Illinois U Library

Transactions

of the

ASME

---

els Performance at Port Washington Station . . . . *W. A. Pollock* 97

mbustion Studies Using the Golay Photothermal Detector With an Infrared Mono-
chromator . . . . *J. T. Agnew* 107

rformance Criteria for Positive-Displacement Pumps and Fluid Motors . . . .
. . . . *W. E. Wilson* 115

sponse Characteristics of Thermometer Elements . . . . . . *A. J. Hornfeck* 121

signing for High-Frequency Induction Hardening . . . . *J. T. Temin* 135

w Forging Acts to Enhance Metal Properties . . . *E. O. Dixon and E. J. Foley* 147

elded Thermocouples for Gas Turbines . . . . . . *A. I. Dahl and E. F. Fiock* 153

ogress Report No. 2 on Tool-Chip Interface Temperatures . . . *K. J. Trigger* 163

tomatic Control of Turbojet Engines . . . . *C. S. Cody* 175

FEBRUARY, 1949

VOL. 71, NO. 2

Transactions

of The American Society of Mechanical Engineers

Published on the tenth of every month, except March, June, September, and Decembe

---

OFFICERS OF THE SOCIETY:

JAMES M. TODD, *President*
K. W. JAFFE, *Treasurer* C. E. DAVIES, *Secretary*

COMMITTEE ON PUBLICATIONS:

J. M. JURAN, *Chairman*
RONALD B. SMITH JOHN HAYDOCK
C. B. CAMPBELL
GEORGE A. STETSON, *Editor* K. W. CLENDINNING, *Managing Editor*

REGIONAL ADVISORY BOARD OF THE PUBLICATIONS COMMITTEE:

KERR ATKINSON—I
OTTO DE LORENZI—II
W. E. REASER—III
F. C. SMITH—IV
TOMLINSON FORT—V
R. E. TURNER—VI
R. G. ROSHONG—VII
M. A. DURLAND—VIII

Published monthly by The American Society of Mechanical Engineers. Publication office at 20th and Northampton Streets, Easton, Pa. The editori
department is located at the headquarters of the Society, 29 West Thirty-Ninth Street, New York 18, N. Y. Cable address, "Dynamic," New York. Pric
$1.50 a copy, $12.00 a year for Transactions and the *Journal of Applied Mechanics,* to members and affiliates, $1.00 a copy, $6.00 a year. Changes of ad
dress must be received at Society headquarters three weeks before they are to be effective on the mailing list. Please send old as well as new address...
By-Law: The Society shall not be responsible for statements or opinions advanced in papers or...printed in its publications (B13, Par. 4)....Entered a
second-class matter March 2, 1928, at the Post Office at Easton, Pa., under the Act of August 24, 1912....Copyrighted, 1949, by The American Socie
of Mechanical Engineers. Reprints from this publication may be made on condition that full credit be given the Transactions of the ASME and th
author and that date of publication be stated.

Fuels Performance at Port Washington Station

By W. A. Pollock,[1] Milwaukee, Wis.

This paper contains recent operating data, a discussion relevant design features, and information comparing ewar and postwar coals as affecting operation of the Port ashington Station of the Wisconsin Electric Power ompany. In order to make the report complete, fuels d station performances are presented.

DESIGN features and the first 15 months of operation of Port Washington's first unit were reported in a previous paper by Fred Dornbrook (1).[2] Reports of subsequent experiences the operation of this first unit and the second unit, after its itial operation late in 1943, have also been published (2–9, clusive).

It is not intended to review in any detail the previously pub- hed record of reliability and economy, but only to supplement d to extend that record to include the most recent data. Table "Average of Daily Operating Data" for unit No. 2, presents erating data similar to those published for the first unit several ars ago.

Furnace Design Warrants Careful Consideration

Careful, conservative furnace design has been one of the most portant factors in sustaining favorable economy and reliability. ith more than 50 per cent of the heat absorption occurring in e furnace of modern boiler units, a furnace possessing the versa- ity to burn low-grade as well as high-grade coal is essential.

Changing coal markets require that coals varying greatly in ture and ash characteristics be consumed, at various loads.

While coping with the ash problem, the furnace must deliver finite quantities of heat to the boiler and superheater, for it largely responsible for costly variations in steam temperature. must burn widely different kinds of fuel with low excess air d with little combustible loss.

One large boiler manufacturer, while discussing the present- y trends in utility steam practice, as reflected in design char- teristics, described a new boiler-furnace installation in the lowing manner: "A simple clean-cut furnace of ample volume low heat-release rates and with solid metal surfaces on all les, top, and bottom. All surfaces to be readily accessible for aning."

That cooler furnaces are considered the best means of providing burning of present-day fuels with the wide variations in char- teristics is evident as the design data on recent installations studied.

In the early days of pulverized-fuel firing, prior to the intro- ction of water-cooled surfaces into the furnace, 13,000 Btu per ft of furnace volume per hr with 13 per cent CO_2 in the exit ses was a practical maximum if refractory maintenance was t to be excessive.

As furnace cooling, in the form of water screens and then water walls, was employed, the maximum furnace heat releases used in large units were increased to 25,000 and 30,000 Btu per cu ft per hr and higher. Changing fuel characteristics during the war and resulting slag accumulations have caused an "about-face" in the thinking, and now the question often asked is, "How large a furnace shall it be?"

Before the trend back toward cooler furnaces had begun, Fred Dornbrook in an earlier paper (10), concluded as follows: "In order to prevent ash from sticking to the inside of any furnace, these surfaces must be designed to cool properly the ash below its plastic state.

"Experiences and data are presented indicating that a practical solution of the so-called 'slagging problem' consists of designing boiler furnaces for such appreciable heat absorption that gases are approximately 200 F below ash-softening temperatures when entering the first rows of boiler tubes."

Lifetime availability records for the two units at Port Washington (see Table 4), are 94.9 per cent for the boilers and 93.5 per cent for the tandem-compound turbines. A 68-boiler-years' availability record produced by the four high-pressure boilers and the high-pressure topping turbines at Lakeside Station, also shown in Table 4, was 94.5 per cent and 96.5 per cent, respectively. Thus with 86 equipment-years of operation, high-pressure boilers are shown to be as dependable as turbines. One-boiler per turbine designs are well justified.

Boiler-unit reliability has a decided bearing upon total investment costs and operating costs. Savings resulting from furnace size are lost if the design lacks reliability and requires more spare boiler units. It is felt that too much emphasis cannot be placed upon reliability.

Prewar and Postwar Coals

How well Port Washington was able successfully to burn the various coals furnished during the war is shown in part by the continued low station heat rates as shown in Fig. 1.

That present coal quality is far below prewar coals is general knowledge. Just how well those operating men charged with the task of maintaining economy records and at the same time carrying unprecedented higher loads have done their job is evident by comparing the annual average coal analysis of 1947 with corresponding values for 1940, a typical prewar year, in Table 5, and by considering the effect of some of the variations on plant operation.

Ash-fusion temperature has decreased 150 deg F and is within 57 deg F of the designed average furnace temperature. Troubles from slag have been avoided only by frequent inspections of the furnaces and by acting upon reports of any slag found when removing ash. Importance of this cannot be overemphasized. Ten-point CO_2 traverses across the boiler width each shift assist in locating hot areas, and act as a guide in making needed air-distribution adjustments.

After 15 months of operation on unit No. 1, it was reported that the first boiler pass had never required lancing. Even with the lower ash-fusion temperatures of the postwar coals, lancing has not been required regularly. Periods of several months often elapse between occasions when extensive lancing is necessary,

---

[1] Senior Test Engineer, Wisconsin Electric Power Company.

[2] Numbers in parentheses refer to the Bibliography at the end of paper.

Contributed by the Fuels Division and presented at the Semi- nual Meeting, Milwaukee, Wis., May 30–June 5, 1948, of The erican Society of Mechanical Engineers.

Note: Statements and opinions advanced in papers are to be lerstood as individual expressions of their authors and not those he Society. Paper No. 48—SA-7.

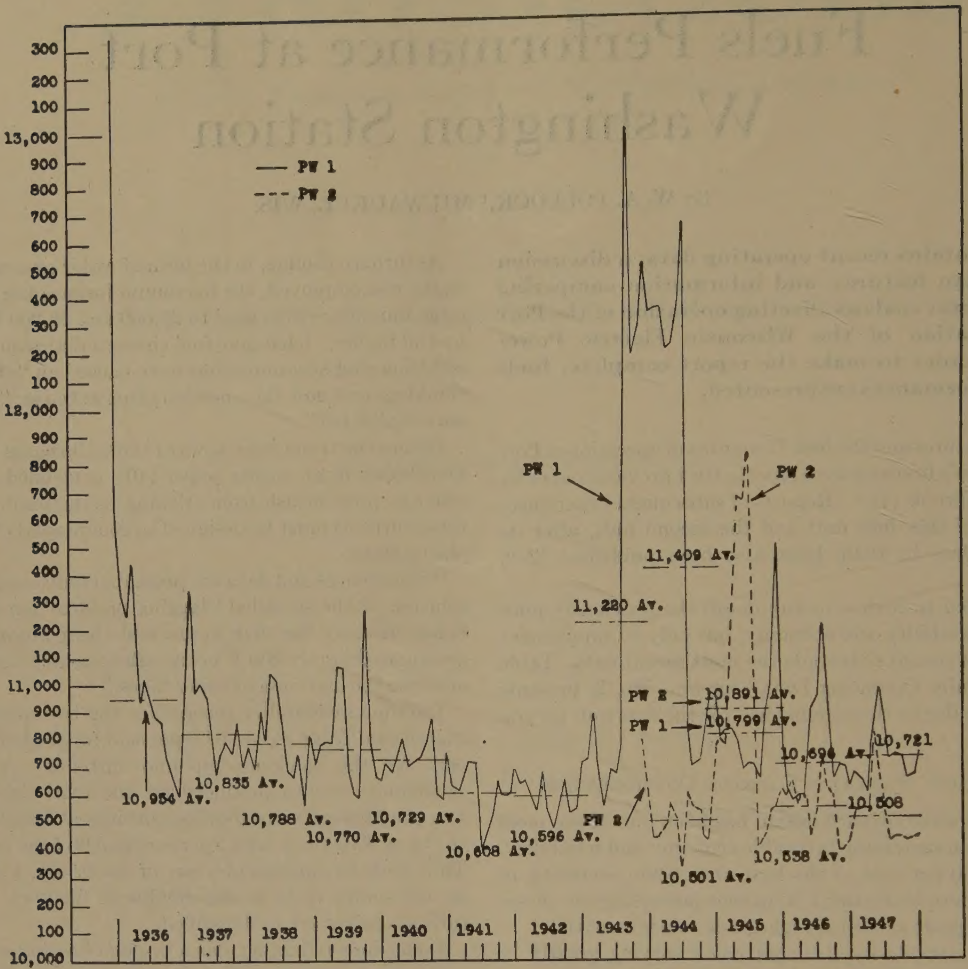

FIG. 1 PORT WASHINGTON STATION HEAT CONSUMPTION, BTU PER NET KWHR

and then it is needed only when first signs of slagging troubles are not followed properly and the cause of the difficulty corrected. No special cleaning has been needed in the furnaces during semiannual outages.

Labor amounting to 0.6 and 0.81 man-hour per boiler-hour is shown as necessary on units Nos. 1 and 2, respectively, to take care of ash removal and to perform all of the lancing and soot-blowing operations necessary to maintain the boiler furnace in proper condition for long-sustained runs, and to regulate steam temperature. All of this cleaning work is readily included in the duties of the boiler-operator helper. The somewhat higher loads carried on unit No. 2 explain in part the higher cleaning hours. The following table gives the record:

	Boiler no. 1		Boiler no. 2	
	Hr per wk	Man-hr per blr-hr	Hr per wk	Man-hr per blr-hr
Ash removal........	14	0.08	28	0.17
Lancing and inspecting...............	28	0.17	42	0.25
Air soot-blower operation...........	10	0.06	10	0.06
Reheater and superheater soot-blower operation.........	49	0.29	56	0.33
Total	101	0.60	136	0.81

It is of interest to note that only 0.12 per cent of the steam generated is needed for soot-blowing. This represents 12 Btu per kwhr increase in station heat rate to provide a means of keeping the heat-absorbing surfaces at the desired cleanliness for uniform operation. The only means of steam temperature control, aside from flame positioning, is by this selective cleaning of heat-absorbing surfaces.

Load reductions at night have been used by some to explain the apparent self-cleaning of boiler furnaces. Two boilers of similar design to those at Port Washington, which are located in stations supplying steam to the Milwaukee central-heating system, have operated continuously at rated capacity for extended periods without slag or ash accumulations which required special attention. Port Washington's boilers have operated at full rating for 16 to 18 hr daily and, on occasions, at full load for more than 48 hr. Lack of system load is normally the only reason for reducing load. There has been nothing to indicate that these boilers could not operate at full loads for extended periods if night-time loads were available.

Continuous operating periods of 8 months have occurred. Six months' continuous operation is the rule. What practically amounts to one outage per year is now practiced, for one of the semiannual outages on each unit is shortened to start on Friday noon and end on Monday morning. The other semiannual outage is ordinarily of 9 days' duration, including two week ends but only 5 full-load days.

It may be concluded that the furnace-cooling still affords a safe margin to cool the ash below its plastic state.

LOWER BTU AND HIGHER ASH VALUES IN POSTWAR COALS

Carrying postwar loads with the postwar coals instead of the coals for which the station was designed has resulted in extra

TABLE 1 OPERATING PERIODS AND REASONS FOR OUTAGES—1947

PERIOD NO.	STARTED	FINISHED	HR. RUN	KWHR GENERATED, MILLIONS	OUTAGE HOURS	OUTAGE REASON
70	12/27/46*	3/21/47	2,039.17	133.655	178.61	General inspection, boiler and turbine.
71	3/29/47	5/14/47	1,117.65	67.918	27.70	Screen tube rupture. Immediate forced outage.
72	5/16/47	8/23/47	2,373.32	146.532	201.55	General inspection, boiler and turbine.
73	8/31/37	9/12/27	294.67	19.423	33.45	Leak in rolled joint and seal weld, rear waterwall downcomer tube. Delayed forced outage.
74	9/14/47	12/26/47**	2,493.88	176.202		
TOTAL	12/27/46	12/26/47	8,318.69	543.930	441.31	
TOTAL	11/22/35	12/26/47	94,649.03	5,516.050	11,382.97	
				Unit No. 2		
20	12/27/46***	1/18/47	531.08	36.298	12.57	Condenser tube leakage. Delayed forced outage.
21	1/18/47	3/15/47	1,328.65	91.006	13.67	Condenser tube leakage. Delayed forced outage.
22	3/15/47	5/2/47	1,151.27	75.514	217.08	General inspection, boiler and turbine. Reseated turbine inlet valves and inspected blading, low-pressure section.
23	5/11/47	10/1/47	3,454.22	227.641	89.56	General inspection, boiler and turbine. Repaired leaky weld and adjacent cuts, radiant reheater.
24	10/5/47	12/26/47****	1,981.90	142.109		
TOTAL	12/27/46	12/26/47	8,427.10	572.568	332.90	
TOTAL	10/27/43	12/26/47	33,694.64	2,172.274	2,622.89	

*This operating period started 8/22/46

**Still in operation.

***This operating period started 9/29/46

****Still in operation.

uipment hours throughout the coal-handling section of the ation. A few of these extras for both units are as follows:

4 tons more coal were required daily or 4 boatloads annually
arloads more coal to remove from the dock, weigh, unload, convey, mill, and burn daily
min extra coal-conveyer time daily
3 extra mill-hours daily
tra air and flue gas for the draft fans

Each of the foregoing items, in addition to meaning extra oor and maintenance cost because of extra operating hours, duces plant output by a definite amount. For example, each ll-hour consumes 250 kwhr. The 6.33 extra mill-hours daily nsume enough energy to operate an 85-hp motor continuously, enough to operate the pump which transfers all of the connsate from one condenser hot well through the steam-jet air mps, generator coolers, and two stages of extraction heating the boiler feed pumps.

The 12.9 per cent ash in 1947 coal versus 8.7 per cent ash in the 40 coal accounts for much of the extra coal-storage and hanng costs described. A total of 178 tons of ash for both units re processed daily in 1947, as compared with 112 ton which uld have been handled for the same total Btu, but with 8.7 per nt ash, the 1940 value. Approximately 50 per cent increased t for ash disposal occurred; 93 cu yd extra of ash had to be posed of, or 7 extra truckloads each day.

PULVERIZED-COAL STORAGE HELPS IN CARRYING LOAD

Full use of storage capacity of the pulverized-fuel bins has en practiced. In 1940 16.7 tons per hr were averaged from the pulverizers which are rated nominally at 15 tons per hr. In 1947 as the operating data show, 15.3 tons per hr were averaged. With 13,000-Btu coal, this would permit rated station capacity; however, at 11,644 Btu per cu ft, 34.5 tons of coal per hr are needed. Thus 10 per cent milling-capacity deficiency exists which is compensated for by drawing down the bin levels at periods of high loads and restoring them during light-load times. Full load could not have been carried, except for the pulverized-coal storage, without installing a spare mill.

How a 13.5-hr mill overhaul is accomplished with the station carrying full load has been previously reported (9).

MILL OPERATION AND MAINTENANCE

The average moisture in the coal to the pulverizers was 7.4 per cent, but the maximum was 14.3 per cent. To dry this higher-moisture coal properly, a higher gas temperature must be used. Flue gas at 830 F has been employed to dry this coal on unit No. 1, where 830 F flue gas entering the air heater is available. On unit No. 2 the flue gas to the air heater averages 700 F and the lifetime average output for its mills has been 0.9 ton per hr lower. Flue gas for mill-drying on units now under construction will be taken from high in the last pass to obtain higher-temperature gas in an effort to raise mill capacity. Flue-gas temperature to the mills will be controlled as on the other units by tempering with gas from the air-heater outlet.

Higher mill repair costs have been referred to earlier in this paper. Just how much higher these costs have been is shown by the comparison between the average life of grinding rings and rolls in 1947, and the best life previously obtained. Seven sets

TABLE 2 AVERAGES OF DAILY OPERATING DATA FOR UNIT NO. 2

DATE, Month Ending	Jan. 26	Feb. 25	Mar. 26	April 25	May 26	June 25	July 26	Aug. 26	Sept. 25	Oct. 26	Nov. 25	Dec. 26	1947 AVE.	4 Year AVE.
COAL, TONS PER DAY														
1. To bunker	656	687	707	659	556	621	621	666	732	661	771*	790*	678*	645*
2. Pulverized	676	705	700	686	604	655	655	706	722	682	733	741	688	659
3. Burned, approx.	676	705	700	687	603	636	653	708	721	682	734	741	688	660
4. Mill hours	43.20	43.89	45.01	44.48	40.32	43.50	46.82	46.67	44.55	44.43	46.78	49.16	44.90	41.18
5. Mill tons/hr.	15.7	16.1	15.6	15.4	14.9	14.6	14.0	15.1	16.2	15.4	15.7	15.1	15.3	16.1
6. Mill system KWH/ton	15.9	15.7	15.3	16.3	16.8	17.4	18.1	15.7	16.1	16.7	15.6	17.3	16.4	15.5
7. Moisture, mill in, %	7.7	7.7	7.3	8.6	7.5	6.9	7.9	7.1	8.0	7.1	7.9	7.9	7.7	7.6
8. Moisture, mill out, %	2.3	2.3	2.3	2.8	2.3	1.9	2.3	2.1	2.4	2.2	2.6	2.3	2.3	2.3
9. No. 3 Mill Fineness % through														
200 mesh	69.90	70.61	74.26	75.75	71.42	68.82	67.11	72.10	71.82	67.05	63.70	65.36	69.83	66.62
100 mesh	89.81	91.30	93.88	93.60	90.48	89.21	89.25	91.77	90.66	87.50	85.61	87.87	90.08	90.34
48 mesh	98.24	98.67	99.35	99.20	98.52	98.06	98.29	98.96	98.69	97.42	96.63	97.70	98.31	98.57
28 mesh	99.88	99.88	99.97	99.95	99.91	99.86	99.89	99.91	99.91	99.81	99.65	99.80	99.87	99.86
20 mesh	99.98	99.99	99.99	99.99	99.99	99.97	99.99	99.99	99.99	99.97	99.93	99.97	99.98	99.98
10 mesh	100	100	100	100	100	100	100	100	100	100	100	100	100	100
10. No. 4 Mill Fineness % through														
200 mesh	69.71	68.15	69.77	64.37	62.20	61.53	67.08	72.64	65.24	63.00	61.35	61.08	65.52	64.62
100 mesh	89.92	88.54	89.48	86.23	84.97	83.85	88.45	91.21	85.58	85.43	84.21	84.69	86.89	88.47
48 mesh	98.11	97.83	97.95	97.05	96.83	96.22	97.97	98.71	96.52	96.79	96.05	96.82	97.24	97.88
28 mesh	99.81	99.79	99.78	99.63	99.68	99.56	99.83	99.90	99.59	99.74	99.43	99.69	99.70	99.76
20 mesh	99.97	99.97	99.95	99.94	99.94	99.89	99.98	99.98	99.94	99.96	99.85	99.95	99.94	99.96
10 mesh	100	100	100	100	100	100	100	100	100	100	100	100	100	100
11. Btu/lb., ash, moist. free	14453	14273	14390	14313	14577	14726	14420	14570	14445	14467	14468	14514	14468	14576
12. Btu/lb., Dry	12700	12466	12607	12643	12800	12865	12544	12733	12360	12576	12505	12520	12602	12907
13. Btu/lb., As Received	11722	11469	11661	11543	11853	11999	11540	11854	11408	11628	11530	11531	11644	11939
14. Moisture, %	7.7	8.0	7.5	8.7	7.4	6.7	8.0	6.9	7.7	6.8	7.8	7.9	7.6	7.5
15. Volatile, %	36.54	35.96	35.98	36.76	35.80	35.70	35.97	35.98	35.50	35.75	35.52	35.81	35.94	35.81
16. Fixed Carbon, %	51.33	51.38	51.63	51.57	52.01	51.66	51.02	51.41	50.08	50.49	50.91	50.45	51.16	52.74
17. Ash, %	12.13	12.66	12.39	11.67	12.19	12.64	13.01	12.61	14.42	13.76	13.57	13.74	12.90	11.45
18. Sulphur, %	2.79	2.52	2.61	2.54	2.54	2.77	2.67	2.79	2.67	2.65	2.40	2.50	2.62	2.49
19. Ash fusion temp. °F.	2095	2093	2114	2119	2169	2189	2180	2140	2196	2196	2181	2210	2157	2153
20. Pulverized Coal Composite Sample														
BTU/LB. Ash, Moisture free	14515	14530	14510	14408	14659	14707	14533	14588	14532	14557	14448	14551	14545	14634
BTU/LB. Dry	12757	12788	12772	12633	12803	12795	12648	12814	12625	12721	12619	12726	12725	12938
BTU/LB. As Received	12515	12519	12504	12355	12534	12622	12395	12583	12347	12505	12341	12459	12471	12666
Moisture, %	1.9	2.1	2.1	2.2	2.1	1.4	2.0	1.8	2.2	1.7	2.2	2.1	2.0	2.1
Volatile, %	36.21	35.98	35.76	35.92	35.49	35.38	35.35	35.63	35.59	35.82	34.83	35.17	35.60	35.53
Fixed carbon, %	51.68	52.03	52.26	51.76	51.85	51.62	51.68	52.21	51.29	51.57	52.51	52.29	51.89	52.88
Ash, %	12.11	11.99	11.98	12.32	12.66	13.00	12.97	12.16	13.12	12.61	12.66	12.54	12.51	11.59
Sulphur, %	2.71	2.49	2.59	2.56	2.37	2.55	2.55	2.46	2.14	2.48	2.13	2.25	2.45	2.38

*This figure includes coal conveyed into #3 Unit green coal bunker which is used for #2 Unit.

TABLE 2 (*Continued*)

DATE, Month Ending	Jan. 26	Feb. 23	March 26	April 25	May 26	June 25	July 26	Aug. 26	Sept. 25	Oct. 26	Nov. 25	Dec. 26	1947 Ave.	4 Year Ave.
BOILER ROOM														
21. Steam, million lb./day	12.646	13.206	13.071	12.539	11.386	12.164	12.238	13.583	13.549	12.957	13.755	13.925	12.919	12.540
22. Feedwater, mil. lb./day	12.609	13.168	13.029	12.510	11.351	12.137	12.209	13.551	13.514	12.926	13.717	13.893	12.885	12.473
23. Ave. output, thd. #/hr.	536	550	554	522	496	506	510	566	565	554	573	580	543	526
24. Hours steaming per day	23.61	24.00	23.58	24.00	22.94	24.00	24.00	24.00	24.00	23.37	24.00	24.00	23.80	23.83
25. Hours banked per day	.29	0	0	0	0	0	0	0	0	0	0	0	.03	.02
26. % excess air	20	19	19	22	26	23	22	21	23	22	20	20	21	20
27. Pressure, lb. G.	1326	1328	1327	1329	1326	1330	1329	1332	1320	1321	1339	1335	1328	1318
28. Feedwater temperature °F.	400	405	405	397	393	397	398	410	407	402	405	406	403	399
29. Feedwater press. # G.	1576	1598	1667	1679	1680	1677	1668	1667	1665	1671	1671	1684	1659	1621
30. B.F. pump eff. % actual	59.8	62.6	68.2	68.0	67.7	68.6	70.0	71.0	70.3	69.9	69.9	70.5	68.1	63.8
31. B.F. pump eff. % standard	62.1	62.5	62.2	61.5	60.7	62.4	63.2	63.8	63.5	63.0	63.1	63.1	62.6	62.8
32. % combustible in fly ash	11.38	11.76	12.08	12.22	11.87	11.21	10.64	7.90	9.23	9.03	10.75	9.63	10.64	11.04
33. Exh. to htrs. thd. lb./day	-	-	-	-	-	-	-	-	-	-	-	-	-	-
Steam Temperature, °F.														
34. Rad. suphtr. out	703	703	701	708	712	712	713	704	703	709	707	704	707	703
35. Con. suphtr. out	838	838	838	840	837	837	838	838	839	837	838	840	838	832
36. Reheater in	561	569	569	565	549	551	553	571	572	566	576	582	566	556
37. Reheater out	810	814	813	810	805	809	811	818	820	820	825	827	815	802
Gas Temperature, °F.														
38. Air heater in	693	698	700	696	679	689	691	711	712	703	707	710	700	702
39. Air heater out	356	364	368	362	339	341	344	359	360	362	364	365	357	356
40. Drop	337	334	332	334	340	348	347	352	352	341	343	345	343	346
Air Temp., deg. F.														
41. Air heater in	176	176	176	176	176	179	181	181	182	183	184	183	180	182
42. Air heater out	480	482	485	481	491	507	508	524	522	517	514	510	502	506
43. F.D. fan in	111	112	116	116	116	124	125	128	123	126	120	117	120	119
44. Rise	369	370	369	365	375	383	383	398	399	391	394	393	382	387
45. % air thru heater	103	101	101	103	102	102	102	100	99	98	98	99	101	100
46. Htr. Perform. % of std.	95	92	91	92	108	112	110	108	107	104	103	102	102	104
TURBINE ROOM														
47. Ave. load, KW	67563	69234	69407	64576	61484	63250	63532	69504	69128	69560	71804	72868	67659	65441
Temperatures, °F.														
48. Throttle	835	835	836	838	835	835	836	836	836	835	837	839	837	831
49. 1st inlet	829	831	831	826	820	824	827	832	832	831	834	836	830	825
50. Reheater in	565	570	573	567	553	553	555	573	574	569	578	584	568	558
51. Reheater out	807	810	809	806	801	804	805	814	816	817	823	826	812	799
52. No. 3 heater	455	458	460	456	442	441	444	456	461	453	459	466	455	445
Pressures, lb. G.														
53. Throttle	1279	1279	1279	1283	1286	1291	1287	1275	1275	1282	1275	1270	1280	1267
54. 1st inlet	1219	1236	1233	1152	1114	1167	1186	1245	1230	1244	1249	1247	1211	1196
55. Reheater in	349	360	365	341	317	323	327	365	365	360	373	380	353	340
56. Reheater out	310	320	325	304	282	287	290	324	324	320	331	337	313	301
57. No. 3 heater	46.0	48.0	48.6	44.6	39.6	40.2	41.0	47.8	48.4	46.6	48.8	50.8	45.9	44.8

TABLE 2 (*Continued*)

DATE, Month Ending	Jan. 26	Feb. 23	March 26	April 25	May 26	June 25	July 26	Aug. 26	Sept. 25	Oct. 26	Nov. 25	Dec. 26	1947 Ave.	4 Year Ave.
Stage Efficiencies, %														
58. 1st in to rehtr. in	77.7	77.2	77.0	78.7	78.8	78.6	78.5	77.2	77.2	77.4	76.6	76.5	77.6	77.5
59. Rehtr. out to No. 3 htr.	85.8	85.5	84.9	84.7	86.5	87.5	87.4	86.6	86.2	87.3	87.2	86.5	86.4	87.0
60. Both	82.4	82.0	81.6	82.2	83.4	83.7	83.6	82.7	82.4	83.2	82.8	82.4	82.8	83.0
61. Cir. Water out, °F.	40.9	41.1	40.7	44.1	50.5	53.3	61.3	67.3	65.2	54.1	52.3	42.2	51.1	50.8
62. Cir. Water in, °F.	35.6	35.8	35.5	39.1	45.6	48.3	56.2	61.7	59.6	48.9	46.8	36.7	45.9	45.8
63. Cir. Water Rise, °F.	5.3	5.3	5.2	5.0	4.9	5.0	5.1	5.6	5.6	5.2	5.5	5.5	5.2	5.0
64. Condensate, F.	51.2	51.8	51.7	54.0	59.3	61.8	69.4	75.7	73.9	63.4	62.1	53.7	60.7	59.7
Exh. Press. "Hg. Abs.														
65. Actual	.39	.40	.40	.43	.51	.56	.73	.89	.88	.59	.58	.44	.57	.56
66. Standard	.37	.39	.38	.42	.50	.54	.69	.84	.83	.57	.55	.40	.54	.54
67. High (+) or low (-)	+.02	+.01	+.02	+.01	+.01	+.02	+.04	+.05	+.05	+.02	+.03	+.04	+.03	+.02
68. Air pump inlet	.30	.30	.29	.32	.40	.44	.60	.73	.73	.44	.42	.29	.44	.44
69. Air leakage, CFM	1.6	1.5	1.6	2.1	2.3	2.1	2.0	1.5	1.6	1.6	1.4	1.4	1.8	1.7
ELECTRICAL														
70. Output, gross, 1000 KWH/day	1592.7	1658.3	1635.1	1552.5	1420.8	1526.4	1532.8	1683.4	1668.3	1630.6	1726.6	1739.2	1613.9	1564.8
71. Output, net 1000 KWH/day	1506.8	1570.6	1549.8	1469.6	1344.2	1446.6	1451.5	1595.1	1580.5	1546.3	1638.9	1649.4	1529.1	1482.8
72. Auxiliaries 1000 KWH/day*	85.9	87.7	85.3	82.9	76.6	79.8	81.3	88.3	87.8	84.3	87.7	89.8	84.8	82.0
73. Auxiliaries, %	5.4	5.3	5.2	5.3	5.4	5.2	5.3	5.2	5.3	5.2	5.1	5.2	5.2	5.2
74. % for coal prep.	.67	.67	.66	.72	.73	.72	.78	.66	.70	.70	.66	.74	.71	.65
75. % for B.R. fans	1.26	1.24	1.23	1.25	1.19	1.15	1.15	1.19	1.21	1.19	1.17	1.20	1.21	1.20
76. % for B.F. pumps	1.97	1.90	1.82	1.89	1.80	1.83	1.80	1.80	1.80	1.79	1.77	1.78	1.83	1.87
77. % for circ. pumps	.86	.83	.85	.84	.90	.86	.89	.84	.86	.87	.83	.81	.85	.91
78. % for miscellaneous	.64	.66	.64	.60	.78	.64	.68	.71	.73	.65	.67	.67	.60	.57
Station Heat Consumption BTU per KWH														
Gross	9975	9989	9996	10237	10066	9998	9892	9931	9869	9805	9869	9893	9955	10039
Auxiliaries	569	558	549	580	581	550	553	547	548	539	532	538	553	558
Net	10544	10547	10545	10817	10647	10548	10445	10478	10417	10344	10401	10431	10508	10597

TABLE 3 USE AND AVAILABILITY DATA FOR UNITS NOS. 1 AND 2

	Unit 1						Unit 2					
	1947			12 Yr. Av.			1947			50 Mo. Av.		
	Boiler	Turbine	Plant	Boiler	Turbine	Plant	Boiler	Turbine	Plant	Boiler	Turbine	Plant
USE FACTOR $\frac{\text{Service Hr.}}{\text{Period Hr.}}$	95.0	95.0	95.0	89.2	89.2	89.2	96.2	96.2	96.2	91.8	92.2	92.2
HOURLY OUTPUT-CAPACITY FACTOR $\frac{\text{Av. Hrly. Output}}{\text{Rated Hrly. Output}}$	76.5	81.7	81.7	66.2	72.9	72.9	78.8	84.9	84.9	76.0	81.9	81.9
ANNUAL OUTPUT CAPACITY FACTOR $\frac{\text{Annual Output}}{\text{Annual Rated Output}}$	72.4	77.6	77.6	59.2	65.1	65.1	75.8	81.7	81.7	69.9	75.6	75.6
ANNUAL DEMAND FACTOR $\frac{\text{Demand Hr.}}{\text{Period Hr.}}$	98.4	96.6	100	92.6	96.9	99.1	98.0	98.3	100	94.1	97.8	100
DEMAND AVAILABILITY FACTOR $\frac{\text{Service Hr.}}{\text{Demand Hr.}}$	96.6	98.5	95.0	96.4	92.1	90.2	98.2	97.9	96.2	97.5	94.3	92.2
ANNUAL AVAILABILITY FACTOR $100 - \frac{\text{Repair Hr.}}{\text{Period Hr.}}$	95.3	98.4	95.0	94.5	92.6	90.0	96.6	96.2	96.2	95.8	92.8	92.2

TABLE 4 AVAILABILITY DATA OF HIGH-PRESSURE BOILERS AND TURBINES

BOILERS

Year	L.S. No. 17	L.S. No. 18	L.S. No. 19	L.S. No. 20	L.S. Av.	P.W. No. 1	P.W. No. 2	P.W. Av.
1931	88.3	92.9	95.0	97.8	92.0			
1932	85.7	98.0	96.4	96.9	93.8			
1933	96.1	98.5	97.6	98.2	97.6			
1934	92.1	96.1	91.7	96.2	94.0			
1935	96.2	95.2	96.0	94.7	95.3			
1936	87.4	95.4	94.4	94.9	93.0	91.1		
1937	92.1	97.1	95.5	95.2	95.0	93.1		
1938	90.8	93.7	92.4	95.6	93.0	98.8		
1939	93.0	96.3	94.1	92.3	93.9	93.4		
1940	90.6	91.9	94.3	95.4	93.1	90.3		
1941	95.3	96.1	93.1	96.5	95.3	96.6		
1942	92.9	95.2	97.2	93.9	94.8	97.1		
1943	94.6	96.8	97.4	97.3	96.5	98.9		
1944	93.0	96.1	96.3	95.7	95.3	95.9	91.4	93.7
1945	93.8	92.6	94.5	93.1	93.5	87.6	98.1	92.9
1946	91.5	94.2	95.1	95.1	94.0	95.9	97.3	96.6
1947	96.9	93.6	95.7	96.5	95.7	95.3	96.6	96.0
Av.					94.5 (68 yr.)			94.9 (16 yr.)

TURBINES

Year	L.S. No. 7	L.S. No. 8	L.S. No. 10	L.S. No. 12	L.S. Av.	P.W. No. 1	P.W. No. 2	P.W. Av.
1931	91.6	93.9	91.7	89.8	91.8			
1932	95.9	95.9	98.7	96.7	96.8			
1933	99.9	98.8	97.6	100.0	99.1			
1934	96.3	98.6	99.9	99.9	98.7			
1935	99.8	96.1	94.5	72.9	90.8			
1936	90.6	93.6	98.9	97.3	95.1	98.1		
1937	97.1	97.1	99.6	98.8	98.2	89.9		
1938	100.0	99.7	95.3	95.8	97.7	96.2		
1939	92.8	99.0	99.7	99.0	97.6	93.0		
1940	100.0	92.8	99.6	97.9	97.6	92.9		
1941	99.6	100.0	95.1	93.8	97.1	100.0		
1942	87.1	95.3	91.4	97.0	92.7	93.5		
1943	100.0	100.0	95.5	94.6	97.5	88.4		
1944	94.8	93.9	99.4	98.5	96.7	88.4	91.0	89.7
1945	97.9	94.0	100.0	96.0	97.0	88.1	89.7	88.9
1946	97.9	97.3	93.5	100.0	97.2	97.7	95.2	96.5
1947	100.0	99.7	99.0	100.0	99.7	98.4	96.2	97.3
Av.					96.5 (68 yr.)			93.5 (16 yr.)

TABLE 5 PREWAR AND POSTWAR COALS

Year	1940	1947
Unit No.	1	2
Av. KWH	58750	67660
Coal Burned Tons/day	551	688
Mill Hrs./day	33.7	44.9
Mill Tons/hr.	16.4	15.3
Proximate Analysis		
BTU/lb. M. & A. F.	14941	14468
BTU/lb. Dry	13644	12602
BTU/lb. A. R.	13005	11644
Moisture, %	4.7	7.6
Volatile, %	34.3	35.9
Fixed Carbon, %	57.0	51.2
Ash, %	8.7	12.9
Sulphur, %	1.27	2.62
Ash Fusion, F.	2310	2157

of rolls and nine rings are represented by the averages for 1947, as follows:

Life of pulverized-grinding parts	Best	1947 average
Tons pulverized per set of rolls.........	147500	65700
Tons pulverized per grinding ring.....	123000	59500

Induced-draft fan wear has increased, but because this maintenance work is part of the regularly scheduled outage work, no direct comparison, as drawn for pulverizer grinding parts, can be made.

Variation in mill output from 14 tons per hr to 16.1 tons per hr, Table 2, is explained primarily by variation in grindability characteristics of the coal.

SUMMARY

A relatively cool furnace, and the storage system of burning pulverized coal, have been shown as big factors in sustaining reliability and economy as daily station output has been increased.

Operating data for unit No. 2 and other often requested data of general interest have been presented.

A comparison is made of prewar and postwar coals, including some figures on extras needed because the postwar coal has had a lower heat value and higher ash. More maintenance chiefly to the pulverizers and the draft fans has been shown to result because of poorer qualities of the 1947 coals.

BIBLIOGRAPHY

1 "The Port Washington Plant—Unique Design Features and Operating Experiences," by F. L. Dornbrook, *Mechanical Engineering*, vol. 58, 1936, pp. 697–704 and 728.

2 "Port Washington's Second Year," by M. K. Drewry, *Combustion*, vol. 9, February, 1938, pp. 18–24.

3 "Port Washington's Third Year," *Combustion*, vol. 10, January, 1939, pp. 16–19.

4 "Port Washington Sustains Its Economy," *Combustion*, vol. 11, January, 1940, pp. 33–34.

5 "Port Washington 1941 Operation," *Combustion*, vol. 13, January, 1942, p. 37.

6 "Port Washington 1942 Experience," *Combustion*, vol. 14, January, 1943, pp. 36–37.

7 "Port Washington Second Unit in Operation," *Combustion*, vol. 15, January, 1944, pp. 30–34.

8 "Port Washington Performance for 1944," *Combustion*, vol. 16, January, 1945, pp. 32–34.

9 "1945–1946 Performance at Port Washington," *Combustion*, vol. 18, January, 1947, pp. 31–34.

10 "Development of a Major Principle in Pulverized-Coal Firing," by F. L. Dornbrook, Trans. ASME, vol. 63, 1941, pp. 261–266.

Discussion

L. H. STARK.[3] The paper presented on the fuel performance at Port Washington Station is not only a progress report of this remarkable station but also a report on the progress of burning coal in a pulverized form.

The research, development, and experience that have taken place since 1918, when John Anderson and Fred Dornbrook conceived the idea that coal could be burned in suspension in a pulverized state, would fill a good-sized volume were it to be related in this manner. The story would reveal what has transpired in this field from the time the Lakeside Station of the Wisconsin Electric Power Company was built when 20,300 Btu were required to produce 1 kwhr (then a world record) to the present report on the 1947 performance of the Port Washington Station of the same company, in which is indicated that the average operation of No. 2 unit in this station is 10,500 Btu per kwhr. This is a reduction of 22 per cent in the heat required to produce 1 kwhr over the period in question.

Those responsible for the results as outlined in the paper will destly tell you that when No. 3 unit goes into operation they ect to better this performance.

---

[3] Plant Engineer, Phoenix Hosiery Company, Milwaukee, Wis. Mem. ASME.

ne of the early conditions experienced was low boiler availa- ty due to furnace slagging and refractory replacement caused furnace temperatures higher than the fusion point of the ash l refractory material. The answer to this problem, as outlined the author, has been a more conservative furnace design in ich by increasing the area of water screens and waterwalls, nace temperatures have been reduced, thereby doubling the t release per cubic foot of furnace volume.

The result has been periods of 6 to 8 months or more of continu- operation which probably aids in justifying one-boiler-per- bine design.

Ve are all aware of the decreased value of postwar versus pre- r coal, not to mention the increase of about 100 per cent in t. Table 5 of the paper is typical of analysis of coals received 1940, as compared to coal received in 1947. The table reveals t coal received in 1947 contained 8 per cent less Btu per pound , 38 per cent more moisture, over 30 per cent more ash, and per cent more sulphur than the coal received in 1940.

Referring to Fig. 1 of the paper, it will be noted that the heat nsumption of boiler No. 1 in Btu per kwhr was practically the ne in 1947 as it was in 1940. Will the author explain how this was accomplished; was it due to better load conditions on the boiler, less boiler outage, more frequent cleaning of heated surfaces, or other reasons not mentioned?

To the writer this is a remarkable performance and could only be attained by having the best of equipment, thorough maintenance, and an operating crew trained to perfection in the duties it has to perform.

AUTHOR'S CLOSURE

The author appreciates Mr. Stark's remarks which supply certain historical and other points of interest which could not be adequately treated in the time and space allotted.

The question is asked why the 1947 Btu per kwhr was essentially the same as in 1940 when more favorable coals were available. Versatility of the conservative design in coping with poorer coals without appreciable economy loss and well-trained operating and maintenance crews who strive to sustain established records under adverse loading conditions have all been contributing factors. At no time in 1947 was there sufficient system capacity to permit loading individual units for economy records even if that had been desired. Capacity factors reported in Table 3 are evidence of this point.

Combustion Studies Using the Golay Photothermal Detector With an Infrared Monochromator

By J. T. AGNEW,[1] PHILADELPHIA, PA.

At the Franklin Institute Research and Development aboratories, a research project is in progress in connection ith which certain techniques in infrared detection and ectroscopy have been developed. This paper contains ie results of some experiments conducted with equip-ient developed in connection with this project which is ponsored by the General Engineering Branch, Signal orps, Army Service Forces, U. S. Army.

I N recent years, it has become obvious in combustion research that new techniques would have to be developed in order to achieve an insight into the reaction kinetics of combustion rocesses. Two types of information badly needed are tempera-re and composition of the reactants in a combustion process as function of time. Knowledge of these two parameters to-ether with pressure would allow a more accurate determination the actual conditions existing at a given instant in a combus-on process such as the explosion in the cylinder of an internal-mbustion engine. A better and more thorough understanding the actual conditions existing throughout the combustion rocess, of course, ultimately would lead to a more efficient con-ersion of the potential energy stored in the fuel to useful energy.

An experimental approach to the investigation of the parame-rs mentioned is the determination as a function of time of the ectral distribution of the radiant energy given off during the mbustion. It would be desirable to determine this spectral stribution over as large a portion of the spectrum as possible, nce many of the radiating components have an identifying band ructure in various regions of the spectrum. A rather large re-on of the spectrum is covered by what are known today as in-ared detectors, although some of these detectors are sensitive so throughout the visible spectrum and partially into the ultra-olet region.

Another factor in favor of using infrared detectors in the initial ase of radiant-energy investigations is that, in the range of mperatures expected to be encountered, say, 530 deg K to 4000 g K, the peak radiant intensity from a black radiator, operating this same temperature range, lies in the infrared region of the ectrum from approximately 0.72 to 5.4 microns. Finally, it is own that many polyatomic molecules have characteristic diation bands in this same region of the spectrum, for example, e water vapor and carbon dioxide bands at 2.7 and 4.4 microns.

All of these factors pointed to the desirability of using infrared thermal detectors for the radiant-energy determinations. erefore, it was decided to investigate the capabilities of various pes of detectors for use as radiant-energy detectors in connec-n with combustion processes.

Classes of Infrared Detectors

Modern infrared detectors can be grouped into the following classifications, depending upon the phenomenon by means of which the thermal energy received is converted into a measurable signal.

Thermoelectric. This is probably the most common type of detector. The thermal energy falls upon a single junction or upon several thermoelements connected in series to give a higher electromotive force. A good example of this type of detector, designed for fast response and high sensititivy, is described by Roess and Dacus (1).[2] They describe a thermocouple consisting of overlapping evaporated layers of bismuth and antimony which has 95 per cent full-scale response in 0.14 sec, and a direct-current sensitivity of 6–7 μ per 10^{-4} watts per sq cm. They also point out the pertinent fact that the single thermoelement has a greater signal-to-noise ratio than the series arrangement. The thermocouple type of detector has increased sensitivity in an evacuated chamber. A good example of the use of such a detector is the bismuth-bismuth tin couple used in the Perkin-Elmer infrared spectrometer. Thermocouples or thermopiles can be constructed which have sensitivities capable of detecting as little as 10^{-10} watts of power, but the speed of response is usually very slow. The slow speed of response of thermoelectric detectors causes amplification difficulties in that the signal must either be amplified by a high-gain direct-current amplifier, with its tendency toward instability, or the signal must be interrupted mechanically or electronically, with the possibility of introducing more noise into the system. In general, the time constant of thermoelectric detectors ranges from a few seconds down to 0.050 sec.

Bolometers. Heat detection by means of bolometers depends upon the fact that, when a material absorbs thermal energy, its resistance changes. In general, this type of detector can be divided into two groups: Metallic conductors, such as gold or platinum foil, which are characterized by low impedance and positive temperature coefficients of resistance; and semiconductors, such as NiO, MnO, and CoO (developed by Bell Telephone Laboratories), which are characterized by high impedance and negative temperature coefficients of resistance. This latter group has been given the name thermistors.

The method of detection consists of allowing the radiation to fall upon a bolometer or thermistor mounted as one leg of a balanced bridge circuit. The change of resistance of the detector causes an unbalanced condition to be set up in the bridge, and a current flows through the system. The electric impulse can be amplified by conventional means. This type of detector, has, in general, higher sensitivity and faster speed of response than the thermoelectric type, the time constant being of the order of a few milliseconds.

An extraordinary application of the case of the bolometer principle for the detection of radiant energy is the development directed by Donald Andrews at Johns Hopkins University. In this application, a columbium nitride bolometer, mounted on a

---

[1] Research Engineer, Franklin Institute Laboratories for Research d Development.

Contributed by the Heat Transfer Division and presented at the mi-Annual Meeting, Milwaukee, Wis., May 30–June 5, 1948, of he American Society of Mechanical Engineers.

Note: Statements and opinions advanced in papers are to be derstood as individual expressions of their authors and not those the Society. Paper No. 48—SA-16.

[2] Numbers in parentheses refer to the Bibliography at the end of the paper.

copper base plate and maintained at temperatures near absolute zero, has been found to have the property of becoming a superconductor over a narrow temperature range. The phenomenon of superconduction is not too well understood, but certain materials have been found to have a very high temperature coefficient of resistance over a narrow temperature range near absolute zero. Thus if it is possible to maintain such a material in this temperature range in a balanced bridge circuit, the reception of very small amounts of radiant energy permits the generation of readily detectable signals.

It was possible to get sensitivities of the order of 5×10^{-10} watts of power at time constants of the order of 0.5 millisec with the superconducting bolometer. Undoubtedly, this type of detector is the most sensitive infrared detector available but its operation must, of course, be accompanied by the equipment necessary to maintain the bolometer at the extremely low temperature. While heretofore this has been rather bulky and cumbersome in so far as portability is concerned, a very compact and portable cryostat has recently been developed.

Pneumatic. The Golay heat cell (2, 3) is an infrared detector which depends for its action upon the expansion of the gas enclosed in a small chamber, due to the heating action caused by the absorption of radiant energy. This detector, developed at the Evans Signal Corps Laboratory, Belmar, N. J., is the type used to obtain the data reported in this paper and will be discussed more in detail later. Sensitivities of the order of 10^{-8} watts of power at time constants of the order of 0.5 to 1 millisec can be obtained with this type of detector.

Another factor to be considered in infrared detectors is their spectral response. The pneumatic detector and the superconducting bolometer have very nearly gray body absorption characteristics, while ordinary thermistors and bolometers as well as thermoelectric detectors may have a spectral region in which their response is poor.

Photoconductive Cells. It has been found that certain materials when exposed to infrared radiation, undergo what might be termed an internal photoelectric effect, in that electrons are liberated and will flow as an electric current if a potential difference is maintained in the vicinity. Two materials known for their ability to produce such an effect are thallium sulphide and lead sulphide. An infrared detector may be realized by allowing radiation to fall on a film of one of these materials across which a potential gradient is developed by means of a gridwork of terminals. The principal disadvantage connected with the use of photoconductive materials as infrared detectors is that they are only sensitive in the near infrared region. For example, the peak response of thallium sulphide is at 0.95 μ and its sensitivity is practically zero beyond 1.45 μ. Lead sulphide has corresponding values of 2.5 μ and 3.6 μ. The development work in this country on materials of this type was largely that conducted at Northwestern University by Prof. R. J. Cashman (4).

Some other possibilities which have been considered for infrared detection but which have not received very extensive application as yet are as follows:

Photoelectric Fatigue. It is known that, when certain types of photoelectric cells are exposed to ultraviolet radiation, the photoelectric current builds up practically instantaneously but, with continued application of the ultraviolet source, the photoelectric current decays due to a phenomenon known as photoelectric fatigue, which may result from an internal space-charge effect. If the photoelectric surface is exposed to infrared radiation after a short period of time, during which the fatigue effect has been allowed to take effect, the photoelectric current suddenly increases again to near its former peak value. The peak developed as a result of radiation with infrared energy could possibly be used as a quantitative measurement of the intensity of the infrared source.

Photoelectric Effect of Adsorbed Alkali Metals. Another possible means of infrared detection, utilizing a photoelectric effect, is to take advantage of the fact that impure sodium chloride crystals which have been exposed to x rays develop rather peculiar properties. Due to the action of the x rays neutral sodium atoms tend to be produced and adsorbed at the internal surfaces. The internal surfaces are necessary as the phenomenon will not take place in a single crystal, but only in an impure crystal with internal surfaces. Now, if a potential is placed across the previously x-irradiated crystal, and it is exposed to light of wave length 4650 Å for sodium chloride, the neutral sodium atoms tend to lose electrons which begin to flow and produce an electric current. However, if the crystal is further irradiated with this light, a fatigue effect somewhat similar to that just described takes place and the current drops off. When the light is turned off, the current drops to a very small but rather constant value, and the crystal is then in a condition to act as an infrared detector. If the crystal is suddenly exposed to infrared radiation, the photoelectric current rises almost instantaneously to a peak and then decays. As before, it is possible that the height of this peak could be used as quantitative measurement of the intensity of the infrared source. Subsequent to irradiation with infrared energy, the crystal assumes the state wherein the adsorbed neutral sodium atoms are again ready for the irradiation with the 4650 Å light. Occasionally it would be necessary to recharge the crystal by the use of x rays.

Phosphors. If certain infrared sensitive phosphors such as CaS, BaS, or ZnS, containing specified amounts of impurities such as Bi, Cu, CaF_2, Li_3PO_4, $Na_2B_4O_7$, or Na_2SO_4, are exposed to ultraviolet radiation, visible light is emitted which could be focused upon a photoelectric cell and measured quantitatively. If the ultraviolet source is turned off, the visible light intensity gradually decays. If, however, a short time after the decay process has begun, the phosphor is exposed to infrared radiation, the visible intensity almost instantaneously increases again to the former maximum level. A quantitative evaluation of this secondary increase due to exposure to infrared radiation might be possible.

It is realized that the theoretical limit to infrared detection by the foregoing means (photoelectric effects, phosphors) is the condition where the energy of an individual photon, corresponding to the frequency of the radiation, is of the same order of magnitude as the energy of motion of the molecules of the material itself. It remains to be determined whether, for the methods of detection just described, this condition will prevail at wave lengths longer than, say, ten microns.

Evaporation and Sublimation. Various techniques come under this general heading. If a thin layer of oil or other material is exposed to an infrared source, the evaporation of a small amount of material causes variations in thickness which could be detected interferometrically. Another possibility is the use of materials which sublime readily. For example, consider a parallel light beam (possibly monochromatic) directed at grazing incidence past the surface of a readily sublimed material to a photoelectric cell. If the surface were exposed to infrared radiation, the increased sublimation could possibly be detected as, (*a*) attenuation of the photoelectric signal due to increased absorption of the light, (*b*) attenuation of the photoelectric signal due to a difference in refraction of the light beam, or (*c*) an interferometric effect using monochromatic light directed on both sides of the sublimator, only one side being exposed to the infrared radiation.

These are only some of the more promising possibilities which should be considered in the search for more efficient methods of infrared detection.

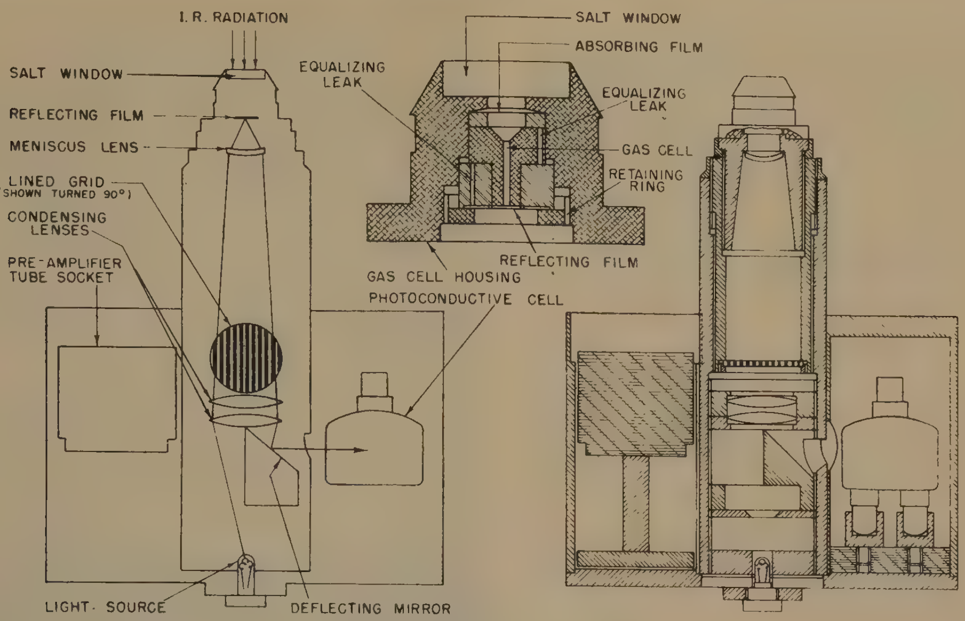

Fig. 1 Photothermal Detector
(Optical system and assembly.)

Pneumatic Detector Selected for Studies

The nature of the work in infrared detection at The Franklin stitute made it necessary to have a detector with high sensiity and fast response time. Also, there was a need for portabil- and a fair degree of ruggedness. Thermocouples and thermoes were considered but eliminated owing to their slow response ne. The cryostat bolometer, from the standpoint of fast reonse time and high sensitivity would have been ideal, but, ce later developments were to include a number of detectors, vas felt that the operation of a spectrograph using a number of supercooled bolometers would run into excessive complexity. e field having been narrowed to room temperature bolometers thermistors) and the Golay pneumatic detector, the pneutic detector was chosen, mainly for two reasons: (*a*) the disvantage of the somewhat complex optical system associated h the pneumatic detector was overbalanced by the somewhat perior sensitivity-response time characteristics, (*b*) the experie gained by Signal Corps personnel in development work on the eumatic detectors was available.

The essential characteristics of the operation of the pneumatic ector may be understood by reference to Fig. 1.

The following is only a brief explanation of the operation of the ector, presented for the convenience of the reader. A deled description of the theory of the pneumatic detector is given the literature by Dr. Golay (2, 3). The infrared radiation sses through a halide (usually sodium chloride) window and kes an aluminized film which forms the closure for one end of iny gas cell. The transmission-absorption characteristics of s film must, of course, be carefully maintained to the proper ue. Energy absorbed or transmitted by the aluminum film is nsferred to the gas in the cell, thus causing a rise in the temature and pressure of the gas. As a result, there is a dilation n antimony film which forms the closure for the other end of gas cell. A path is provided for gas leakage around the coment parts forming the gas cell, and the impedance to the flow gas can be varied. This adjustment has much to do with the sitivity of the detector. The dilation of the antimony film is ected and evaluated by means of an optical system which inporates a lined grid to provide light modulation to a light-senve cell. The antimony film acts as a mirror. Light from a small filament passes through one half of a pair of condensing lenses which focuses the light on the antimony film forming one end of the gas cell. Immediately after leaving the second condensing lens, the light passes through the top half of a lined grid, consisting of alternate transparent and opaque lines. A small meniscus lens placed near the antimony film causes an image of the top half of the grid to be formed on the lower half of the grid after reflection from the antimony film.

Thus, with quiescent conditions, and the proper positioning of the grid and lenses, a minimum amount of light passes through the lower half of the grid to the light-sensitive cell. Theoretically, no light would pass through if the image of the opaque spaces on the top half of the grid were formed on the transparent spaces of the bottom half of the grid. Reception of infrared energy and the resultant dilation of the antimony mirror causes a shift in the position and dimensions of the grid image with the result that some light passes through the lower half of the grid to the light-sensitive cell.

The light-sensitive cell used was a thallium-sulphide photoconductive cell, which has been found to have a higher signal-to-noise ratio than ordinary phototubes or photomultipliers, for the degree of light intensity used in this application. The reception of increasing amounts of energy causes larger signals up to a certain point when more energy results in the passage of less light through the grid combination and a decreased signal results. However, at low energy levels, the response is linear.

A detector of the type described was used in conjunction with a special low-dispersion monochromator, the schematic diagram of which is shown in Fig. 2. The two small sections of the same large parabolic mirror, used, respectively, for collimation M_1, and focusing M_4, are essentially equivalent to two small off-axis parabolic mirrors. The radiation enters slit S_1 and strikes parabolic mirror M_1. From there parallel rays travel to the 60-deg prism of sodium chloride. The prism and mirror M_2 are arranged according to the Wadsworth type of mounting, wherein the rays that pass through the prism at the angle of minimum deviation are reflected from plane mirror M_2, at an angle to the rays incident to the prism-mirror combination of twice the angle θ between the perpendicular to the prism base and a line parallel to the face of M_2.

Hence for this monochromator, the total deviation of the rays which pass through the prism at minimum deviation is 90 deg. From M_2, parallel rays strike plane mirror M_3, and are again deviated through 90 deg to mirror M_4, which would ordinarily focus them at S_1, but plane mirror M_5 is interposed in their path to deflect the rays through slit S_2 which is mounted on the pneumatic detector.

The electronic signal obtained from the light-sensitive cell of the detector is amplified and fed to an oscilloscope where it is photographed. Due to the low dispersion of the monochromator, accurate calibration was somewhat of a problem. The calibration in the visible region was made accurate, by means of a photographic plate of the mercury-arc spectrum. The atmospheric water vapor and carbon dioxide frequencies in absorption were taken as 2350 cm^{-1} and 3750 cm^{-1}, respectively. These data in combination with refractive index data from the literature and check points from a variable-temperature oxidized brass surface heater gave a calibration which is believed accurate to ±0.05 micron.

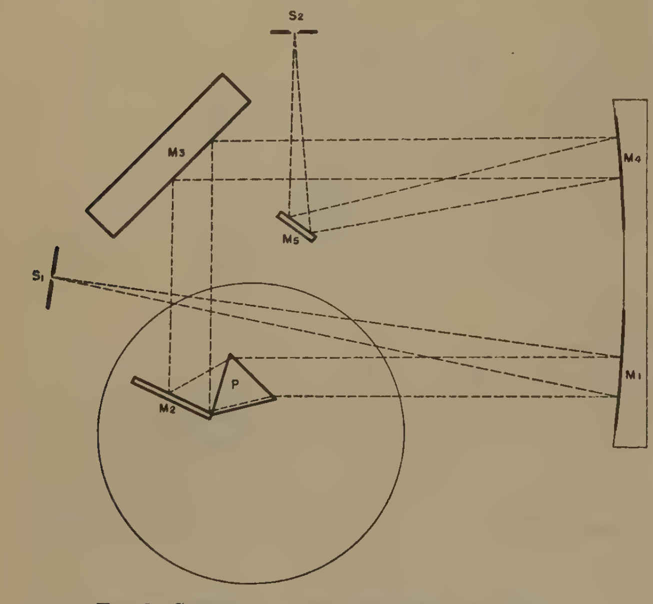

Fig. 2 Schematic Diagram of Monochromator

Use of Low-Dispersion Monochromator and Pneumat Detector

The use of this low-dispersion monochromator with the pne matic detector permits the determination of the spectral distrib tion of phenomena existing for very short intervals of time (the order of a few milliseconds) or the determination of the spe tral distribution, as a function of time, for phenomena existing f longer periods of time. A study of the latter type has been ca ried out and will be described.

A methane-air mixture containing approximately 8 per ce methane was ignited by means of a spark in a bomb, the cro section of which is shown in Fig. 3. The procedure for the fillin and exhausting of the bomb was as follows: Subsequent to a explosion, the valve to the vacuum pump was opened and th products of combustion pumped out until the pressure in th bomb was approximately 1 in. Hg. Then the atmosphere valv was opened and atmospheric air allowed to fill the bomb. Th atmosphere valve was closed and the bomb again pumped out t a pressure of 1 in. Hg. The valve to the methane tank was the opened and methane was allowed to flow in until the pressure rise as indicated by a mercury manometer, was 6.1 cm Hg. On th basis of barometric pressure of 30 in. Hg or 76.2 cm Hg, a partia pressure of methane of 6.1 cm would give approximately an 8 pe cent by volume mixture. After the bomb had received the charge of methane, the methane valve was closed and the atmosphere valve opened wide to allow the air to rush in and mix with the methane. A period of approximately 2 min was allowed fo mixing and partial quieting of the turbulent conditions caused by the entrance of air into the tank.

On the basis of the foregoing procedure, the amount of previous products of combustion in the freshly prepared charge should not exceed $^1/_{900}$ or 0.11 per cent of the total mixture. It is realized that the real percentage composition of the mixture, as prepared, depended upon the existing barometric pressure and upon the validity of Dalton's law of partial pressures. No attempts were made to control to a fine degree the composition of the mixture in these first experiments which were more or less of an exploratory nature.

After the bomb had been filled with the combustible mixture, the shutter was set in motion to intercept, at intervals, the radiation emitted from the burning gas through the sodium chloride window. The monochromator was adjusted to the desired wave length and the spark ignited. The sweep circuit of the oscilloscope was set in motion simultaneously, and a short time-delay relay allowed the sweep to travel a short distance before the

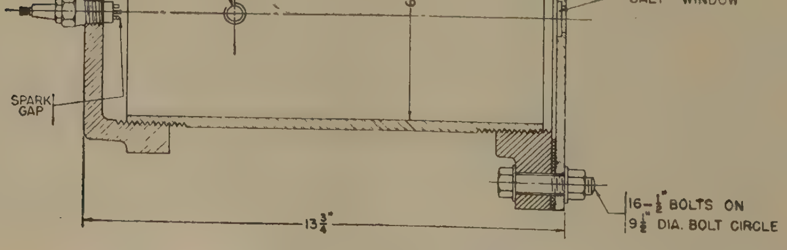

Fig. 3 Combustion Bomb

park was ignited. With the ignition of the spark, the com- ustion process began, and the energy emitted from the reac- ion at a given wave length, as chosen by the monochromator, was ent to the gas cell of the pneumatic detector. The detector was djusted for high sensitivity and the time required to reach 63 er cent of the maximum signal was approximately 7 millisec. he shutter was arranged for equal off and on times of 17.35/2 illisec. This was the most convenient value, as dictated by the evolutions per minute of the motor used to drive the shutter. hus it was possible to obtain time slices of the energy intensity t a given wave length at intervals of 17.35 millisec. The entire rocess was repeated for a series of wave lengths, 65 different ave lengths being taken in the spectral region from 1 micron to 1 microns.

Measurements by Oscilloscope

A typical oscilloscope trace is shown in Fig. 4. This trace was btained by a simple time exposure during the combustion. The ace, as shown in Fig. 4, traveled from left to right, the first ownward streak from the left being caused by the ignition of e spark. The maxima and minima of the trace tended equalize around a centralized base line which itself tended to ift, depending upon the strength of the signal. The actual in- nsity, at a given time was obtained by measuring the distance ertically downward from a maximum to the line joining the o minima on either side of the maximum being measured. It n readily be seen in Fig. 4, how this distance builds up and ecreases with time. The distance in time from successive max- na or minima was 17.35 millisec. It will be noticed in Fig. 4, at the peaks get closer together as they progress toward the d of the trace. This was done purposely by using a logarith- ic horizontal sweep. This arrangement allowed the peaks to spread more at the beginning of the combustion, where it was sired to determine the position of the first few peaks accu- tely with relation to the spark. Energy from the combustion ocess was detected visually for a time lasting from 1 to 1.5 sec.

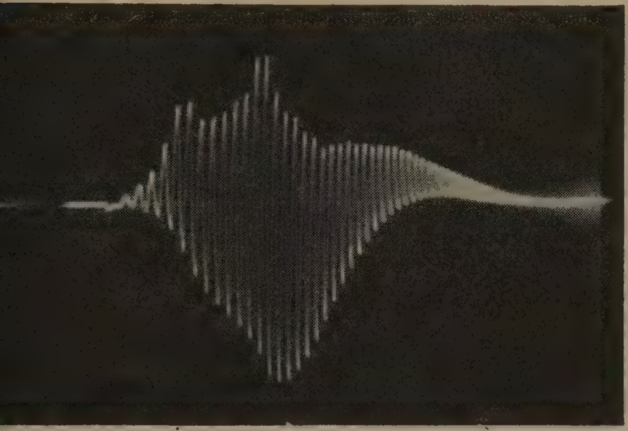

Fig. 4 Typical Oscillogram

By evaluating the traces as indicated, curves such as those own in Fig. 5, were obtained. These curves are for wave ngths of 1.0, 2.7, 4.5, and 10.0 microns, respectively. The attering of points in the case of 1 and 10 is due to the fact that e detector is being operated in the region where its rather low- equency noise level has been reached. Sixty-cycle pickup was nsidered, but the basic frequency of the noise indicated is ap- oximately 30 cycles. The attenuation necessary to represent four of these curves on a single chart is indicated.

Several peculiar properties of these curves must be discussed.

It will be noticed that there is a small intensity peak in the vicinity of 90 millisec on all the curves. This small peak was present at every wave length, but it is yet to be determined whether it is due to a phenomenon caused by the combustion process or the geometry of the bomb itself. Later tests to be conducted with different-shaped bombs and a correlation with pressure should clarify this point.

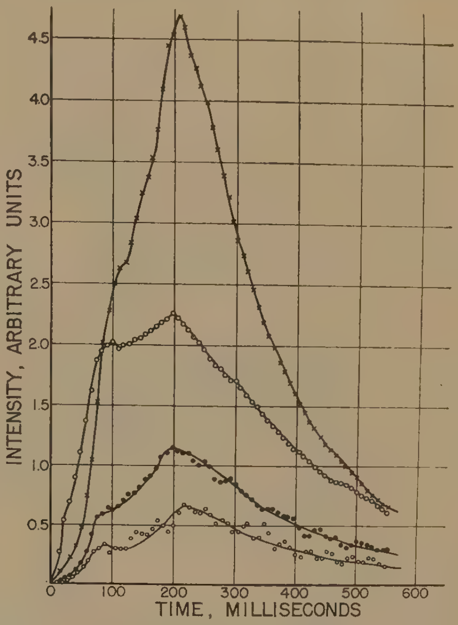

Fig. 5 Intensity as a Function of Time for Various Wave Lengths

° = 1.0 μ, ordinates × 1 (bottom curve)
× = 2.7 μ, ordinates × .05
° = 4.5 μ, ordinates × .05
● = 10.0 μ, ordinates × 1.1

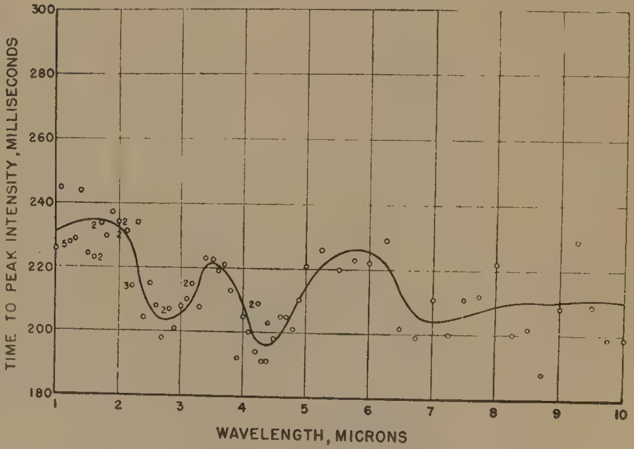

Fig. 6 Variation of Time to Peak Intensity

The next point to be considered is that the time to reach the main peak of intensity is different for the various wave lengths. Variations in the mixture prior to the combustion could contribute to this inconsistency, but an examination of the curve shown in Fig. 6 reveals some interesting data relative to this point. In Figs. 7 and 8 it can be seen that there are pronounced emission peaks in the vicinity of 2.8 and 4.5 microns, and a broad peak in the vicinity of 6.75 microns. In Fig. 6 it can be seen that the time to reach the peak intensity tends to be lower in these same spectral regions.

Figs. 7 and 8 represent spectral intensity as a function of time

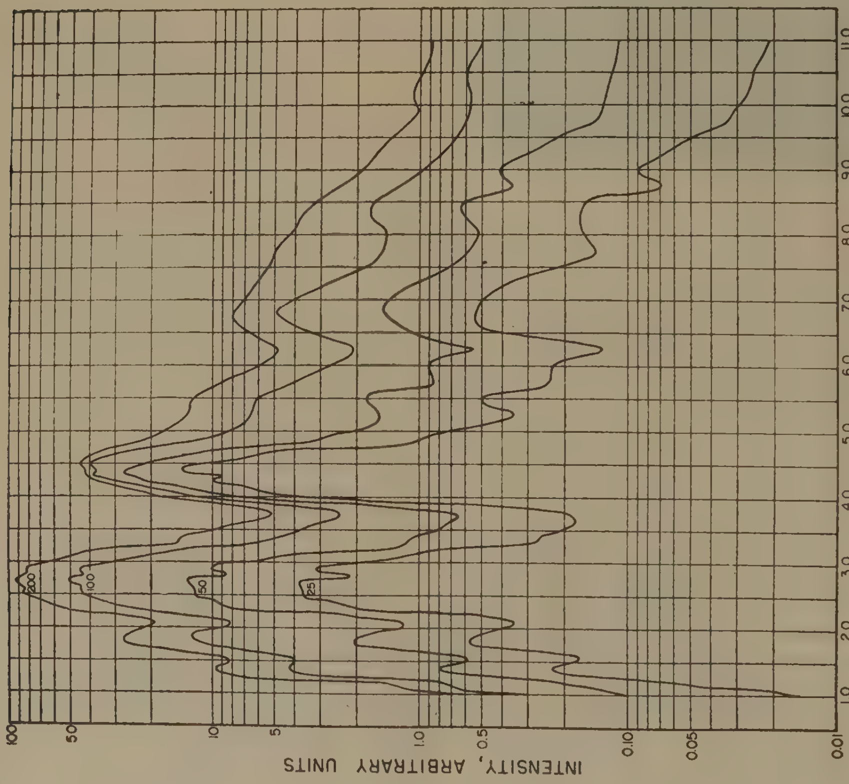

Fig. 7 Spectral Distribution of Radiation From 8 Per Cent Methane Combustion From 25 to 200 Milliseconds

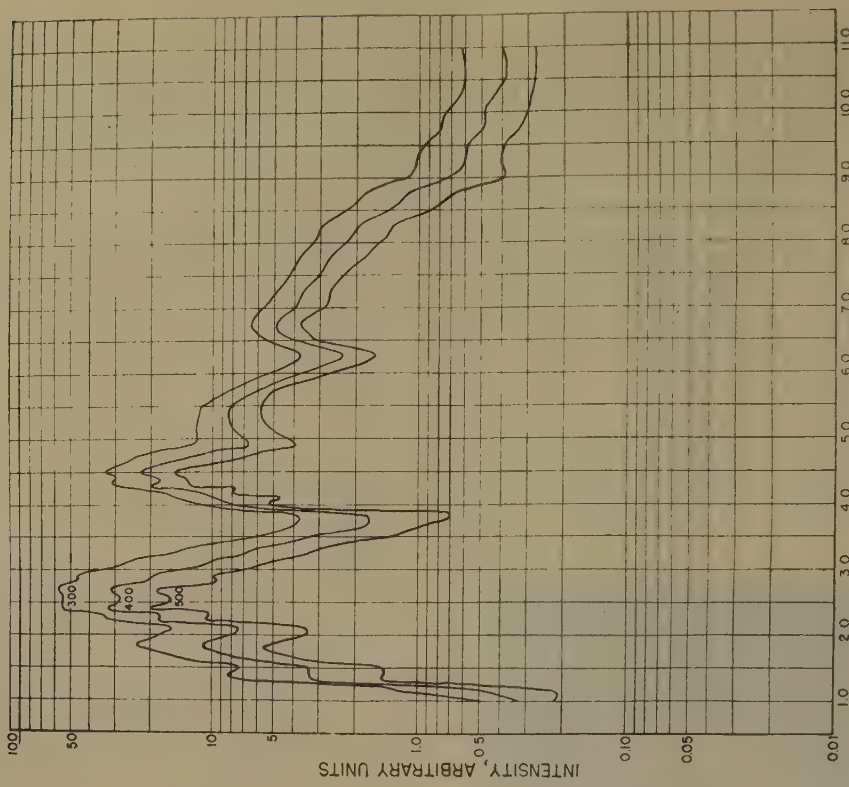

Fig. 8 Spectral Distribution of Radiation From 8 Per Cent Methane Combustion From 300 to 500 Milliseconds

r the radiation emitted during the combustion process. In g. 7, progressing upward, the successive curves are for times 25, 50, 100, and 200 millisec. The curves in Fig. 8 are, ogressing downward, for times of 300, 400, and 500 milliconds. In preparing the curves in Figs. 7 and 8, from the pe of curves shown in Fig. 5, it was necessary to determine the ost probable time for the peak intensity to be reached for a ven wave length. Undoubtedly, there would be some variion in this time from trial to trial at a given wave length, so at, since for most wave lengths in these experiments only one al was made, there is some doubt as to whether the time to ak intensity for that particular trial would be exactly the lue which would be obtained for an average of, say, ten trials. nerefore the curve shown in Fig. 6 was used to determine the ost probable time to peak intensity for a given wave length, and e times as measured were corrected to this most probable time. is felt that this procedure would result in a more reasonable esentation of the curves shown in Figs. 7 and 8. The curves in gs. 7 and 8 are drawn with the intensity ordinate on a logahmic scale. This was necessary because of the large range of tensities covered. The curves as presented are not corrected r the overlapping effect, due to the use of a fairly wide slit of 0 μ.

The complete analysis of the curves requires considerable time d will be presented in a later paper. However, the following marks apply to the curves as presented: At 25 millisec there e well-defined emission peaks at 1.42 and 1.80 microns, two broad aks covering the range 2.4–2.9 μ and 4.1–4.6 μ, and other aks at 5.5 μ, 6.0 μ, and 6.75 μ. There are irregularities, alost completely masked, in the range 3.2–3.7μ. Methane is own to have a band in this region so that the minimum in the cinity of 3.3 μ in the early stages of the combustion may be abrption by unburned methane. The development of these aks can be followed with time. The rather complicated structre of the 2.4–2.9 μ and 4.1–4.6 μ bands is probably somewhat due self-absorption. The OH radical is known to have a fundaental frequency corresponding to a wave number of 3570 cm^{-1}, a wave length of 2.8 microns. A well-defined minimum at 2.8 μ n be seen at 25 millisec. This minimum grows less pronounced to a time of 200 millisec, but becomes slightly more prounced at later times. The complete time analysis of the specl distribution could not be satisfactorily reproduced in Figs. 7 d 8. Only those curves corresponding to the times indicated uld be presented.

Discussion of Tests

The primary purpose in conducting the methane combustion s to examine the feasibility of using the data obtained for the termination of the prevailing temperature of the combustion ocess as a function of time. There is considerable difference of inion as to whether the characteristic radiation emitted by ated polyatomic molecules (for example, the water-vapor and rbon dioxide molecules at 2.7 and 4.5 microns) is of a thermal or a chemiluminescent nature. If the radiation is of a thermal ture, a determination of spectral brightness and emissivity at y two wave lengths should give the proper temperature with e application of the established radiation laws. Experiments this nature, using the wave length 2.7 and 4.4 microns were rried out by Schmidt (5) and are discussed in the text by Lewis d von Elbe (6).

Another view of the problem is given by Gaydon in his text (7). can be seen in Figs. 7 and 8, that the existence of the charteristic radiation emission peaks (assuming the radiation is of hermal nature) results in an effectively higher emissivity in se spectral regions. It will be noticed also that the relative ensity of the emission peak near 2.7 μ, as compared to the peak at 4.5 μ, tends to increase at the beginning of the combustion process and decrease near the end of the time for which the process was analyzed. The ratio of the intensity of the peak at 2.7 μ to that of the peak at 4.5 μ is plotted in Fig. 9, as a function of time. It will be noted that the peak ratio is reached near a time corresponding to the time in Fig. 5 for which the peak intensity for the radiation at various wave lengths is a maximum.

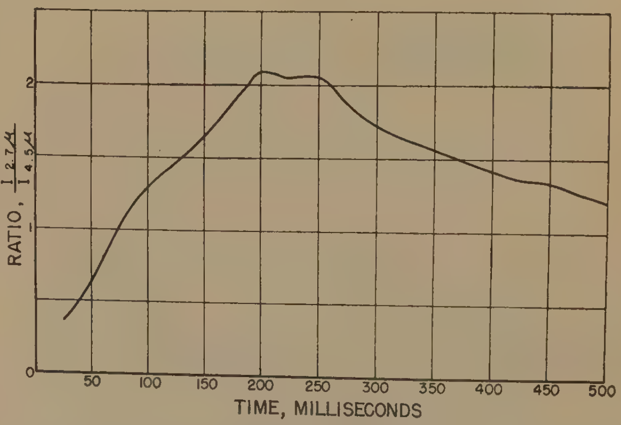

Fig. 9 Relative Intensities of Bands at 2.7 μ and 4.5 μ as a Function of Time for 8 Per Cent Methane in Air Spark-Ignited Combustion

Mixture strength and moisture content are known to have considerable influence upon the ratio of intensities of the bands at 2.7 μ and 4.5 μ, but the effect of temperature undoubtedly is of primary importance, the band at 2.7μ probably being favored at higher temperatures (see ref. (7), chapter X). There are two phenomena present in the data which might lead to a clearer understanding of the nature of the radiation from combustion processes similar to the one studied. One of these is to be seen in Fig. 5. Subsequent to the first discontinuity in the vicinity of 90 millisec, the rate of increase of intensity at 4.5 μ is much slower than that at 2.7 μ and also much slower than the rate of increase of intensity prior to the discontinuity near 90 millisec. The other phenomenon is the effect previously referred to and illustrated in Fig. 6, namely, that the peak intensity at wave lengths where strong emission is present is reached sooner than at wave lengths where none of the characteristic radiation exists. Further study of these two effects may furnish information relative to thermal-equilibrium conditions during the combustion.

On the strength of two very broad assumptions, (*a*) that the radiation of 2.7 μ and 4.5 μ is purely of a thermal nature (no chemiluminescence), and (*b*) that the source giving rise to the radiation can be treated as a gray radiator at these wave lengths, it is possible to calculate the temperature for the combustion process as a function of time. This can be done by finding the value of T which satisfies the following equation

$$\frac{I_{2.7}}{I_{4.5}} = \frac{(4.5)^5}{(2.7)^5}\,\frac{e^{\frac{14320}{4.5T}} - 1}{e^{\frac{14320}{2.7T}} - 1}$$

By carrying out such a calculation, the results shown in Table 1 were obtained. The low values of temperature undoubtedly were due to the fact that factors other than temperature, such as total mass and relative proportions of the radiating components, have considerable influence on the ratio of the bands at 2.7 μ and 4.5 μ. However, the fact that the maximum temperature, as calculated, was reached at a time corresponding to the peak intensity at all the spectral wave lengths, is not to be overlooked.

TABLE 1 TEMPERATURE CALCULATIONS FOR 8 PER CENT METHANE IN AIR SPARK-IGNITED COMBUSTION

RATIO, $\frac{I_{2.7\mu}}{I_{4.5\mu}}$	TIME, ms	T, °K	T, °C
0.367	25	600	327
0.633	50	708	435
1.012	75	842	569
1.280	100	935	662
1.448	125	989	716
1.613	150	1053	780
1.852	175	1132	859
2.080	200	1205	932
2.044	225	1195	922
2.043	250	1200	927
1.864	275	1140	867
1.705	300	1080	807
1.630	325	1051	778
1.544	350	1025	752
1.481	375	998	725
1.415	400	975	702
1.366	425	953	680
1.331	450	948	675
1.243	475	925	652
1.206	500	900	627

CONCLUSION

The primary purpose of this paper was to indicate what can be done in this field with the equipment developed. Further work will be carried out, of a more precise nature, with a large-aperture infrared spectrograph, utilizing a bank of ten photothermal detectors. This unit will be capable of determining the spectral intensity, as a function of time, simultaneously at ten different wave lengths. Further experiments will be directed toward a true determination of the temperature as a function of time, the incorporation of a pressure gage to determine pressure as a function of time, the effect of type and exposed area of surface, and other effects.

ACKNOWLEDGMENTS

The author wishes to express his deep appreciation to Miss Lois Leach, Technical Assistant, Franklin Institute Research Laboratories, for her invaluable assistance in conducting the experiments and evaluating the results. Special thanks are also due to Miss Rachel Franklin, Research Physicist, for her many valuable suggestions and time spent in discussing the results. The work would have been prolonged indefinitely without the timely assistance of the following, all employed in the Research Laboratories of the Franklin Institute: Mr. Robert Benn, Mr. Howard Warshaw, Mr. William Foote, Mr. Ami Berkowitz, and Mr. Albert Bazarian.

BIBLIOGRAPHY

1 "The Design and Construction of Rapid Response Thermocouples for Use as Radiation Detectors in Infrared Spectrographs," by L. C. Roess and E. N. Dacus, *Review of Scientific Instruments*, vol. 16, July, 1945, pp. 165–172.

2 "Theoretical Consideration in Heat and Infrared Dete With Particular Reference to the Pneumatic Detector," by M. Golay, *Review of Scientific Instruments*, vol. 18, May, 1947, pp. 356.

3 "A Pneumatic Infrared Detector," by M. J. E. Golay, *R of Scientific Instruments*, vol. 18, May, 1947, pp. 357–362.

4 "Development of Stable Thallous Sulfide Photocondu Cells for Detection of Near Infrared Radiation," OSRD Re Department of Physics, Northwestern University, Oct. 31, 1945

5 "Prüfung der Strahlungsgesetze der Bunsenflamme," b Schmidt, *Annalen der Physik*, vol. 29, 1909, p. 1027.

6 "Combustion Flames and Explosions of Gases," by B. L and G. von Elbe, The Macmillan Company, New York, N. Y., 19

7 "Spectroscopy and Combustion Theory," by A. G. Gay Chapman and Hall, Ltd., 1942.

Discussion

F. B. Downing.[3] The author's analysis of energy releas the combustion of methane introduces a quantitative spectral proach to combustion processes which promises to elucidate portant steps in the kinetics of flame propagation and explosi The wealth of literature on combustion research is a sound in of the importance of combustion to science and civilization, bu is also a confession of the complexity of the subject and the n for new and simplifying methods of scientific approach. T chemical engineer, the development of techniques for establish the kinetics of combustion is important not only for improvi the efficiency of power generation, but for directing the process valuable chemical products.

Application of the Golay pneumatic detector to this resear takes advantage of the high sensitivity and rapid response of t gas cell. However, it is believed the Society is particularly fo tunate in having the practical experience and knowledge of co struction and assembly of the detectors coincide with the com bustion research. More rapid and successful development ca be anticipated, since here full knowledge of the advantages an limitations of the instrumentation will be applied simultaneous with the planning of experiments and the interpretation of data.

The General Engineering Branch, Signal Corps, is to be congra ulated for sponsoring this project and for releasing this introdu tory review of the equipment and method of attack.

AUTHOR'S CLOSURE

In Figs. 7 and 8 it will be noticed in connection with the ban at 4.5 μ that the long tail on the long-wave-length side is present This long tail was a subject of considerable discussion at the re cent Symposium on Combustion, Flame, and Explosion Phenom ena held at the University of Wisconsin during the week of Sep tember 6. Papers presented by Shirleigh Silverman, of the Ap plied Physics Laboratory, Johns Hopkins University, and G. B B. M. Sutherland, Pembroke College, University of Cambridge indicated some interesting possibilities in connection with temperature determinations by the use of the radiation from carbo dioxide on the long-wave-length side of the 4.3 band. This matter will be discussed further in subsequent papers.

---

[3] Assistant Director, Jackson Laboratory, E. I. du Pont de Nemours & Company, Wilmington, Del.

Performance Criteria for Positive-Displacement Pumps and Fluid Motors

By W. E. WILSON,[1] RAPID CITY, S. DAK.

**The comparison of performance characteristics of posi-
e-displacement pumps and fluid motors on the basis
dimensionless performance coefficients and dimension-
s efficiency curves is presented as a substitute for the
esent methods. It is shown that the coefficients describe
rformance adequately and are subject to significant
erpretation in terms of the geometry of the unit. The
nensionless efficiency curve is shown to have advantages
presenting a wide range of data and in prediction of per-
mance characteristics under any specified operating
nditions.**

Introduction

THE general confusion with regard to methods of presenting positive-displacement-pump and motor performance data with particular reference to lack of agreement in definition
terms led to the preparation of the method of performance-
a analysis and comparison described in this paper. Clarifica-
n of definitions of efficiencies, and the introduction of coeffi-
nts of performance and their definitions are attempted in order
provide a logical and adequate means of describing perform-
ce.

Performance Equations

The performance of a pump can be described in terms of two
ple equations (1),[2] one of which expresses the delivery and
other the torque as a function of the pertinent variables.
ese equations are

$$Q = Dn - \frac{c_s D \Delta P}{2\pi\mu} - Q_r \ldots\ldots\ldots\ldots\ldots\ldots\ldots [1]$$

$$T = \frac{\Delta p D}{2\pi} + c_d D\mu n + c_f \frac{D}{2\pi}\Delta p + T_c \ldots\ldots\ldots [2]$$

ere

= delivery in units of volume per unit time
= displacement in units of volume per revolution
= speed of rotation in revolutions per unit time
= coefficient of slip
= pressure differential across pump
= dynamic viscosity of the liquid
= loss in delivery due to cavitation in the neighborhood of the inlet
= torque required to drive the pump in units of force times distance
= viscous-drag coefficient
= dry-friction coefficient
T_c = frictional torque which is independent of speed and pressure

Similar equations can be written for a fluid motor, differing only in the signs of the terms after the first on the right-hand side of the equations. In all cases the system of units used must be consistent.

The power output P_{out} and power input P_{in} of the pump can be expressed directly from the equations for torque and delivery, making use of the basic relationships

$$P_{\text{out}} = Q\Delta p$$

$$P_{\text{in}} = 2\pi T n$$

The resulting equations for power are then

$$P_{\text{out}} = [Dn - c_s \frac{D}{2\pi}\,\frac{\Delta P}{\mu} - Q_r]\ \Delta P \ldots\ldots\ldots\ldots [3]$$

$$P_{\text{in}} = 2\pi\left[\Delta p \frac{D}{2\pi} + c_d D\mu n + c_f \frac{D}{2\pi}\Delta p + T_c\right] n \ldots [4]$$

The ideal power P_i of the pump is given by

$$P_i = \Delta p D n$$

The power output and power input can be written in terms of the ideal power thus

$$P_{\text{out}} = P_i\left[1 - c_s \frac{\Delta p}{2\pi\mu n} - \frac{Q_r}{Dn}\right] \ldots\ldots\ldots\ldots\ldots [5]$$

$$P_{\text{in}} = P_i\left[1 + c_d \frac{2\pi\mu n}{\Delta p} + c_f + \frac{2\pi}{D}\,\frac{T_c}{\Delta p}\right] \ldots\ldots\ldots [6]$$

It is obvious that the power output is always less than the ideal power and the power input is always greater than the ideal.

Efficiency can be defined in a general manner as the ratio between an ideal and an actual quantity. This leads to the distinguishing of three different efficiencies, namely, volumetric efficiency, torque efficiency, and over-all efficiency.

The volumetric efficiency η_v is the ratio between the actual delivery and the ideal delivery, thus

$$\eta_v = \frac{Dn - c_s\, D/2\pi\ \Delta p/\mu - Q_r}{Dn}$$

or

$$\eta_v = 1 - c_s \frac{\Delta p}{2\pi\mu n} - \frac{Q_r}{Dn} \ldots\ldots\ldots\ldots\ldots [7]$$

In a similar manner the torque efficiency η_T is defined as the ratio between ideal torque and actual torque, thus

$$\left.\begin{aligned} \eta_T &= \frac{\Delta p\ D/2\pi}{\Delta p\ D/2\pi + c_d D\mu n + c_f\ \Delta p\ D/2\pi + T_c} \\ \text{or} \\ \eta_T &= \frac{1}{1 + c_d \dfrac{2\pi\mu n}{\Delta p} + c_f + \dfrac{2\pi}{D}\,\dfrac{T_c}{\Delta p}} \end{aligned}\right\} \ldots [8]$$

President, South Dakota School of Mines and Technology;
nerly Pump Division, Sundstrand Machine Tool Co. Mem.
ME.

Numbers in parentheses refer to the Bibliography at the end of
paper.

ontributed by the Hydraulic Division and presented at the
ni-Annual Meeting, Milwaukee, Wis., May 30–June 5, 1948, of
AMERICAN SOCIETY OF MECHANICAL ENGINEERS.

OTE: Statements and opinions advanced in papers are to be
erstood as individual expressions of their authors and not those
he Society. Paper No. 48—SA-14.

The over-all efficiency η of the pump is defined as the ratio of power output to power input which is expressed, from Equations [5] and [6] thus

$$\eta = \frac{1 - c_s \dfrac{\Delta p}{2\pi\mu n} - \dfrac{Q_r}{Dn}}{1 + c_d \dfrac{2\pi\mu n}{\Delta p} + c_f + \dfrac{2\pi}{D}\dfrac{T_c}{\Delta p}} \qquad [9]$$

It can be demonstrated readily that the over-all efficiency is the product of volumetric and torque efficiencies

$$\eta = \eta_v \eta_T \qquad [10]$$

The maximum efficiency which can be obtained with any particular pump is determined by the equation for over-all efficiency, and is expressed in a very simple and significant form when certain assumptions concerning relative magnitudes of terms are made. If one assumes that Q_r and T_c are zero, the efficiency Equation [9] can be written in the following form

$$\eta = \frac{1 - c_s \dfrac{\Delta p}{2\pi\mu n}}{1 + c_d \dfrac{2\pi\mu n}{\Delta p} + c_f} \qquad [11]$$

This equation is interesting from the standpoint that the efficiency is expressed in terms of the coefficients c_s, c_d, and c_f, and the dimensionless parameter $(2\pi\, \mu n)/(\Delta p)$ only, indicating that the maximum efficiency is a function of the coefficients only. The approximation made by neglecting T_c and Q_r is very frequently valid. In addition, the neglect of these terms provides an expression for efficiency which may be used as a guide, giving as it does a measure of the maximum efficiency attainable with the pump so long as the clearances are unchanged.

In order to obtain the expression for maximum efficiency, Equation [11] is differentiated with respect to the parameter $(\mu n)/(\Delta p)$, and the result set equal to zero, thus

$$\frac{d\eta}{d\left(\dfrac{\mu n}{\Delta p}\right)} = \frac{c_s/2\pi \left(\dfrac{\Delta p}{\mu n}\right)^2}{1 + c_d \dfrac{2\pi\mu n}{\Delta p} + c_f} - \frac{\left[1 - \dfrac{c_s}{2\pi}\left(\dfrac{\Delta p}{\mu n}\right)\right] c_d 2\pi}{\left(1 + c_d \dfrac{2\pi\mu n}{\Delta p} + c_f\right)^2} = 0$$

Solution of this equation for the critical value of $(\mu n)/(\Delta p)$ yields

$$\frac{\mu n}{\Delta p} = \frac{c_s}{2\pi}\left[1 + \sqrt{1 + \frac{1 + c_f}{c_s c_d}}\right] \qquad [12]$$

When this value of $(\mu n)/(\Delta p)$ is substituted in Equation [11] there results for maximum efficiency, $\eta_{\max}$, the expression

$$\eta_{\max} = \frac{1}{1 + c_f + 2c_s c_d \left[1 + \sqrt{1 + \dfrac{1 + c_f}{c_s c_d}}\right]} \qquad [13]$$

It is significant that the maximum efficiency is dependent upon the product of c_s and c_d and not upon the value of each individually. This makes possible the presentation of the maximum efficiency as function of the pump coefficients in the very simple manner indicated in Fig. 1.

Significance of Coefficients

The method of defining the coefficients c_s, c_d, and c_f requires that they be dimensionless numbers which can be shown to be ratios of lengths involved in the geometry of the pump or flui motor. Consideration of the slip coefficient and the gener equation for flow between parallel plates reveals that the sli coefficient can be represented by an equation in the followin manner: The general equation for slip flow, Q_s, between paralle plates is (1)

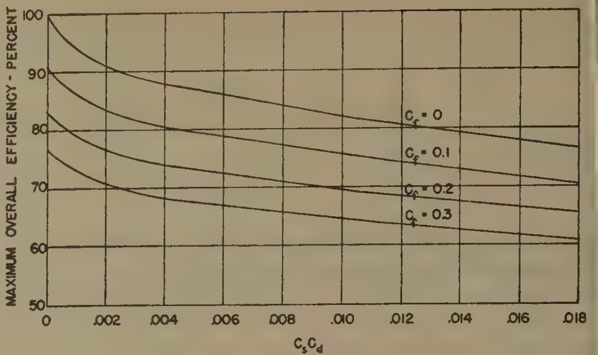

Fig. 1 Calculated Maximum Over-All Efficiency Positivi Displacement Pump

$$Q_s = \frac{\Delta p\, b\delta^3}{12\,\mu l}$$

where b is the width of the passage, l is the length, and δ is th perpendicular distance between the plates. Equating this to th second term of Equation [1], which is the slip

$$c_s = \frac{\pi}{6}\frac{b\delta^3}{lD}$$

The displacement is proportional to the product of the square o the rotor radius R and the length of the rotor L, hence

$$c_s \sim \frac{\delta^2}{R^2}\frac{\delta}{L}\frac{b}{l}$$

which indicates the general nature of this coefficient.

Since the coefficient of slip is a ratio of pertinent lengths in a pump or motor, it is descriptive of the effect of the geometry of the unit on the slip. A series of geometrically similar pumps would have identical slip coefficients, thus performing identically in so far as volumetric efficiency is concerned.

A similar demonstration shows that c_d, which is also a dimensionless coefficient, made up of geometrical ratios, identical for a homologous series of units, can be expressed

$$c_d \sim \frac{R}{\delta}\frac{b}{L}\frac{l}{R}$$

The coefficient c_f is a function of the coefficient of friction between contacting metals, the dimensions of the unit, and its elastic properties; hence would not be expected to be identical for a homologous series. However, it is dimensionless and is useful in comparing performance of pumps and motors with particular reference to wear characteristics.

The product of slip and drag coefficients $c_s c_d$ is significant as a measure of the excellence of the design from the standpoint of the proportioning of the clearances which exist between various elements of the pump or motor. It has been shown (4) that in the case of a simple vane pump there is an optimum clearance for operation at any particular value of the parameter $(\mu n)/(\Delta p)$. This demonstration may be extended to include all types of positive-displacement pumps and motors as will be shown.

In order to show that there is an optimum clearance for opera-

ı at a particular value of the parameter $(\mu n)/(\Delta p)$, the effi-
ıcy equation is investigated, making use of the relationship
ween the coefficients c_s and c_d and the clearance just developed.
this purpose these coefficients are expressed

$$c_s = c_s' \frac{\delta^3 b}{R^2 Ll}; \quad c_d = c_d' \frac{Rbl}{\delta LR}$$

ostitution of these quantities in the general efficiency Equation
] yields

$$\eta = \frac{1 - c_s'[(\delta^3 b)/(R^2 Ll)][(\Delta p)/(2\pi\mu n)]}{1 + c_d'\left(\frac{Rbl}{\delta LR}\right)[(2\pi\mu n)/(\Delta p)] + c_f} \quad \ldots\ldots [14]$$

e form of the equation indicates that for any given value of
$)/(\Delta p)$, there is a value of δ between zero and infinity which
es a maximum efficiency.

DETERMINATION OF COEFFICIENTS

The numerical value of the coefficients of the pump may be
ermined experimentally as will be outlined briefly. This pro-
lure has been discussed in greater detail elsewhere (2), and is
iewed here simply to provide ready reference.

The torque and delivery of the pump should be measured under
ıditions of constant liquid temperature at the pump intake, for
ious pressures and speeds. The data are best plotted as
wn in Fig. 2. The slope of the torque lines is $c_d D\mu$ as indi-
ed. The slope of the delivery lines is the displacement D.
owing μ, the value of c_d can be calculated.

The torque at zero speed is found by extending straight lines
ough the plotted points for torque versus speed at constant
essure. This yields values of torque which are independent
speed and equal therefore to the sum

$$T_c + c_f \,\Delta p \frac{D}{2\pi} + \Delta p \frac{D}{2\pi}$$

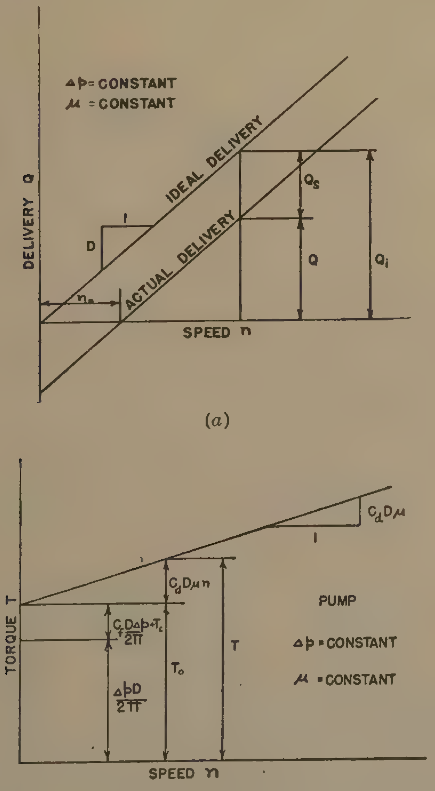

(a)

(b)

FIG. 2

The delivery at zero speed is determined in a similar manner. This delivery is negative and is the slip at the given pressure.

If the torque at zero speed and the slip are plotted as indicated in Fig. 3, the values of T_c and c_f, and c_s can be found as indicated. The slope of the torque line is

$$\frac{D}{2\pi}(1 + c_f)$$

the intercept on the vertical axis is T_c, and the slope of the slip-pressure line is $c_s(D/\mu)$. Since D and μ are known, c_f and c_s can be calculated.

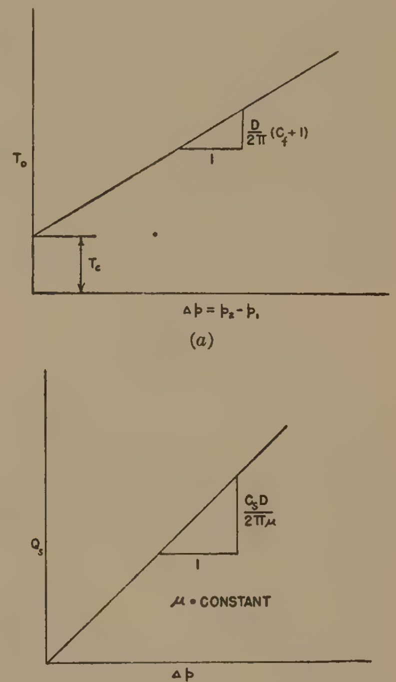

(a)

(b)

FIG. 3

EXPERIMENTAL RESULTS

In Table 1 are shown experimentally determined pump and motor coefficients which have been established by the procedure outlined. Pumps of several different manufacturers are included in the list. Most pumps were stock models, although some were in various stages of development. In no case were the pumps operated at a speed sufficiently high to indicate conclusively the magnitude of Q_r.

The value of the drag coefficient c_d is of the order of magnitude which one would expect from a consideration of the dimensions of pumps of the type under consideration. Calculated values of viscous torque indicate that the coefficient c_d will generally be of the order of magnitude of 10^4 to 10^5.

The slip coefficient in most cases is larger than would be expected from calculated values of slip. However, the coefficient is extremely sensitive to clearance values, being a function of the cube of the clearance (3). It is not subject to great accuracy of calculation since tolerances are relatively large compared to the clearance. In addition, heating of the liquid in slip passages, due to high rates of shear, results in a reduced viscosity and increased slip. This causes an experimental determination of a slip coeffi-

TABLE 1 PUMP AND MOTOR COEFFICIENTS

Hydraulic unit	D cu in./rev.	T_c in-lb	c_d	c_s	c_f	$c_s c_d$	Calc η_{max}
A Internal-gear pump	1.205	13	5.95×10^4	3.35×10^{-7}	0	0.0199	75.7
B Internal-gear pump	2.965	0	9.77×10^4	1.02×10^{-7}	0.0446	0.0100	79.0
C Spur-gear pump	2.965	0	10.25×10^4	0.48×10^{-7}	0.179	0.0050	74.3
D Vane pump	2.865	0	7.30×10^4	0.477×10^{-7}	0.212	0.00348	74.1
E Herringbone-gear pump	0.652	4	1.20×10^4	9.00×10^{-7}	0.200	0.0108	69.0
F Piston motor	2.060	7	22.9×10^4	...	0.067	...	..
G Piston motor	1.000	12	9.3×10^4	...	0.094	...	..
H Piston motor	3.365	17	6.46×10^4	...	0.0875	...	..
I Internal-gear pump	1.800	13	5.06×10^4	1.6×10^{-7}	0.075	0.0081	78.3
J Piston pump	3.600	0	16.8×10^4	0.15×10^{-7}	0.045	0.0020	87.0

$$\eta_{max} = \frac{1}{1 + c_f + 2c_s c_d \left[1 + \sqrt{\frac{1 + c_f}{c_s c_d}}\right]}$$

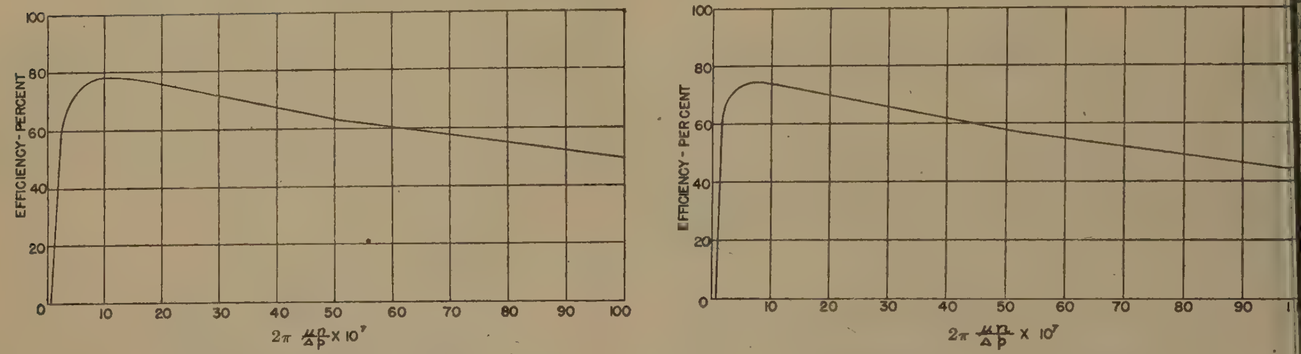

(*a*) Over-All Efficiency Pump B

(*b*) Over-All Efficiency Pump C

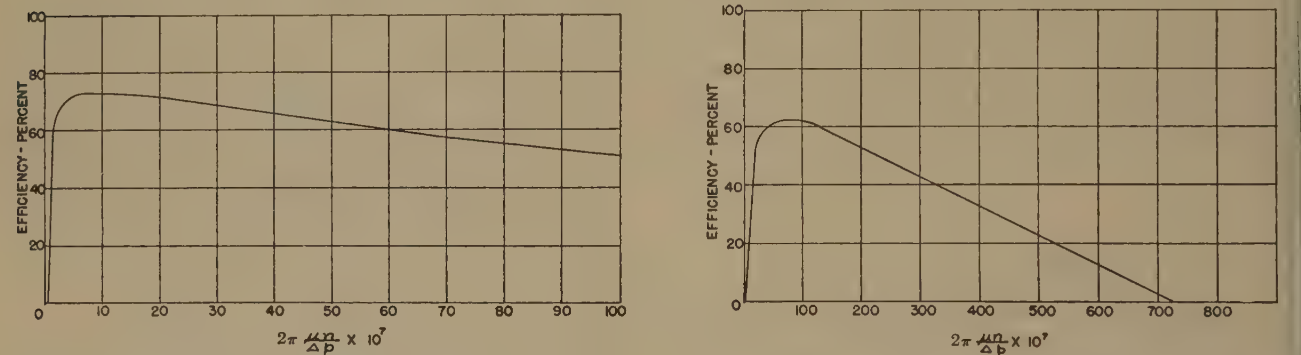

(*c*) Over-All Efficiency Pump D

(*d*) Over-All Efficiency Pump E Operating as a Motor

Fig. 4

cient, based upon viscosity at the pump inlet, to include the heating effect of the shear.

The values of c_f in many cases are excessive and indicate the necessity for additional consideration of dry frictional drag by the designer. This coefficient is an indication of the occurrence of metal-to-metal contact, and it is to be expected that a pump or motor which exhibits a large value of this factor will show signs of wear in a relatively short time.

The torque T_c is very much like that associated with the coefficient c_f, differing only in the fact that it is independent of pressure. It is desirable to eliminate it in all designs. With few exceptions, the value of T_c has been kept down to a reasonable value.

Dimensionless Efficiency Curves

The plotting of performance data in the form of dimensionless efficiency curves is a means of presenting a wide range of data in compact form as well as an excellent means of predicting performance outside the range of the experimental data, that is, at values of μ, n, or Δp not readily obtained experimentally. Since performance is a function of the parameter $(\mu n)/(\Delta p)$ and not μ, n, and Δp individually, an infinite number of combinations of these quantities is represented by a single experimental point giving an efficiency at a specified value of $(\mu n)/(\Delta p)$.

Using the experimentally determined values of the performance coefficients in Equation [13], the expression may be written for the efficiency of the given unit. From this equation a curve can be plotted. This curve can be used safely to extrapolate beyond the range of the experimental data, provided due consideration is given to the possibility of reduced delivery due to cavitation in the neighborhood of the inlet.

The calculated value of maximum efficiency, shown in Table 1, is obtained by assuming $T_c = 0$. Comparison of pumps on the basis of this efficiency may be carried out if due allowance is made for the effect of T_c. Specifically, pumps A and E cannot attain the maximum efficiency indicated but will approach it when the pressure differential is very large.

The plotting of efficiency as a function of the parameter is illustrated in Fig. 4 where the efficiency of pumps, B, C, and D, and motor E are shown. Since T_c is zero for each of these pumps, this plotting is even more significant, showing as it does the actual formance characteristic over a wide range of values of vis- ity, speed, and pressure.

CONCLUSIONS

The use of the coefficients c_s, c_d, and c_f, and the torque T_c, to cribe the performance of a pump or fluid motor, is a method of nparing performance on a common basis.

The interpretation of the performance characteristics in terms hese coefficients and T_c constitutes a method of isolating weak- sses in design thus assisting in redesign for improved perform- e.

The presentation of performance data in the form of dimension- efficiency curves offers a means of showing a wide range of a in compact form as well as a means of determining suita- ity of the unit for an intended service.

BIBLIOGRAPHY

"Rotary Pump Theory," by W. E. Wilson, Trans. ASME, vol. 1946, p. 375.

"Method of Evaluating Test Data Aids Design of Rotary mps," by W. E. Wilson, *Product Engineering*, vol. 16, 1945, pp. –656.

"Rotary-Pump Theory," by W. E. Wilson, Trans. ASME, vol. 1946, p. 373.

"Design Analysis of Rotary Pumps to Obtain Maximum Effi- ncy," by W. E. Wilson, *Product Engineering*, vol. 17, 1946, pp. –141.

Discussion

. H. **MAUDE.**[3] It is interesting to note that the paper applies all types of positive-displacement pumps, regardless of design e and the natural pressure limitation of each design. In gen- l, and eliminating pumps of special manufacture, the engineer learned to select a certain design type of pump according to ximum circuit pressure, and these limitations may be stated follows:

Gear pumps for pressures not exceeding 1000 psi.

Radial vane pumps for pressures not exceeding 2000 psi.

Radial piston pumps for pressures over 2000 psi, and gen- lly up to 3000 psi. Certain small and special pumps of this e may be obtained for even higher fluid pressures.

n quite a number of pressing operations the "load-deforma- " curve is of approximate parabolic form, somewhat similar to t given in a paper by the writer.[4] In a direct pumping scheme ress operation, a high-low dual pump set is prescribed, which vides a high-volume low-pressure pump in conjunction with a ller-volume high-pressure pump. During the preliminary t of the pressing stroke, the combined discharges of both ps are employed up to the limit pressure of the low-pressure p, after which the low-pressure high-volume pump is auto- ically by-passed, and the final part of the pressing stroke is pleted by the high-pressure pump alone. By careful selec- of pumps and pressures, it is seen that it is possible to keep motor efficiently employed up to its rated capacity throughout rge part of the pressing cycle and thus make an economic in- lation.

n selecting such a high-low combination pumping unit, the gner must also have knowledge of the oils which these pumps handle:

Gear pumps will pump any press circuit oil employed.

Radial vane pumps will not operate on an oil heavier than SAE No. 20W. Generally the oil is specified as 150-225 SUV at 100 F. Heavy oils cause suction cavitation.

3 Radial piston pumps require a heavy oil, sometimes as high as SAE 40 to 50, and having a viscosity of 920 SUV at 100 F. The internals of the pump obtain their lubrication from a prescribed leakage from the pistons operating in the bronze cylinder body, which leakage is limited to 3 per cent maximum of pump discharge.

All oils for hydraulic circuits should possess temperature stability so that there is as little reduction in viscosity with temperature rise as is possible.

From the foregoing it will be noted that a low-pressure radial vane pump cannot be used in association with a radial piston pump, because of the difference in circuit oil requirements.

Referring to the author's researches into what he terms "dry friction" and its magnitude, this is a variable factor depending largely upon manufacturing inaccuracies. All machines made along the lines of quantitative production are made to certain prescribed tolerances and allowances with selective assembly. Nevertheless, in assembly, small misalignments plus approaching high and low dimensions compound to give a pump not exactly to true standard, so that on test, it immediately develops undue heat. This is the "dry-friction" factor and the remedy is hand-fitting to bed in the mating parts.

O. E. **TEICHMAN.**[5] The author of this paper is to be commended for applying dimensional analysis and similitude to the analysis of performance data of positive-displacement pumps and fluid motors. The plotting of efficiency data, obtained from performance tests, against the dimensionless parameter $(\mu n)/(\Delta p)$ gives a very effective means for comparing a variety of operation conditions. The coefficients of viscous drag c_d, slip c_s, and dry friction c_f, derived from the discharge-speed and torque-speed diagrams, give the designer a basis for evaluating various design features and their influence on the over-all efficiency. The diagram given in Fig. 1 of the paper, showing the maximum efficiency as a function of the product $c_s c_d$ for various values of c_f, is indicative for the limitations in performance of certain designs.

From the simplifications made to obtain Equation [11] of the paper, as well as from the diagrams, Figs. 2(*a*) and (*b*), it is understood that only straight-line relationships of torque speed and discharge speed are used in the analysis. Experimental data usually show that there is only a limited speed range where this holds true. The term Q_r in Equation [1] is a function of the speed causing, for the pump, a downward bend of the discharge-speed curve in the higher speed range. The torque-speed relationship is linear only in the region of "perfect" lubrication. For low values of $(\mu n)/(\Delta p)$, imperfect film lubrication sets in similar to conditions as observed on journal bearings, where the coefficient of friction and consequently the friction torque increase sharply below a certain minimum value of $(\mu n)/(\Delta p)$ for any given ratio of bearing diameter to clearance in the bearing. Under certain conditions, this will affect the maximum efficiency obtainable, giving a smaller $\eta_{\max}$ at a somewhat higher $(\mu n)/(\Delta p)$, as compared with the values corresponding to Equations [11] and [13].

Another uncertainty is attached to using viscosity values in the approach lines for $(\mu n)/(\Delta p)$, neglecting local heating and change of viscosity at the locations in the pump where the slip and torque losses occur. It will always pay to check these conditions before any extrapolation beyond the range of experimental data is applied.

With regard to nomenclature, it should not be out of order to

---

Assistant Chief Engineer, Industrial Division, Dominion Engi- ing Company, Limited, Montreal, Canada.

'Principles in the Design of Modern Hydraulic Machinery," by . Maude, *Dominion Engineer*, vol. 14, August, 1947, fig. 21, p. 12.

[5] Supervisor in Fluid Mechanics, Armour Research Foundation, Chicago, Ill. Mem. ASME.

raise a question concerning the term "cavitation" as used in connection with Q_r. Would it not be better to reserve this term to conditions where "vapor-filled cavities" are encountered, the collapse of which causes the phenomenon called "cavitation erosion?" In oil-hydraulics, would not "aeration" or "separation" be better terms for the formation of cavities that are mostly filled with air?

Author's Closure

Mr. Maude summarizes present practice and general limitations on positive-displacement pumps and motors, opening as he does so the topic of the design of pumps and motors for special purposes. The limitations with respect to pressure and type of oil cited by Mr. Maude are to a considerable extent the result of standard practice with reference to clearances. The basic significance of the clearances built into a positive-displacement unit when fully appreciated should result in designs capable of performing satisfactorily under conditions now deemed outside the practical range.

Mr. Maude's observations on the significance and cause of dry friction are extremely pertinent. It it unlikely that the average designer appreciates fully the magnitude of the energy loss associated with relatively slight metal-to-metal contacts when high speeds are involved.

Mr. Teichman discusses several very basic topics, among which are imperfect lubrication, variation of liquid viscosity due to local heating, and nomenclature. As Mr. Teichman points out, the linear relationships suggested in this paper exist only for limited ranges of the parameter $\frac{\mu n}{\Delta p}$. Deviations due to breakdowns of the lubrication are apparent in all experimental studies providing the low-speed high-pressure ranges are investigated. Much significant research remains to be done in determining completely the consideration which must be given to this fact in design.

The effect of viscosity variation on performance is a factor of prime importance in design. The comp[illegible]e problems which arise in attempting to predict th[illegible]y given set of circumstances are so great that [illegible]ulating a design procedure have been taken[illegible]sing field of research exists in this area.

Mr. Teichman very properly questions the use of the word cavitation to describe the formation and decay of air-filled pockets. Prof. R. T. Knapp, authority on cavitation has expressed the opinion that this phenomenon shou[illegible]erly be considered cavitation. It would seem that usage and custom must ultimately determine the choice of word.

Response Characteristics of Thermometer Elements

A. J. HORNFECK,[1] CLEVELAND, OHIO

Speed of response of the thermometer element is an important factor in the accurate measurement and control of tempera[illegible] industrial processes. This paper discusses th[illegible] of the time constant as a basis of comp[illegible]ts and shows quantitatively by means [illegible]ves the effects of varying the design factors su[illegible] size, materials, and internal element structure. Th[illegible] relation between the heat-transfer rate from the surrounding medium to the socket wall and the element response is shown by response data for a number of designs tested in air and water. Methods are given for determining [illegible]mperature versus time response curves of elements in a medium whose temperature is changing suddenly, uniformly, and sinusoidally as a function of time.

SPEED OF RESPONSE AS A FACTOR IN TEMPERATURE MEASUREMENT AND CONTROL

In almost all applications involving the measurement and control of industrial processes, temperature is of fundamental importance as a guide to the successful operation of these processes. Temperature of the medium is usually inferred from the temperature of an immersed element such as a thermocouple, a resistance wire, or a bulb filled with expansible liquid or gas. This element is heated by any or all of the three modes of transfer, i.e., convection, conduction, and radiation. While conditions can be controlled in the laboratory so that temperatures can be measured and reproduced to an extraordinary precision, such conditions do not generally exist in industrial processes.

In many cases the heat-transfer rate to the temperature-measuring element or its protective socket is a factor determined by the process and is not controllable. Also, the thermal element must be sufficiently massive to withstand corrosion and mechanical shock and is generally enclosed in a socket whose thickness and construction are determined by pressure and other factors. Several commercial-type socket assemblies for resistance-thermometer elements are shown in Fig. 1. The design and application factors determine the lag of the element temperature behind that of the medium and sizable errors may result under conditions of change. Consequently an important consideration in the accurate measurement and control of the temperature of industrial processes is the response characteristic of the measuring element.

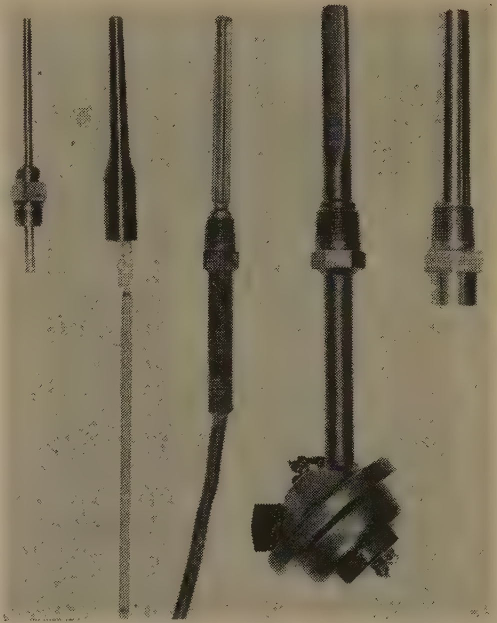

FIG. 1 SEVERAL COMMERCIAL-TYPE RESISTANCE-THERMOMETER SOCKET ASSEMBLIES

A great deal of justifiable emphasis has been placed on those factors which are important to fundamental accuracy such as purity and reproducibility of thermocouple and resistance-element materials, aging and contamination of materials, instrument accuracy, and the like. The application sources of error including response lag are equally important but in many cases are neglected or minimized because of a lack of specific information and data to enable the engineer to properly evaluate these factors in analyzing his special problems of temperature measurement.

The importance of the response characteristic in the accurate measurement and control of temperature was recognized in certain vital processes engaged in during the last war. Consequently a specific development was organized and carried out to determine the correlation between the physical factors and the speed of response of thermal elements and to design elements based on this study to have the fastest response consistent with all the other desirable features involved, such as mechanical strength, corrosion resistance, and minimum conduction and radiation errors. The physical factors include the thermal properties of the medium as well as the geometry of the thermal elements and the properties of the materials making up the element and its protecting socket. Since the completion of this development, further investigation has been carried out to determine additional data and to extend the methods and analysis to more general application. The object of this paper is to summarize these test results and to correlate these results to the physical factors. The tests were made with various designs of elements and sockets in media ranging from stagnant air to flowing water in order to cover a wide range of heat-transfer rates.

Although most of the response data were obtained using resistance-thermometer and thermocouple elements in metallic sockets, the method of analysis and the conclusions can be extended in a general way to all types of thermal elements including thermal control devices. Certain differences in the design and

---

[1] Research Engineer, Bailey Meter Company.

Contributed by the Industrial Instruments and Regulators Division and presented at the Industrial Instruments and Regulators Division Meeting, Philadelphia, Pa., Sept. 13–17, 1948, of The American Society of Mechanical Engineers.

NOTE: Statements and opinions advanced in papers are to be understood as individual expressions of their authors and not those of the Society. Paper No. 48—IIRD-2.

materials making up these elements will of course influence the characteristics. For example, the stem lag of partially immersed elements such as mercury thermometers is a complicating factor as discussed in an article by Noyes (5).[2] However, in all cases the problem is fundamentally one of transient heat flow. A completely general and rigorous mathematical solution is probably not possible and certainly not practical to the design and application engineer. The methods employed in this paper involve a combination of relatively simple theory of equivalent heat-flow circuits with heat-transfer data and specific response data to establish a basis for determining with reasonable accuracy the response of thermal elements. The present state of knowledge of heat-transfer coefficients and thermal properties of materials at various temperatures does not justify more rigorous methods. In a few cases where temperature of the medium can change frequently and rapidly, such as surrounding air temperatures of an aircraft, a knowledge of the response characteristic might be as important as steady-state accuracy. However, in most industrial applications, approximate calculation of the response lag to 10 or 20 per cent is satisfactory. The problem, in general, is to obtain the highest speed of response in a specific heat-transfer medium and consistent with good design practice.

The Thermal Time Constant as the Elementary Basis for Comparison

A bare resistance thermometer element or thermocouple immersed in a heat-transfer medium can be considered as a single lumped thermal capacity exchanging heat through a single lumped conductance as shown in Fig. 2*a*. This circuit also approximates that of a mercury-in-glass thermometer, bare gas-filled bulb, or thermostatic element of the expansion type. In many applications it is also a reasonably accurate representation of the heat-flow circuit even when the sensitive element is enclosed in a protecting tube or socket. A more general treatment of the element in socket case is considered later on in this paper.

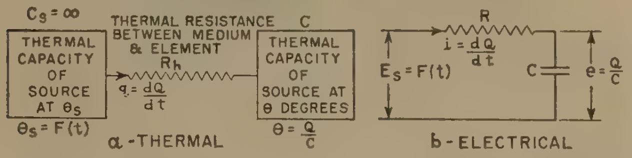

Fig. 2 (*a*) Thermal Circuit of the Elementary Thermometer (*b*) Analogous Electric Circuit of the Elementary Thermometer

The thermal circuit is exactly analogous to the electric circuit shown in Fig. 2*b* in which the capacitor C is charged to a potential e through a resistance R from a source such as a battery or generator. The source in either case is assumed to have an infinite capacity so that flow of current or heat into or out of it has no effect on the potential. This potential as represented by voltage or temperature is considered to be varying as some function of time denoted as $\theta_s = F(t)$.

The differential equation for the thermal circuit is

$$F(t) = RCd\theta/dt + \theta \quad \text{[1]}$$

If the temperature of the medium changes suddenly from an original steady-state value of θ_0 degrees to a new value of θ_m degrees, the temperature of the element at time t is

$$\theta = \theta_0 + (\theta_m - \theta_0)\,(1 - e^{-t/RC}) \quad \text{[2]}$$

The temperature lag expressed as a part of the total temperature change is

$$L = \frac{\theta_m - \theta}{\theta_m - \theta_0} = e^{-t/RC} \quad \text{[3]}$$

The product RC is the time constant symbolized as t_0. It has units of time and is numerically equal to the time required for the element lag to be reduced to $1/e$ or 0.368. In other words, when $t = t_0$, the element will have accomplished 63.2 per cent of the total medium temperature change. If the natural logarithm of L is plotted as a function of t the resultant curve is a straight line having a slope equal to $-1/t_0$.

Since thermal conductance U is a more familiar factor than resistance, the thermal time constant is perhaps better represented by the ratio of thermal capacity to thermal conductance. Symbolically, $t_0 = C/U$.

In very few industrial applications does the temperature of a process medium change suddenly enough to be considered instantaneous as assumed in this analysis. In test or laboratory work, temperature elements may be exposed to such conditions as, for example, when immersed suddenly in a bath or fluid stream. However, regardless of how the medium is changing, the time constant is the basic factor which determines the response of the thermometer element.

A number of response equations for changing medium temperatures are listed as follows: These solutions are based on the assumption of an elementary thermometer element, but apply with certain limitations to most applications.

1 *Condition.* The medium changes at a constant rate of r degrees per unit time beginning at θ_0 deg at 0 time

$$\theta = \theta_0 + r\,[t - t_0(1 - e^{-t/t_0})] \quad \text{[4]}$$

and

$$L = \frac{\theta_0 + rt - \theta}{rt} = \frac{t_0}{t}\,(1 - e^{-t/t_0}) \quad \text{[5]}$$

For large values of t the lag in degrees is simply

$$L_s{}^\circ = rt_0 \quad \text{[6]}$$

2 *Condition.* The medium changes at a constant rate of r degrees per unit time for a period of t_a units of time.

In the interval from $t = 0$ to $t = t_a$ the response and lag are given by Equations [4] and [5]. From $t = t_a$ to $t = \infty$ the response is given by the following equation

$$\theta' = \theta_0 + rt_a - rt_0\,(1 - e^{-t_a/t_0})\, e^{\frac{-(t - t_a)}{t_0}} \quad \text{[7]}$$

and

$$L = \frac{t_0}{t_a}\,(1 - e^{-t_a/t_0}) e^{\frac{-(t - t_a)}{t_0}} \quad \text{[8]}$$

3 *Condition.* The temperature of the medium changes as a periodic sinusoidal function of time about a mean value of θ_0 in accordance with the equation $\theta_s = \theta_0 + \theta_m \sin (2\pi ft)$. This might be the case with a hunting control cycling at a frequency of f cycles per unit time. The complete response equation is

$$\theta = \theta_0 + \frac{\theta_m}{1 + w^2\,t_0{}^2}\,[wt_0e^{-t/t_0} + \sqrt{1 + w^2t_0{}^2}\,\sin\,(wt - \tan^{-1} wt_0)] \quad \text{[9]}$$

At steady state

$$\theta = \theta_0 + \frac{\theta_m}{\sqrt{1 + w^2t_0{}^2}}\,\sin\,(wt - \tan^{-1} wt_0) \quad \text{[10]}$$

---

[2] Numbers in parentheses refer to the Bibliography at the end of the paper.

where $w = 2\pi f$ and $\tan^{-1}(wt_0)$ is the lag angle of the temperature of the element behind that of the medium.

Equation [10] is recognized more familiarly as that of the voltage on a condenser in series with a resistance across an alternating-current power source.

For large values of f and t_0 it is apparent from Equation [10] that the element will not measure instantaneous medium temperature, but rather the average temperature θ_0. The ratio of the amplitude of the element temperature to that of the medium is $\frac{1}{\sqrt{1+w^2t_0^2}}$. The lag in degrees between the element and the medium at time t is given by Equation [11]

$$L^\circ = \frac{wt_0\,\theta_m}{\sqrt{1+w^2t_0^2}}\sin\left(wt + \tan^{-1}\frac{1}{wt_0}\right)\ldots\ldots\ [11]$$

In general, if the known or assumed variation of the temperature of the medium can be expressed as an analytical function, the response of the measuring element can be determined by solving the differential Equation [1]. Conversely, the temperature of the medium can also be inferred from the response record of the temperature of the measuring element.

The time constant t_0 is the single constant of the elementary thermometer which determines its response. Since the response is an inverse function of t_0, it is sometimes more convenient to compare elements on the basis of $1/t_0$ which is defined in this paper as the response factor Rf.

Experimental Procedure

If the elementary thermometers at a uniform temperature θ_0, are suddenly immersed in a medium at temperature θ_m, it is assumed that the response will be the same as if the element were immersed in a medium whose temperature is changed suddenly $(\theta_m - \theta_0)$ deg. Consequently, the response of an element determined by sudden immersion will be the same as defined by Equation [2]. The time constant can be obtained directly from the curve of per cent response plotted versus time by observing the time required for 63.2 per cent of the total change. A better method consists in determining the slope of the lag curve plotted on semilog coordinates. Equation [3] expressed in logarithm form is

$$\ln L = \frac{-t}{t_0}$$

and

$$t_0 = \frac{-t}{\ln L} \text{ where } \ln L = \text{logarithm of } L \text{ to base e}$$

Since the ordinates of the semilog paper are distributed according to logarithm to base 10, the expression for log L becomes

$$\log L = -t/t_0 \log_e = -0.435\ t/t_0$$

and

$$t_0 = -\frac{0.435\ t}{\log L}$$

or

$$t_0 = \frac{0.435\ tn}{n}\ldots\ldots\ldots\ldots\ldots\ldots\ldots[12]$$

where n = number of cycles of plotting.
tn = time given by the intersection of the lag curve with the time axis.

For example, assume that log L is plotted over the range 1 to 0.01 in which case $n = 2$ and

$$t_0 = \frac{0\ 435\ tn}{\log 1 - \log 0.01} = \frac{0.435\ tn}{2} = 0.2175\ tn$$

In determining test data it was found convenient to use an electronic-type recorder of the continuous-null-balance type such as described in a recent paper (10) by Dickey and Hornfeck. A round-chart instrument was used by speeding up the chart movement from 24 hr to 48 sec. A high-speed recorder mechanism was used to enable the recording pen to travel across the chart in less than 1.5 sec. The typical response curve on the round chart is a spiral record as shown in Fig. 3, and each test was run until the records overlapped indicating no further significant change in temperature.

This equipment was generally quite satisfactory in obtaining response data of industrial-type thermometer elements. However, fine-wire thermocouples and bare resistance thermometers in liquids and high-velocity air streams were found in some instances to have speeds of response greater than that of the recorder. Since these are simple elements, it is usually possible to extrapolate actual test data of heavier elements or elements

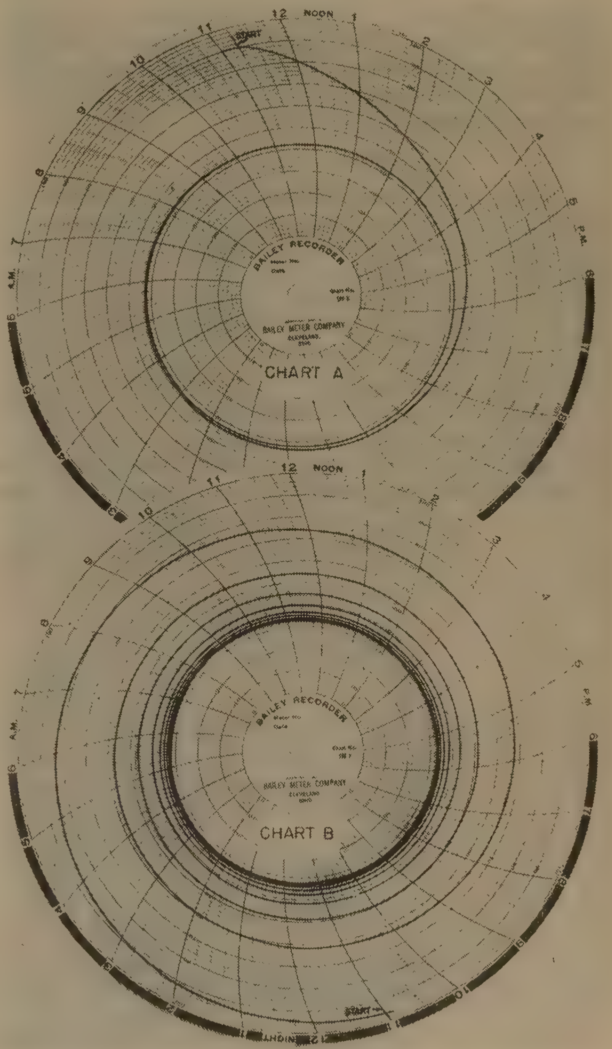

Fig. 3 Typical Response Records Obtained With a Round Chart Recorder; Time Scale, 1 Hr = 2 Sec

(Chart A, cooling curve of element in water; Chart B, cooling curve of same element in air at 50 fpm velocity.)

in low-heat-transfer media to determine the response of lighter elements or similar elements in high-heat-transfer media.

In making tests special effort was made to minimize such factors which might falsely distort the response curve. These include: 1, time of transfer of element to medium to initiate the response; 2, nonuniform heating or cooling of the element, particularly the enclosed-socket type; 3, longitudinal transfer of heat down the socket or element leads to the head exposed to a different temperature from the medium: 4, variations in temperature of the medium during test; and 5, change in heat-transfer factors of the medium and thermal properties of the elements over the range of temperature.

The time required for full immersion was less than $^1/_4$ sec and had negligible effect on the response tests except in a few instances. Factors 2, 3, 4, and 5 were minimized by making most of tests at or near ambient temperatures and the total rise or fall of temperature relatively small (generally under 100 F). In spite of these precautions certain deviations of the response curves from those predicated by simple theory were occasionally observed.

In general, it is believed that the response data on the particular elements tested are accurate to ±2 per cent in water and ±5 per cent in the air stream. The accuracy with which these data can be extrapolated or interpolated to specific industrial installations depends on how accurately the heat-transfer coefficients and the effect of variations in design, i.e., shape and size of the socket, from those tested can be calculated.

Response Test Data

Resistance Thermometers. The majority of the response tests were conducted on resistance-thermometer elements both bare and in protecting sockets. This is justifiable on the basis of the increased use of the resistance thermometers in industrial-process and aircraft applications where speed of response, sensitivity, and accuracy obtainable with this type of element are in many cases necessary or desirable. Furthermore, widespread use of the resistance thermometer for industrial applications is of relatively recent origin although it has been used as laboratory standard for precision thermometry for many years. Except for two recent papers (1, 2) little literature is available on the response lag and other sources of application error on this type of thermometer.

A number of commercial and experimental designs were analyzed and tested. These are shown in Fig. 4. All but one o the designs tested used platinum wire as the sensitive elemen and because of the very small thermal capacity of the actua wire, the data would apply as a close approximation to copper o nickel wire elements. It will be noted from the figures that ther are two basic types of construction: 1, the separable socket an element type (Fig. 4*a* to 4*f*) in which the internal element can b readily removed for replacement and repair, and 2, the integra type as shown by types 4*g* and 4*h* in which the sensitive element and the bulb form a single unit which cannot be disassembled The first design has the advantage of permitting the use of a standard internal element in all types of sockets whether for high or low pressure or corrosive or noncorrosive atmosphere. The second design, because of its integral construction, can be made to have a higher speed of response when applied alone but it has the major disadvantage of requiring a second protecting socket in many applications.

The single time constant t_0 defines the response characteristic of bare elements in any heat-transfer medium. While the response of an element in a socket may deviate from a straight line on a semilog graph, these more complex thermometers can be approximately compared on the basis of an equivalent time constant. Table 1 summarizes the data on the various thermometer elements tested in air and water. The data show the response of the elements for a wide range in velocity of the air.

At low velocities the time constant of the element is determined almost entirely by the heat-transfer coefficient to the socket and the thermal capacity of the socket. Consequently the response factor, $1/t_0$ for a particular socket is a function of the air velocity as shown by the curves in Fig. 5. The slopes of these curves in this region are theoretically equal to the exponent of the velocity term in the expression for the heat-transfer coefficient from air or other gases to round cylinders. The exponent increases somewhat with velocity as indicated by these curves. At high velocities it will be noted that the response curves begin to droop and if the velocity were increased indefinitely, the response would ultimately become constant at a value equal to the conductance between the inner wall of the protecting socket and the sensitive element divided by the thermal capacity of the internal element. This factor may be called the internal response

TABLE 1 EQUIVALENT TIME CONSTANTS OF SEVERAL EXPERIMENTAL AND COMMERCIAL RESISTANCE-THERMOMETER ELEMENTS DETERMINED BY TEST IN AIR AND WATER

Element and socket		Time constant — t_0 — sec			
Reference figure	Description	350 ft per min	Air at 950 ft per min	5300 ft per min	Water at 60 ft per min (approx)
4*a*	Bare flat element	5.6	4.1	2.6 at 1800	less than 1 sec
4*b*	Bare flat element with guard springs	34.5	24	15 at 1800	less than 1 sec
Element 4*b* in socket 4*c* Flat	Element in high-pressure socket		136		23
Element 4*a* in socket 4*d*	Low-pressure high-speed unit	49	33.5	15.5	1.3
Element 4*e* in round stainless (18-8) socket	Silver springs socket d_2 = 0.600 in. d_1 = 0.563 in.	55.5	40	16.5	7.5
Same	Same with Inconel springs	81.0	65.0	42	31.8
4*e* in brass socket	Silver springs socket d_2 = 0.593 in. d_1 = 0.568 in.	38.5	29.0	13.3	6.0
Same	Same with Inconel springs	67.5	55.0	38.0	30.5
4*e* in aluminum socket	Silver springs socket d_2 = 0.600 in. d_1 = 0.563 in.	30.5	25	12	5.0
4*f* element in round stainless steel socket	Low-pressure round unit	32.5	24	13.3	5.1
4*g* stainless steel socket	Integral unit socket not separable	68	47	18	1.6
4*h*	Integral unit for low pressure and temperature applications	43	28	10	0.9
4*h* in $^3/_4$-in. OD separable brass socket				48.3	5.7

NOTE: Average temperature: air = 130 F, water = 100 F; range of temperature change: air = 100 F, water = 40 F; pressure: atmospheric 29.6 in. Hg. (approx).

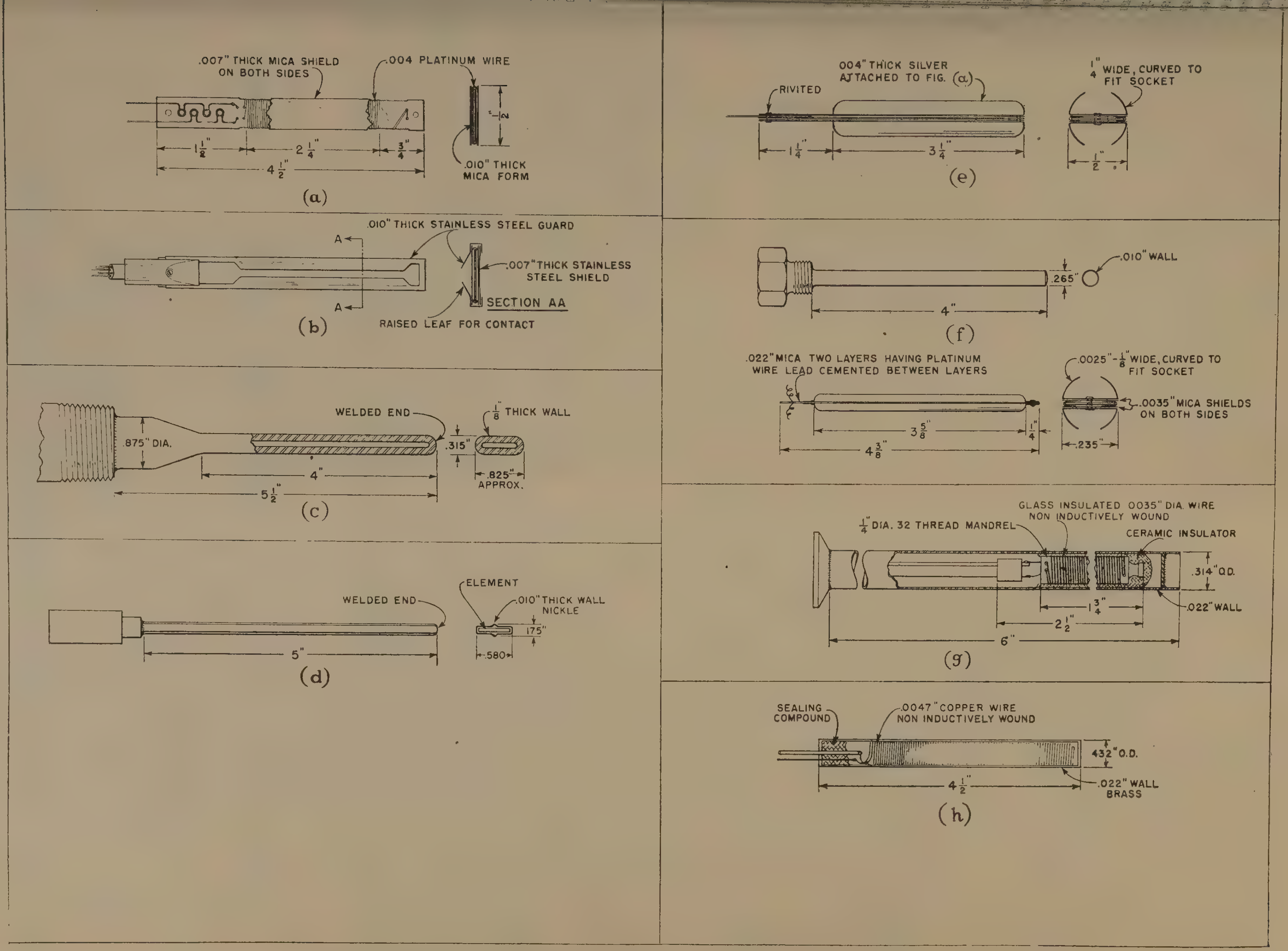

Fig. 4 Experimental and Commercial Resistance-Thermometer Elements and Sockets

[(*a*) Basic flat element; (*b*) flat element in spring guard holder for flat sockets; (*c*) industrial socket—flat, heavy wall type for high pressures; (*d*) thin-wall, high-speed socket for low pressures; (*e*) flat element similar to (*a*) with round conducting and holding springs for round sockets; (*f*) element similar to (*e*) but smaller in size. Assembled in small-diameter, thin-wall AN-type socket and suitable for low and moderate pressure: (*g*) integral-type element and socket assembly for low and moderate pressures; (*h*) high-speed integral element and socket assembly suitable for low temperatures and pressures only.]

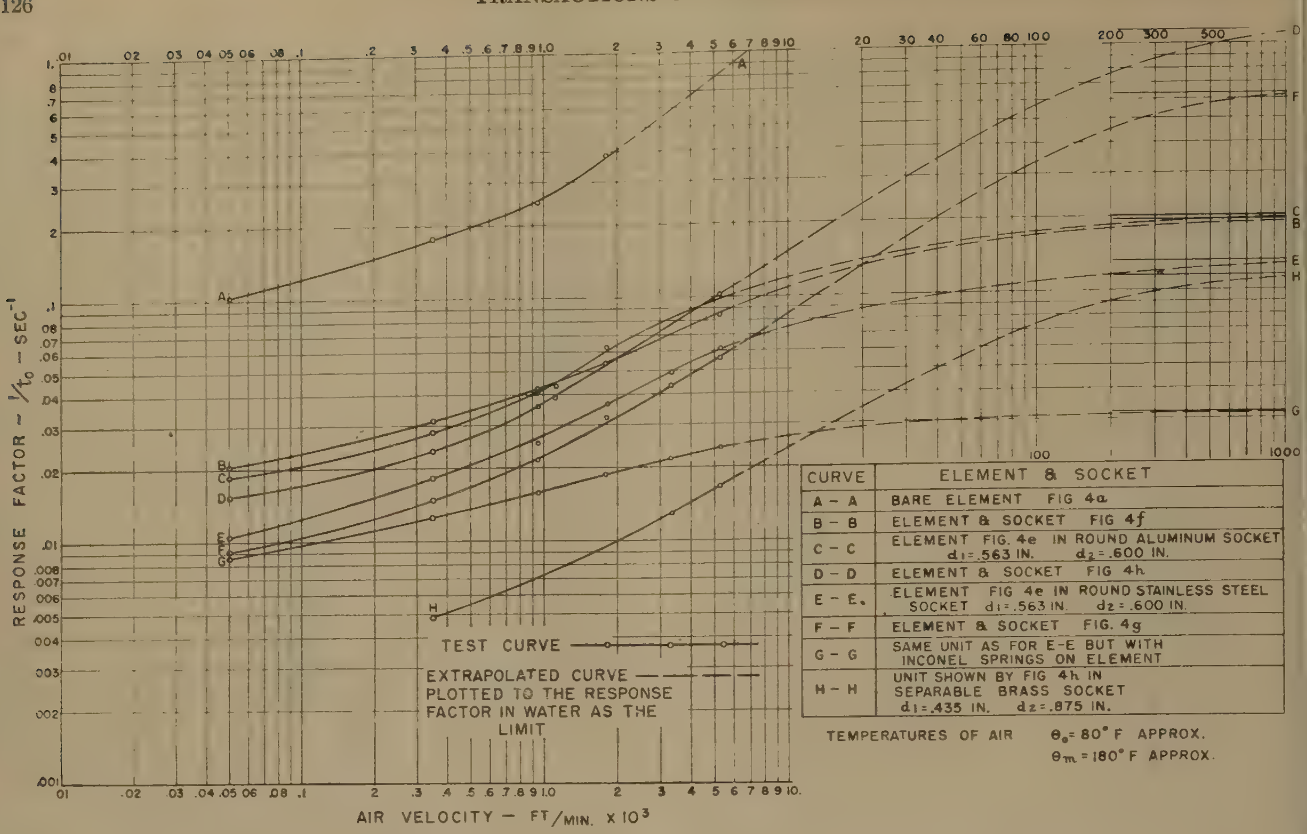

Fig. 5 The Variation of Response Factor (Reciprocal of Time Constant) With Air-Stream Velocity

factor. It will be observed that for integral units, which have extremely small internal time constants, the response increases indefinitely with velocity over the test range. On the other hand elements which have an appreciable internal time constant show considerable drooping at higher velocities.

In most liquids with the possible exception of relatively viscous oil the equivalent time constant is determined principally by the internal thermal conductance and capacity. Exceptions exist in the case where the socket wall thickness is very great for extremely high-pressure applications and where the socket material is limited to metals such as stainless steel or to nonmetals which have a high thermal capacity and a low thermal conductivity. Consequently an excellent method to determine the internal time constant is to obtain the response characteristic in water. This is particularly accurate for very thin-wall sockets. In Fig. 6 the time constant of the resistance-thermometer element shown in Fig. 4*e* enclosed in a round socket is plotted as a function of diameter ratios. This figure shows the relatively small effect of socket thickness on response in a high-heat-transfer medium. For example, the stainless-steel socket with silver conducting springs shows variation of time constant with socket thickness down to a wall thickness of about $^7/_{32}$ in., beyond which point there is relatively little change indicating that most of the remaining lag is internal. The brass socket with Inconel conducting springs shows considerably less effect produced by changes in the socket size because the low thermal conductivity of the Inconel compared to silver increases the internal time constant.

Table 2 shows the time constants of several elements in various fluids. In general, other things being equal, the heat-transfer coefficient and the response factor will be approximately inversely proportional to some function of the kinematic viscosity, which is the ratio of absolute viscosity divided by the density. The data indicate that in most liquids the response is higher than in air and other equivalent gases at even high velocity.

TABLE 2 TIME CONSTANTS OF SEVERAL RESISTANCE THERMOMETER ELEMENTS IN VARIOUS HEAT-TRANSFER MEDIA

Element and socket			Liquids at approx. 60 fpm velocity							
Reference figure	Description	Air 1800 fpm	Water	Acetone	Carbon tetrachloride	Alcohol synthetic	Benzene	Ethyl acetate	Heavy oil	Lavite (molten salts)
4*b*	Bare flat element with guard springs	15	less than 1	2.5	3.6		2.5	2		
4*b* in 4*c*	Flat element in high-pressure socket	76	23							23
4*a* in 4*d*	Low-pressure high-speed unit	24	1.3	3.1	2.5	2.9	2.2	2.7	9.4	
4*f* in round socket	Low-pressure round unit	18.5	5.1	8.7	8.5	7.4	8.5	8.7		
4*g* Stainless-steel socket	Integral unit	31.0	1.6	3.7	4.2	2.7	3.2	3.2		
4*h*	Integral unit	19.0	.9	2.6	2.7	2.0	2.5	2.7	25	

Note: Average temperature: air = 130 F, Lavite = 600 F, other liquids = 100 F; Range of temperature change: air = 100 F, Lavite = 400 F, other liquids = 40 F.

THERMOCOUPLES

Thermocouples either bare or in protecting sockets exhibit the same type of response characteristic as resistance thermometers. This is obviously true since the thermal circuit from the heat-transfer medium to the sensitive thermocouple element is basically the same as that of the resistance thermometer. Table 3 shows the time constants of various thermocouple elements.

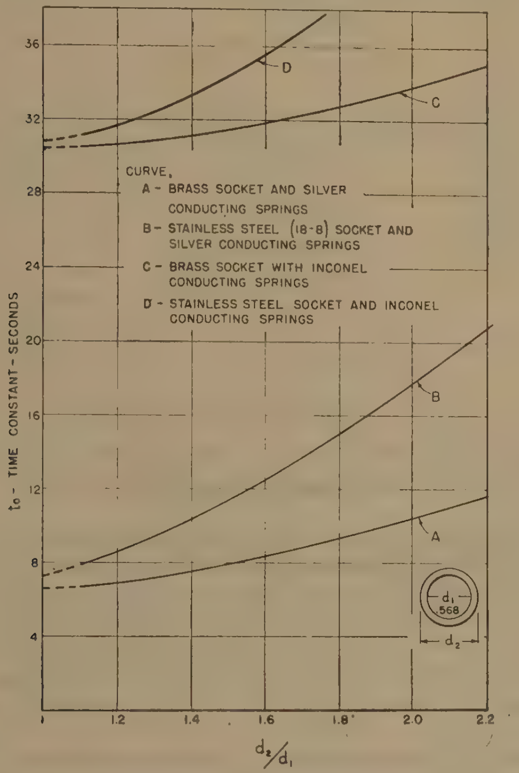

FIG. 6 TIME CONSTANTS OF SOCKET-ENCLOSED ELEMENTS IN WATER AS A FUNCTION OF SOCKET SIZE
[Element shown in Fig. 4(e).]

If the thermocouple does not touch the walls of the enclosed socket, the thermal resistance between the inner wall of the socket and the thermocouple element is high compared to the thermal resistance between the heat-transfer medium and the outer wall of the socket. Consequently, as the data show, this type of installation is very sluggish under all conditions. If the thermocouple makes good contact with the socket or is welded or soldered into the end of the socket or, as in some cases, if the socket itself forms one of the thermocouple conductors, the internal lag is generally small or negligible and the time constant is determined almost entirely by the thermal capacity of the socket and heat-transfer coefficient to it from the medium. In general, the bare thermocouple will have a response similar to that of the bare resistance-thermometer element except that additional lag may be introduced by the support on which the resistance wire is wound. Since the bare thermocouples tested were of larger wire size than the resistance thermometers, they are somewhat slower as indicated by the specific data.

DETERMINATION OF RESPONSE FROM BASIC DATA AND BY EXTRAPOLATION OF TEST RESULTS

The test thermometer elements have been compared on the basis of a single equivalent time constant. While this may not be mathematically correct in so far as defining the complete response curves, it does serve as a satisfactory criterion of comparison. On the other hand if the response is to be predetermined by calculation from basic data or by extrapolating test data for new heat-transfer conditions, the equivalent time constant can be calculated only if the thermometer is physically equivalent to a single thermal capacity in series with the boundary resistance. Strictly speaking only a bare element can be so represented, but in practice the socket-protected element often has a response characteristic defined by a single exponential function. Consequently it is relatively easy to calculate the time constant of such an element providing the thermal capacity and heat-transfer rates are known. The time constant is given by the simple equation

$$t_0 = C/U = \frac{\rho V c}{h A} \qquad [13]$$

where

ρ = density of material
V = volume of element
c = specific thermal capacity of element material (specific heat)
A = surface area
h = heat-transfer rate from medium to element surface.

TABLE 3 EQUIVALENT TIME CONSTANTS OF THERMOCOUPLES

Thermocouple and socket		Time constant — t_0—sec					
Unit no.	Description	Air 50 fpm	350 fpm	1150 fpm	3350 fpm	5300 fpm	Water at 60 fpm
1	Bare No. 14 wire iron-constantan	20	13	8	7.4	5.3	Less than 1
2	Bare No. 19 wire chromel-alumel	12.5	7.7	3			Less than 1
3	Same as No. 1 in round brass socket $^7/_8$ in. OD, $^9/_{16}$ in. ID	750	325	198	135	103	Erratic
4	Same as No. 2 in round brass socket $^5/_8$ in. OD, $^7/_{16}$ in. ID	332	150	109	59	39	Erratic
5	No. 20 wire iron-constantan in $^5/_8$ in. OD, $^7/_{16}$ in. ID brass socket. Wire not touching wall.	362	283	171	111	78	76.5
6	Same as No. 5 but thermocouple silver-soldered to socket wall	282	144	77	38	30.5	2.7
7	No. 20 wire iron-constantan couple soldered into $^1/_4$-in. brass cube	56	36	22.0	12	8	Less than 1
8	Same as No. 7 but couple soldered to $^1/_4$-in. aluminum cube	35	19	14	6	4.5	Less than 1
9	Commercial thermocouple and socket assembly. No. 12 wire in steel socket $^9/_{16}$ in. OD, $^7/_{16}$ in. ID		220	136	79	73	57

NOTE: Average temperatures: air = 130 F, water = 100 F; range of temperature: air = 100 F water = 40 F.

Any consistent set of units may be used. Generally the time constant is expressed in seconds and dimensions in inches. Consequently it will be found convenient to express the foregoing quantities in the following units

ρ = lb/in.^{3}
V = in.^{3}
c = Btu/deg F-lb
A = in.^{2}
h = Btu/deg F-in.^{2}-sec = Btu/deg F-ft^2-hr × 1.93 × 10^{-6}

If, as usually is the case, the element consists of two or more materials in close thermal contact, as, for example, a thermocouple or a resistance element wound on a thin mica card, the total thermal capacity ($C = \rho Vc$) must be determined by summing up the individual capacities.

To illustrate the accuracy with which the time constant can be calculated for the elementary thermometer the integral-type element shown in Fig. 4*h* is taken as an example. Specifically the response of this element as a function of air velocity is plotted in Fig. 7 and compared against the test curve. In this case the calculations were relatively simple since nearly all the thermal capacity lies in the socket itself and the resistance is determined almost solely by the heat-transfer rate from the air to the socket. Occasionally it may be difficult to calculate the factor $\rho Vc/A$ in Equation [13]. An example is a bare thermocouple in which the proportions of the two metals are not known. In this case it is usually a relatively simple matter to determine this factor from a single response test under controlled conditions. By Equation [13], $C/A = \dfrac{\rho Vc}{A} = t_0 h$ where t_0 is the time constant determined by the specific test and h is the calculated heat-transfer coefficient. The response or the time constant of this element can then be calculated for any other condition so long as the heat-transfer factors are known.

Calculation of the Response Curve From t_0

Since the elementary thermometer response is determined by a single time constant and by the temperature change of the medium to which it is exposed, a complete response curve can usually be calculated if these are known. Fig. 8 shows the general temperature-lag curves for an elementary thermometer plotted in terms of dimensionless time t/t_0. These curves apply to a medium whose temperature changes suddenly, continuously at a uniform rate, or for a period of time at a uniform rate. From these curves it is possible to determine the response of a specific element providing the time constant and the rate of temperature change of the medium are known. Fig. 9 is a calculated response curve derived from Fig. 8 for a specific element having a time constant of 20 sec subjected to a change in temperature of 2 deg per sec for 40 sec.

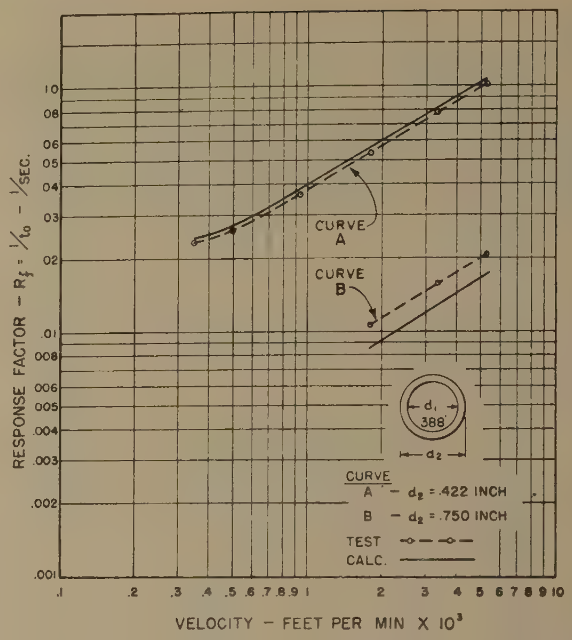

Fig. 7 Calculated and Test Curves Showing the Relation Between the Time Constant and Air-Stream Velocity for Element in Fig. 4(*h*).

Socket and Element Design Factors

1 *Socket Mass.* The effect of the mass of the socket is il-

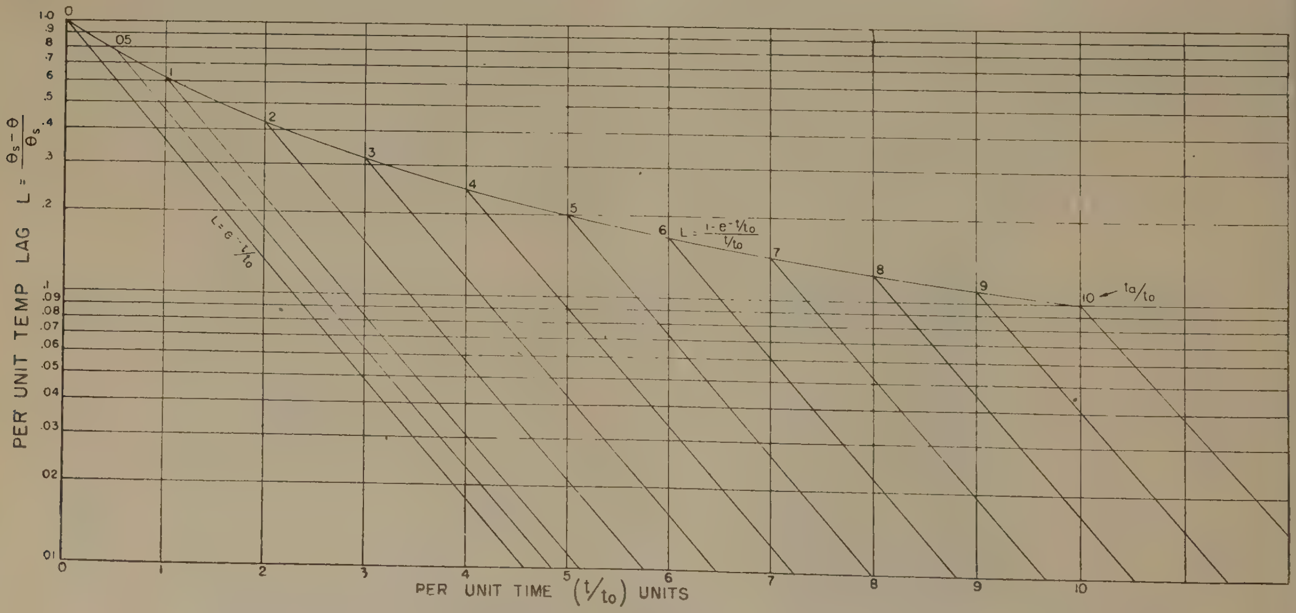

Fig. 8 Generalized Temperature-Lag Curves of an Elementary Thermometer

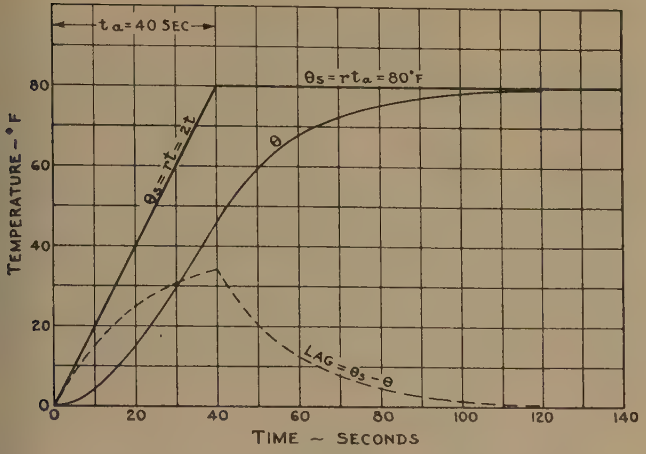

FIG. 9 DERIVED RESPONSE AND LAG CURVES FOR A SPECIFIC ELEMENT AND CONDITION
(t_0 = 20 sec, t_a = 40 sec, r = 2 deg per sec.)

lustrated in the curves in Fig. 10 which show the experimental and calculated relation between time constant, t_0, and diameter ratio d_2/d_1. These curves were obtained on the separable socket type of element shown in Fig. 4*e* enclosed in a round protecting tube. The internal element and the internal diameter are constant throughout the tests. Calculated results were obtained by determining the total thermal capacity of the complete structure including the internal element as well as the socket. The thermal conductance between the air stream and socket wall was calculated from heat-transfer factors available in the literature (3, 4, 7). The following equation was used to determine the equivalent time constant

$$t_0 = t_1 + t_{12} + t_2 \ldots\ldots\ldots\ldots\ldots [14]$$

$$= C_1/U_1 + C_2/U_1 + C_2/U_2 \ldots\ldots\ldots\ldots\ldots [15]$$

In this equation U_1 is equal to the thermal conductance per inch length between the heat-transfer medium and the socket wall, and U_2 equals the thermal conductance between the inner wall of the socket and the sensitive element.

In terms of the sockets' dimensions this equation is as follows

$$t_0 = \frac{(a^2 - 1)d_1c_v}{4ah} + \frac{C_2}{\pi a d_1 h} + \frac{C_2}{U_2} \ldots\ldots\ldots\ldots [16]$$

where $a = d_2/d_1$
c_v = specific heat of socket per unit volume = ρc
h = heat-transfer factor between medium and socket wall.

As will be shown later this equation is only an approximation since the exact response of the complex element of this nature cannot be calculated precisely by summing up the individual time constants; but it does yield an equivalent total time constant. It is a fairly satisfactory basis for comparison of elements. For large sockets the last two factors of this equation become negligible and the response is determined almost entirely by the socket itself. The intersection of the curve with the $d_2/d_1 = 1$ axis is the internal time constant t_2 plus the mutual time constant t_{12} and is equal to the sum of the last two factors in Equation [16]. At higher velocities the conductance between the air stream and the socket wall becomes greater than the internal conductance of the element and consequently the response is determined primarily by the internal time constant t_2.

2 *Socket Material.* The effect of the thermal properties of the socket on the response depends on the application, i.e., the heat-transfer rate from the medium to the socket wall. In any case the conductivity of the material is not important except where the socket wall is very heavy or where a nonmetallic material such as a ceramic is used.

In media such as air at low or moderate velocity where the heat-transfer rate is relatively small the specific heat of the socket c is important as indicated by Equation [16]. As the heat-transfer factor increases, the socket time constant becomes less important and in water the response is determined primarily by the internal time constant. This is shown by data in Table 4.

3 *Internal Element Construction and Materials.* In applications in which a high heat-transfer rate exists between the me-

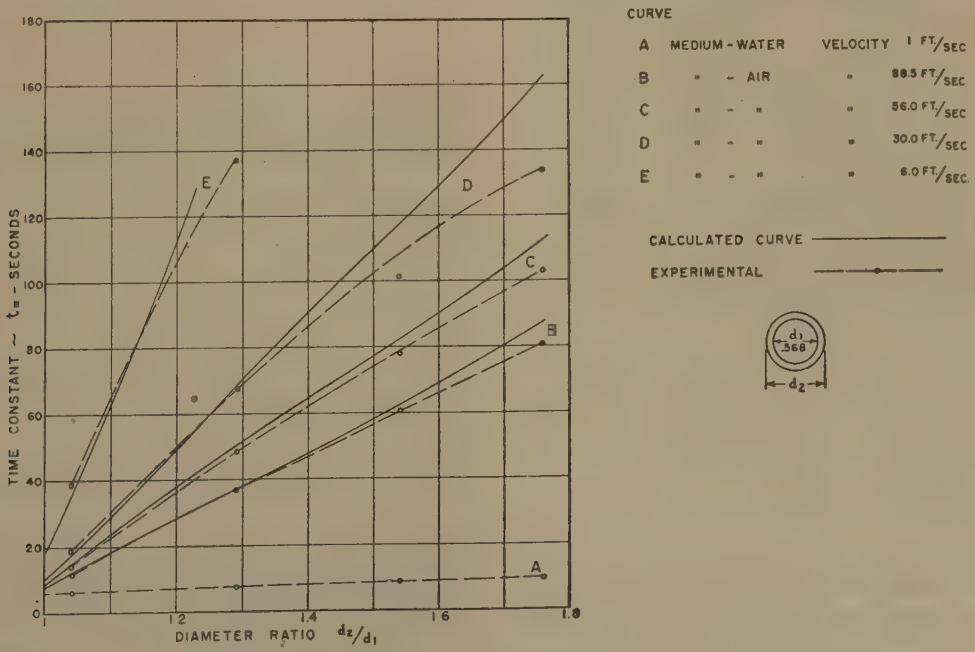

FIG. 10 TIME CONSTANT OF THERMOMETER ELEMENT AS A FUNCTION OF SOCKET SIZE
(Element shown in Fig. 4(*e*) enclosed in brass socket.)

TABLE 4 TIME CONSTANT AS A FUNCTION OF SOCKET MATERIALS USED IN SOCKETS AND ELEMENTS

Element	Socket material	C_v	Time constant Air 50 fpm	5300 fpm	Water 60 fpm
Fig. 4*e* with silver springs in round socket d_2 = 0.600 in. d_1 = 0.563 in.	18–8 Stainless steel	0.0348	90.5	16.5	7.5
	Brass	0.0292	76.2	14.2	6.0
	Aluminum	0.0178	55.0	12.0	5.0

dium and the socket wall the internal time constant is of primary importance. This factor is determined by the total thermal capacity of the internal element and the equivalent thermal conductance between the inner socket wall and the sensitive portion of the element. In contrast to the socket the thermal conductivity of the internal element is as important as specific heat. This is especially true of the electric insulating material which is always required in the resistance-thermometer element and generally in the thermocouple. Table 5 lists the thermal properties of more commonly used materials one or more of which may form the internal element or the protecting socket. The conductivity and specific heat are given in consistent units for purposes of easy use in calculations of conductance and total capacity.

TABLE 5 THERMAL PROPERTIES OF MATERIALS

Material	Temp F	Density lb per in.^{3}	K = Thermal conductivity Btu-in. per sec-°F-in.^{2}	C_v = Specific heat Btu per °F-in.^{3}
Aluminum	32	0.0975	2.71×10^{-3}	17.7×10^{-3}
	212		2.75	17.8
	572		3.08	18.0
Brass	32	0.310	1.30	
70% Cu	212		1.39	29.2
30% Zn	572		1.46	
Copper	32	0.322	5.18	29.6
	212		5.05	30.4
	572		4.91	31.8
Gold	212	0.698	3.91	21.8
Monel	80–212	0.322	0.347	40.9
Nichrome				
62 per cent Ni—15 per cent Cr		0.296	0.182	31.7
80 per cent Ni—20 per cent Cr		0.303	0.181	32.4
Silver	212	0.376	5.55	21.2
Mercury	32	0.491	0.082	16.3
Inconel	100–212	0.307	0.200	33.4
Nickel	32	0.313	0.833	32.8
	212		0.787	36.6
	572		0.741	44.0
Platinum	64	0.773	0.932	24.4
	212		0.970	
Steel (mild)	212	0.284	0.606	33.5
	932		0.509	34.6
Stainless steel (18-8)	212	0.290	0.218	34.8
	572		0.254	
Mica	122	0.104	0.0058	21.4
Glass				
Crown	70	0.0904	0.0168	14.6
Pyrex		0.0811	0.0151	16.2

The effect of changing one component material of the internal element shown in Fig. 4*e* is demonstrated by the test data in Table 6.

TABLE 6

Element	Socket	Time constant — sec Air 350 fpm	Air 5300 fpm	Water 60 fpm
Fig. 4*e* with silver springs	18-8 Stainless steel d_1 = 0.563 in. d_2 = 0.600 in.	55.5	16.5	7.5
Fig. 4*e* with Inconel springs		81	42.0	31.8

The time constant using silver conducting springs is less than the value obtained using Inconel springs as would be predicted from the fact that silver has a much higher thermal conductivity. The proportional difference is much greater in water than in air since the internal time constant is the dominant factor in water.

More Exact Treatment of the Response of the Socket-Protected Element

The use of a single equivalent time constant obtained by summing the individual constants of a complex thermometer is only approximately correct in determining the complete response curve. This is particularly true if the constants t_1, t_2, and t_{12} are approximately equal to one another. In the more exact analysis the thermometer cannot be represented by the simple circuit shown in Fig. 2 in which the total capacity and total resistance are lumped into a single series circuit. In almost all applications involving the use of metallic protective sockets a reasonably good correlation between experimental and calculated response can be obtained by assuming a two-element type of circuit such as shown in Fig. 11. This equivalent thermal circuit is based on the assumption that the actual element consists of two thermal resistances and two thermal capacities in series-parallel combination. One resistance is formed by the thermal resistance between the medium and the socket wall and the other resistance is the equivalent thermal resistance between the inner wall of the socket and the sensitive measuring element. Similarly one thermal capacity is that of the protecting socket and the other thermal capacity is that of the internal element.

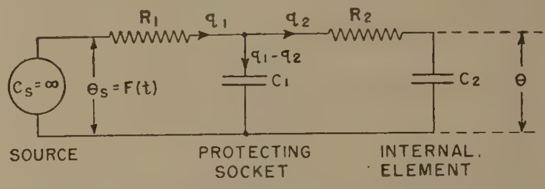

Fig. 11 More Exact Circuit of the Socket-Protected Element

The differential equation for the circuit is given by

$$F(t) = R_1C_1R_2C_2\frac{d^2\theta}{dt^2} + (R_1C_1 + R_1C_2 + R_2C_2)\cdot\frac{d\theta}{dt} + \theta \quad [17]$$

The coefficients in Equation [15] may be expressed in terms of the various time constants defined previously.

$$F(t) = t_1t_2\frac{d^2\theta}{dt^2} + t_0\frac{d\theta_2}{dt} + \theta \quad [18]$$

If the thermometer element is subjected to a sudden change in temperature, $(\theta_m - \theta_0)$, the following response equation of temperature as a function of time is readily derived

$$\theta = \theta_0 + (\theta_m - \theta_0)\,[1 - e^{-at}(\cosh bt + P\sinh bt)] \quad [19]$$

where $a = \frac{t_0}{2t_1t_2}$

$$b = \frac{\sqrt{t_0^2 - 4t_1t_2}}{2t_1t_2} \text{ and } P = \frac{t_0}{\sqrt{t_0^2 - 4t_1t_2}}$$

The per unit lag is as follows

$$L = \frac{\theta_m - \theta}{\theta_m - \theta_0} = e^{-at}(\cosh bt + P\sinh bt) \quad [20]$$

Good correlation can generally be obtained by the use of these equations to predict the response of the socket-protected element. Calculated and test response curves are compared in Fig. 12. It will be observed that the most serious error in using the simple response, Equation [2], would occur in the period of initial change. The socket-protected element has a zero rate of change of temperature during this period as compared to a maximum rate of change of temperature of the elementary thermometer. This initial response lag is particularly serious from the standpoint of control since it is desirable that the instrument and consequently the control senses the temperature change of the medium immediately.

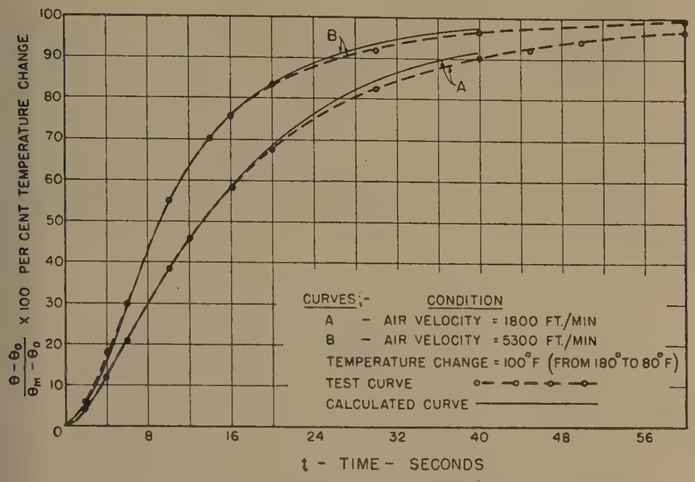

FIG. 12 EXPERIMENTAL AND CALCULATED RESPONSE CURVES FOR A SOCKET-PROTECTED ELEMENT

[Curves based on a sudden change in temperature of the medium. Element shown by Fig. 4(*e*) with silver springs in round aluminum socket. OD = 0.600 in., ID = 0.563 in.]

As in the case of the elementary thermometer the response equation for the complex thermometer can be calculated for any change in the temperature of the medium which may be expressed in analytical form. Several examples are given as follows:

1 Medium temperature increases at a constant rate r beginning at a value of θ_0 deg. The function t given in the general equation is $F(t) = \theta_0 + rt$.

Substituting this function in Equation [18] and solving for θ yields the temperature of the sensitive element at any time t, after the application of this function.

$$\theta = re^{-at}\left[\left(\frac{at_0 - 1}{b}\right)\sinh bt + t_0 \cosh bt\right] + r(t - t_0) + \theta_0 \qquad [21]$$

The lag in degrees at any time t is given by the following equation

$$L = r\left\{t_0 - e^{-at}\left[\left(\frac{at_0 - 1}{b}\right)\sinh bt + t_0 \cosh bt\right]\right\}. \qquad [22]$$

At steady state the response equation reduces to

$$\theta_s = r(t - t_0) + \theta_0 \qquad [23]$$

and the lag is determined by the total equivalent time constant t_0, as shown by the following equation

$$L_s = rt_0 \qquad [24]$$

2 The temperature of the medium changes during the interval from $t = 0$ to $t = t_a$ at the rate of r deg per sec. It is constant at a value rt_a thereafter.

For the interval from $t = 0$ to $t = t_a$ Equation [19] applies. When $t = t_a$, $\theta = \theta_a$ = the value obtained by substituting $t = t_a$ in Equation [21]. At this value of time the differential equation for the response is the same as for a sudden change in temperature. The solution of this equation yields the following response expression for values of t greater than t_a

$$\theta = r\,t_a + \theta_0 - e^{-at'}\left[\frac{(art_0 - a\theta_a)}{b}\sinh bt' + (rt_a - \theta_a)\cosh bt'\right] \qquad [25]$$

where $t' = t - t_a$

3 Steady-state response for sinusoidal cycling temperature conditions with the applied temperature changing in accordance with the following equation

$$F(t) = \theta_0 + \theta_m \sin wt \qquad [26]$$

The temperature of the internal element as a function of the constants of the equivalent circuit and the applied temperature of the medium can be calculated relatively simply by alternating-current circuit analysis. The steady-state solution is given by the following equation

$$\theta = \frac{\theta_m}{\sqrt{(1 - w^2t_1t_2)^2 + w^2t_0^2}} \sin\left(wt - \tan^{-1}\frac{wt_0}{1 - w^2t_1t_2}\right) \qquad [27]$$

If the medium is changing in accordance with some other function, the response can be calculated in a similar way. However, these response expressions for the complex thermometer become somewhat cumbersome, and, in general, it is satisfactory to use the simple circuit for the elementary thermometer and the total equivalent constant. This is particularly true because of the relative inaccuracy of heat-transfer data and the difficulty in determining the exact values of the various thermal resistance and capacities.

THERMALLY MASSIVE SOCKETS AND ELEMENTS

The simple theory based upon the heat-flow circuit shown in Fig. 2 and Fig. 11 has proved to be quite satisfactory for predicting the response of thermometer elements in most ordinary applications. However, if the socket is quite massive or is constructed of materials which have a high specific heat and a low thermal conductivity, the actual response may deviate considerably from the response predicted from the simple theory. Typical examples are extremely heavy-walled sockets for high-pressure applications and ceramic sockets for high-temperature applications. Other examples are gas or liquid expansion systems in which the sensitive medium is a relatively poor thermal conductor. All of these elements may be considered as being thermally massive. Exact analytical treatments to determine the response of these elements is difficult because the heat-flow path can no longer be considered as a simple circuit consisting of lumped constants. Approximations can of course be made by representing the heat-flow paths by a sufficient number of circuit elements; but the derivation of a response equation based on such circuits is relatively difficult and yields complicated and cumbersome expressions. The use of a calculating system using electric-circuit analogy such as developed by Paschkis (8) is suggested as a means for determining generalized response curves.

The effect on the response of a thermally massive unit is demonstrated graphically in Fig. 13, which shows the experimental and calculated response curves for a resistance thermometer element in a stainless-steel socket. It will be observed that the actual response curve deviates considerably from the calculated curve based on a single exponential and to a less extent from a calculated curve based on the more exact treatment, using the circuit in Fig. 11. The test curve shows no observable temperature change of the sensitive element for the first several seconds, and this initial or transfer lag is the time required for the tempera-

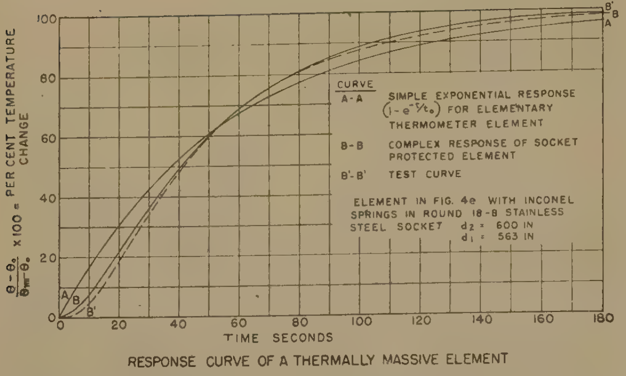

Fig. 13 Experimental and Calculated Response Curves for a Thermally Massive Element

ture wave to penetrate or be transmitted to the sensitive wire of the element. This lag might be called the initial or transfer lag and will increase with the thermal mass of the socket. If other factors remain constant, this initial dead time will be some function of the ratio of the specific heat of the socket material to the thermal conductivity and the higher this ratio the longer the lag. For example, an aluminum socket of the same dimensions as the stainless-steel socket tested under the same conditions shows no appreciable initial lag.

Discussion and Conclusions

On the basis of the test results and analysis presented in this paper, it may be concluded that the equivalent time constant is a satisfactory basis for comparing the speed of response of totally immersed thermometer elements. A single time constant defines quite accurately the response of the bare or elementary thermometer and, less accurately but generally to a good approximation, the response of the socket-protected thermometer. There is believed to be no justification for the use of some other factor such as the time required for 90 or 99 per cent of the temperature change to take place, particularly since these values of time have no direct relation to the physical constants of the thermometer and because they are relatively difficult to obtain experimentally.

The relation between the thermal constants of the thermometer and the heat-transfer properties of the medium to the time constants and the response characteristics of thermometers is shown both experimentally and analytically. The data and analysis show that only the bare or elementary thermometer can be compared under all conditions on the basis of a time constant obtained by a single test in a specific medium. It is not generally reliable to compare the socket-encased element response for all applications on the basis of a single test, as for example in water, since the equivalent time constant or over-all response is determined by three individual time constants. It is possible and often the case that one element may be faster in water but slower in some other medium such as air. However, it is often possible to calculate the response of the socket-protected element for various conditions on the data obtained by a single test.

It should be emphasized that the data and equations in this paper apply only to symmetrical and totally immersed elements, in which the temperature-responsive material such as the resistance wire or the thermocouple junction is heated or cooled uniformly. Furthermore, investigation is also restricted to applications in which the heat-transfer coefficient from the medium to the element and the thermal properties of the elements are constant and not affected by temperature over the change. This is not believed to be a serious restriction, since in most cases of continuous measurement and control, the response of the thermometer to relatively small temperature changes of the medium is important. If the response of thermometers to very wide temperature changes, particularly at high temperature where the nonlinear coefficient of radiation becomes important, is desired, the data and method outlined in this paper must be modified and amplified to obtain accurate response information.

Unsymmetrical elements and elements which may exchange heat with the outside, as for example partially immersed glass-stem thermometers and socket-enclosed thermometers having large stem-conduction errors, are excluded by the foregoing restrictions. Radiation elements such as thermocouple and resistance bolometers are also outside the classification of thermometers considered. These cannot be handled by the generalized analysis and data presented here, but usually must be treated in a more specialized and probably more complicated manner.

BIBLIOGRAPHY

1 "Heat Flow Effects in a Resistance Type Thermometer," by N. P. Millar, Transactions AIEE, vol. 64, 1945, pp. 678–685.

2 "Response Time and Lag of a Thermometer Element Mounted in a Protecting Case," by W. N. Goodwin, Transactions AIEE, vol. 64, 1945, pp. 665–670.

3 "The Basic Laws and Data of Heat Transmission," by W. J. King, *Mechanical Engineering*, vol. 54, 1932, pp. 275 and 347.

4 "Heat Transmission," by W. H. McAdams, second edition, McGraw-Hill Book Company, Inc., New York, N. Y., 1945.

5 "Stem Lag of Industrial Thermometers," by Bradford Noyes, *Instruments*, vol. 15, 1942, pp. 449–452 and 454.

6 "Conduction of Heat in Solids," by H. W. Carslaw, second edition, Dover Publications, New York, N. Y., 1945.

7 "Some Simplified Heat Transfer Data," by Margaret Fishenden and O. A. Saunders, The Institute of Fuel, vol. 9, 1945, pp. 62–71 and 74.

8 "A Method for Determining Unsteady-State Heat Transfer by Means of an Electrical Analogy," by V. Paschkis and H. D. Baker, Trans. ASME, vol. 64, 1942, pp. 105–112.

9 "Operational Circuit Analysis," by V. Bush, John Wiley and Sons, Inc., New York, N. Y., 1929.

10 "Electronic-Type Instruments for Industrial Processes," by P. S. Dickey and A. J. Hornfeck, Trans. ASME, vol. 67, 1945, pp. 393–398.

11 "Thermometric Time Lag," by Rudolph Beck, Trans. ASME, vol. 63, 1941, pp. 531–543.

Discussion

V. Paschkis.[3] The author presents an approach to the control problems which is to be commended not only for the treatment itself but also because it recognizes the thermal aspect of the problem.

From a heat-transfer viewpoint the following questions should be raised, which it is hoped will be clarified in the author's closure:

1 In the section "The Thermal Time Constant as an Elementary Basis for Comparison," the author states that he made "most of the tests at or near ambient temperature and the total rise or fall of temperature was relatively small." By arranging his experiments in this manner he obtains values of the boundary conductance h, which may be considerably different from those obtained in actual practice.

2 When comparing the resistance of the temperature-sensitive element with that of the boundary layer, it would be helpful to introduce the ratio of the two resistances (film resistance/internal resistance) which ratio is, in heat transfer, usually designated by the letter m. A large number of experiments and calculations can be reduced in presentation by using this dimensionless parameter.

3 In the "Calculation of the Response Curve From t_0," the author says that in the calculated values the boundary conduct-

---

[3] Technical Director, Heat and Mass Flow Analyzer Laboratory, Columbia University, New York, N. Y. Mem. ASME.

ance which he calls "thermal conductance between air stream and socket" was calculated based upon literature, namely, his references (3, 4, 7). In order to check the author's procedure, it would be desirable to indicate the actual values he used.

4 In the section "Socket Material," it is stated that the effect of thermal properties of the socket on the response depends upon the application. This again would be more easily explained by using the m value mentioned before.

In the last section the author discusses the more complex circuits required to calculate massive sockets. Without going into the question whether for the thinner sockets the representation of his Fig. 2(b) is permissible, the author agrees that for heavier sockets it is not. He suggests a circuit similar to Fig. 11 but it is questionable if it would not be necessary to represent both the protecting socket and the internal element by several sections. As the author points out, such circuits become mathematically unmanageable. The electric-analogy method lends itself readily to the solution of the more complex circuits.[4]

D. G. Prinz.[5] The method described in the paper employs a *step* input function. As an alternative, it is suggested to make use of an input function consisting in a short *impulse*. Experimentally, this would involve the transfer of the thermometer from a low-temperature medium to a high-temperature medium for a brief interval, and its immediate return to the original medium.

The advantages gained from this modification are due to the fact that the response to an impulsive input is (apart from a constant factor) equal to the derivative (with respect to time) of the response to a step input. A point of inflection in the step-input response curve corresponds to a maximum in the impulse-input response curve, and this maximum can be located much more accurately.

Considering the initial shape of the curve, i.e., the part immediately following $t = 0$, it is seen that the response curve to step input makes a sharp angle with the t-axis for a single-capacity system, while for a two-capacity system this curve is rounded off, starting tangentially to the t-axis. A third time constant does not alter qualitatively the character of the curve.

For an impulse input, the response curve shows an infinitely steep rise for a single-capacity system, and a finite rise, forming a sharp angle with the t-axis, for a two-capacity system; the presence of a third time constant can, in this case, be detected by the same "rounding off" which characterizes the step response in the two-capacity case. Actually, a certain amount of rounding off will always occur due to the finite duration of the pulse, but this can, in principle, be reduced to any desired extent by decreasing the pulse duration.

A quantitative method for the determination of the two time constants characterizing a two-capacity system can be based on the following construction:

The response curves to unit impulse are calculated for various values of the ratio $m = T_1/T_2$ of the two time constants. These curves will show maxima A_m occuring at times t_m. Altering the temperature and time scales by division with A_m and t_m, respectively, a new set of curves is obtained in which a maximum of height 1 occurs at the value 1 of the argument, independent of the parameter m.

Any experimental pulse-response curve of a two-capacity system can now be redrawn to a scale in which its maximum coincides with one of the maxima of the calculated curves. It will then entirely coincide with one curve of this set, and the value of m for this curve, together with the scale factor, determines the time constants T_1 and T_2.

The method suggested here should be useful for the study of other types of multicapacity systems; the experimental procedure becomes particularly simple when the input pulse can be produced by the rapid turning on and off of a power supply.

It is regretted that details of the calculations (which were carried out in England), and a diagram of the response curves cannot be made available in time for this discussion; it is hoped to publish them at a later date.

Author's Closure

The author wishes to thank both Dr. Paschkis and Dr. Prinz for their kind comments. Their suggestions indicate the need and value of additional investigation concerning the response of thermometers and other control elements. There is an ever-increasing need for such information in practical and useful form for engineers who are responsible for the design and application of instruments and control.

The following comments are made in reply to the specific questions raised by Dr. Paschkis:

1 The test conditions were purposely restricted to obtain consistent data unaffected by factors such as the change of the boundary conductance h with temperature.

2 The use of dimensionless parameters m defined by Dr. Paschkis as the ratio of the socket film resistance to the internal resistance may have simplified and also made more general some of the data and curves presented in the paper. Better still the ratio of the two time constants involving both thermal capacity as well as resistance might have been employed to advantage. It is interesting to note that if this ratio is either much larger or much smaller than unity, the response reduces to the simple exponential function.

3 Most of the heat-transfer data for air to the sensitive-element protecting sockets was obtained from curves given in reference (7). It is felt that the presentation of detailed calculations of heat-transfer data was beyond the scope of this paper.

4 The author did not intend to imply that the circuit shown by Fig. 11 is a mathematically complete representation for heavy-wall sockets. However, the analysis was limited to this circuit and the simpler one shown by Fig. 2 because the more complex representation becomes, in the words of Dr. Paschkis, "unmanageable" and yields response equations of little practical value to the engineer.

It is indicated by the discussion of Dr. Prinz that the impulse method for obtaining response may have certain advantages in some instances over the step input method used by the author. This appears to be particularly the case if it is desired to obtain the separate time constants of a multicapacity system. The method whereby the impulse-response data is obtained and the manner in which the curves are plotted is not made entirely clear by this discussion. One serious objection to this method as compared with the method used in the paper might be the difficulty in obtaining experimental data.

It is hoped that the details of Dr. Prinz's method will be published soon. It should be a valuable contribution to this field.

---

[4] "A Method for Determining Unsteady-State Heat Transfer by Means of an Electrical Analogy," by V. Paschkis and H. D. Baker, Trans. ASME, vol. 64, 1942, p. 105.

[5] Ferranti Ltd., Instrument Department, Moston, Manchester 10, England.

Designing for High-Frequency Induction Hardening

By J. T. Temin,[1] Cleveland, Ohio

High-frequency induction-hardening methods are being incorporated in the production of industrial parts to a greater extent than ever before. The design requirements are fairly rigid if the best results are to be obtained. These design principles are given specific treatment by the author. Special fixtures and machines for a variety of applications of the process have been developed and these are described at some length. The discussion includes metallurgical aspects of the induction-hardening process.

ORIGINALLY the production engineer was assigned the problem of adapting the technique of high-frequency induction hardening to the part being manufactured. Now, however, the induction-heating process has progressed to the point where the design engineer is requested to design the part so that induction-heating methods can be used to meet the hardening requirements.

Many design problems found in high-frequency induction-heating applications are going unanswered because there are too few engineers trained for this type of work. Also, because of the accelerated pace during the war, application and designing engineers, since, have had little opportunity to study, reorganize, and assimilate the technical advances made.

Then, too, the engineer seems reluctant to adopt induction-heating for hardening because some latent fear exists of using a tool so startling in its application, and misapprehension of the requirements for its operation. It can be said that the combined subjects of metallurgy, and electrical and heat-transmission engineering do present a formidable obstacle to the new user of induction-heating machines.

The field is unique indeed. The metallurgist finds that he can no longer ignore such terms as kilocycles, kilowatts per square inch, kilovolt amperes, and power. As in the case of the metallurgist, the mechanical and the electrical engineer must become familiar with such terms as microstructure, austenite, martensite, and hardness depth.

Applications for high frequency induction-heating are increasing rapidly and already have been widely used in such fields as hardening crankshafts, camshafts, gears, piston pins, wearing surfaces of many kinds, guide rails, knife-edges, and many others. Examples of parts which have been induction-hardened are shown in Figs. 1 and 2. The designing engineer assigned to the job can be qualified if he is familiar with the fundamental heating requirements, metallurgical fundamentals, and types of fixtures now in use.

Definition of Induction Heating

Simply stated, induction heating is "the heating of a nominally conducting material due to its own I^2R losses when the material is placed in an electromagnetic field." Thus if a steel rod is inserted in an inductor coil, Fig. 3, which carries an alternating current, the varying magnetic field caused by the ampere turns of the coil, couples the steel rod and induces a voltage which in turn causes a circulating current, the same as it would induce a current in a closed loop of copper wire. Once the bar is positioned properly in the inductor, the depth to which the heat penetrates into the rod is a function of the physical characteristics of the steel, that is, the metallurgy of the steel, the frequency of the current, and the power used.

Physical Characteristics and Metallurgical Considerations

Fundamentally, to obtain an acceptable hardness in a magnetic steel bar, the material must be heated to a temperature above its upper critical point and quenched within a limited time, in order to convert the austenitic solution into a final structure known as martensite. Since martensite is considered the hardest component of steel, it becomes most desirable as the end result.

Thus if we were to assume that an annealed steel rod were to be made from SAE 1045 specification, that is, a steel containing approximately 0.45–0.48 per cent carbon, we would note from the iron-carbon equilibrium diagram that the temperature of the steel must be raised to 1450 F in order to obtain complete austenitic solution. Of course increasing the carbon content of the steel, or adding alloying elements varies the critical temperature at which austenite forms. From the time-temperature transformation curve, commonly known as the S-curve, we would note that the steel must be quenched from the austenitic state within a definite time and at a certain minimum rate, in order to make the conversion to martensite possible. The reasons for martensite forming are still a matter of discussion among metallurgists and are not of concern in this paper, except for the fact that the hardened area to be metallurgically correct must consist of a martensitic structure.

Depth of Hardness

Subsequent discussion may be simplified by reviewing briefly the general understanding of hardness as shown in Fig. 4. When a bar is heated inductively, the surface tends to reach the critical temperature first and, if the heating cycle is short, as in the case of hardening, the temperature in each succeeding layer drops rapidly to the point where the core may still be at room temperature. Fig. 4 shows a cross section of a steel rod made from SAE 1045 material which has been hardened inductively, using 10,000-cycle frequency and quenched with water. Owing to the variation in temperature, there exists a demarcation zone below which there has been no change in previous microstructure. The depth measured from the surface to the demarcation zone, indicated by the letter *Z*, is known as the heated depth. If the hardness of the heated depth were checked with a Rockwell tester, the reading would indicate maximum hardness at the surface and a very low hardness at the demarcation zone. The hardness reading takes a decided drop after the demarcation zone and records the original hardness of the unchanged core.

In this paper, the hardened depth, commonly referred to in

---

[1] Commercial Engineer, Tocco Division, Ohio Crankshaft Company.

Contributed by the Machine Design Division and presented at the Semi-Annual Meeting, Milwaukee, Wis., May 30–June 5, 1948, of The American Society of Mechanical Engineers.

Notes: A companion paper, "Design and Manufacture for Profit," by H. B. Osborn, Jr., was presented at the same session and published in *Mechanical Engineering*, vol. 70, 1948, pp. 805–810.

Statements and opinions advanced in papers are to be understood as individual expressions of their authors and not those of the Society.

Paper No. 48—SA-32.

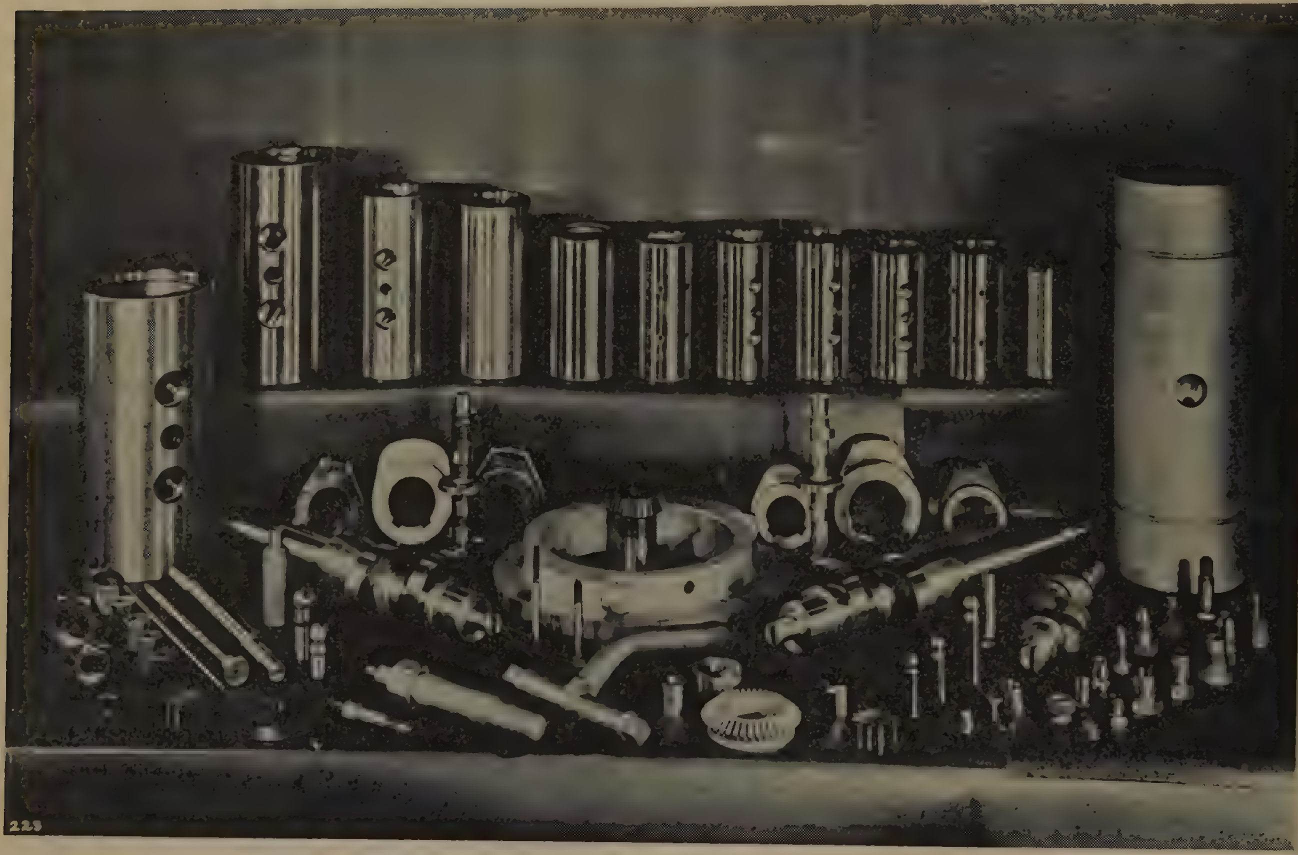

Fig. 1 Various Types of Parts Which Have Been Induction Hardened

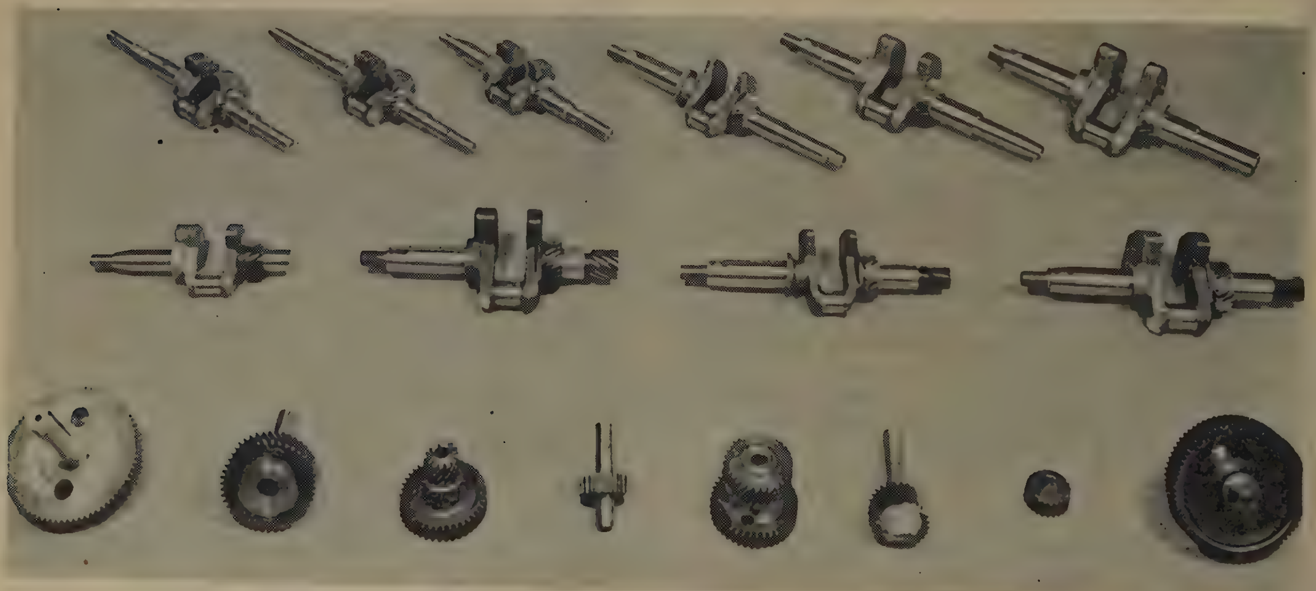

Fig. 2 Various Types of Gears and Crankshafts Which Have Been Induction Hardened

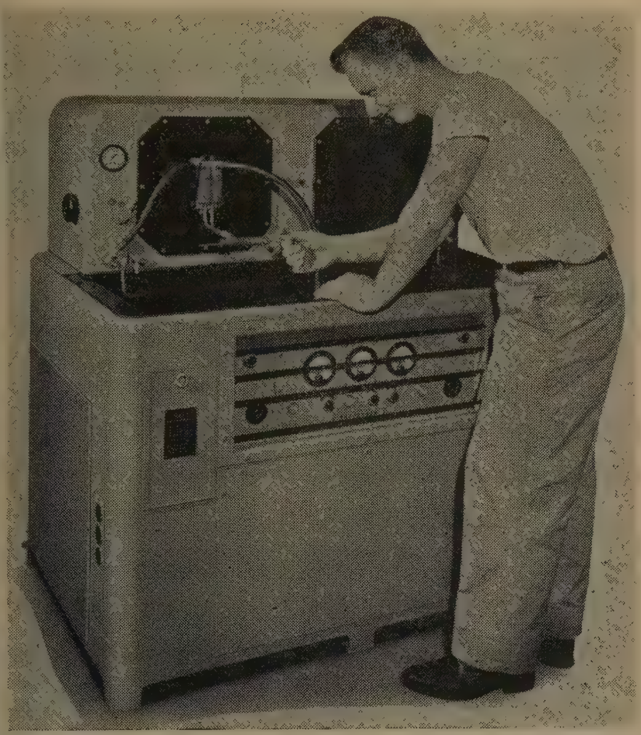

Fig. 3 Steel Bar Inserted in a Multiturn Inductor Coil Located on a High-Frequency Induction-Heating Machine

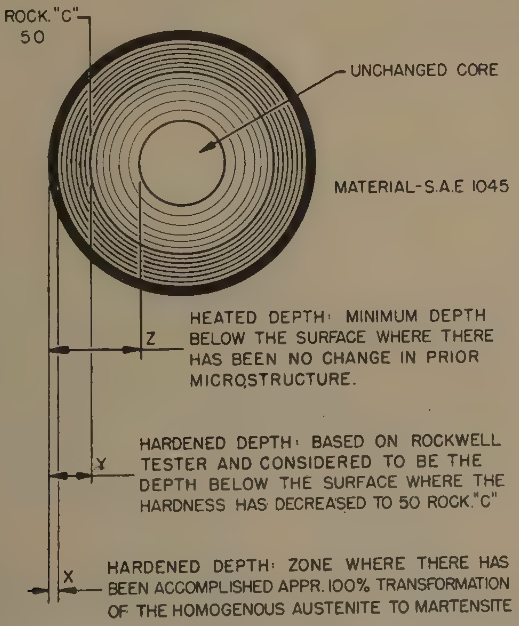
ROCK."C" 50
UNCHANGED CORE
MATERIAL-S.A.E 1045
Z
HEATED DEPTH: MINIMUM DEPTH BELOW THE SURFACE WHERE THERE HAS BEEN NO CHANGE IN PRIOR MICROSTRUCTURE.
Y
HARDENED DEPTH: BASED ON ROCKWELL TESTER AND CONSIDERED TO BE THE DEPTH BELOW THE SURFACE WHERE THE HARDNESS HAS DECREASED TO 50 ROCK."C"
X
HARDENED DEPTH: ZONE WHERE THERE HAS BEEN ACCOMPLISHED APPR. 100% TRANSFORMATION OF THE HOMOGENOUS AUSTENITE TO MARTENSITE

Fig. 4 Gradation of Hardness in Induction-Heated SAE 1045 Steel Bar

(Diameter 1 in.; frequency 10,000 cycles.)

induction heating, is considered to be the depth below the surface where the hardness, as indicated by the Rockwell tester, has decreased to 50 RC or approximately 50 per cent martensite, and is indicated by the letter Y. Owing to the gradation of the temperature, complete solution was not obtained in the areas which did not reach the critical temperature. Consequently, on cooling, in place of approximately 100 per cent martensite, there appears a mixture of softer constituents. Although this is not completely correct metallurgically, for all practical purposes metallurgists consider this structure acceptable.

The hardened depth indicated by the letter X is known as the metallurgically correct structure for maximum hardness, and the structure is approximately 100 per cent martensite. Because of its high hardness and resistance to wear, martensitic structure is desired in applications where the surface is subjected to continuous wear, such as, bearing surfaces, guiding surfaces, cam surfaces, piston pins, knife-edges, raceways, and ever so many other applications.

Importance of Time in Induction Hardening

A point worth noting is that the transformation into the austenitic solution does not take place immediately but is a function of time as well as of the previous structure of the steel. In general, the previous structures of most steels can be grouped into four classifications, namely, annealed, spheroidized, normalized, and quenched and drawn, or heat-treated. The annealed state, containing a mixture of pearlite and ferrite, takes the longest time to go into austenitic solution, and the heat-treated state, consisting of fine sorbitic structure, takes the shortest time. In fact, when heating the annealed or spheroidized specimens, it is often necessary to increase the temperature and time to obtain the solid solution.

Since the time required for induction hardening is short, the conversion into the austenitic solution must be quite rapid. For example, Fig. 5 shows crankshafts with pin-throw areas of various diameters. The diameters vary from $^3/_4$ in. to $2^3/_8$ in. and the heating time varies from $1^1/_2$ sec to $5^1/_2$ sec. Thus in part (*a*), an acceptable hardness was obtained by heating the bearing surfaces to the austenitic temperature in $1^1/_2$ sec and quenching. This is quite a contrast with previous methods of heating where time was measured in terms of minutes, hours, and days.

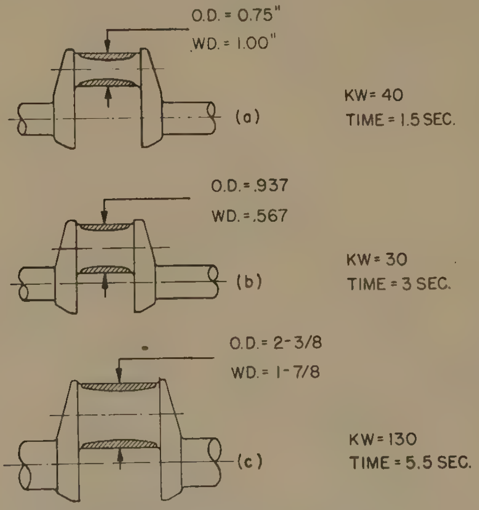

Fig. 5 Illustrating Relative Short Heating Time in Hardening Bearing Surfaces on Various Crankshafts

If two specimens of different heat-treatment were to be heated and quenched for the same period of time, we would find a difference in the hardened depth. Thus by way of illustration, Fig. 6 shows two steel bars; one is annealed and the other has been previously heat-treated. If the two specimens are separately heated, but under the same hardening conditions of power density and heating time, the heated depth will be the same, but the hardness depth of the quenched and drawn part, due to the rapid conversion into the solid solution, is greater than in the annealed specimen.

What is more important to the user, however, is the now apparent fact that since there is a rapid transition into the austenitic state with a resulting increase in hardening depth, the heating time can be decreased and the quenched and drawn specimen quenched faster to obtain a shallower hardness depth than is possible with any of the other three types of steels previously structured. This point is illustrated in Fig. 7 which again shows two specimens, one annealed, and one quenched and drawn. In order that the end results may be comparable, it is assumed that hardness depth in each case is 0.010–0.015 in. below the surface, and that depth is composed of approximately 100 per cent martensite. The two specimens are then heated under identical conditions and power density and, as indicated in the sketch, the quenched and drawn specimens require a minimum time of 0.97 sec and the annealed specimens require a minimum time of 1.5 sec or almost twice the time of heating.

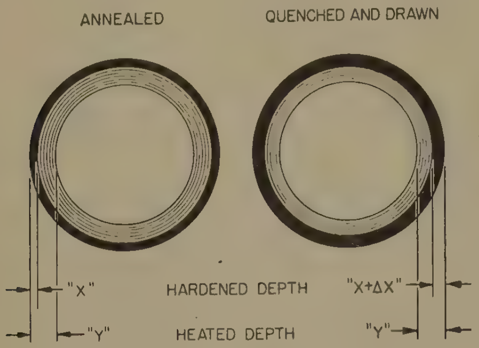

Fig. 6 Illustrating Depth Hardness Versus Previous Structure in SAE 1045 Steel Specimen

(10,000-cycle frequency, $1^3/_8$ in. diam; same density, kw per sq in.; same heating time, sec.)

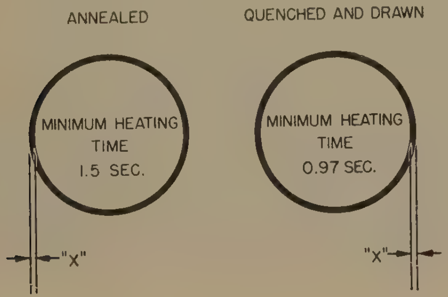

Fig. 7 Illustrating Relationship of Minimum Heating Time Between Annealed and Quench-Drawn Specimens in Obtaining Equal Depth Hardness

(SAE 1045 steel rod; diameter $1^3/_8$ in.; 10,000-cycle frequency; power used approximately 15 kw per sq in.)

Power and Hardened Depth

Of equal importance to the design engineer is his understanding of the effect on hardened depth due to increasing the energy input to the work part. Generally speaking, increasing the energy increases the hardness depth. Thus, illustrated in Fig. 8, are three specimens of an SAE 1045 annealed-steel rod showing the hardness depth with various energy inputs. The hardness depth, denoted by the letter Y, increased from 0.096 in. to 0.132 in. to 0.132 in. as the energy input increased from 22.5 kw-sec per sq in. to 39 kw-sec per sq in. In order that the data presented have practical significance, the tests performed were on the basis of the surface containing an acceptable metallurgical structure consisting of complete martensite for a depth of 0.010 in. to 0.015 in., denoted by the letter X.

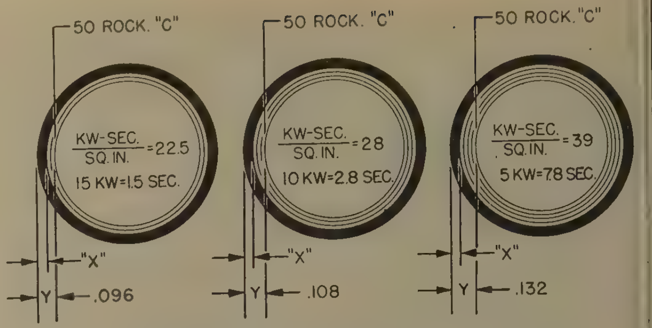

Y= HARDENED DEPTH BASED ON ROCKWELL TESTING AND CONSIDERED TO BE DEPTH BELOW THE SURFACE WHERE THE HARDNESS HAS DECREASED TO 50 ROCKWELL "C"

Fig. 8 Illustrating Relative Hardness Depth With Various Energy Input Into Test Part

(SAE 1045 steel part; diameter $1^3/_8$ in.; 10,000-cycle frequency; annealed previous structure.)

However, to complete the general picture, it is necessary to analyze the results and the conditions under which the tests were performed. Thus, for example, the first specimen in Fig. 8 shows that 0.096 in. hardened depth was obtained with 22.5 kw-sec per sq in. applied energy; that is, the specimen was heated using a power density of 15 kw per sq in. and a heating-time cycle of 1.5 sec. If the heating cycle were increased to 2.6 sec to produce a total energy input of 39 kw-sec per sq in., an energy input similar to the third specimen, the possibilities are that the depth hardness of 0.132 in. would not be obtained, nor would the martensitic depth be the same. In fact, increasing the time may result in the surface overheating, causing grain growth, and resulting in a decrease in surface hardness.

The same method of analysis can be used for the third specimen, where hardness depth is given as 0.132 in., when the energy input was 39 kw-sec per sq in. Thus the power density was 5 kw per sq in., and the heating time 7.8 sec. If the heating time were to be decreased to 4.7 sec to produce a total energy of 22.5 kw-sec per sq in. similar to the first specimen, in all likelihood the depth hardness of 0.096 in. would not be obtained. In fact, laboratory tests show that the time would be insufficient for the previous microstructure to go into solution. As a result of this underheating, no martensite would be obtained, the resulting hardness would be very low, and the metallurgical structure might be unacceptable.

Frequency Considerations

The effect of frequency on hardness depth is an equally important factor to be considered. Due to the phenomena of skin effect, the induced current tends to hug the surface. The higher the frequency, the greater the tendency for the current to hug the surface, the less depth heated, and the shallower the depth hardness.

When reference is made to hardness depth, as a result of the higher-frequency currents, it is necessary to consider the added effects due to the heat transmission in the steel specimen; for although electronic frequencies may produce an almost instant critical temperature on the surface, the heat will tend to be conducted toward the center of the bar at a rate which is a function of the characteristics of the steel. If the part is not quenched within an extremely short time, instead of obtaining a surface hardness with the electronic frequency, the net result would be a hardness depth equivalent to using the lower frequencies.

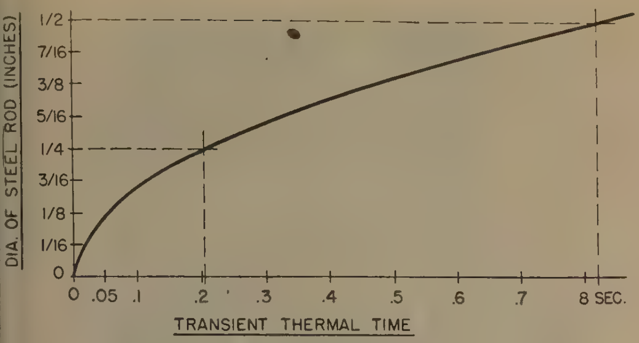

FIG. 9 TRANSIENT THERMAL TIME VERSUS BAR DIAMETER

Fig. 9 shows a theoretical curve which illustrates quite clearly the importance of conduction in a steel bar that is being induction-hardened. The curve is plotted to show the transient thermal time versus diameter of the steel bar when the surface of the bar is assumed to be, and maintained, at 1650 F. The transient thermal time indicates the time interval for the heat to be conducted from the surface of the bar to the center. For example, if we were to inductively heat a steel bar $^1/_2$ in. diam, and the temperature of the surface of the bar were to be raised in almost zero time to 1650 F, in approximately 0.8 sec, the temperature of the center of the bar will also be raised to 1650 F. Consequently, if it is desired to obtain a surface hardness that is metallurgically correct, the bar must be quenched in less than 0.8 sec. However, we have seen that a lapse of time is necessary for the previous structure to be converted into the solid-solution phase; hence if solid solution is not obtained in 0.8 sec, through-hardness will be obtained in quenching. Again, if solution does take place in less than 0.8 sec, then split-second quenching will be required with precision mechanical setup so that no delay exists.

TYPES OF HARDENING PROCESSES

A helpful guide for designing parts with surfaces to be induction hardened is to become familiar with the various types of inductors already available, and the methods in which they are employed. Fig. 10 shows a few of many types of inductors, each designed for a particular heating application. Parts that are to be designed for induction-hardening may fall into any one, or all, of the four general induction-heating classifications:

1 Stationary heating method.
2 Progessive heating method.
3 Continuous heating method.
4 Oscillatory heating method.

Often the type of heating process used is governed by the production requirements as well as by the metallurgical limitations. Whichever process is used, the inherent advantages of induction-hardening should not be misused. Fixtures must be designed for precise control of the heating and quenching cycle. The operation must be dependable to insure proper location at all times, and the loading and unloading time must be at a minimum. As previously pointed out, the quenching requirements are sometimes a split-second operation and a delay either way, quenching too soon or too late, may result in a metallurgically incorrect specimen.

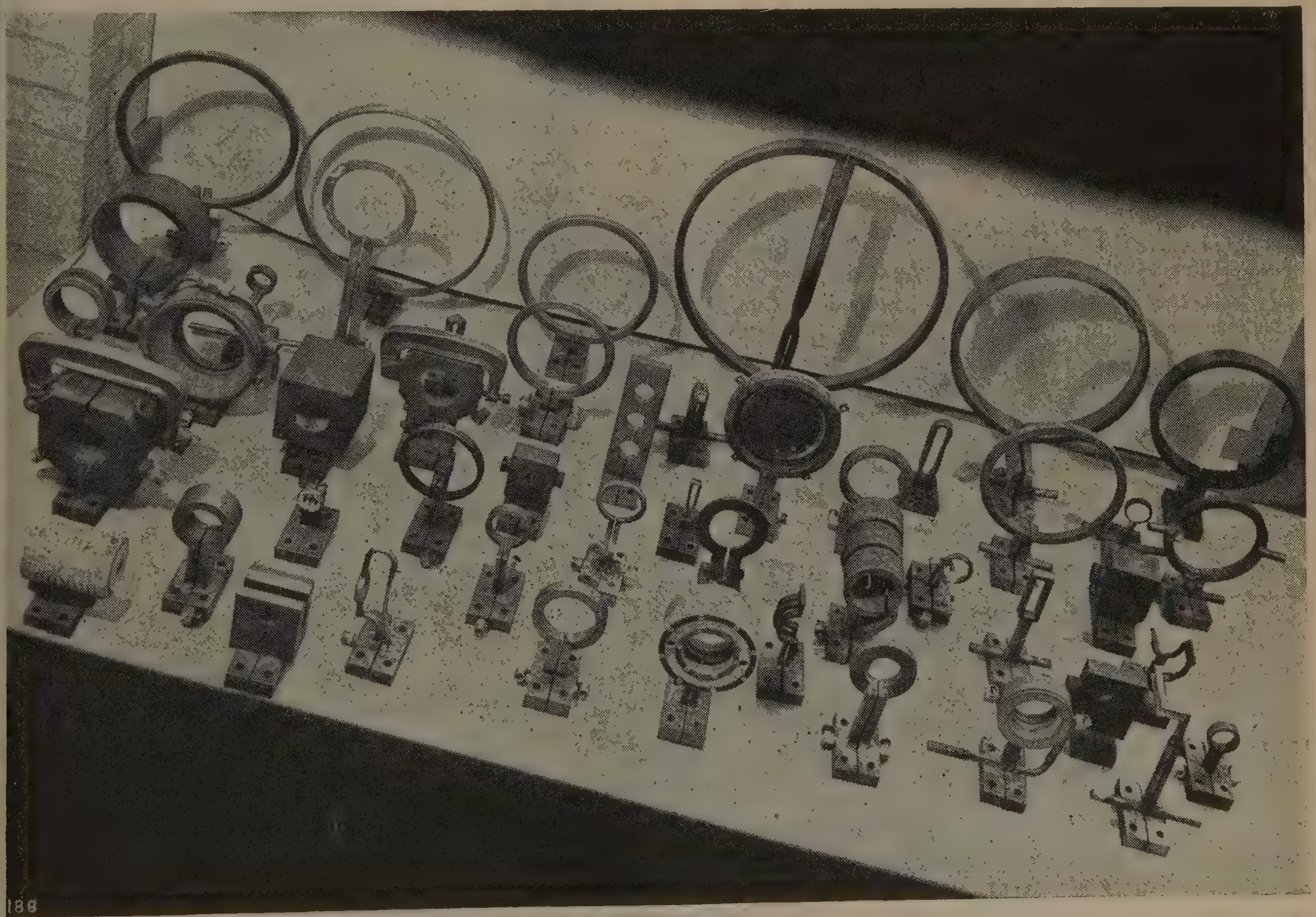

FIG. 10 INDUCTOR BLOCKS AND INDUCTOR COILS USED IN HIGH-FREQUENCY INDUCTION-HEATING APPLICATIONS

Designing Parts for Stationary Hardening

Stationary heating for hardening is the most common form of heating, and parts must be designed with finished locating areas to permit exact positioning. If various parts, similar in dimensions, are to be hardened, considerable savings in tooling cost can be realized by designing standard locating areas. Stationary positioning is adapted to heating short length, eccentric, and miscellaneous contours. Fig. 11 shows a simple post-type fixture designed to locate a spherical head stud accurately in an inductor block. The inductor is machined for cooling and quenching, and for obtaining a surface hardness over the spherical surface.

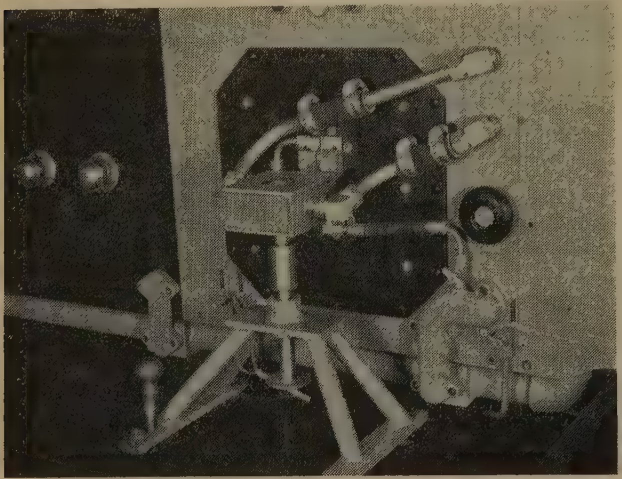

Fig. 11 Post-Type Fixture and Inductor Block Designed for Hardening Spherical Surfaces of Ball Studs

The heating and quenching cycle is controlled accurately by timers on the induction-heating machine, and the purpose of the fixture is merely to provide proper positioning during the very short heating cycle. The ball stud is located manually in the fixture by the operator and can be loaded from the top by inserting the part through the block and positioning the threaded end in the locators of the fixture. After the heating and quenching cycle the operator merely forces the plunger up, a process which raises the stud and locator and permits the operator to remove the stud and replace it with a green part.

To avoid the "fishtail" effect occurring at the split section of the inductor block, the part to be hardened should be rotated during the heating operation. Consequently, if at all possible, the parts should be designed symmetrically to permit rotation in the inductor. If the metallurgical requirements are critical, and the fishtail effect must be avoided, the ball stud may be rotated simply by mounting the plunger in a bearing and twisting the knob of the plunger during the heating cycle.

There are various post-type fixtures which can be adapted for stationary heating. If the production requirements are small, limiting the amount of funds that can be allocated for tooling, then post-type fixtures similar to Figs. 12 and 13 can be used to advantage.

Stationary positioning is of course not limited to the fixtures of the post type. There are many stationary fixtures whose designs are limited only by the ingenuity of the designer. Where the parts are long, yet require selective hardening, V-fixtures can be used to advantage. For example, Fig. 14 shows a simple V-type fixture which supports a two-throw crankshaft during the heating and hardening of one of the pin areas. The shaft extensions on either side of the eccentrics are long enough so that there is positive location on the V-supports. The second throw area is used for the locating surface in order to position the area to be heated in the inductor. Any slight variation in position may cause the hardened contour to shift, and, in addition, a loss of power will exist by the heat being dissipated into the cheeks. Consequently, parts should be designed for finished surfaces at the time of induction hardening, so that areas to be heated can be located accurately.

If the design calls for a massive part to be located, the V-supports can be positioned on dollies similar to Fig. 15. The

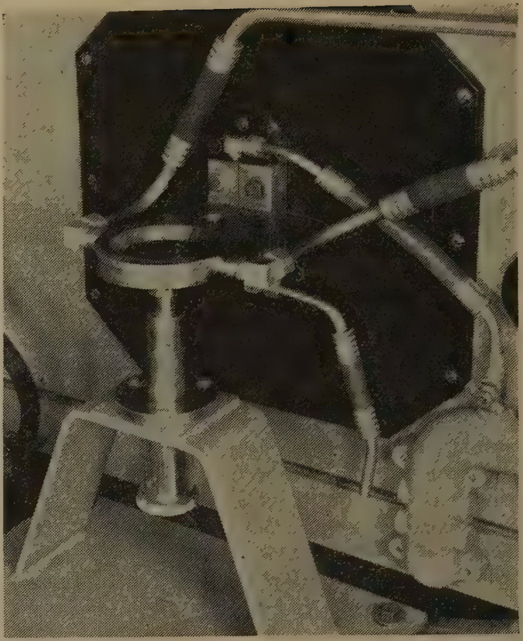

Fig. 12 Post-Type Fixture With Slotted Locator

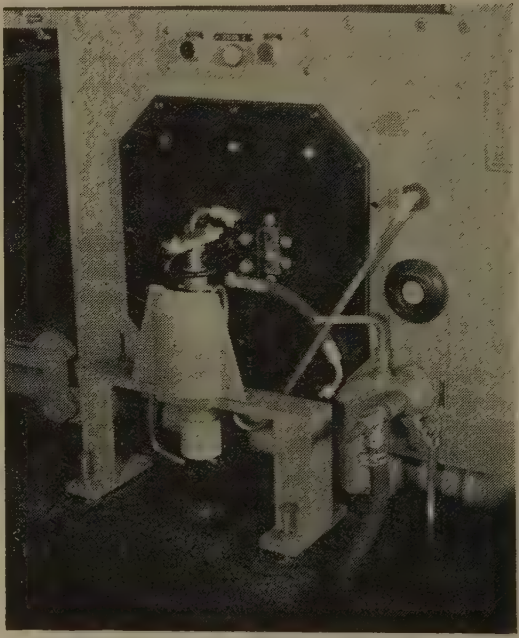

Fig. 13 Inductor and Fixture Assembly for Hardening Bottom Slot on Adjusting Screw Which Is Manually Elevated Into Inductor

(Part was previously carburized, and trouble was encountered with "ears" heating off. Now made of SAE 1045; completely machined, and then hardened.)

entire dolly assembly is then rolled into position, locating the area to be heated in the inductor. Large crankshafts with many crankpins, such as those used on automobiles, Diesel engines, and for ship propulsion, can be processed on tunnel-line induction-heating assemblies as shown in this illustration. The crankshafts are positioned on V's assembled on dollies and are rolled on their tracks from one station to the next, processing one throw area at a time.

Holes, slots, narrow widths, and sharp edges are to be avoided when designing an area to be hardened inductively. Since a very high current circulates around the area, an obstruction may cause a very high current density at a particular point and result in that area overheating. Thus, for example, the oil holes in the crankshaft, shown in Fig. 15, present a critical area, but cannot be avoided since the oil holes must be drilled in the area before hardening. In order to prevent the areas surrounding the holes from overheating and cracking, the holes are plugged with copper tubing or steel inserts, and sometimes wooden plugs.

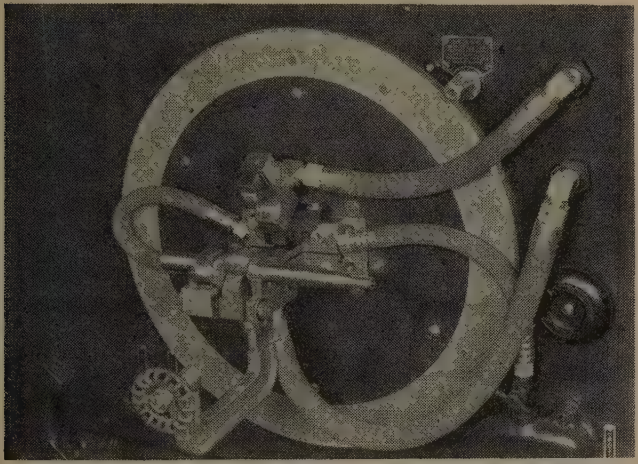

Fig. 14 V-Type Fixture and Split-Inductor Assembly for Hardening Throw Area on Crankshaft

Parts designed for induction-hardening, using stationary heating methods, offer the following advantages among others:

1 Inductors can be contoured to eccentric and nonsymmetrical surfaces.
2 Inexpensive fixtures can be used.
3 Fixtures can be designed readily to locate and position parts.
4 Quench nozzles and quench chambers are located more readily.

Locating cannot be too strongly stressed, not only for stationary setups, but for all types of heating methods. Parts should be so designed as to permit stops and positioning devices on fixtures to locate from finished dimensions at the time of hardening. The air gap between the surface to be heated and the inductor should remain constant during the heating cycle. When a magnetic material is heated inductively, there is a magnetic force exerted on the part until the temperature of the part has reached and passed the Curie point and the part has ceased to be magnetic. Also to be considered, a fact often overlooked, is the continued existence of electromotive force above the Curie point. Consequently, the part should be designed to permit the locating section to be gripped firmly by the fixture. A slight movement of the part may cause one side of the part to overheat and the opposite side to underheat, resulting in a nonuniform hardness and a varying hardened pattern.

Progressive Hardening

Cylindrical bars, rods, splines, pins, and shafts of various diameters and lengths are well adapted to induction-hardening, using the progressive heating method. A practical rule to follow is that if the length exceeds $2^1/_2$ in., it is desirable to harden the section progressively. For example, if a shaft 2 in. diam and $2^1/_2$ in. long were to be surface-hardened, using a stationary fixture, the area to be heated would be approximately 15.7 sq in. Assuming that a heating factor of 10 kw per sq in. is required to obtain a satisfactory hardness contour and hardened depth, a machine rated for approximately 150 kw would be required.

Fig. 15 V- and Dolly Supports Used for Locating Crankshafts in Tunnel-Line Induction-Hardening Setup

If, however, we resort to progressive hardening, an inductor block can be machined for cooling and quenching, and designed to scan the entire area. Thus if the block were to be $^1/_2$ in. wide, the total area heated at any one time would be approximately 3 sq in. Assuming the same heating factor of 10 kw per sq in. to apply, a 30-kw machine would be sufficient.

Fig. 16 illustrates a special progressive type of fixture capable of processing shafts up to 36 in. long. The shaft is held stationary between the centers, and the inductor block scans the surface, heating and quenching the shaft as the block progresses up the shaft. Vertical fixtures of similar type can be designed to process bars as long as 7 and 8 ft. In most applications where the part must be supported, center holes should be machined in the ends so that simple center locators can be used.

A progressive-type fixture recently designed varies from the foregoing in that the inductor is fixed, and the part to be hardened is passed through the inductor. A fixture incorporating this type of design is shown in Fig. 17 and is known as the "Toccotrol" fixture. Of particular interest is the electronic contro device, Fig. 18, incorporated with the fixture and controllin the entire heating and quenching cycle. With added control it is possible to regulate the speed of the shaft through th inductor as well as to regulate rotation of the shaft, and, at th same time, to limit the time the power is on and off. The cam arrangements and limit switches on the control rack can be prese for several heating and hardening sequences during a singl down-travel of the carriage. Once the cycle has been set, al functions are automatic, and the only requirements of the operator are to locate the shaft between the centers on the carriag and to press the starting button.

This type of fixture can be used for stationary and selectiv

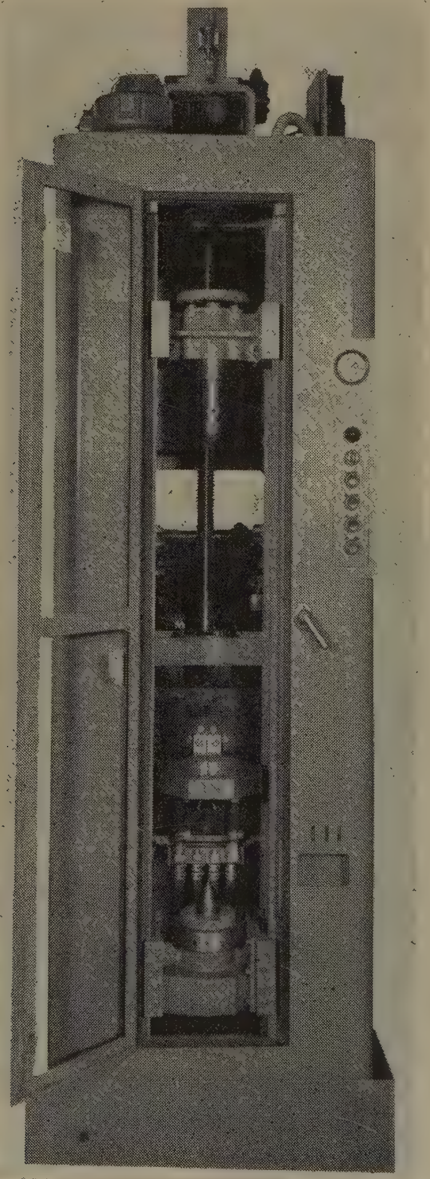

Fig. 16 Progressive Vertical Fixture With Movable Inductor

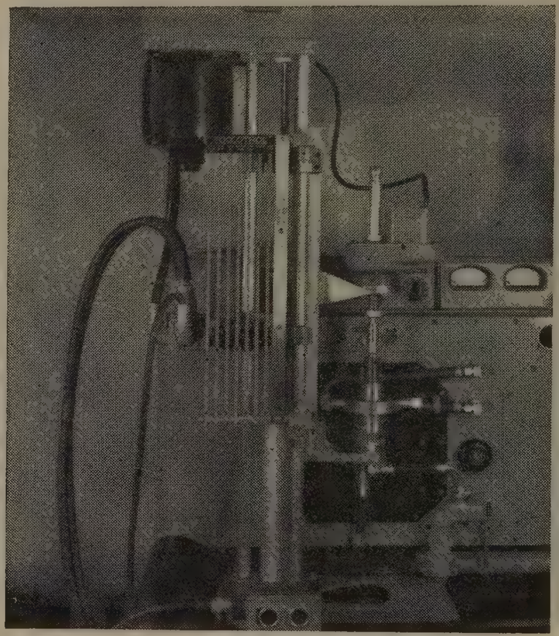

Fig. 17 "Toccotrol" Progressive Hardening Fixture

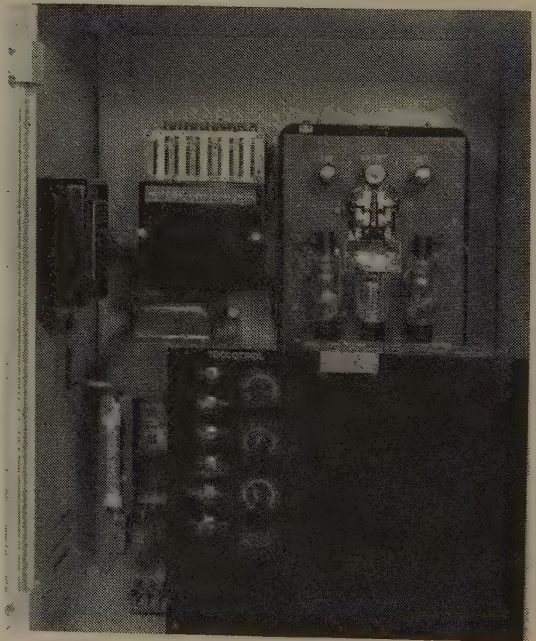

Fig. 18 Open Panel View of Electronic Controls for "Toccotrol" Progressive Fixture

hardening as well as for progressive hardening. Its unusual versatility and flexibility make this fixture adaptable for a wide variety of induction-heating applications.

In designing parts to be hardened by induction-heating and using the progressive-type fixtures, care must be exercised that no protruding area interferes with the inductor as the part passes through the block, or as the block scans the part. Should such obstructions occur in the design, the inductor must be increased in diameter for clearance and consequently cause a loosely coupled circuit, resulting in an inefficient process. An alternate step would be to use a split-type inductor, as shown in Fig. 14. In many cases, however, production requirements may not permit the loss of time in opening and clamping the inductor. Metallurgical requirements also may call for a hardened surface up to the shoulder of the protruding area, but because of this protrusion the quench water will not pass over the heated area and consequently the result will be a nonhardened surface.

Although the technique has been developed satisfactorily to harden irregular surfaces, such as slots, threads, splines, grooves, and the like, using induction-heating methods, caution should be exercised in the design which combines such areas with straight surface hardening. Unless inductors are specifically designed to harden irregular surfaces, for example, a slot or a splined area, difficulties may be encountered not only from the overheating as previously mentioned, but also from the erratic splashing caused by the quenching water on the irregular surface.

One of the outstanding features of induction-hardening is the tendency to minimize distortion, especially where a long bar is to be surface-hardened. Tests on many parts indicate that distortion can be minimized further by rotating the part during the heating and quenching operation. If, however, the surface to be hardened contains an obstruction or irregular surface, as mentioned, rotation may have to be eliminated because of the uncontrolled splashing.

Continuous Hardening

Invariably the costs of the tooling required to harden a part continuously is greater than the tooling costs for induction-heating methods using stationary or progressive fixtures; but in many cases this cost is justified by the increased production and minimum labor requirements. Continuous fixtures include, among others, conveyers, rotating tables, pushers, and indexing and cam control mechanisms. If parts can be designed for hopper feeding and chute spills, Fig. 19, manual loading can be eliminated, making the entire process completely automatic.

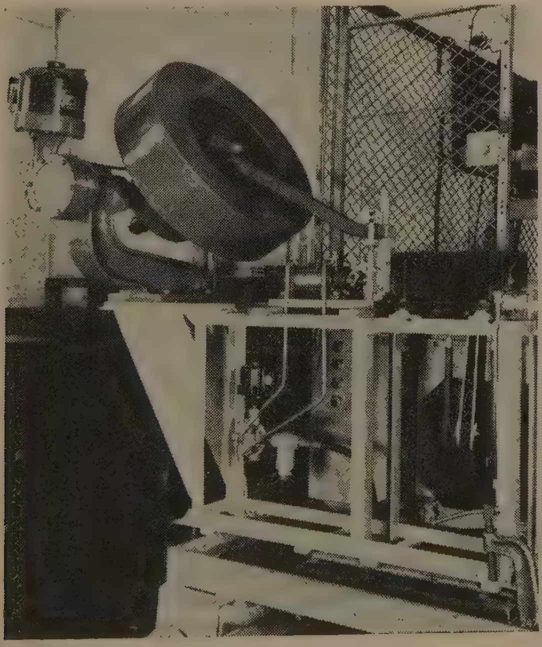

Fig. 19 Hopper-Feed Mechanism Used in Induction-Hardening Application

Whatever method is used, the designer must exercise caution so that the part can be positioned properly and located during heating. Tooling is often the greatest burden in a manufacturing process; consequently, in designing a part, consideration should be given to the fact that continuous loading and unloading will cause locators to wear. Locating areas should provide sufficient length and clearance, so that spring or tension devices used on fixtures can be insulated from any heat which possibly may destroy its elasticity. At all times it must be kept in mind that induction-heating is a direct result of the magnetic lines of force or flux produced by the inductor, and that any metal passing through the magnetic field, be it the part to be processed, or be it the fixture, will be heated. Although the fixture may be designed to resist high temperature, close coupling of metallic parts of the fixture to the inductor may absorb power, and as a result destroy the heating cycle and cause the part to be underheated.

Fig. 20 shows a continuous-hardening fixture of the rotating-table type. The application consists of hardening the ball end of the stud. The stud end is sufficiently long in this case for the locator to be designed well below the magnetic field of the coil and still locate the ball head in the induction coil. With a shortened stud extension, the table locators would have to be raised in order for the ball end to enter into the channel inductor. Consequently the locators would have to be made of nonmagnetic material, such as stainless steel, brass, or ceramic material.

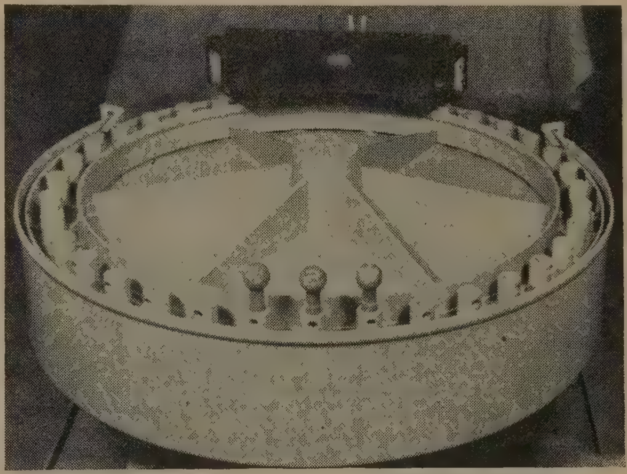

Fig. 20 Rotating-Table Fixture for Hardening Ball Studs Continuously

Fig. 21 illustrates a continuous roll-type fixture which is used for hardening and annealing round bar stock. The minimum length which can be processed with this type of fixture is $4^{3}/_{4}$ in. The cross section of the bar stock may vary from the round to rectangular, or polygonal cross section, and the same fixture can be used, except for a change in roller design.

The following example illustrates to the design engineer how the hardness requirements can be met through the practical applications of metallurgical fundamentals and simple fixture design, when the design of the part to be hardened is fixed: Shown in Fig. 22 is a unique rotating cam fixture mounted on a 450,000-cycle high-frequency induction-heating machine, used

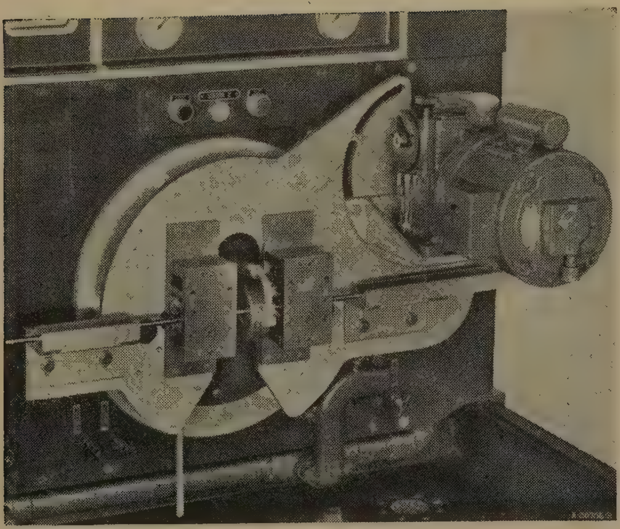

Fig. 21 Roller-Type Continuous Fixture Used for Hardening Bar Stock

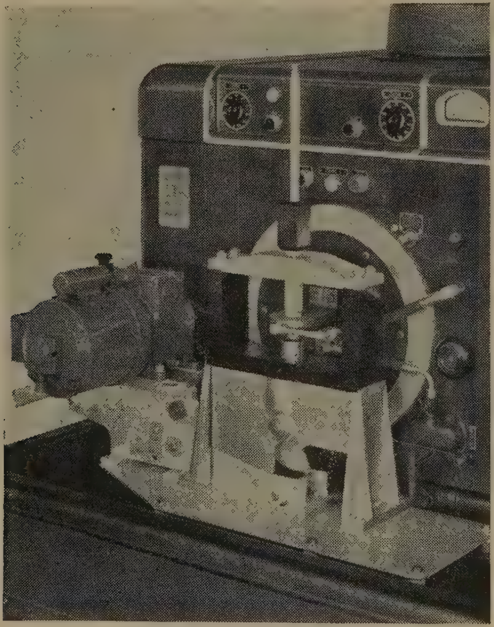

Fig. 22 Generated Cam-Feed Fixture Used for Hardening Chain-Link Pins

for hardening small link pins for chain conveyers. Thousands of link pins per day were required, and the metallurgical specifications were exacting, necessitating precise control over the heating cycle.

The pins were approximately 1 in. long and $^{3}/_{16}$ in. diam, made of heat-treated SAE 4065 steel. Specifications required maximum surface hardness of good metallurgical structure over the center body, and approximately $^{1}/_{8}$ in. at each end was to remain soft. The soft ends were necessary for a riveting operation during the assembly of the chains.

The pins were fed through a funnel opening and passed down through a long tube into an inductor block machined for cooling and quenching. The pins rode on the periphery of a generated cam and consequently progressed downward at a constant rate as the radii of the cam gradually decreased. As the full length of the pin emerged, the pin was flicked out by the cam notch and the following pin automatically rode on the maximum outside diameter of the cam. The production rate was governed by the revolution and the number of notches in the cam.

Obviously, with the heating cycle set for continuous operation, the entire length of the pin would be hardened unless the power was cut off as the ends of each pin entered and left the inductor. This would be undesirable in view of the mechanical difficulties to maintain breakers and relays which must operate more than 4 times every second to maintain a production approaching 15,000 pins per hr.

The problem was solved by taking advantage of the fact that time and temperature are required for the previous microstructure of the pin to go into the austenitic solution, in order that on quenching, the hard martensitic structure can be obtained. The generated cam was redesigned so that the periphery decreased at a greater rate at the end of the heating cycle, thus causing an increase in vertical speed of the pin at the precise instant the ends of the pins passed through the inductor. Since the power cycle was set for one speed, any increase in speed would cause the pin at that particular time to be underheated. Consequently, on quenching, the previous microstructure of the pin would not convert to a hardened structure.

Parts Designed for Oscillatory Heating for Hardening

Parts designed with flat surfaces and valleys to be hardened may require an oscillating heating method since it may not be possible to obtain a uniform temperature over a wide surface by the methods described. Wall-thickness variations, drilled holes, grooves, and the like may cause areas to overheat while adjacent areas have not reached the critical temperature; consequently, an inductor is passed over the surface of the part at a predetermined frequency until the heat has soaked into the part long enough to result in a uniformly heated surface. Oscillating heating is not usually recommended because of the experimental work required to obtain an acceptable heating cycle. In addition, considerable setup time is necessary with automatic equipment, and relatively long heating cycles.

Conclusion

In view of the accelerated production requirements, high-frequency induction-hardening methods are being incorporated more and more in the design specifications. Considerable progress already has been made in the development of fixtures and machines for a variety of applications. A review of the technique involved can serve as an excellent background for the designing engineer.

In summarizing, it has been pointed out that factors such as production requirements, metallurgical limitations, and fixture designs exert their influence on the final part to be hardened.

Acknowledgment

The author wishes to extend his appreciation for the material assistance given by J. T. Vaughan and J. B. Wadhams of OCCO Research and Development Section.

Discussion

A. S. Hamilton, Jr.[2] This discussion is from the point of view of the user of the equipment described, and without too specific knowledge of the fine points of heat-treating.

The frequencies used for this process are mentioned only twice, and, with the large difference between 10,000 cycles and 450,000 cycles, one is led to wonder about the significance of the frequency and why such variations exist.

---

[2] Consulting Engineer, Rochester, N. Y. Mem. ASME.

In mentioning the construction of the locators or work-holding devices, the author states that nonmagnetic materials, such as stainless steel, brass, or ceramic materials may be used. During the war the writer was familiar, in detail, with two types of high-frequency heating units, one of which (a Tocco machine) was used continuously for soft-soldering of two parts of a brass diaphragm assembly, and the other of which was used for general heat-treating, as well as for silver-soldering two brass pieces. Although it may be possible to use metallic nonmagnetic work holders at some frequencies, it has been the writer's experience that ceramic, bakelite, formica, or asbestos board had to be used for locators or work-holding fixtures.

With these exceptions, the paper presents in simplified form the type of work which can be handled by high-frequency induction-hardening in a manner that can be understood readily by one not too well versed in the subject.

D. C. K. Mitchell.[3] In the hardening of steel by the usual furnace practice, a quenching temperature of approximately 1450 F is normally contemplated, depending upon the analysis of the material. With induction surface-hardening, it is not unusual to employ temperatures around 1600 F, and, in some cases even higher, which is often surprising to persons familiar with the older furnace practice.

Normally, we associate higher temperatures with increased grain growth from our experience with furnace practice. However, we should bear in mind that grain growth is a function of temperature and time, and therefore where the surface to be hardened is brought up to temperature in the very short period of time usually attendant upon the induction-heating process, grain growth does not have time to take place.

Experience has shown that with a given analysis of steel, two similar parts, the one hardened by conventional furnace methods and the other surface-hardened by induction, a finer grain structure may often be expected in the induction-hardened sample, even though the surface temperature at the time of quenching may have been 150 to 200 F higher than that used for the furnace-hardened sample.

J. B. Wadhams.[4] Clarification is submitted of the depth to which heat penetrates under the heading "Definition of Induction Heating."

Once the bar is properly positioned in the inductor, the depth to which the heat penetrates into the bar is a function of the physical properties of the bar, such as its size, shape, molecular density, specific heat, resistivity, permeability, thermal and electrical conductivity, and previous metallurgical structure, as well as the frequency of the currents induced therein, the power absorbed, and the time consumed.

Further clarification of the interpretation of Fig. 9 seems in order:

For example, when bars to be surface-hardened by induction are of the order of $^1/_2$ in. OD or less, one might draw the conclusion that the use of higher-frequency energy should suffice to produce light case depths. This is not always the case because of the limiting heat-conduction factors which occur when the bar or load size is small.

Fig. 9 of the paper is a calculated plot of bar diameter in inches for a medium-carbon steel versus time of application of temperature to that bar. The curve drawn is the product of a logarithmic and Bessel function. Its derivation springs entirely from physical and thermal considerations. This characteristic is obtained by assuming that the outer surface of a given bar size was raised instantaneously from room temperature to 900 C and held at this condition. The abscissas were computed to determine how much time would pass under the foregoing surface condition before the center line of the bar was likewise raised to 900 C by conduction. Although this highly theoretical condition does not occur in practice, nevertheless, it is a useful tool in guiding the engineer when the problem of surface-hardening small-diameter bar stock exists. The term "transient thermal time" was picked for lack of a better definition for this time interval. Therefore this curve might be considered as obtainable by the use of induction energy, where its power density is very large but finite, and its frequency infinite, so that the initial depth of current penetration would be zero.

In practice, it is recommended to use this interpretation of transient thermal time. If one is able by induction to induce sufficient power at a given high frequency into a small-diameter bar to surface-harden it, then it is necessary to interrupt the heat and quench immediately before this transient thermal time has passed; otherwise the bar will be through-hardened upon quenching.

Several points on this characteristic have been well borne out in practice. For one example, $^3/_{16}$-in-OD pins 1 in. long have been surfaced-hardened in a stationary position by using 500-kc energy with power densities of the order of 50 to 100 kw per sq in., and heating times of a fraction to 1 sec. It was found that if the heating cycle were lengthened $^1/_{10}$ sec, through-hardening of the pin resulted, everything else being the same. This result tends to verify the transient thermal time for this size of bar diameter as shown in Fig. 9.

Author's Closure

The author welcomes Mr. Mitchell's comments and field experience which verify the fact that an induction-hardened bar under limited conditions will have a higher hardness reading than can be obtained by the conventional furnace method. To explain this superhardness, it is necessary to consider the reasons for hardness in a martensitic structure. These are still controversial in nature and, to date, have not been explained completely. It may be due to the extremely homogeneous austenite resulting from the rapid carbide diffusion and, as Mr. Mitchell points out, with an attendant small grain size. It may be due to internal strain setup, owing to rapid cooling with a backing of unaffected metals. J. B. Austin[5] refers to the theory that the hardness is associated with the tetragonal structure of martensite and is essentially a structure distorted by the principles of carbon atoms and possessing no planes on which gliding is easy. Whatever explanation is used for the resulting high hardness due to induction hardening, we who have worked in the laboratory do not find it unusual; in fact, we view it as commonplace to produce a hardened surface with a few points higher hardness readings than can be obtained under ordinary conditions.

To Mr. Hamilton, we should like to say that it was not our intention to limit the manufacture of the locator to ceramic materials only. Many types of materials, such as ceramics, refractories, and plastics are used under specific conditions. It is to be noted, however, that there are very few plastics or fibrous materials which can stand up in service when heated to 600 F or over. Since the temperature for induction hardening approaches 1600 F, materials used for locating devices may deteriorate rapidly and become a maintenance problem if too closely located to the heated area. For example, transite is used in great quantities in making housings and fixtures supports as well as locators in induction applications. Transite, a composition of cement and asbestos, will pick up 15 per cent moisture and eventually may become waterlogged and disintegrate if placed within a water-quenched area. Although varnish is often used to coat the transite to make it water-repellant, heat and service eventually cause the varnish to wear off.

---

[3] Induction Heating Specialist, Rudel Machinery Company, Inc., New York, N. Y.

[4] The Ohio Crankshaft Company, Cleveland, Ohio.

[5] "Current Theories of the Hardening of Steel Fifty Years Later," by J. B. Austin, *Metals Progress*, vol. 54, August, 1948, p. 201.

Where the locators can be positioned at a distance from the area heated, various types of materials, as pointed out by Mr. Hamilton, can be used and are used by us in our laboratory and in the many fixtures which we design. If in locating an area to be heated the locator must come in contact with material at high temperature, a critical problem exists which few plastics, refractories and ceramics can meet. It is for this reason, in many continuous heating applications, for example, slug heating, that Nichrome tubes are used. Nichrome will stand high temperature and is nonmagnetic. In addition, if the diameter of the Nichrome tubing is small in comparison to the part that is heated, little power will be absorbed. A second example is found in locating ball-bearing races which are through-heated and hardened one at a time. The ball-bearing races are heated to over 1800 F and oil-quenched in position. Our experience shows that locators made from stainless steel are very satisfactory, and the knife-edges which support the race have a high service life.

Frequency has little to do with the type of material used in making fixtures. It is necessary of course to use caution when high voltage, which is associated with electronic frequencies, is used. For example, some electronic high-frequency sets have stud posts with over 10,000 volts across their terminals, and these studs appear in the working area. Materials used in fabricating the inductor housing of integral locating fixture must have high dielectric strength and corrosion-resisting properties in order to minimize any voltage breakdown during service.

Discussion in this paper was limited to 10,000 and 450,000 cycles because these two frequencies are standard and are used in industry. Standard equipment is now available with most induction-heating manufacturers, and these frequencies can be adapted to over 90 per cent of all induction-heating applications. Frequencies used in induction hardening range from as low as 1000 cycles to as high as 3,000,000 cycles. In specific induction-heating applications, frequencies as low as 60 cycles are being used.

The points for clarification, as presented by Mr. Wadhams, are gratefully received. All too often users of induction-heating equipment and induction-heating designers neglect to consider the fact that the heated depth is affected by the heat conducted through the part. The importance of heat transmission h been emphasized by Dr. H. B. Osborn, Jr.,[6] which illustrat that the heated depth is due to the depth of high-frequenc current penetration and the additional depth from thermo he flow; thus

$$\left.\begin{aligned} D_1 &= \sqrt{4/F} \\ D_2 &= \sqrt{0.0015T} \\ D_T &= D_1 + D_2 \end{aligned}\right\} \text{(heating to 1600 F minimum)}$$

D_1 = depth in inches of metal in which most of heat generate
F = frequency in cycles per second
D_2 = additional depth in inches resulting from thermal he flow
T = heating time in seconds.
D_T = total depth

The author wishes to state that there does not exist today a accepted common definition of hardened depth. In this pap we have considered the hardened depth to be that depth at whic the hardness range has decreased to 50 RC and experiment work was with steel containing 0.40–0.50 per cent carbon. It to be noted that steels with lower carbon content are also indu tion-hardened, but because of insufficient carbon may not reac 50 RC, even on the surface. Yet these heat-treated materia are considered to have a hardened depth.

In some circles, the hardened depth is considered to be th depth below the surface at which the hardness reading has decreased to one half of the over-all range of hardness. For example, if the surface of the steel is 47 RC and the core is 15 RC the hardness range is 32 RC. The hardened depth would the be considered to be that point below the surface where the hardness has decreased to 31 RC.

Where the steel is carburized, carburized depth often become the hardened depth. Many manufactureres consider the hardened depth to be that depth at which the microstructure has bee affected to show a hardness reading greater than the hardnes of the original core. It should be pointed out, however, that, i a majority of cases, the user maintains a hardness-depth specification which is governed by proved service of the part to withstand wear.

---

[6] "Design and Manufacture for Profit," by H. B. Osborn, Jr. *Mechanical Engineering*, vol. 70, 1948, pp. 805–810.

How Forging Acts to Enhance Metal Properties

BY E. O. DIXON[1] AND E. J. FOLEY,[2] CUDAHY, WIS.

Heretofore unrecognized effects of high impact pressures eveloped by forging steel in closed dies have been studied. lechanical properties are compared for conditions of arying restraint to metal flow. Forging tests have been evised to permit analysis of impact pressure with and ithout accompanying plastic flow as separate effects. igh impact pressures developed in drop forging contribte substantially to the improvement in ductility and otched-bar toughness. This is demonstrated under onditions of negligible plastic flow.

INTRODUCTION

METALLURGICAL literature contains numerous references to the effects of forging upon the physical properties of steel. Heretofore, maximum emphasis has been aced upon development of grain flow with directed methods of ot-working. The refinement of crystalline structure from that ccurring in the original ingot and the increase in ductility and ughness, particularly in the direction of greatest plastic flow ave been discussed.

It is the purpose of this paper to evaluate the effect of the ot-working method upon the physical properties of steel. The ope of the investigation includes the effect of hammer-forging r reductions increasing from zero to 96 per cent, when open es are used. In order to evaluate more completely the effect forging upon properties, steel was forged under conditions of straint employing closed dies. In the closed-die studies, llet material reduced 80 and 92 per cent by rolling was emoyed. The effect of forging ingot material in closed dies was bserved in order to evaluate more completely how the high ressures used in drop-forging influence properties of steel.

NATURE OF FORGING METHODS

There is at best among designers only a general understanding the effect of hot-working upon physical properties. It is kely that designers of heavy equipment, using components rged directly from the ingot, have been confronted more riously with the effect of hot-working upon directional properes than have designers of forgings made in drop hammers emoying closed dies.

An ingot is a casting which possesses inherent weakness springg from the solidification mechanism. The resultant structure somewhat coarse and may vary from a massive columnar ystallization at its periphery to an equiaxed crystalline structure thin the body of the ingot. The solidification of such a large ass proceeds relatively slowly, resulting in some segregation. oids due to entrapped gas and shrinkage cavities can exist. onmetallics are distributed in varying degree in accordance th the mechanism of solidification. The mechanical design of an ingot is such as to promote maximum soundness throughout the body of the cast form and to concentrate imperfections in a special easily removed section called the hot top. Ingots, particularly those designed for subsequent forging, thus represent the maximum in metallurgical quality obtainable by freezing molten metal masses of the sections typically used.

Hot-working an ingot, whether by forging or rolling, has not only the object of producing a desired geometry, but also that of altering structure, breaking up segregates, and actually welding cavities or voids. The nonmetallic segregate is distorted and broken up and, to some extent, redistributed, and the inherent coarsely crystalline structure is reduced to one that is finer. Direction of metal flow and amount of reduction affect distribution and shape of the nonmetallics, imparting a definite influence on the grain flow associated with wrought steel.

To the users of various types and sizes of forgings, the term "forging" may have widely different meanings. To the designers of large industrial equipment, a forging is a large shape up to several feet in diameter, hot-worked directly from an ingot which may be as large as 110 in. diam and weigh up to 500,000 lb. Ingots are forged in hydraulic presses of up to 12,000 tons capacity using flat dies, and the shape produced must be deemed a crude approximation of the finished component. Tooling and equipment required in the production of such forgings are large, and the process involved is costly. However, the insurance of greater uniformity in dynamic properties and internal soundness has convinced engineers that greatest ultimate economy and satisfactory performance are to be had through the use of such forgings. Steam-turbine spindles, generator rotors, marine propulsion shafting and pressure vessels for the power, oil, and chemical industries are a few examples of forgings made directly from the ingot.

To other users of forgings, the process implies use of steam hammers equipped with flat dies and employing material which has received prior plastic work from the original ingot by rolling. The kinetic energy developed by the freely falling weight of ram, rod, and piston, accelerated by pressure of expanding steam in the cylinder, is released quickly when die contact is made with the steel being forged. Steel is hot-worked by the high impact pressures developed when the kinetic energy developed by the falling weight is absorbed in a very small time interval. The contour of the forging produced is a rough approximation of the finished part. Forgings vary in weight, ranging from a few ounces to several thousand pounds. This method of production is particularly adaptable where quantities involved do not warrant sinking dies, or where dimensional geometry precludes the production of a drop forging.

Steam drop hammers are the principal source of large quantity production of forgings whose shape resembles closely the design of the finished component. Drop forgings are used for most dynamically loaded aircraft parts, in heavy-duty truck and tractor applications, in the automotive industry, and for deep-well drilling tools, to mention but a few of their many uses. The size of drop forgings may vary from several ounces up to 3500 lb. Ratings of the steam drop hammer range from a few hundred pounds up to 50,000 lb. High kinetic energy, developed by falling weight of ram, rod, and piston which is ac-

---

[1] Chief Metallurgical and Mechanical Engineer, Ladish Company. em. ASME.

[2] Research Metallurgist, Ladish Company.

Contributed by the Metals Engineering Division and presented the Semi-Annual Meeting, Milwaukee, Wis., May 30–June 5, 48, of THE AMERICAN SOCIETY OF MECHANICAL ENGINEERS.

NOTE: Statements and opinions advanced in papers are to be derstood as individual expressions of their authors and not those the Society. Paper No. 48—SA-60.

celerated by pressure of expanding steam, is dissipated suddenly on contact with the steel being forged. The unique manner in which the high impact pressures build up as forging proceeds will be developed further in this discussion.

Board drop hammers are used to a large extent in the production of smaller drop forgings. Kinetic energy is developed by a freely falling weight from a constant height for successive strokes. Energy dissipation and impact pressures developed follow the same pattern as in the case of the steam drop hammer. Since terminal velocity developed in the board drop hammer is purely a function of height of fall, a few comparisons may be made with the steam drop hammer. Terminal velocities of 30 fps have been measured for steam drop hammers having a stroke of 4 ft. An equivalent terminal velocity in the board drop hammer requires a free fall height of approximately 16 ft. Since length of stroke for equivalent terminal velocities is much greater with the board drop hammer, the number of blows per unit time is less. However, in practice, it is not practicable to design and operate a hammer having a free fall height sufficiently great to give a terminal velocity equal to that of a steam drop hammer. Mechanical difficulties also limit the falling weight that can be used economically in a board drop hammer. Actual forging practice, then, limits the size of board drop hammers used with the result that steam drop hammers constitute the source of impact-forging equipment developing maximum kinetic energy.

Forging in closed dies, however, may be done using several types of equipment in addition to the drop hammer. Mechanical and hydraulic presses are used widely for production of contour or closed-die forgings of relatively small size. Forging machines, often referred to as upsetting machines, likewise may be used to produce certain of the shapes made with presses and hammers. The design of the forging machine and its manner of operation make it especially valuable for forging only a portion of a bar as in a pinion shaft. It also affords a most economical method of gathering stock for subsequent final forging operations. Where the production quantities and standardization of forgings warrant, highly specialized forging equipment has been designed for the performance of specific tasks. Such equipment as rock-bit pointing and mushroom-valve forming machines are examples of specialization in the production of forgings made in closed dies.

It is not the purpose of this paper to discuss the choice of methods of forging as they are affected by economies of production or design. All of the forging equipment has its sphere of usefulness in the forging industry. Each is used to meet the problems posed by forming of specific shapes and sizes in various quantities. However, we may consider the manner in which certain of these various tools work steel in the forging operation.

OPERATING PRINCIPLES OF PRESSES AND HAMMERS

Presses, whether mechanical or hydraulic, and forging machines when used to operate closed dies, impart an increasing pressure upon the steel reaching a maximum at the end of the stroke. Energy available is a function of a definite mechanical linkage or piston relationship. Rate of energy dissipation is, in general, much slower than that with impact forging tools.

The steam hammer, whether flat die or drop hammer, differs in operating principle from press or forging machine. Energy obtained by the falling weight of ram, rod, and piston, is increased by pressure of expanding steam against the piston. The amount of energy may be varied within wide limits by regulating the length of stroke and pressure cycle employed. The gravity drop hammer, however, differs from the steam hammer in that energy is received only from the freely falling weight of the ram, generally from a height constant for successive blows.

When steel is forged in open dies, regardless of method, the only restraining action is resistance of the hot metal to the forces acting upon it and friction between metal and die surfaces. Where action is slow and time of contact is long, the dies exert a chilling effect upon the steel. When the action is fast and die contact time is short, as in the steam hammer, chilling effect is minimized.

When steel is forged in closed dies, regardless of method, material flows in a fashion affected by its internal resistance to deformation and the frictional relationship of steel and die surfaces. As the steel fills the die impression, resistance to metal flow increases and a condition approaching complete restraint to metal flow is developed. Excess metal is forced out as flash, cooling quickly and increasing the resistance to further flow.

We may at this point compare the relative action of different types of forging equipment when the die is filled and the forging is almost at desired thickness. A condition of great restraint to metal flow exists as just mentioned. Mechanical and hydraulic presses or forging machines require increased power to perform the finishing operation. This increase is due to internal resistance to metal flow because of drop in temperature and the restraining action imposed when excess steel is forced out of the impression as flash. Maximum pressure is built up, gradually increasing to a maximum at the end of the stroke.

ENERGY ANALYSIS OF DROP HAMMER

An analysis may be made of the energy dissipated upon impact when using a drop hammer. If we consider the terminal velocity of a 50,000-lb steam drop hammer at a measured value of 30 fps, kinetic energy available at the moment of impact is about 700,000 ft-lb. Measurements of die-contact time with the steel pose several problems which have not been solved at present. However, we know that in the final finishing blows a forging may be reduced as little as 0.005 in. Considering total deflections in the hammer and its foundation, it has been approximated that the striking mass of 50,000 lb is brought to rest in about 0.020 in. This would result in the short contact time of only 0.00011 sec., resulting in a dissipation of more than 10,000,000 hp. It is doubtful if any other metalworking equipment produces as great force on the metal being forged as does a steam drop hammer when steel is struck under conditions of great restraint. It is the very high rate of release of energy which produces this extreme pressure on forging in closed dies.

Previous investigators do not appear to have considered separately the two factors of high impact pressures and metal flow in studying the effects of forging. As will be shown herein, these effects can be separated for investigational purposes. It will be demonstrated that pressure alone contributes a substantial proportion of the improvement gained through forging.

INITIAL STUDIES OF FORGING EFFECTS

While grain flow is associated with open and closed-die forgings, as with other methods of producing wrought shapes, an impression appears to exist among some users of forgings that a difference exists in strength parallel with and transverse to the direction of grain flow. It will be of interest to analyze facts revealed by past and present experimental work. Competent investigators, as early as 1925, have shown that while differences in static tensile strengths in various directions are small, improvement in ductility and dynamic strength is produced in all directions by forging. Moreover, improvement in notch toughness and endurance values is consistently greater in the direction of maximum plastic flow.

Data may be referred to at this time illustrating the effect of open-die forging on longitudinal and transverse properties.

TABLE 1[a] EFFECT OF CROSS-SECTIONAL REDUCTION IN FORGING UPON MECHANICAL PROPERTIES

Cross-sectional reduction, per cent	As-cast ingot		75		87.5		96	
Test direction	Longitudinal	Transverse	Longitudinal	Transverse	Longitudinal	Transverse	Longitudinal	Transverse
Elastic limit, psi	36900	36700	45300	44000	46800	46800	45000	42400
Yield point, psi	45600	41000	47500	48300	47500	47500	46200	43300
Maximum stress, psi	86000	87500	81600	82000	79600	80000	80800	80800
Elongation, per cent	19.7	18.2	30.8	29.0	33.4	22.2	33.1	28.5
Reduction of area, per cent	25.8	23.6	57.4	48.4	58.3	23.8	58.7	43.5
Izod, ft-lb	16.7	17.0	34.0	27.3	61.7	30.0	74.0	29.0

[a] Original data of Aitchison and Johnson[3] converted from tons per square inch to psi.

Aitchison and Johnson[3] studied directional properties of several analyses. Data for a carbon steel are shown in Table 1. The original material used in this study was trepanned to obtain a $13^{1}/_{2}$-in-diam section from the center of a 28-in. octagonal ingot. Center location was chosen to obtain only equiaxed material in the as-cast condition. Reductions of 75, 87.5, and 96 per cent, respectively, were made by open-die-forging methods. Material was tested after normalizing at 1562 F (850 C). Composition tested was as follows: Carbon 0.34, manganese 0.79, sulphur 0.063, phosphorus 0.046, silicon 0.13, nickel 0.15, chromium 0.22. No appreciable difference was found for longitudinal or transverse ultimate strength, elastic limit, and yield point. The difference between longitudinal and transverse Izod values was found to be greater than the variation in ductility.

In fatigue tests on the foregoing material and other analyses, Aitchison and Johnson[3] observed a maximum deviation of 17 per cent fatigue strength of longitudinal and transverse specimens. The results of their fatigue tests are shown in Table 2.

TABLE 2 EFFECT OF REDUCTION IN FORGING UPON ENDURANCE STRENGTH

Condition	Endurance limit, psi	
	Longitudinal	Transverse
As cast	±29200	±28300
75 per cent reduction	±36300	±33700
87.5 per cent reduction	±36300	±30300
96 per cent reduction	±35800	±33700

Mechanical properties such as ultimate strength, elastic limit, and yield point showed little variation with forging direction. Improvement in ductility, toughness, and fatigue strength was greater in each case for longitudinal tests than for transverse specimens. While the average endurance limit observed for the as-cast material was ±28,700 psi, the average endurance value for reduction of 75 to 96 per cent was ±34,300 psi. The minimum improvement in endurance was approximately 7 per cent. Hence the effect of forging upon fatigue strength is equivalent to substantial improvements in life or maximum load under conditions of widely fluctuating stress.

Comparison of Open-Die and Closed-Die Forging

About 4 years ago, initial data obtained by forging equivalent shapes in open dies and in closed dies gave a first quantitative indication of the greater improvement in toughness and ductility resulting from closed-die forging as compared to open-die forging. In this experiment two shafts were forged to $4^{1}/_{4}$ in. diam using 4-in. round-cornered square billets of the following chemistry: Carbon 0.23, manganese 0.90, phosphorus 0.022, sulphur 0.026, silicon 0.018.

The open-die shaft forging was made under a 2500-lb hammer using flat dies. The forging was air-cooled from a finishing temperature of 1850 F, using 75 blows to make the forging. The closed-die forging was forged in a 12,000-lb hammer employing 8 blocking and 11 finishing blows, and the finished forging was air-cooled from a temperature of 2040 F. Properties obtained from each forging are given in Table 3.

Noticeable particularly is a major improvement in transverse ductility obtained by forging in closed dies under conditions of great restraint and with extremely high impact pressures.

A second experiment of similar nature was performed employing alloy steel of NE 8744 chemistry and following forging with heat-treatment to obtain higher mechanical properties. Results of this series of tests are given in Table 4.

These results indicate likewise a distinct improvement in transverse ductility when forging in closed dies. The strength properties in both tests show no substantial difference with variation in direction.

Having obtained initial information showing increased transverse ductility in the closed-die forging, as compared with open-die forging, a question arose regarding the effect of impact without appreciable plastic flow. In order to evaluate the effect of high pressure without plastic flow versus high pressure with plastic flow, a third experiment was performed.

Test billets of SAE X-4340 were machined into cylinders $3^{3}/_{4}$ in. diam × $8^{1}/_{4}$ in. long. A second group of test pieces was machined into cylindrical form $4^{1}/_{2}$ in. diam × 6 in. long. All

TABLE 3 COMPARATIVE EFFECT OF FORGING IN OPEN AND CLOSED DIES UPON MECHANICAL PROPERTIES

	Open-die forging			Closed-die forging		
Direction of specimen axis	Longitudinal		Transverse diametral	Longitudinal		Transverse diametral
Location of specimen	Surface	Center		Surface	Center	
Ultimate strength, psi	83500	73700	69250	80500	74000	74200
Yield point, psi	54400	48000	48750	56800	47700	52000
Elongation in 2 in., per cent	32.4	35.5	11.0	36.2	38.5	26.0
Reduction of area, per cent	70.2	63.3	13.7	73.2	73.7	48.4

TABLE 4 COMPARATIVE EFFECT OF FORGING IN OPEN AND CLOSED DIES UPON MECHANICAL PROPERTIES

	Open-die forging			Closed-die forging		
Direction of specimen axis	Longitudinal		Transverse diametral	Longitudinal		Transverse diametral
Location of specimen	Surface	Center		Surface	Center	
Ultimate strength, psi	127000	124500	122000	127300	130300	124100
Yield strength, 0.2 per cent	98000	97000	100000	98000	101300	103700
Elongation in 2 in., per cent	19.6	18.5	5.0	20.2	19.0	15.0
Reduction of area, per cent	60.5	49.3	13.4	58.9	52.9	37.0

---

[3] "The Effect of Grain Upon the Fatigue Strength of Steels," by L. Aitchison and L. W. Johnson, *Journal of Iron and Steel Institute*, vol. 111, 1925, pp. 351–378.

test pieces came from the same bar. A set of forging dies was sunk with the bottom die machined so as to contain snugly the $4^1/_2$-in-diam pieces when heated to forging temperature. The top die was flat. Total pressure was confined to the specimen being forged by means of a suitable cold cylinder used on top of each piece to transmit all of the impacting pressure to the test specimen. In this manner the $3^3/_4$-in-diam pieces were upset to the diameter of the die cavity and then subjected to repeated impacts. The $4^1/_4$-in-diam test pieces were not upset appreciably for they just fitted the cavity. These latter pieces, however, were subjected to impact pressure with negligible plastic flow. Tensile tests made on these specimens, illustrating the relative effect of impact pressure with and without accompanying plastic flow, are shown in Table 5. The SAE X-4340 tested in the heat-treated condition, represented a condition of higher strength properties. Included for comparison are data on rolled billet material tested in the heat-treated condition.

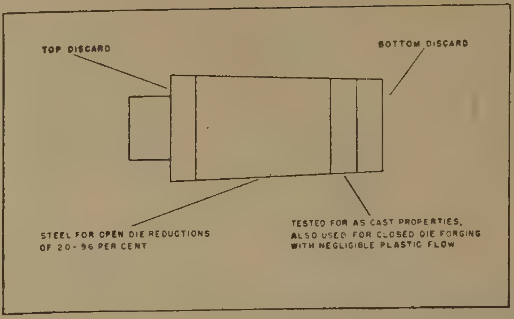
TOP DISCARD
BOTTOM DISCARD
STEEL FOR OPEN DIE REDUCTIONS OF 20-96 PER CENT
TESTED FOR AS CAST PROPERTIES, ALSO USED FOR CLOSED DIE FORGING WITH NEGLIGIBLE PLASTIC FLOW

Fig. 1 Diagram Showing Forging Test Locations for a 25-In. Ingot

TABLE 5 MECHANICAL PROPERTIES OF UPSET AND COMPRESSED SAE X-4340, COMPARED WITH ORIGINAL BILLET MATERIAL

Condition	Direction	Ultimate strength, psi	Yield strength 0.2 offset psi	Elongation, per cent	Reduction of area, per cent	Charpy impact, ft-lb
Rolled	Longitudinal	143900	127500	18.8	49.4	34.3
Upset	Longitudinal	146300	127700	17.2	49.8	32.5
Compressed	Longitudinal	147000	129000	17.7	53.3	35.7
Rolled	Transverse	143900	128100	12.8	31.6	21.3
Upset	Transverse	147200	128100	15.3	40.5	27.5
Compressed	Transverse	150300	134300	14.3	38.0	23.6

The results in Table 5, taken as the average of three determinations in each case, indicate clearly that transverse ductility, as measured by reduction of area, and toughness, as determined by the notched-bar test, are improved by closed-die forging. Of particular interest, however, is the fact that these properties are improved primarily by the high pressures developed in the closed-die forging. This is brought out in the test where the material was compressed by high impact pressure with negligible plastic flow.

Current Experimental Program

The tests described provided sufficient background on heretofore unrecognized phases of the effect of closed-die forging to pose new and unanswered questions. Engineers are constantly considering designs that will employ forgings which can develop high dynamic strength and endurance properties. It is obvious that the strength values, as determined by static tensile tests, are not the only criteria of successful performance, but are related to and depend upon the resultant dynamic properties and ductility developed. Construction of large drop hammers with ratings as high as 50,000 lb have permitted engineers to design, as drop forgings, components weighing up to 3500 lb.

Keeping in mind the nature of trends in engineering design, a long-range experimental program has been developed to study effects of closed-die forging upon mechanical properties. Included for study are such phases as the following:

1 Trend shown by the dynamic properties, endurance strength, and notched-bar toughness, for steels developing highest strength in static tensile tests.

2 Effect of varying prior plastic work by rolling, with emphasis on lower cross-sectional reduction from ingot.

3 Effect of increased pressures developed by hammers of higher rating.

Since the scope of such work is necessarily large, a portion of the work undertaken and completed at present may be discussed at this time. Tests were devised to evaluate effect of open-die forging with increasing reduction upon mechanical properties of an alloy steel heat-treated to an ultimate strength of 165,000—185,000 psi. Comparison was established with properties in the original ingot. Material which had received 80 and 92 per cent prior plastic work, respectively, in rolling was forged in closed dies. A portion of the closed-die forging was done permitting 20 per cent upset. Forging was also done with negligible plastic flow to observe effects of impact pressure alone. In order to gather background on effect of closed-die forging, where little prior work had been done by rolling, ingot material was forged in closed dies with negligible plastic flow. The portion of work completed at present is based upon static tensile, bend, and preliminary Charpy notched-bar studies. Endurance tests, while under way, are not included in this paper.

Material used in this investigation was electric-furnace steel of the following composition:

Carbon.......	0.40	Silicon.............	0.26
Manganese....	0.75	Nickel.............	1.73
Phosphorus...	0.015	Chromium..........	0.71
Sulphur.......	0.025	Molybdenum.......	0.26

One 25-in. ingot of 8500 lb weight was employed to provide cast material for test and for forging to varying reductions using an 8000-lb double-frame steam hammer equipped with flat dies. Fig. 1 illustrates per cent reduction and location of test material.

One 25-in. ingot was rolled to 7-in. round-cornered square billets. Another 25-in. ingot was rolled to 16-in. round-cornered square billet, although none of this section was used in this investigation. The balance of the heat was rolled from 25-in. ingots to 11-in. round-cornered billets yielding 86,210 lb in this size. Thus the 7-in. and 11-in. billets represent 80 and 92 per cent reduction, respectively, by rolling as prior plastic work.

Specimens were machined from 7-in. and 11-in. billet material for forging tests in closed dies employing a 5000-lb steam drop hammer for the closed-die tests. A schematic representation of test-specimen shape, per cent reduction, and direction of work with respect to grain flow is shown in Fig. 2.

The specimens used for closed-die tests, permitting 20 per cent upset, were cylindrical. Those specimens used for the 0 per cent upset tests were machined as a frustrum of a cone. Allowance was made so that the specimen when hot just dropped snugly into the die. This permitted forging the specimen under complete restraint with negligible metal flow. Location of the machined specimen, with respect to its original position in the billet, was maintained by use of stainless-steel pins located in the bottom of the piece. An unheated machined cap was placed on top of each forging specimen after it was dropped into the lower die. The purpose of this cap, or cold top, was to permit ready removal of the specimen from the lower die after forging. Locking of the cold top to the specimen was achieved with a few light hammer blows, upsetting the forging around the cone on the cold top. An illustration of a forged test piece with attached cold top is shown in Fig. 3.

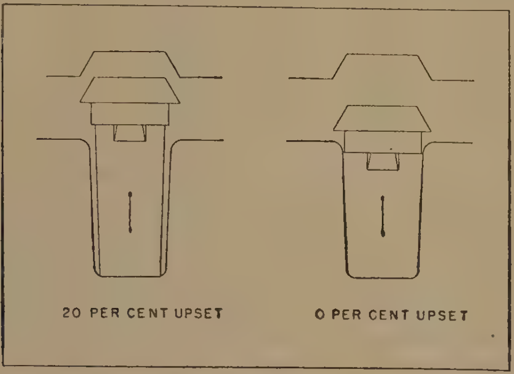

FIG. 2 DIAGRAM OF CLOSED-DIE-FORGING PROCEDURE, SHOWING AMOUNT OF PLASTIC WORK, FORGING, AND ORIGINAL GRAIN-FLOW DIRECTION

A total of 36 test pieces were forged by this method, 8 of which were of heat-resisting alloys not tested as of this writing. All closed and open-die forgings of SAE 4340 were cooled slowly after forging.

Surface, mid-radius, and center sections with longitudinal and transverse grain flow were prepared for each stage of reduction, where obtainable, from the material forged in open dies. The material was cut into slabs approximately 3 × 8 × $1^1/_8$ in.

FIG. 3 CLOSED-DIE TEST FORGING WITH ATTACHED COLD TOP

Material forged in closed dies was sectioned into slabs $1^1/_8$ in. thick to provide test material from surface, mid-radius, and center sections, where obtainable, and possesing longitudinal and transverse grain flow.

All material was heat-treated by normalizing, hardening, and tempering. The complete thermal history, including forging temperatures, is summarized as follows:

Forging: 2175 F–2230 F; cooled at 10 F per hr
Normalize: 1625 F; cooled in air
Heat: 1525 F; quenched in oil at 130 F
Temper: 1000 F
Hardness: 3.10–3.20 Bhd, or 363–388 Bhn

After heat-treatment, standard 0.505-in. tensile test bars were machined and tested. Bend tests were made using specimens having $^3/_8$ × $^3/_{16}$-in. cross section, and a bend radius of $^1/_2$ in. Impact tests were made using standard Charpy specimens with a milled notch.

RESULTS OF CURRENT EXPERIMENTAL WORK

In order to establish preliminary trends in this investigation, properties at the mid-radius test location, with reference to the original billet or ingot, were determined. These are included in the results obtained to date. Results of longitudinal and transverse tensile tests for various cross-sectional reductions in open-die forging are shown in Fig. 4.

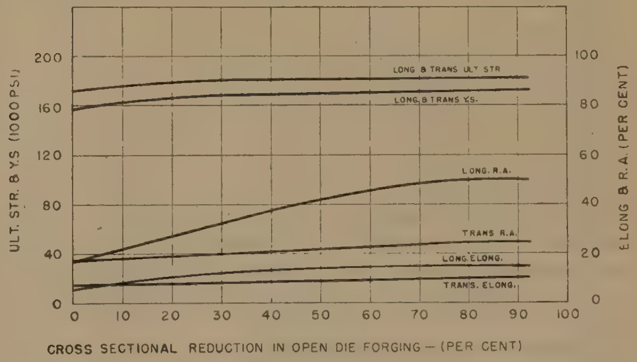

FIG. 4 MID-RADIUS TENSILE PROPERTIES VERSUS REDUCTION IN OPEN-DIE FORGING

No apparent difference exists between longitudinal and transverse ultimate strength or yield strength from the original ingot through increasing stages in reduction by open-die forging. Significant variation in ductility is noticed, however. Improvement in ductility is greater in the longitudinal direction for increased cross-sectional reduction in open-die forging. Reduction of area appears to be a more sensitive indication of ductility than does elongation for steel heat-treated with resultant ultimate strength of 120,000 to 180,000 psi. This has been observed in many tests performed on die blocks and piston rods where little variation in ductility as measured by elongation is noted. However, low reduction of area has been observed in those components having unsatisfactory service life, yet possessing elongation comparable with material giving satisfactory performance.

A comparison of the effect of forging methods is illustrated in Table 6. Ingot material was tested from a mid-radius location. Material from the same ingot location was forged in closed dies with negligible plastic flow. A marked improvement in ductility may be noted due to impact pressure alone. Closed-die forging with negligible plastic flow and with 20 per cent upset, likewise

TABLE 6 COMPARATIVE STATIC TENSILE TESTS FOR OPEN AND CLOSED-DIE FORGING AND INGOT MATERIAL FROM MID-RADIUS TEST LOCATIONS

Cross-section reduction from ingot, per cent	Forging method	Longitudinal				Transverse			
		Ultimate strength, psi	Yield strength, 0.2 per cent, psi	Elongation in 2 in., per cent	Reduction of area, per cent	Ultimate strength, psi	Yield strength, 0.2 per cent, psi	Elongation in 2 in., per cent	Reduction of area, per cent
0	As-cast ingot	173200	160000	6.0	14.6	169700	153000	8.0	18.4
0	Ingot material, closed die, zero per cent upset	172500	160000	11.0	34.7	181000	167500	14.0	42.2
80	Open die	184000	170000	16.0	50.8	181000	174500	10.0	22.7
80	Closed die, zero per cent upset	172200	155000	16.0	51.1	180000	167000	11.5	27.5
80	Closed die, 20 per cent upset	170700	157500	15.0	46.6	172500	152500	10.0	27.2
92	Open die	180000	170000	15.0	49.2	181500	175500	9.0	20.6
92	Closed die, zero per cent upset	170200	152500	15.5	49.2	175700	157500	12.0	28.2
92	Closed die, 20 per cent upset	175700	161500	16.0	50.6	173500	163000	10.0	36.7

shows an increase in transverse ductility over open-die forgings for comparable cross-sectional reductions from the original ingot. It may be noted that impact pressure alone causes a marked improvement in transverse ductility.

Effect of cross-sectional reduction and forging method upon Charpy impact strength is shown in Table 7.

TABLE 7 VARIATION IN CHARPY IMPACT STRENGTH WITH FORGING METHODS FOR MID-RADIUS TEST LOCATIONS

Cross-sectional reduction, per cent	Forging method	Charpy impact, ft-lb	
		Longitudinal	Transverse
0	As-cast ingot	14	12
0	Closed die, zero per cent upset	18	21
80	Open die	24	15
80	Closed die, zero per cent upset	23	15
80	Closed die, 20 per cent upset	24	15
92	Open die	26	15
92	Closed die, zero per cent upset	24	15
92	Closed die, 20 per cent upset	22	14

The greatest improvement in notched-bar toughness over as-cast material is shown in the longitudinal direction. Closed-die forging on ingot material with negligible plastic flow has resulted in a distinct improvement.

Bend tests were performed on mid-radius material using bend bars with $^3/_8 \times {}^3/_{16}$-in. cross section and a bend radius of $^1/_2$ in. Mid-radius ingot bend bars broke at 56 and 89 deg for longitudinal and transverse directions. Longitudinal and transverse specimens taken from comparable ingot material, forged in closed dies with negligible plastic flow, withstood the 180-deg bend test satisfactorily. All wrought steel, forged by open and closed-die methods, was bent 180 deg without failure.

SUMMARY

The purpose of this investigation has been to study the effect of reduction and of forging method upon the mechanical properties of steel. Neither amount of reduction nor method of forging alters the strength properties at a given hardness level with regard to direction of grain flow. A successive series of experiments on steel treated to varying ranges of strength show superior transverse ductility and notched-bar toughness developed by the extremely high pressures used in closed-die forging. That pressure alone in closed-die forging effects an improvement in transverse ductility has been demonstrated by tests in which amount of plastic deformation was negligible. It is felt that this aspect of the high pressures developed in closed-die forging has been overlooked heretofore.

The advantage that may be realized from this method of hot-working lies in the ability to improve properties in regions of highest stress. Such effects may be realized by drop-forging, the process yielding shapes whose geometry follows closely the design of the finished part. While some designers feel that full advantage cannot be taken of higher ductility, because of inability of a design to function with high deflections, very often operating stresses of a high order or overload conditions require deformation for a very small gage length. Such condition can arise in a fillet. If the resulting deformation in the restricted area is met by ample ductility, the result is satisfactory performance. On the contrary, low ductility in such a region can result in a preliminary crack leading to ultimate failure. The operation of gas turbines has shown that bucket wheels possessing highest center ductility have attained the best performance, again illustrating the relation of ample ductility to service life.

The nature of the results obtained to date on the effect of forging method point definitely to the need for further work in this field. Inasmuch as high pressure with no appreciable plastic flow has shown a material improvement in ductility of ingot material, the question has arisen concerning effect of closed-die forging on billet material of large cross section with less plastic work from the ingot stage. This is of decided importance in view of the growing demand for forgings produced by the largest steam drop hammers. Further investigation is needed to show the effect of higher pressures, tested by using hammers of greater rating. Studies of effect of closed-die forging on endurance properties in fatigue are in progress at the present time.

Shielded Thermocouples for Gas Turbines

By A. I. DAHL[1] and E. F. FIOCK,[1] WASHINGTON, D. C.

In gas turbines, the gases are normally much hotter than the surrounding walls, so that radiation from a thermocouple in the gas stream to the walls may cause considerable error in observed values of gas temperature. Effective radiation shielding of the measuring junction can be accomplished by pressing a small tubular shield of silver, gold, or platinum directly on an oxidized junction of base-metal thermoelements. The construction, calibration, and performance of junctions with pressed shields of low surface emissivity are described, and the results to date of service tests in gas turbines are discussed. Experimental results on the rate of response of various junctions to sudden changes in temperature, and means for increasing this rate are presented.

Introduction

The recent development of the gas turbine as a practical power plant for applications on land, sea, and in the air has been accompanied by the wide use of thermocouples for indicating gas temperatures in the range up to approximately 2000 F. Many problems related to this application have assumed considerable importance, in both the evaluation of power-plant performance and in the development of satisfactory controls. These include evaluation, in terms of indicated temperature, of the heat transfer to or from the sensing element by conduction, convection, and radiation, the effects of gas velocity, and the rate of response of the element to sudden changes in temperature. Of these diverse problems, this paper deals only with the control and evaluation of the radiation correction, and with the response rate of thermocouples. The experimental work was done at the National Bureau of Standards, with the Bureau of Ships, Department of the Navy, as sponsor.

General Considerations

The temperature attained by a thermocouple junction, immersed in a stream of hot gas, is seldom identical with the temperature of the gas, but instead is characteristic of a steady state at which the rate of heat transfer from the gas to the junction by convection, impact, and friction is equal to the rate of heat transfer from the junction to the surroundings by radiation and conduction. If the junction can "see" the flame, it may also receive heat by direct radiation over a limited solid angle. Assuming that the gas is transparent to radiation, the following equation holds at a steady state

$$h_c(T_s - T_i)A_1 + I + \sigma\epsilon\epsilon_f(T_f^4 - T_i^4)xA_1 = \sigma\epsilon(T_i^4 - T_w^4)A_1 + (kA_2/a)(T_i - T_w) \quad \text{[1]}$$

in which

h_c = coefficient of heat transfer by convection
T = absolute temperature
A_1 = surface area of junction
σ = Stefan-Boltzmann radiation constant
ϵ = surface emissivity of junction
ϵ_f = emissivity of flame
x = fraction of total solid angle over which junction sees the flame
k = coefficient of thermal conductivity of thermocouple wires
A_2 = cross-sectional area of thermocouple wires
a = depth of immersion of junction

Subscripts s, i, w, and f mean static, indicated, wall, and flame, respectively, and refer to the gas, junction, wall, and flame.

The quantity I represents the rate of heat transfer to the junction due to directed motion of the gas, and is the resultant of directed impact and friction in the boundary layer of gas around the junction. The magnitude of I depends primarily upon the velocity and heat capacity of the gas, and to a lesser extent upon the configuration of the junction and the nature of the flow around it. The discussion which follows is limited to gas velocities sufficiently low that I can be neglected for practical purposes.

The stem conduction term may be conservatively approximated by $(kA_2/a)(T_i - T_w)$. Its effect may be made negligibly small by proper attention to thermocouple design and installation (1, 2),[2] by the use of small wires, and by adequate immersion. If it is assumed also that the junction cannot see the flame, the foregoing equation becomes simply

$$T_s - T_i = (\sigma\epsilon/h_c)(T_i^4 - T_w^4) \quad \text{[2]}$$

which expresses the departure of the temperature indicated by the junction from the static temperature of the gas, resulting from radiation alone. Since the radiation intensity increases as the fourth power of the absolute temperature, the correction due to radiation losses assumes considerable importance at the temperatures experienced in gas turbines.

The use of shields to reduce the radiation correction has been common practice for many years. The most common type consists of coaxial tubes surrounding the measuring junction (3, 4), and the effectiveness of such shields increases with the number employed. Units of this type, however, are difficult or impossible to install in many locations throughout a gas turbine; they create undesirable disturbances to gas flow, and are slow to respond to changes in temperature.

Another well-known method of reducing the radiation error (5) is to decrease the emissivity of the surface of the junction itself, that is to decrease the value of ϵ in the equations given. This approach seemed to offer the most promise for the development of an instrument having the characteristics desired for service in gas turbines, and therefore was followed in the present investigation.

Test Equipment

The equipment used to produce streams of exhaust gas in which these tests and calibrations were made is shown diagrammatically in Fig. 1. It consists essentially of a blower supplying air to a single combustor from a German Jumo 004 turbojet engine, with controls for inlet air and fuel, and a bleed line in parallel with the test section on the burner discharge. Gas temperature is adjusted by controlling the inlet air and fuel rates, and the velocity in the test section can be varied by means of the valve in the bleed line.

---

[1] Physicist, National Bureau of Standards.

Contributed by the Heat Transfer Division and presented at the Semi-Annual Meeting, Milwaukee, Wis., May 30–June 5, 1948, of The American Society of Mechanical Engineers.

Note: Statements and opinions advanced in papers are to be understood as individual expressions of their authors and not those of the Society. Paper No. 48—SA-29.

[2] Numbers in parentheses refer to the Bibliography at the end of the paper.

The test section is a 4-ft length of 6-in. standard iron pipe, provided with three hatches for convenience in installing various instruments, and located far enough downstream from mixing and flow-straightening devices that the temperature and velocity are sensibly uniform over a central core 3 in. diam. Numerous junctions peened into the test section are used to indicate wall temperatures.

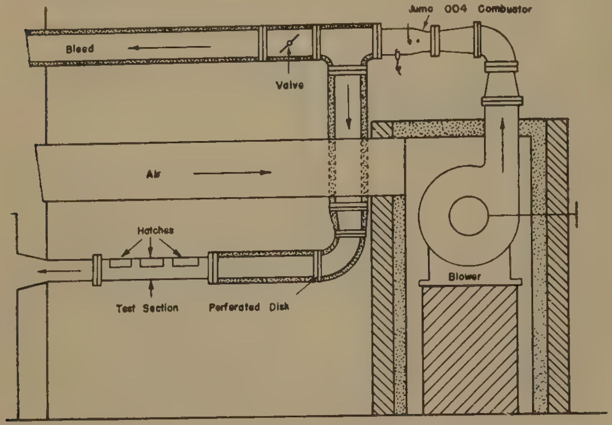

Fig. 1 Diagram of Combustion System

The equipment provides gas flows from 2 to 7 lb per sec ft^2 and gas temperature up to 1500 F. It is anticipated that the range of the present measurements will be extended considerably with new equipment now being constructed.

Junctions With Pressed Shields

Theory and Construction. From Equation [2] it will be seen that the effect of radiation to the surroundings is directly proportional to the surface emissivity ϵ, of the thermocouple junction. The emissivities of base-metal thermocouple materials (oxidized surfaces) range from about 0.80 to 0.95. The emissivity can be reduced temporarily by polishing the junction, but the surfaces reoxidize rapidly at elevated temperature. However, silver and gold have an emissivity of from 0.03 to 0.05 and platinum from 0.12 to 0.18. Since these metals are not subject to oxidation, they retain their effectiveness as radiation shields at all temperatures below their melting points.

Thus by covering the junction of a chromel-alumel thermocouple with a layer of silver, the rate of heat transfer by radiation from the junction to the surroundings will be reduced by a factor of about 18, with only a slight decrease in the rate of heat transfer from the gas to the junction by convection. Fig. 2 illustrates the construction of such a silver-shielded junction.

A junction is made between the base-metal thermoelements in a conventional manner, such as by autogenous welding. The resulting bead is dressed to the form of a disk having a thickness about equal to the diameter of the wires. A $^{3}/_{4}$-in. length of fine silver, gold, or platinum tube, $^{1}/_{8}$ in. OD × 0.020 in. thick, is flattened so that it will slip freely over the disk and the wires. After the disk and about $^{1}/_{2}$ in. of the adjoining wires have been oxidized by heating to a dull red in a mild air-gas flame, the disk is inserted to the approximate center of the flattened tube. The flattening of the tube is then continued in a press or vise until the junction is held firmly by the tube, which becomes about 0.2 in. wide and 0.04 in. thick when No. 22 thermocouple wires are used.

Such a shielded junction is simple to construct, reasonably rugged, and has small physical dimensions, so that it is easy to install, it creates little disturbance to flow, and it responds rapidly to sudden changes in gas temperature.

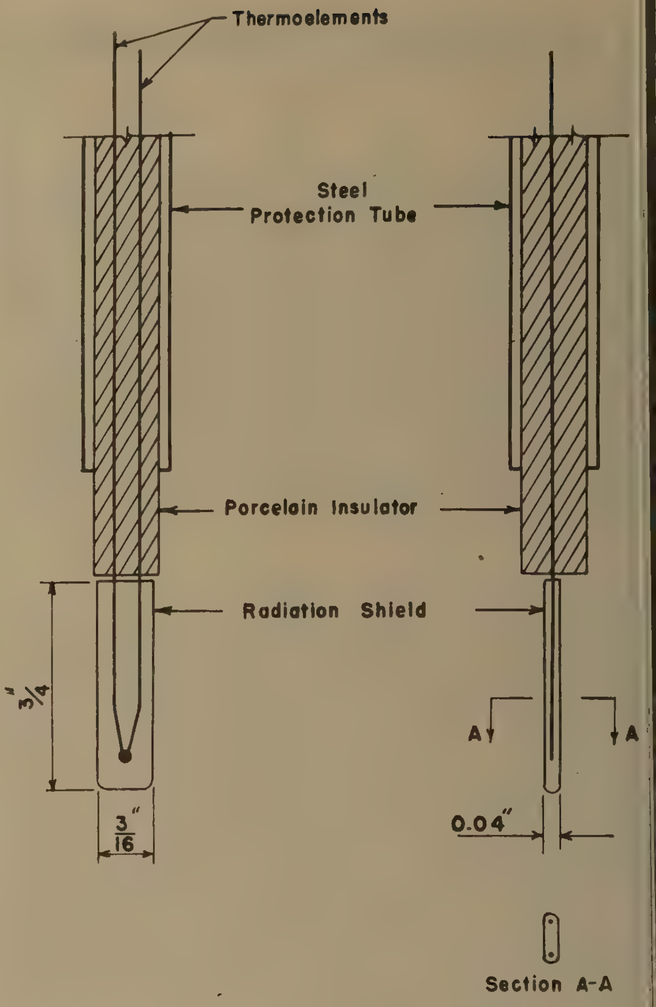

Fig. 2 Details of Junction With Pressed Radiation Shield

Protection and Mechanical Stability of Shielded Junctions. Although shielded junctions of the type described, supported only by two-hole porcelain insulating tubes, are suitable for laboratory use, some mechanical protection is essential for service applications. For use in exhaust gas, it has been found that a guard tube of Type 347 stainless steel, slotted to permit the flow of gas over the shield, meets this need. Fig. 3 shows an unguarded junction, and two with guards of the type mentioned. From the standpoint of ease of installation, the advantage of making the guard the same diameter as the support tube is obvious. Numerous tests have shown that these guards have no significant effect upon the calibration or the performance of the shielded junctions.

Preliminary service tests of silver-shielded junctions made of No. 22 chromel-alumel wire in operating gas turbines showed that, while the mechanical strength was adequate in one unit, the wires failed between the silver and the porcelain tube in another. The obvious methods for increasing the strength are to increase the size of the thermocouple wire, to decrease the thickness and length of the shield, and to provide mechanical support in addition to that of the wires themselves.

The use of large thermoelements has the disadvantages of larger heat loss by conduction and of decreased rate of response. The first of these is not serious, and the second is of little importance in some applications. Hence shielded junctions of No. 14 chromel-alumel have proved satisfactory in one application in

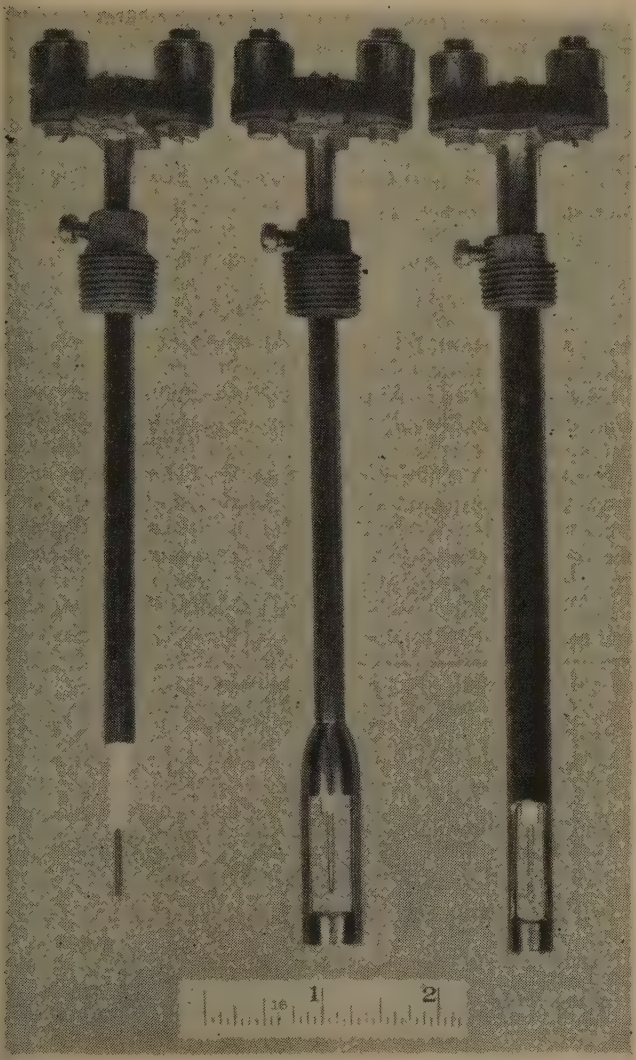

FIG. 3 SHIELDED THERMOCOUPLE PYROMETERS

which those made from No. 22 wires failed. In this case additional mechanical support, as well as the larger wire, was required because of the severe service conditions.

The use of pressed shields of silver, gold, or platinum less than about 0.02 in. thick is not recommended from the standpoint of strength, because these metals become relatively soft at the temperatures under consideration.

To study the effect of shield length, the performance of various shielded junctions was compared with that of a junction having a shield $^3/_4$ in. long. The relative magnitudes of the corrections with shields of various lengths are given in Table 1. It will be noted that little advantage is to be expected from making the shield longer than $^3/_4$ in., but that the radiation error increases appreciably as the length of the shield is reduced below this value.

TABLE 1 RELATIVE MAGNITUDE OF RADIATION CORRECTION

Junction with $^3/_4$ in. shield	1.0
Junction with $^1/_2$ in. shield	1.2
Junction with $^1/_4$ in. shield	1.5
Junction with $^1/_8$ in. shield	3.6
Bare junction	11.0

For increased mechanical support, various methods, including anchoring the shield to the porcelain insulating tube and to a similar porcelain tube, supported from the end of the guard tube, have been tried. However, the method which seems most satisfactory, both from the standpoint of construction and performance, is that shown in Fig. 4. A lower support is provided by inserting a nichrome loop in the end of the flattened shield tube before the latter is pressed to final shape. The nichrome support is then passed through appropriate holes in a disk anchored in the end of the guard tube. Thus the nichrome limits the possible movements of the shielded junction to an extent which virtually eliminates failure of the wires by fatigue.

Preliminary tests of silver-shielded junctions in an operating gas turbine indicate a life of several hundred hours in all locations except between the combustor and the turbine. At the latter location the junctions fail in less than 50 hr of continuous service, regardless of the gas temperature.

The leading edge of the silver shield of a junction that has failed is badly pitted, and both the chromel and alumel elements have deteriorated within the shield and for some distance up the porcelain insulating tube. The direct impingement of incandescent carbon particles on the shield, and possible effects of sulphur in the fuel, are being investigated at present.

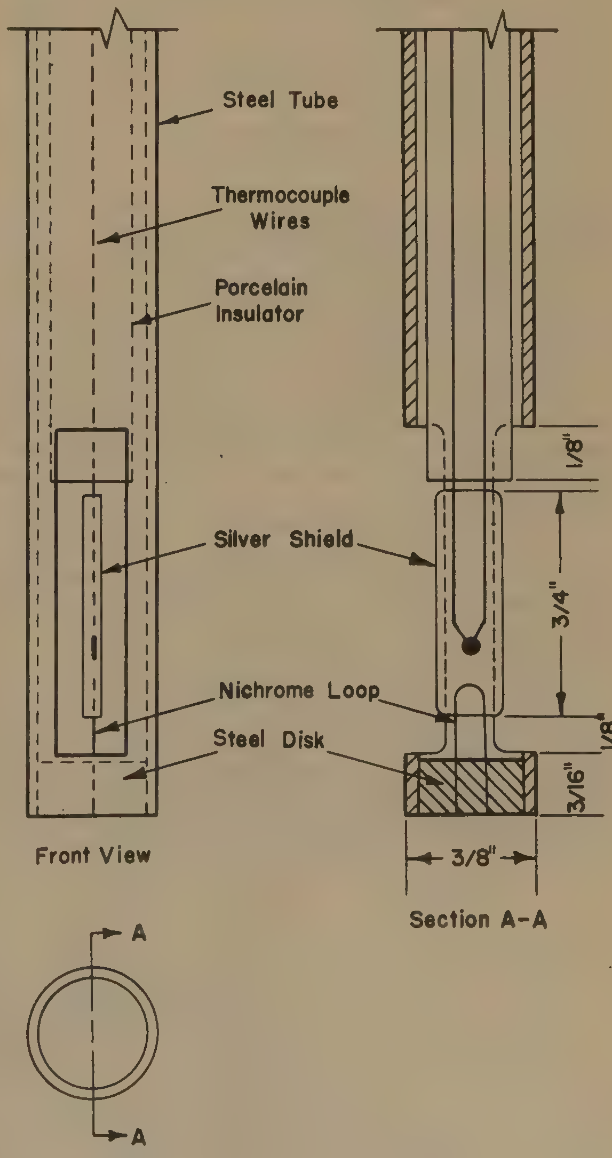

FIG. 4 SHIELDED JUNCTION WITH ADDED MECHANICAL SUPPORT

DETERMINATION OF RADIATION CORRECTIONS

Laboratory Standard Thermocouple for Gas-Temperature Measurements. If the effects of radiation are to be determined experimentally, the first requirement is a laboratory standard instrument which is free from such effects. Fig. 5 shows a pyrometer in which a bare thermocouple junction is surrounded by a cylindrical shield, the temperature of which can be controlled by a second electrically heated shield. The inner shield is a silver tube $5^1/_2$ in. long × 1 in. OD × 0.04 in. thick. The outer shield of stainless steel is provided with a heating element of nichrome ribbon, insulated from the tube with mica. The heating element is divided into three approximately equal sections, each section being provided with individual current control. Three chromel-alumel junctions peened into the silver shield are used to indicate its temperature. By adjusting the heat supplied electrically to each section of the steel shield, the temperature of the silver shield can be brought to uniformity and to equality with that of the junction. When this condition prevails, the junction temperature approaches that of the gas, since there can be no appreciable heat interchange by radiation.

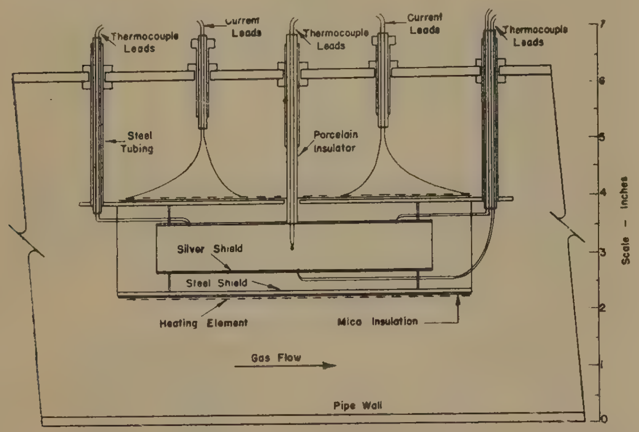

FIG. 5 LABORATORY STANDARD THERMOCOUPLE FOR MEASURING GAS TEMPERATURE

It will be apparent that much time and care are required in the use of such a laboratory standard instrument. After it had been used for the careful calibration of several silver-shielded chromel-alumel junctions, it became evident that a more convenient standard could be devised by making use of a junction with a pressed shield.

Secondary Standard. This instrument consists simply of a silver-shielded junction mounted centrally within two coaxial, unheated tubes, as shown in Fig. 6. The inner silver tube is 6 in. long × 1 in. OD × 0.04 in. thick, and the outer Inconel tube is 7 in. long × 2 in. OD × 0.04 in. thick. The shielded junction can be inserted and removed without disturbing the tubes. Junctions peened into the silver indicate the temperature of the inner shield.

After a direct intercomparison of the primary and secondary standards showed that there was no choice as to performance, the latter was used exclusively, because of its greater convenience.

Calibration of Junctions With Pressed Shields. These junctions are made from wire for which the temperature-emf relation is known from previous calibrations (6). The actual temperature of any junction is determined by measuring its emf with a semi-precision potentiometer, applying the correction thereto for the calibration of the wire, and reading the temperature corresponding to this corrected emf from a standard table (7).

During a calibration experiment, various junctions are located in the test section as shown in Fig. 7. Those at locations 1, 2, and 3 are silver-shielded junctions used for control purposes. The junction to be calibrated is used at location 4, the calibration being accomplished by a substitution method using the secondary standard with a silver-shielded junction made of the same wire as the test junction. The procedure is as follows: With the test junction at location 4, a measurement is made. The secondary standard is then substituted for the test junction, and a second measurement is made at identical operating conditions, as indicated by the junctions at locations 1, 2, and 3. Thus one run of each pair gives the temperature attained by the test junction, and the second gives the true temperature of the gas at the same location and under identical conditions. The difference thus observed is

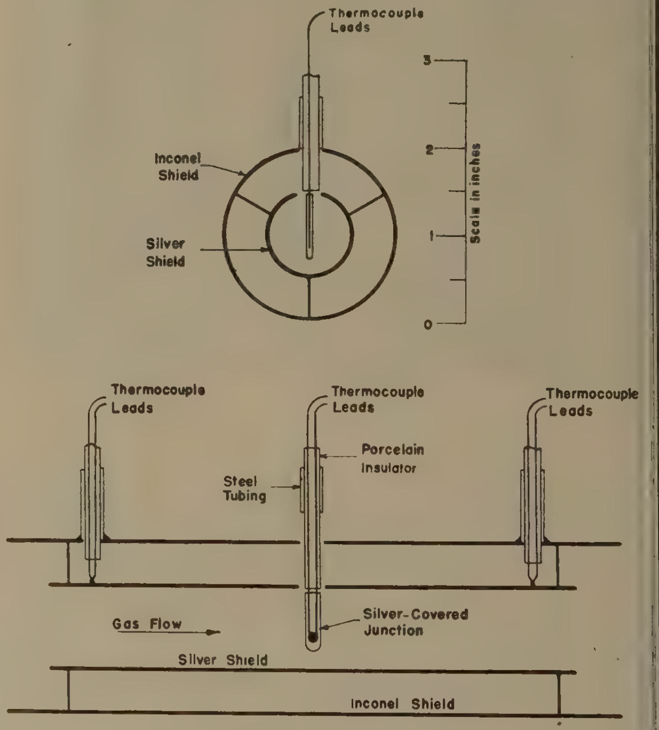

FIG. 6 SECONDARY STANDARD THERMOCOUPLE FOR CALIBRATION PURPOSES

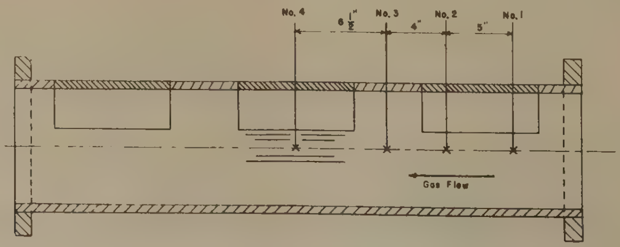

FIG. 7 ARRANGEMENT OF TEST SECTION FOR CALIBRATIONS

the temperature drop due to radiation from the test junction. Errors which might otherwise arise from conduction along the wires and from wire calibration are avoided completely by this method. Runs of this type were made for both silver and platinum-shielded chromel-alumel junctions over the following ranges: Wall temperatures, 700 to 1400 deg F; gas temperatures, 1000 to 1500 F; and gas flows, 1.5 to 7 lb per sec ft^2.

Silver-Shielded Junctions. The results obtained for silver-shielded junctions are presented graphically in Fig. 8. To illustrate the use of this figure, assume that a silver-shielded junction in a gas stream indicates 1379 F, when the wall temperature is 1165 F, and the gas flow is 3.8 lb per sec ft^2. From the point on the base line corresponding to 1379 F, proceed vertically to the curve which would correspond to a wall temperature of 1165 deg F. This involves interpolation between the curves for 1100 and 1200 F. Then proceed horizontally to the right until the flow line representing $G = 3.8$ is reached. From this point, proceed vertically downward to the base line, where the correction, amounting to 4 deg F, can be read.

It is believed that the corrections for radiation loss determined from Fig. 8 will be in error by less than ±2 deg F, when the correction is less than 10 deg F, and by less than $^1/_5$ of the correction when the latter exceeds 10 deg F. It is emphasized that the corrections are applicable to silver-shielded junctions of the size and shape specified. Small changes in dimensions are probably unimportant, but large changes would involve changes in the value of convection coefficient, and hence also in the corrections.

Although it has been found that silver-shielded junctions may be used in gas streams having uniform temperatures up to 1700 F, the large variations which usually exist at the turbine inlet make it inadvisable to use silver shields when the average temperature is thought to exceed about 1500 F, since local temperatures may at times exceed the melting point of silver.

Silver shields which are burnished when new, quickly assume a whitish bloom upon exposure to exhaust gas at elevated temperature. It is probable that this change at the surface takes place before a calibration can be made, so that the results in Fig. 8 actually apply for this type of surface. At any rate, no change in radiation correction has been detected with the length or conditions of service. The expected deposition of products of incomplete combustion upon the shields has not occurred in the test system, and has not been reported in service.

Gold as a Material for Radiation Shields. Gold has about the same emissivity as silver, but melts about 185 deg F higher. Therefore gold-shielded chromel-alumel junctions should be useful in exhaust gas of uniform temperature up to about 1900 deg F, or at the turbine inlet in streams with an average temperature of about 1700 F. Because the greater cost of gold does not seem to be justified by the small extension of the useful range which it provides, and because, even though gold were used, advantage could not be taken of the full useful range of base-metal thermocouples, no attempts have been made to calibrate gold-shielded junctions.

Platinum-Shielded Junctions. Platinum, with a melting point of 3225 F, is more than adequate from this standpoint as a shield for the common base-metal thermoelements. As a shielding material it has at least two disadvantages over silver and gold, namely, its emissivity is about 0.18, or approximately 3.5 times as high; the well-known ability of platinum to catalyze reactions must not be overlooked. The first of these means merely that the radiation correction, under given operating conditions, will be about 3.5 times that for silver. Even so, the correction for a platinum-shielded junction is only about $^1/_3$ that for a bare junction.

It was considered desirable, in the course of the present work, to investigate the possibility that heat developed by sur-

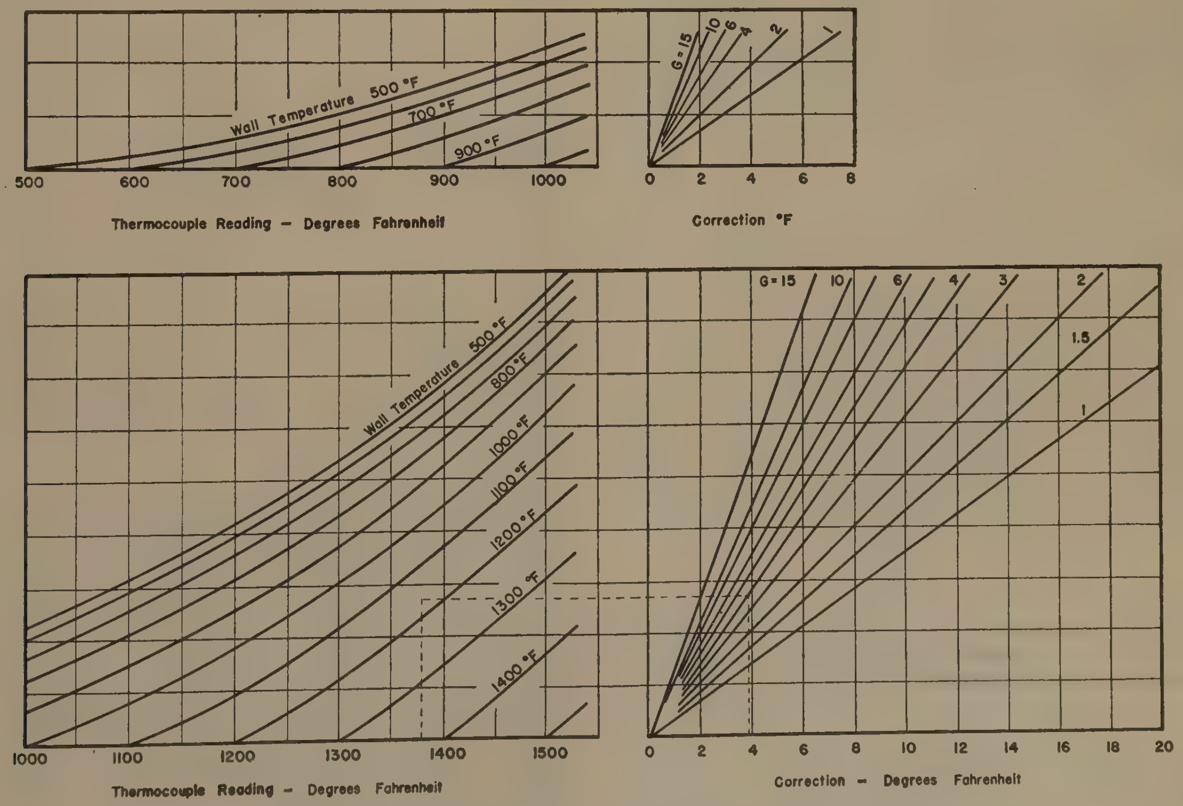

Fig. 8 Radiation Corrections for Silver-Shielded Junction

face reaction would change the temperature of a platinum-shielded junction.

These studies consisted of direct comparisons of silver- and platinum-shielded junctions in exhaust gases of various compositions and temperatures. During these comparisons the radiation correction for both junctions was reduced to zero by making the temperature of the gas and of the walls identical. This could be accomplished in the apparatus, Fig. 1, by running gas at 1500 deg F through the well-lagged test section until the wall temperature reached a value previously selected, then quickly reducing the gas temperature to this same value by reducing the fuel rate.

The composition of the gas passing over the test junctions was varied by adding metered quantities of hydrogen or of propane far enough downstream from the burner so that the excess fuel did not ignite. Samples of the gases passing through the test section were withdrawn through a water-cooled sampling tube and analyzed in a mass spectrograph.

Briefly summarized, these tests showed that at relatively low gas temperatures, the platinum-shielded junctions reached a steady-state temperature more than 25 deg F above the gas temperature. This difference increased with the percentage of either hydrogen or propane, and decreased as the gas temperature was raised. Slightly below 1200 deg F, the difference in temperature indicated by the two test junctions became zero, regardless of the amount of raw fuel added, and it remained zero at temperatures up to 1400 deg F, which was the highest wall temperature that could be maintained. It is not expected that surface reactions will have a significant effect upon the temperature attained by a platinum-shielded junction above 1200 deg F, but this will be checked experimentally when new test equipment becomes available.

It is concluded that platinum-shielded chromel-alumel junctions may be used in the range 1200 to 2000 deg F without fear of error from surface reactions. Radiation corrections for such junctions were determined by direct comparison with silver-shielded junctions in the range of gas temperatures from 1200 to 1500 deg F, and over the ranges of wall temperatures and flows mentioned previously. The correction for a platinum-shielded junction can be obtained by getting the correction for a silver-shielded junction from Fig. 8, then multiplying this value by 3.5.

Comparison of Radiation Corrections for Various Pyrometers. Fig. 9 presents a comparison of the radiation corrections for five difference instruments at a mass flow rate of 6 lb per sec ft^2 and a temperature difference of 200 deg F between the gas and the walls.

Rates of Response of Thermocouples

If a thermocouple is to be used for control purposes, such as to limit the gas temperature at the turbine inlet to a safe value, it must respond rapidly to sudden changes in temperature but need not indicate the true temperature of the gas. The rate of response of a thermocouple is usually expressed as its characteristic time τ, which may be defined as the time in seconds required to undergo 63 per cent of the change in temperature to which it is subjected instantaneously. This definition comes from the equation

$$\Delta T = (T_2 - T_1)(1 - e^{-t/\tau}) \qquad [3]$$

expressing the increase ΔT, in the temperature of the junction with time t, when the temperature of the gas in which it is immersed is increased instantaneously from T_1 to T_2. Furthermore

$$\tau = C_j/A_1h_c \qquad [4]$$

in which C_j is the heat capacity of the junction, and the other quantities have the meanings assigned previously.

It will be noted that the characteristic time of a given junction varies with the coefficient of heat transfer by convection, and hence with the rate of gas flow.

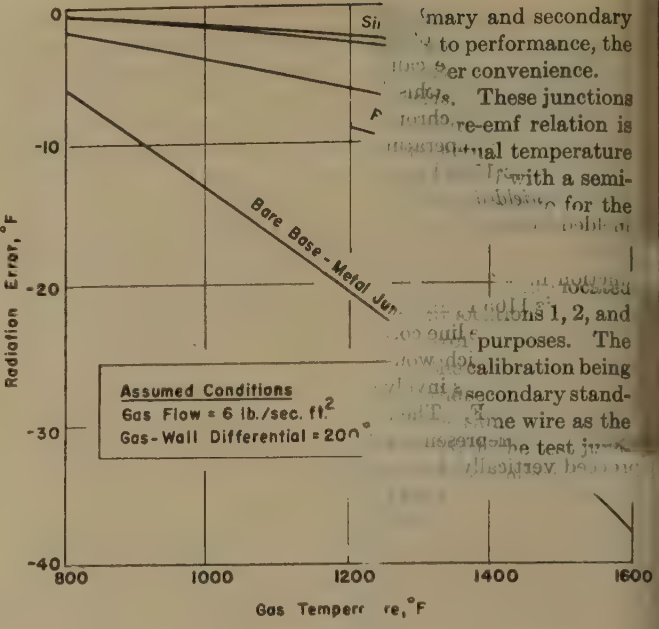

FIG. 9 RADIATION ERROR FOR VARIOUS JUNCTIONS

Various types of thermocouples have been subjected to sudden changes of temperature in the apparatus shown in Fig. 10. The direct emf of the test junction is chopped, amplified, and recorded on a direct-inking oscillograph, typical records being reproduced in Fig. 11. Some of the results are summarized in Table 2.

TABLE 2 CHARACTERISTIC TIMES OF THERMOCOUPLES IN EXHAUST GAS

Flow rate, lb per sec ft^2			2.2	4.2	6.8
Type of junction	Wire gage	Shield thickness in.	Time, sec		
Silver-shielded Ch-Al	22	0.020	3.1	2.2	1.8
Silver-shielded Ch-Al	22	0.014	..	..	1.5
Silver-shielded Ch-Al	22	0.008	..	..	1.1
Silver-shielded Ch-Al	22	0.005	..	..	1.0
Bare Ch-Al	18	...	2.2	1.6	1.2
Bare Ch-Al	22	...	1.3	1.0	0.8
Bare Ch-Al	28	...	0.54	0.41	0.34
Bare Ch-Al	36	...	0.17	0.12	0.10
Bare Ch-Kn	40	...	0.11	0.08	0.07
Bare Ch-Kn	44	...	0.07	0.05	0.04

Not even the bare junctions which are sturdy enough to withstand operating conditions, i.e., those made of wire at least as heavy as No. 22 gage, respond quickly enough for some control applications. For this reason, certain combinations of junctions which respond more rapidly than single junctions have been investigated.

One possible way of obtaining a greater change in emf in a given time is to use a multijunction thermocouple of the type illustrated in the insert of Fig. 12. Junctions a, b, and c are close together, so that all are at essentially the same temperature during steady-state operation. At all times the resultant emf (E_m) of this unit is the sum of the individual values E_a, E_b, and E_c, proper account being taken of polarity. Thus for the system shown, $E_m = E_a + E_b - E_c$. When all junctions are at the same temperature, $E_m = E_a = E_b$, and the steady-state emf of the unit approaches that of a single junction at the same temperature.

It can be shown that the resultant temperature change ΔT_m indicated by the multijunction when subjected to an actual temperature change ΔT_0 is

$$\Delta T_m/\Delta T_0 = 1 - e^{-t/\tau_a} - e^{-t/\tau_b} + e^{-t/\tau_c} \qquad [5]$$

he temperature dro
Errors which might
vires and from wir
method. Runs of
platinum-shielded
ranges: Wall tem
tures, 1000 to
Silver-Sh

perature is
point on the base li
to the curve whi
1165 deg F. This
1100 and 1200
the flow line ro

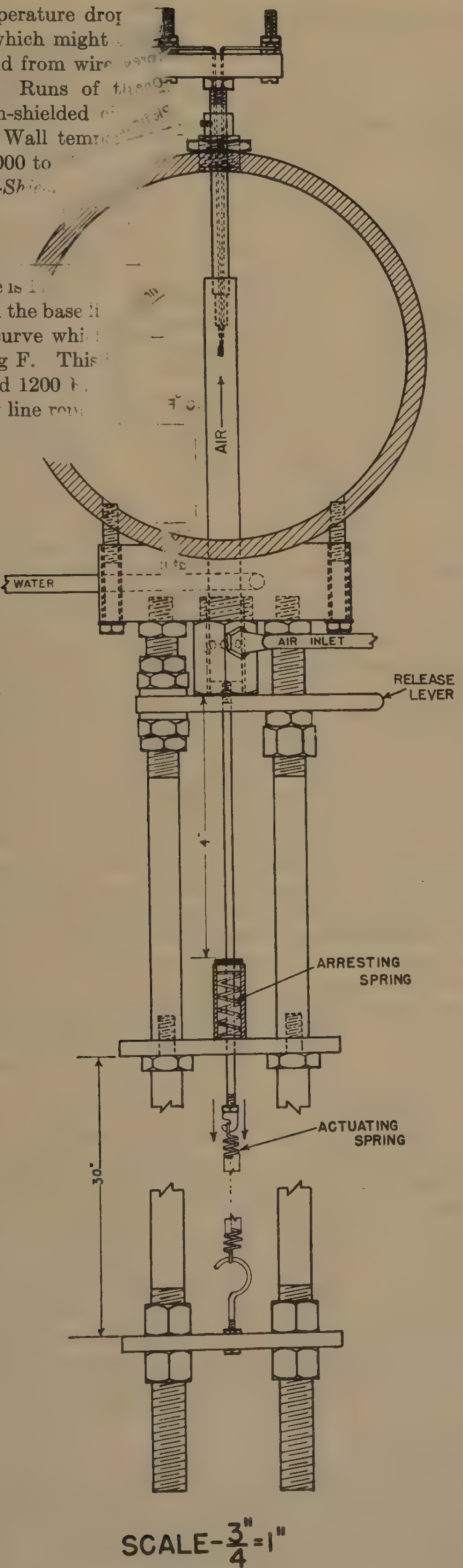

FIG. 10 APPARATUS FOR SUBJECTING JUNCTIONS TO SUDDEN CHANGES IN TEMPERATURE

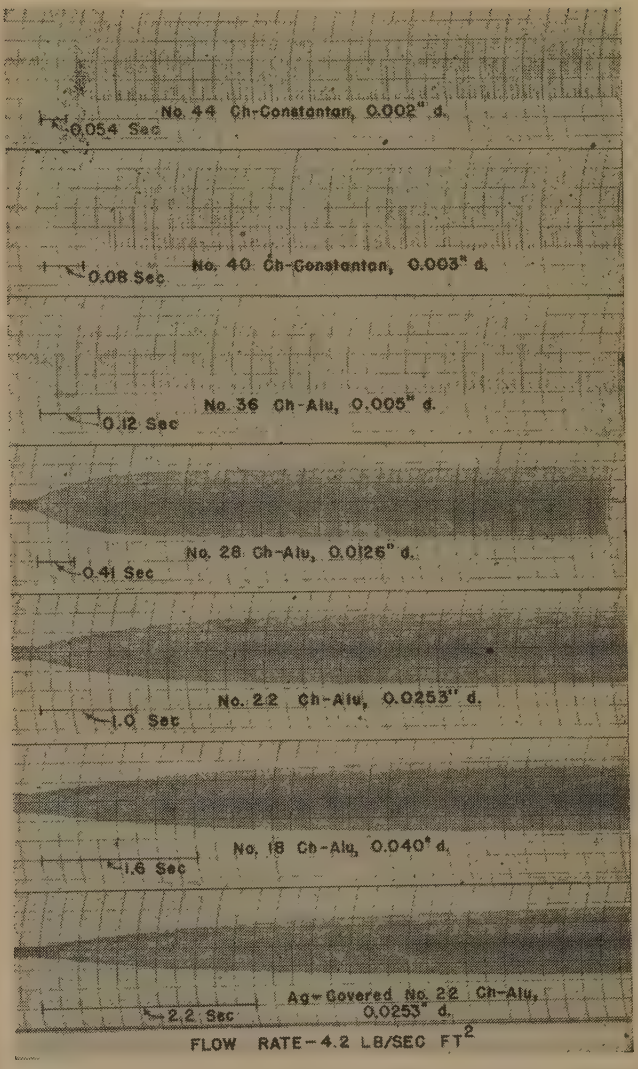

FIG. 11 TYPICAL RESPONSE CURVES OF THERMOCOUPLES

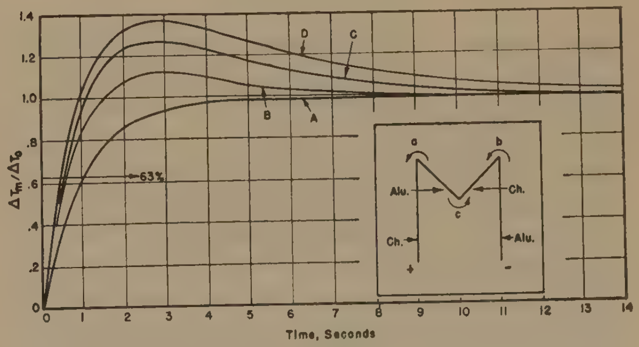

FIG. 12 RESPONSE CURVES OF MULTIJUNCTION THERMOCOUPLES

Fig. 12 is a plot of $\Delta T_m/\Delta T_0$ against time, for an assumed constant value of ΔT_0 and for the following assumed values of τ: For all curves $\tau_a = \tau_b = 1$. For curves A, B, C, and D, τ_c = 1, 2, 3, and 4, respectively. Curve A is identical with that for a single junction, and it can be seen that the time required to reach the line marked 63 per cent decreases as τ_c is increased, i.e., as the lag in junction *c* becomes greater.

On the basis of this theory the three types of multijunctions illustrated in Fig. 13 were constructed and tested. In type A the lag of the intermediate junction was increased by using heavier wire for this junction. In types B and C, one and two intermediate junctions, respectively, are embedded in alundum cement which provides the thermal lagging. The results obtained with these units confirm the theoretical values indicated in Fig. 12, namely, that the response time of the multijunctions is approximately one half that for a bare single junction made of the same wire.

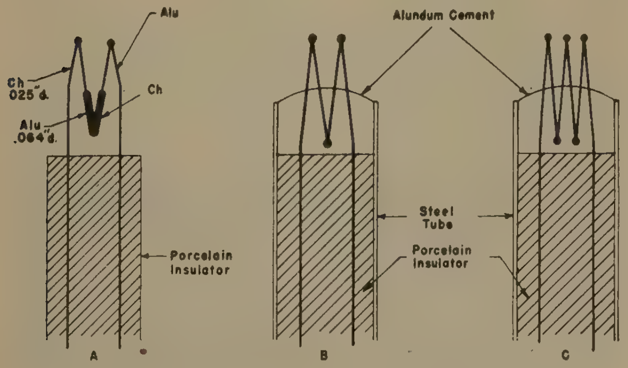

Fig. 13 Typical Multijunction Thermocouples

Summary

In gas turbines, the gases are normally much hotter than the surrounding walls, so that radiation from a thermocouple in the gas stream to the walls may cause considerable error in observed values of gas temperature. Effective radiation shielding of the measuring junction can be accomplished by pressing a small tubular shield of silver, gold, or platinum directly on an oxidized junction of base-metal thermoelements. The construction, calibration, and performance of junctions with pressed shields are described, and the results to date of service tests in gas turbines are discussed. Experimental results on the rate of response of various junctions to sudden changes in temperature, and means for increasing this rate, are presented.

BIBLIOGRAPHY

1 "A Graphical Determination of Unshielded-Thermocouple Thermal Correction," by W. M. Rohsenow, Trans. ASME, vol. 68, 1946, p. 195.

2 "The Use of Thermocouples in High-Velocity Gas Streams," by E. F. Fiock and A. I. Dahl; published in the May, 1948, *Journal of the Society of Naval Engineers.*

3 "Measurement of High Temperatures in High-Velocity Gas Streams," by W. J. King, Trans. ASME, vol. 65, 1943, p. 421.

4 "Development of Temperature Probe, Multi-Shielded Type," by H. W. Emmons, Report to Elliott Company, Jeannette, Pa., 1944.

5 "Temperature, Its Measurement and Control in Science and Industry," by H. F. Mullikin, Reinhold Publishing Corporation, New York, N. Y., 1941, p. 775.

6 "Methods of Testing Thermocouples and Thermocouple Materials," by W. F. Roeser and H. T. Wensel, National Bureau of Standards, *Journal of Research* RP 768, vol. 14, 1935, p. 247.

7 "Standard Tables for Chromel-Alumel Thermocouples," by W. F. Roeser, A. I. Dahl, and G. J. Gowens, National Bureau of Standards, *Journal of Research* RP 767, vol. 14, 1935, p. 239.

Discussion

Florence F. Buckland.[3] Equation [3] of this paper gives the rate of response of the thermocouple. It might be helpful to pursue the definition of the characteristic time τ a little further,

$$\tau = \frac{c\rho}{h}\frac{V}{A}$$

where c is specific heat of the assembly, ρ is weight density, h is surface-heat-transfer coefficient, A is surface area, and V is volume.

For control purposes, it is desirable to make τ as small as possible. It may be reduced by decreasing c, ρ, or V, or by increasing h or A. For a solid cylinder of a given material in an air stream with a known velocity and temperature, the response time is proportional to the 1.4 power of the radius. However, the assembly is not solid, nor is it a cylinder, so there is some leeway in the design that might be used to advantage. There is the possibility of putting fins on the shield (a watchmaker's job) or perhaps making the shield of 20-mil wire wound tightly about the thermocouples so that the area for heat transfer is greater by $\pi/2$ and the weight less by $\pi/4$. This arrangement might play havoc with the necessary mechanical strength, but if it were feasible, the response time should be one half as long.

T. P. Kirkpatrick.[4] The authors are to be commended for their work in developing a very helpful improvement in thermocouples suitably designed for measuring the temperature of hot gases traveling at relatively high velocities.

The writer has been privileged to collaborate in the first tests of silver-shielded thermocouples in the Allis-Chalmers 3500-hp gas turbine at the U. S. Naval Engineering Experiment Station at Annapolis, and in the subsequent application of thermocouples of this type for measurement of the gas temperature in this turbine plant.

A brief review of the steps leading to the adoption of the silver-shielded thermocouple for this application may be of interest. Conventional shielded-thermocouple designs were rejected after analyses of installation difficulties and the uncertainties regarding their ruggedness in gas streams with velocities in the order of 100 fps, which correspond to mass flows in the order of 12.5 lb per sec-ft^2, and temperatures up to 1500 F. Early trials of a completely enclosed thermocouple design indicated errors of undesirable magnitudes.

A protected tip or single-shielded thermocouple design was then developed. This, together with the graphical method for determination of the thermal correction, developed by Dr. Warren M. Rohsenow,[5] was adopted.

The first trial of the silver-shielded thermocouple in this turbine produced striking results. One of the four single-shielded thermocouples in the 1350 deg F inlet-gas duct was replaced by the silver-shielded couple. At the time the inner walls of the duct were 25 deg F cooler than the gases at the thermocouple locations near the center of the duct. The silver-shielded couple indicated temperatures approximately 10 degrees hotter than the semi-shielded couples. The fuel supply was then abruptly cut off. This reduced the gas temperatures below those of the hot walls. The silver-shielded couple reflected the expected reversal in radiation by indicating lower temperatures than the single-shielded couples. Computed radiation corrections applied to the single-shielded couples brought the temperatures into agreement within 1 or 2 deg.

When the Allis-Chalmers gas turbine was reinstrumented subsequent to its installation in a new laboratory building, nineteen silver-shielded thermocouples were installed for measurement of gas temperatures at stations where accurate temperatures were of greatest importance to the performance test data. Design de-

---

[3] General Engineering and Consulting Laboratory, General Electric Company, Schenectady, N. Y. Mem. ASME.

[4] U. S. Naval Engineering Experiment Station, Annapolis, Md.

[5] Authors' Bibliography (1).

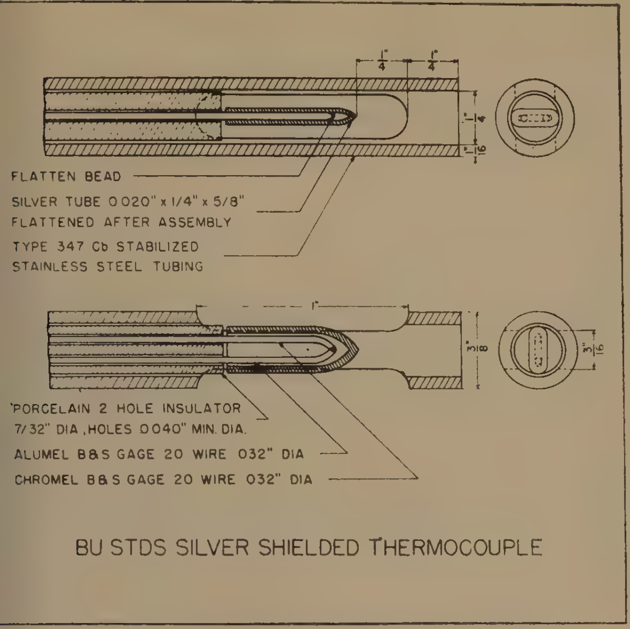
1/4
1/4
1/16
FLATTEN BEAD
SILVER TUBE 0.020" x 1/4" x 5/8" FLATTENED AFTER ASSEMBLY
TYPE 347 Cb STABILIZED STAINLESS STEEL TUBING
5/8
5/16
PORCELAIN 2 HOLE INSULATOR 7/32" DIA, HOLES 0.040" MIN. DIA.
ALUMEL B&S GAGE 20 WIRE .032" DIA
CHROMEL B&S GAGE 20 WIRE .032" DIA
BU STDS SILVER SHIELDED THERMOCOUPLE

IG. 14 Bureau of Standards Silver-Shielded Thermocouple

ails for these thermocouple assemblies are shown in Fig. 14 of his discussion.

Three couples were equally spaced around a 3-in. circle concenric with the center of the duct at each station. This was done to rovide a better average of the gas temperature and for insurance gainst casualty to a couple during a test run. The nineteenth ouple was installed in the turbine where space did not permit the se of three.

In the past 10 months, silver-shielded couples have been used uring something over 1100 hr of turbine testing. Over 100 hours f this testing have been with 1500 F inlet-gas temperatures.

Test results have indicated a gratifying reduction in the spread f data, much of which must be credited to the silver-shielded ouples and refinements in calibration developed for us by the uthors at the Bureau of Standards.

Deterioration of silver shields experienced in this service has been due principally to two undesired and abnormal conditions:

(*a*) Soot, resulting from incomplete combustion, will tarnish or darken the silver and reduce its ability to minimize radiation effects.

(*b*) Abrasive matter in the gas stream such as silica or metal scale tends to honeycomb and darken the leading edges of the silver.

Where such abnormal conditions are not present, the silver shields quickly gain a bright granular surface bloom and appear to retain their brightness as long as the gas remains clean.

Cross-sectional microphotographs of silver-shielded thermocouples recently removed from the gas turbine disclose much higher rates of intergranular attack on the chromel and alumel wires than experienced on similar wires without the silver shields. This is particularly true of the alumel wires.

As far as known at this time this intergranular attack does not seriously impair calibrations of the thermocouples until shortly before complete failure occurs. It does shorten the useful life of the silver-shielded couples, and it is hoped that the authors' future investigations will provide means of minimizing or eliminating this tendency.

Authors' Closure

The use of fins on the thermocouple junction, as suggested by Mrs. Buckland, has been tried. On small junctions the mechanical difficulties incident to the use of fins would seem to make the scheme impractical, despite the resulting increase in response rate of the junction.

Recent data obtained on silver-shielded chromel-alumel junctions in both the Allis Chalmers gas turbine at NEES and at the NBS have shown that the deterioration of the shielded junctions referred to by Mr. Kirkpatrick resulted from sulphur in the fuel. With fuels of low sulphur content, no deterioration of the shielded junction has been observed.

The authors are deeply grateful for the co-operation and assistance of the gas-turbine laboratory, NEES, Annapolis, in procuring service test results.

Progress Report No. 2 on Tool-Chip Interface Temperatures

By K. J. TRIGGER,[1] URBANA, ILL.

This report is a continuation of Progress Report No. 1 which was presented in 1947 before the Society. The investigation is principally concerned with the effects of cutting speed upon cutting temperature, chip thickness, and chip hardness, when steel at various hardness levels is machined with cemented-carbide tools. In most of the tests conducted, a steel-cutting grade of carbide tool was used. This type contained tungsten, titanium, and tantalum carbides and is referred to as a triple-carbide tool. A straight tungsten-carbide tool was used in one series of tests in order to compare the performance with that of the triple-carbide composition. The cobalt content of each grade was normal for the particular type and intended cutting service. Details of the tests are given in this paper.

CUTTING-TEMPERATURE MEASUREMENTS

THE cutting temperatures of the tests to be discussed in the present paper were measured in the same manner as those which were reported previously, and they are subject to the same interpretation as indicated in Progress Report No. 1 (1).[2] The discussion of the present results must take into account some revisions of the cutting temperatures previously reported. In the preceding paper it was pointed out that the carbide-tool insert, the carbide contact rod, and the carbide calibration bar must all be of the same chemical composition. If this condition exists, the temperature-millivolt relationship established in calibrating the steel-carbide thermocouple applies in the determination of temperatures from the tool-chip millivolt data. Conversely, if the calibration bar and carbide insert were not chemically alike any temperatures so determined were potentially in error.

TABLE 1 TEMPERATURE-MILLIVOLT RELATIONSHIPS OF VARIOUS CEMENTED CARBIDES WITH MILL-ANNEALED NE9445 STEEL

Carbide sample	Manufacturer	Carbide type	Reference-junction temperature, deg F	Millivolts at			
				1000 F	1200 F	1300 F	1400 F
1} Duplicates	A	Triple carbide	61	11.70	13.84	14.91	16.00
2	A	Triple carbide	67[a]	11.60	13.74	14.82	15.92
3	A	Triple carbide	75	10.62	12.57	13.54	14.55
4[b]	A	Triple carbide	74	11.03	13.07	14.10	15.16
5} Duplicates	B	Triple carbide	68	9.91	11.78	12.78	13.78
6	B	Triple carbide	75[c]	9.84	11.71	12.70	13.69
7	A	Tungsten carbide	67	12.80	15.44	16.70	18.10
8	B	Tungsten carbide	66	14.12	16.95	18.30	19.65

[a] To correct to same reference temperature as sample No. 1 add 0.09 mv.
[b] From calibration test in Report No. 1 (1).
[c] To correct to same reference temperature as sample No. 5 add 0.07 mv.

Subsequent to the presentation of Report No. 1, it was established that the carbide calibration bar and carbide insert were of the same grade but not of the same composition. Therefore the millivolts "generated" at the tool-chip interface could not be converted, accurately, to temperatures by use of a steel-carbide calibration curve when the calibration bar was different, chemically, from the carbide insert. (When the carbide materials were obtained, it was understood that they were from the same lot of carbide mixtures.)

During the entire course of this investigation, many calibration tests have been conducted and the variation in the temperature-emf relationship may be observed by a study of Table 1. The chemical composition of any given grade of cemented carbide is probably controlled within reasonably close limits, but apparently, slight changes in chemistry may have a rather large effect on the temperature-emf relationship. Furthermore, it is conceivable that the method of pressing (hot versus cold) may have a significant effect upon the loss of cobalt and thus alter the thermoelectric effects of the carbide.

It may be observed from Table 1 that duplicate carbide samples have the same temperature-millivolt characteristics. Comparison of samples 1 and 2, or 5 and 6, when corrected to the same calibration reference temperature, indicate virtually identical emf for a given temperature. On the other hand, samples 2 and 3, for example, show from 1 to $1^1/_2$ mv difference for the same temperature even though of the same grade and manufacture. Comparison of samples 2 and 5 reveals about $1^3/_4$ to 2 mv difference at the same temperature. These samples are of the same type of carbide but of different manufacture. Some variations in chemistry are undoubtedly present. A similar trend is noticed in samples 7 and 8, which also reveal the marked difference between the temperature-millivolt relationship of tungsten carbide as compared with the triple-carbide composition.

In order to appreciate the significance of the difference in chemistry, consider a case in which the carbide tool insert consisted of sample 2, Table 1. During cutting an indicated 13.74 mv generated at the tool-chip interface would correspond to a cutting temperature of 1200 F. If, however, the calibration bar were of different composition, e.g., sample 3, this 13.74 mv would be equivalent to about 1320 F. The error, 120 F, is due to the difference between samples 2 and 3 which, while of the same grade and manufacture, are of considerably different temperature-emf characteristics.

---

[1] Professor, Department of Mechanical Engineering, University of Illinois. Mem. ASME.

[2] Numbers in parentheses refer to the Bibliography at the end of the paper.

Contributed by the Research Committee on Metal Cutting Data and Bibliography and the Production Engineering Division and presented at the Semi-Annual Meeting, Milwaukee, Wis., May 30–June 5, 1948, of THE AMERICAN SOCIETY OF MECHANICAL ENGINEERS.

NOTE: Statements and opinions advanced in papers are to be understood as individual expressions of their authors and not those of the Society. Paper No. 48—SA-51.

As a consequence of these observations, all of the tests herein reported are based upon the use of carbide inserts, contact rods, and calibration bars which were not only made from the same lot of carbide mix but which were all cold-pressed and all sintered alike. Therefore any error due to chemical variation should be at an irreducible minimum.

An assumption in Report No. 1 must also be modified. Based upon one preliminary test it was assumed that the heat-treated condition of the steel member had little effect upon the calibration curve. The magnitude of difference reported previously was about 0.10 mv for a calibration with the steel in the annealed state as compared with the steel quenched and tempered to 1050 F. Duplicate subsequent calibrations with the new carbides have indicated that the difference is somewhat greater, about 0.25 mv, for the heat-treated steel and that it becomes progressively greater as the tempering temperature is lowered to 950 F and 850 F. Accordingly, this report takes into consideration the effect of heat-treatment upon the temperature-emf relationships. Some of the cutting speed-cutting temperature tests previously reported have been repeated, and some new tests are included in this report.

In Fig. 1 are shown the various calibration curves of the triple carbide-steel thermocouple for the different heat-treatments of the steel member. In each calibration a new steel member was prepared and heat-treated as indicated. Check calibrations were conducted in most instances and the curves were, if possible, based upon the same reference-junction temperature. It is apparent that the heat-treatment of the steel does have a significant effect upon the temperature-millivolt relationship, particularly in the tempering range of 850 F to 950 F. The curves in Fig. 1 were used to determine the cutting temperatures for all tests in which the triple carbide was used. The millivolt data obtained during a cutting test (at the existing cold-junction temperature) were corrected to the reference-junction temperature of the calibration curve by use of the appropriate curve at the right of Fig. 1.

Fig. 2 compares the temperature-millivolt relationship of the triple carbide with the tungsten-carbide composition. The steel member was in the same condition in each test. The much greater emf of the tungsten carbide-steel couple is obvious. At 1200 F the difference is in excess of 5 mv. Curve 2, Fig. 2, was used to determine cutting temperatures in those tests involving the tungsten-carbide tool.

Test Procedure

The general method of testing was the same as that heretofore used. The feed was held constant at 0.01 in. per revolution; the depth of cut was 0.100 in. and the tool shape was held constant with the specifications as follows: Back rake, 0 deg; side rake, 4 deg; end relief, 7 deg; side relief, 7 deg; end cutting-edge angle, 8 deg; side-cutting-edge angle, 0 deg; and nose radius $^3/_{64}$ in. The setting angle was 90 deg in all tests; the tool was finished with a 400-grit diamond hone and was set on the center line of the workpiece. All tests were conducted without coolant. The test stock consisted of NE9445 mill-annealed to 183 Bhn and quenched and tempered at 850 F, 950 F, and 1050 F to 401, 352, and 311 Bhn, respectively. The test logs were 3 to 5 in. diam, and $1^1/_2$ to 2 ft long. During the tests, chips were collected from each run and measurements of chip thickness and hardness were obtained.

Results of Tests

Cutting Speed-Cutting Temperature Tests. The results of the cutting speed-cutting temperature tests are shown in Tables 2, 3, and 4, and the relationships are plotted on logarithmic coordinates in Figs. 3 and 4.

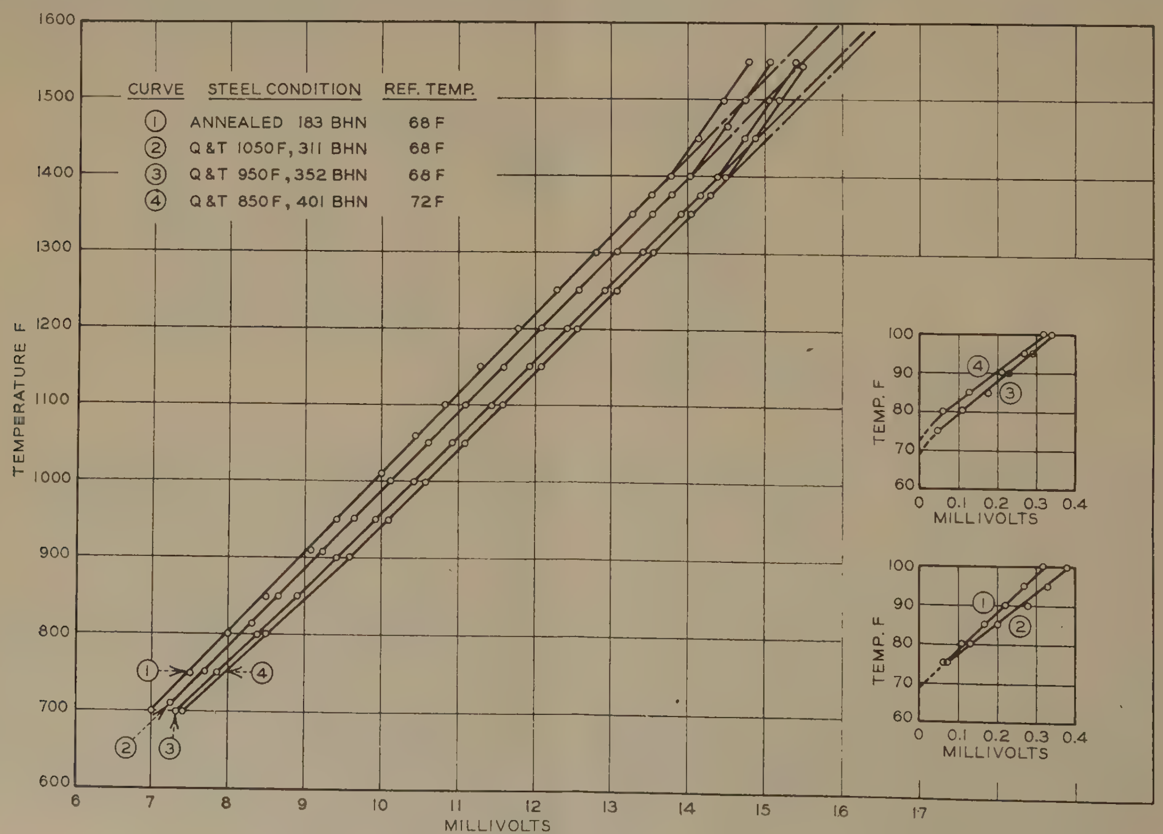

Fig. 1 Calibration Curves NE9445 Steel Versus Triple Carbide

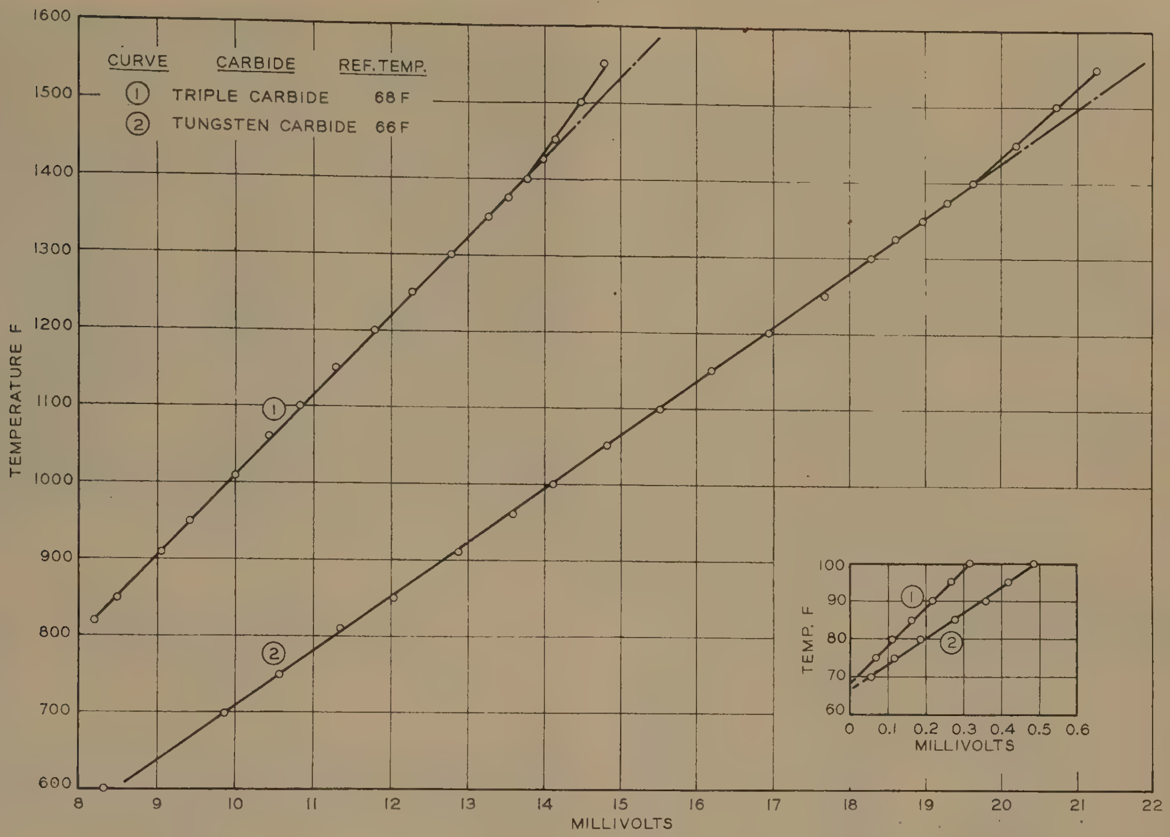

FIG. 2 CALIBRATION CURVES NE9445 STEEL ANNEALED VERSUS CEMENTED CARBIDES

TABLE 2 CUTTING SPEED-CUTTING TEMPERATURE RESULTS; VARIABLE HARDNESS

Steel: NE9445.
Tool: Triple carbide. 0-4-7-7-8-0-$^3/_{64}$.
Feed: 0.01 in. per rev. Depth of cut: 0.100 in. Cut: Dry

Mill annealed 183 Bhn				Quenched and Tempered at 1050 F to 311 Bhn			
Cold-junction temperature, 75 F				Cold-junction temperature, 80 F			
Cutting speed, sfpm	Corrected mv[a]	Cutting temperature, deg F	Chip thickness, in.	Cutting speed, sfpm	Corrected mv	Cutting temperature, deg F	Chip thickness, in.
101	10.19	1030	0.044	55	10.16	1003	0.041
118	10.49	1061	0.041	64	10.42	1030	0.037
140	10.92	1105	0.039	76	10.80	1070	0.034
164	11.14	1128	0.037	90$^1/_2$	11.20	1110	0.031
189	11.63	1180	0.035	104	11.41	1131	0.028
227	12.02	1218	0.032	124	11.74	1165	0.025
263	12.36	1255	0.030	147	12.12	1203	0.023
312	12.84	1304	0.029	170	12.42	1233	0.022
365	13.24	1345	0.028	200	12.88	1282	0.021
413	13.70	1393	0.027	237	13.29	1324	0.020
498	14.22	1445	0.026	272	13.72	1367	0.019
				321	14.25	1422	0.018

[a] Millivolt readings corrected to calibration reference-junction temperature.

TABLE 3 CUTTING SPEED CUTTING TEMPERATURE RESULTS; VARIABLE HARDNESS

Steel: NE9445.
Tool: Triple carbide. 0-4-7-7-8-0-$^3/_{64}$.
Feed: 0.01 in. per rev. Depth of cut: 0.100 in. Cut: Dry.

Quenched and tempered at 950 F to 352 Bhn				Quenched and tempered at 850 F to 401 Bhn			
Cold-junction temperature, 69 F				Cold-junction temperature, 78 F			
Cutting speed, sfpm	Corrected mv	Cutting temperature deg F	Chip thickness, in.	Cutting speed, sfpm	Corrected deg F	Cutting temperature deg F	Chip thickness, in.
43	10.13	970	0.036	37	10.16	957	0.034
50	10.49	1006	0.032	44	10.71	1012	0.029
59	10.82	1040	0.030	52	11.07	1050	0.027
71	11.15	1072	0.028	61	11.42	1085	0.025
83	11.52	1110	0.026	73	11.82	1126	0.023
97	11.81	1138	0.024	86	12.07	1150	0.021
114	12.19	1177	0.022	100	12.40	1183	0.020
137	12.59	1216	0.021	118	12.75	1218	0.019
157	12.95	1253	0.020	142	13.14	1258	0.018
185	13.40	1297	0.019	163	13.49	1294	0.017
220	13.81	1340	0.018	192	13.96	1341	0.016
253	14.24	1383	0.018				

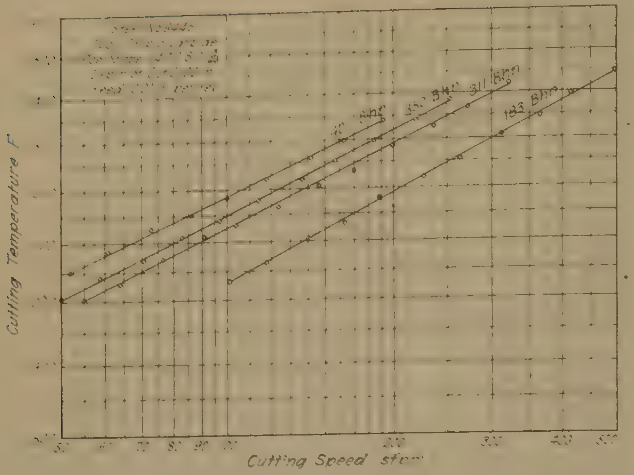

Fig. 3 Cutting Speed-Cutting Temperature Relationships Using Triple-Carbide Tool

TABLE 4 CUTTING SPEED-CUTTING TEMPERATURE RESULTS

Steel: NE9445 mill-annealed 183 Bhn
Tool: Tungsten carbide. 0-4-7-7-8-0-$^3/_{64}$
Feed: 0.01 in. per rev. Depth of cut: 0.100 in. Cut: Dry
Cold-junction temperature 76 F

Cutting speed, sfpm	Corrected mv	Cutting temperature, deg F	Chip thickness, in.
101	12.28	868	0.043
118	14.18	1004	0.043
140	14.72	1041	0.042
164	15.00	1062	0.039
189	15.51	1098	0.036
227	16.04	1135	0.033
263	16.74	1185	0.032
312	17.25	1223	0.031
365	18.09	1284	0.030
413	18.74	1330	0.030
498	19.32	1372	0.030
118	13.50	955	...
118	13.96	987	...

In Fig. 3 the type of carbide, tool shape, depth of cut, and feed are held constant, and the hardness of the steel is varied. The cutting speed-cutting temperature relationships are all straight lines on logarithmic co-ordinates and are of the form $T = CV^n$. The equations of the various lines are as follows:

Hardness Bhn	Equation
183	$T = 387\ V^{0.212}$
311	$T = 459\ V^{0.195}$
352	$T = 466\ V^{0.197}$
401	$T = 499\ V^{0.188}$

These relationships are of the same form as those previously reported though the constants are appreciably lower and the exponents slightly different (0.001 to 0.006).

An increase in the hardness results in a higher cutting temperature at any selected cutting speed. Considering only the quenched and tempered steels, it is seen that at a selected cutting temperature, 1200 F, for example, the cutting speed decreases linearly with an increase in the hardness. This is shown in the lower curve of Fig. 5. If the curve were extended to include the annealed steel, the straight-line relationship does not hold. However, it appears reasonable that extrapolation to some quenched and tempered hardness level, say 250 Bhn, is justified since the structure is of the same kind, namely, tempered martensite, whereas the annealed structure consisted of fine spheroidized carbides in ferrite. In view of the chemical difference in the carbide materials previously used and the unwarranted assumption in Report No. 1, Figs. 3 and 5 are submitted as the revised effect of hardness upon the cutting speed-cutting temperature relationship.

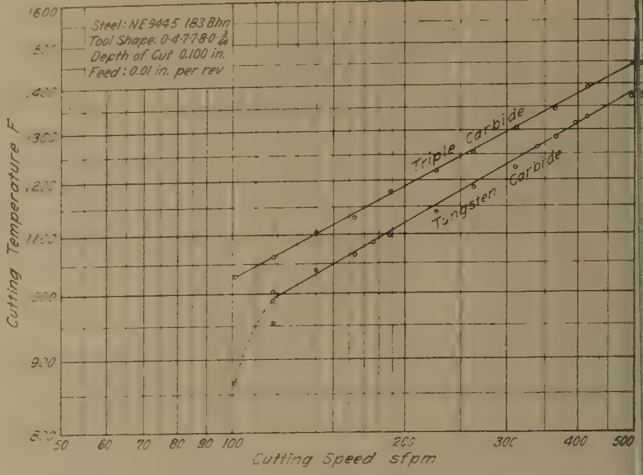

Fig. 4 Cutting Speed-Cutting Temperature Relationships Using Annealed NE9445 Steel

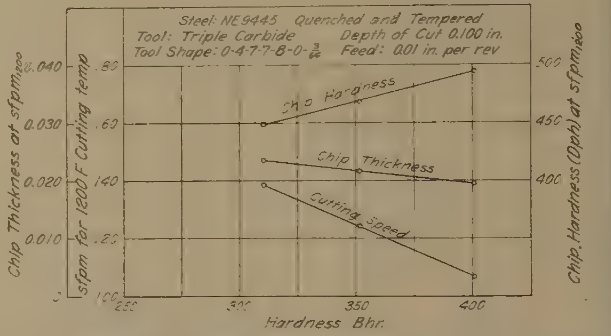

Fig. 5 Effect of Workpiece Hardness on Chip Thickness, Chip Hardness, and Cutting Speed

Fig. 4 compares the cutting speed-cutting temperature relationship for annealed N9445 when cut with two types of carbide tools. The upper curve is for the triple carbide tool and the lower curve is for the tungsten-carbide composition. The triple carbide was a standard steel-cutting grade while the tungsten carbide was primarily intended for cast iron, aluminum, magnesium, and all materials other than steel.

The equations of the straight-line portions of the curves are $T = 387\ V^{0.212}$ and $T = 333\ V^{0.229}$ for the triple-carbide tool and tungsten-carbide tool, respectively. Evidently, lower temperatures result with the tungsten-carbide tool, though there were some characteristics of the chip which may have caused the difference. Consider the lower speed range and dotted portion of the curve for the tungsten-carbide tool. It may be noted that the cutting temperature for the 101-sfpm test is nearly 100 F below the straight-line portion of the curve if the latter were extended, and also that for the 118-sfpm test there are three points which constitute quite a spread in cutting temperature. Fig. 6 is a macrograph of the three chips, representing the three points for the 118-sfpm test. The chip on the left has most of the separating surface torn or scuffed, indicating the presence of a large built-up edge on the tool, and it is consequently a type-3 chip as classified by Ernst (2). The center chip is the result of a succeeding test, and is partially clear although there is still evidence of appreciable gouging and scuffing due to the built-up edge. The right chip, from a still later test, is about two-thirds clear although gouging due to a built-up edge is evident.

These tests were made in succession, each one of the usual duration, about 10 sec, and each successive millivolt reading was

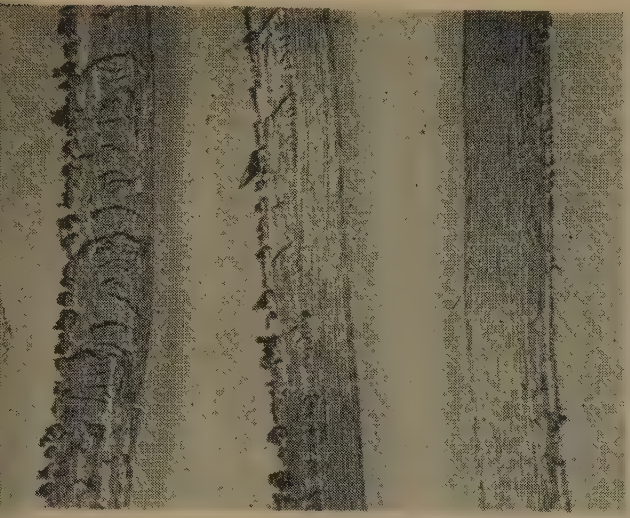

13.42 mv 955 F 13.88 mv 987 F 14.18 mv 1004 F

Steel: NE9445 annealed, 183 Bhn
Tool: tungsten carbide
Depth of cut: 0.100 in.
Feed: 0.01 in. per revolution

FIG. 6 CHIPS FROM 118-SFPM TEST; × 3½

igher. The variation in the millivolt reading has previously een attributed to the effect of the built-up edge which is to emove some of the many parallel thermocouples from the ource of heat and also perhaps to introduce a new thermocouple. t is thought that the difference in the adhesive nature of the tool urface may be the cause of the observed variation. The "nas- ent" surface of the freshly ground tool may have a higher ad- esive nature than a surface very slightly oxidized by the cutting temperature. A similar effect has been observed in the triple-carbide tools where the cutting temperature is usually a little lower after a high-speed test than it was prior to the formation of a slightly discolored tool surface. In these observations with triple-carbide tools no variable due to cratering was apparent.

Fig. 7 shows a series of chips using a tungsten-carbide tool on annealed NE9445 and depicts the gradual clearing up of the separating surface of the chip as the cutting speed is increased. The chip gradually changes from type 3 to type 2. It was observed that by the time the chip cleared up (385 fpm in Fig. 7), the tool had begun to crater and would have failed upon further usage. Evidently the duration of tool-chip contact has an important bearing upon the tendency to adhesion of the chip and the tool.

Fig. 8 shows a series of chips using a triple-carbide tool on the annealed steel. It is seen that, at all speeds shown, the chip may be classified as type 2, there being no significant built-up edge on the tool.

A comparison of Figs. 7 and 8 reveals sharp contrast in the tendency of the chip to adhere to each type of tool. The adhesion temperature (temperature of incipient welding of chip and tool) is dependent upon the steel hardness and upon the composition of the carbide. Since, in this comparison the steel hardness is the same, the difference lies in the tool. W. Dawihl (3) cites a difference of about 275 F in the adhesion temperature of a tungsten-carbide tool, as compared to one containing both titanium and tungsten carbides when each was tested against a steel of about 85,000 psi (170 Bhn). The lower adhesion temperature, or greater adhesive tendency, of the tungsten-carbide composition accounts for the formation of a built-up edge over a widespread range. That the built-up edge eventually disappears must be attributed to the extremely short time of contact and also to the decreased friction on the tool surface. Even though the cutting temperatures are lower with tungsten carbide, the tool life is impaired by the tendency of the chip to adhere to the

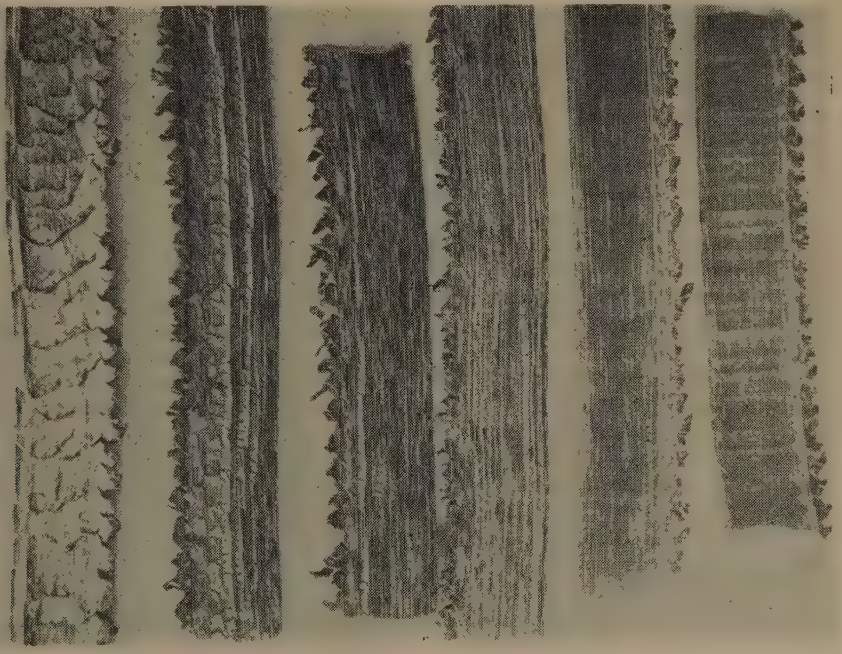

sfpm 109 131 153 211 285 385

Steel: NE9445 annealed 183 Bhn
Depth of cut: 0.100 in.
Feed: 0.01 in. per revolution

FIG. 7 TYPICAL CHIPS USING TUNGSTEN CARBIDE TOOL; × 4½

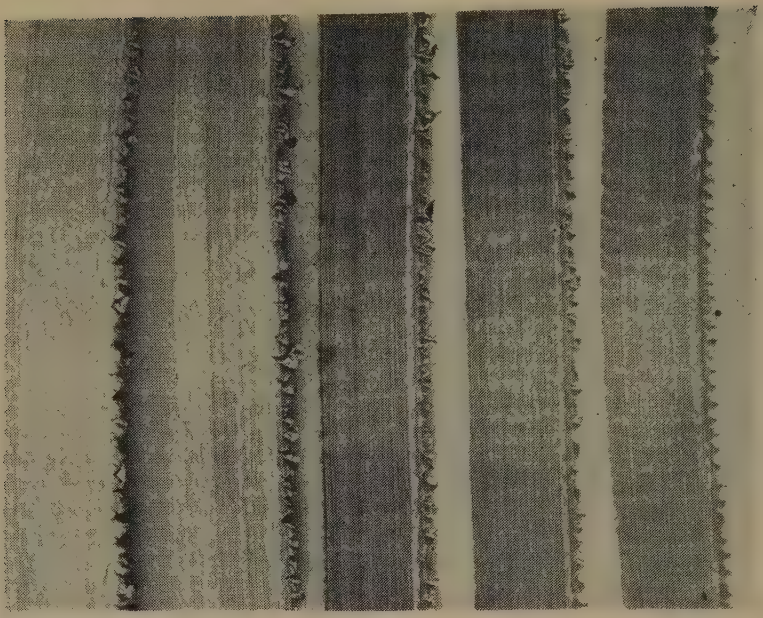

Steel: NE9445 annealed, 183 Bhn
Depth of cut: 0.100 in.
Feed: 0.01 in. per revolution

FIG. 8 TYPICAL CHIPS USING TRIPLE-CARBIDE TOOL; × $4^1/_2$

tool, and, upon subsequent removal, break out some of the tool material.

Fig. 4 also points out a possible basic fault of the two-tool thermocouple. At a speed of 150 sfpm, for example, the cutting temperature of the triple carbide is 70 F higher than that of the tungsten carbide.

If two different tool materials were used as members of a two-tool thermocouple and such a temperature difference prevailed, the so-called "law of intermediate metals" (4) is violated. Combinations such as high-speed steel and cemented carbide do not appear feasible since the usable speed ranges do not overlap appreciably. If triple-carbide tools are used at very low speeds on annealed steel, chips of the type shown in Fig. 7 result and, as a consequence, the millivolt readings are lowered unduly. Similarly, when high-speed steel is used as a tool, the separating surface of the chip is generally quite rough within the usable speed range of the tool. This may be attributed to the low adhesion temperature of high-speed steel (3). However, if the two tools were both of the same grade of carbide, but of different compositions, as illustrated by samples 2 and 5, Table 1, the two-tool thermocouple should function satisfactorily.

Chip-Thickness Results. Chip-thickness measurements were made with micrometer calipers using care to select a straight section of the chip. An average of five readings taken at random was made on the chips from each test in which the triple-carbide tool was used. Chip-thickness measurements made in the manner described represent the thickness to the peaks of the stepped exterior surface of the chip and are therefore slightly greater than the mean chip thicknesses. Samples of chip from two tests, 95 sfpm and 465 sfpm, were mounted in lucite and examined in section longitudinally. A number of areas were measured, using a microscope with a filar micrometer eyepiece, and it was found that the mean chip thickness was about 91 per cent of maximum chip thickness in each of these tests. The readings taken with the micrometer calipers were readily reproducible, and they are used in Fig. 9 as the chip-thickness values.

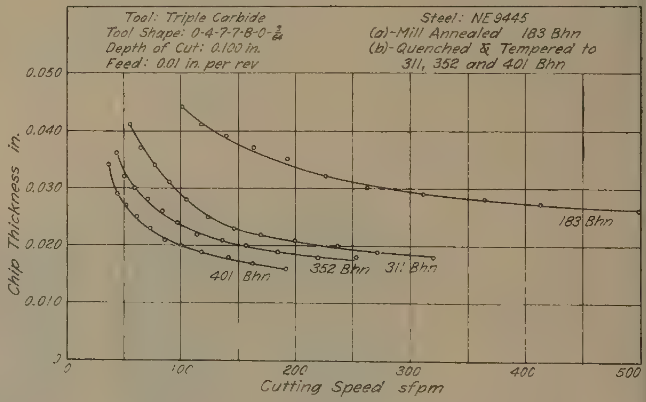

FIG. 9 EFFECT OF CUTTING SPEED ON CHIP THICKNESS

Fig. 9 shows the effect of cutting speed upon chip thickness for annealed and heat-treated NE9445 steel. It is noted that the chip thickness decreases quite rapidly (in fact, as a power function) as the cutting speed is increased from the minimum value and then at a slower rate as the speed is further increased. Eventually, a condition obtains in which the chip thickness is almost independent of cutting speed. At a constant cutting speed, the chip thickness of the heat-treated steel is much less than that of the annealed steel. Considering only the heat-treated steels, it is apparent that the chip thickness bears approximately an inverse relationship to the Brinell hardness of the workpiece. This is well illustrated in the middle curve in Fig. 5 which shows the effect of hardness upon the chip thickness at a cutting speed corresponding to a cutting temperature of 1200 F.

While the cutting conditions herein used cannot be considered as meeting the requirements for orthogonal cutting, as specified by M. E. Merchant in his papers (5, 6, 7), it is of interest to apply some of Merchant's relationships to the results of these chip-thickness measurements. In these tests the chip width, where measured, was about $^1/_8$ in. (varied from approximately

0.118 to 0.133, depending upon the steel hardness and cutting speed), an accurate measurement being impossible due to the sawtooth edge. Hence the chip was not of the same width before and after removal and therefore the following shear angles are based upon the chip-thickness ratio r_t as defined by Merchant (6), and it is the ratio of t_1, the thickness of the "uncut" chip (feed) to t_2, the mean chip thickness after removal (91 per cent of measured thickness). The diameter of the stock was 5 in. (the back rake of the tool was 0 deg and the side rake, 4 deg; the true rake angle α is then practically 4 deg). Using Merchant's equation

$$\tan \phi = \frac{r_t \cos \alpha}{1 - r_t \sin \alpha}$$

the shear angle ϕ may be approximated (to the degree to which the cutting conditions approximate orthogonal cutting).

If the foregoing equation for the shear angle were applied to the heat-treated steels, it was found that the shear angle increased with an increase in cutting speed, and also that the shear angle became greater as the hardness of the steel was increased. The effects of steel hardness are indicated in Table 5 which compares the steels at constant cutting speed and Table 6 in which the cutting temperature is 1200 F.

TABLE 5 EFFECTS OF STEEL HARDNESS AT CONSTANT CUTTING SPEED, 150 SFPM

Steel condition	r_t	ϕ
Annealed 183 Bhn..............	0.292	16° 33′
Heat-treated 311 Bhn...........	0.484	26° 28′
Heat-treated 352 Bhn...........	0.549	29° 38′
Heat-treated 401 Bhn...........	0.632	33° 22′

TABLE 6 EFFECTS OF STEEL HARDNESS; CUTTING SPEED FOR 1200 F CUTTING TEMPERATURE

Steel condition	r_t	ϕ
Annealed 183 Bhn..............	0.33	18° 36′
Heat-treated 311 Bhn...........	0.467	25° 44′
Heat-treated 352 Bhn...........	0.511	27° 50′
Heat-treated 401 Bhn...........	0.566	30° 25′

According to Merchant (7) the influence of temperature, rate of shear, and shearing strain upon the shear angle are all secondary as compared to the effect of compressive stress upon shear strength. If the chip thickness is compared at a cutting speed for a fixed cutting temperature, under which condition the velocity of chip travel is nearly constant, at about 45 fpm, the variables mentioned are still further reduced. Thus the change in shear angle, Table 6, or chip thickness, Fig. 5, as the hardness is increased may be due to a difference in the effect of compressive stress upon shear strength as well as the change in shear strength.

It has been observed (3) that the propensity to adhesion decreases with an increase in the strength and hardness of the steel being cut. The resultant decrease in the friction of the chip on the tool surface causes an increase in the shear angle ϕ. It is also concluded that the chip friction decreases with increased cutting speed perhaps because of greater plasticity of the chip surface. These latter effects appear to account for the observed trends in chip thickness.

Chip-Hardness Test

Samples of the chips from each test with the triple-carbide tool were used for the study of chip hardness at or near the separating suface of the chip. Three sections of chip 1/2 in. to 3/4 in. long were chosen at random and mounted in bakelite in a metallographic specimen mounting press. The separating surface of the chip was left exposed in the process, and this surface was then hand-ground on 2/0 paper, rough-polished with No. 500 silicon-carbide grain, and finished with levigated alumina on a broadcloth wheel. Due to slight irregularities in the chip surface, the polishing operations left some areas of the chip surface in the "as-cut" condition.

The chip hardness was measured with a Tukon[3] tester. The indenter consisted of a square-base diamond pyramid having an apex angle of 136 deg, which was forced into the chip by a load of 2 kg. The hardness so measured is expressed as the diamond-pyramid hardness (dph) and is numerically slightly greater than the equivalent standard Brinell number.

The 2-kg load was chosen in order that the hardness reading could be superficial yet have a large enough indentation to facilitate accurate measurement. The greatest depth of indenter penetration in any chip occurred in the annealed steel cut at 545 sfpm. In this test the average diagonal of the indenter impression was 0.105 mm which corresponded to an indentation of 0.015 mm, or approximately 0.0006 in. Since the chip thickness was 0.026 in., it is evident that there was no possibility of the indenter breaking through the chip. The diamond-pyramid hardness test is sensitive to slight variations and some deviation in the readings should be expected.

During some preliminary studies of chip hardness, a number of hardness surveys were made across the separating surface of several chips. These tests revealed a total variation of about 30 hardness numbers or a deviation of 15 from the mean. The preliminary tests also included random measurements of chip hardness on the separating surface and the opposite, or exterior, surface of the chip. Table 7 summarizes the results of such tests.

TABLE 7 CHIP-HARDNESS DATA; (1 KG LOAD)

(All cuts at 0.100 in. depth and 0.01 in. per revolution feed)

Cutting speed, sfpm	Workpiece condition	Diamond-pyramid hardness (average) Separating surface	Diamond-pyramid hardness (average) Opposite surface
40	Heat-treated 352 Bhn	502	502
208	Annealed 183 Bhn	351	349
390	Annealed 183 Bhn	333	338

NOTE: The over-all variation was approximately ±10 hardness numbers.

A few tests were taken directly on the unpolished portions of the separating surface. Such tests indicated very little difference between the hardness at that location and the hardness on a polished area (of the order of 0.0002–0.0003 in.) slightly removed from the separating surface.

For the chip-hardness values in this paper, a minimum of ten hardness readings were taken at random on the three sections of chip (which were selected at random from each test) and the diamond-pyramid hardness is reported as the arithmetic average of these readings.

Fig. 10 shows the effect of cutting speed upon the chip hardness of the annealed and heat-treated NE9445 steel. The hardness of the uncut stock is shown by points on the zero cutting-speed

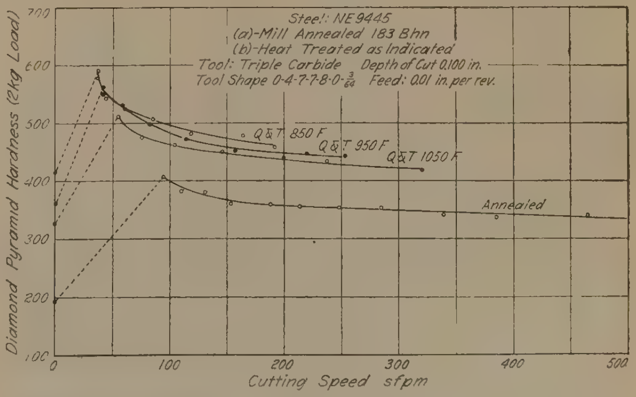

FIG. 10 EFFECT OF CUTTING SPEED ON CHIP HARDNESS

line. It is noted that check tests on two of the steels show a spread of the points. Several check tests were conducted with the surface repolished, in an attempt to evaluate the effect of repolishing on the hardness. In some tests the check values were a little higher (10 points) while in others they were somewhat lower. It is possible that there is some effect due to polishing per se. It may be that the hardness of the chip changes somewhat as the test area approaches a position equidistant from the two surfaces. Further tests are necessary, however. In order to represent the chip-hardness picture properly, the hardness lines in Fig. 10 should be considered as being the mean of a hardness band about 20 diamond-pyramid numbers in width.

---

[3] Wilson Mechanical Instrument Company, New York, N. Y.

Fig. 10 shows clearly the effect of cutting speed upon the chip hardness. The general trend of the curves is reminiscent of the relationship between chip thickness and cutting speed. As the cutting speed is increased, the chip hardness apparently attains a minimum value, after which it becomes virtually independent of speed.

An increase in cutting speed should decrease the chip hardness. This is due largely to a combination of effects: (*a*) A higher rate of heat generation, i.e., higher chip temperature; and (*b*) less time for heat loss so that more heat is available to promote recovery and/or recrystallization of the cold-worked chip material. This so-called adiabatic effect is very noticeable at the end of a high-speed (700 to 800 fpm) cutting test. As the feed is disengaged, the backlash of the feed mechanism causes a final thin chip, which, at high speed, becomes so hot that it ignites and burns. The heat generation is so rapid that the time for loss is nil. This coupled with the low thermal capacity of the thin chip causes the latter to be heated to ignition temperature.

Metallographic examination of a section of a chip from the annealed steel cut at 95 sfpm (1010 F) revealed no signs of recrystallization. The original spheroidized structure was clearly evident. A section of chip cut at 465 sfpm (1430 F) indicated recrystallization at both surfaces of the chip. It is concluded therefore that the chip hardness should decrease with speed, up to some limit, when it thereafter is substantially constant since the recrystallization temperature of the steel has been attained.

Considering the data in Table 7, apparently the two surfaces of the chip attain essentially the same temperature during the cutting operation as judged by the hardness after cold-working.

The chip hardness exceeds that of the workpiece because of the work-hardening due to the plastic deformation. Obviously, the greater the work-hardening capacity of the steel, the greater is the increase due to cold-working. Therefore the greatest increment of hardness should occur in the annealed steel. Conversely, a quenched and tempered steel is of lower work-hardening capacity, and the increase due to cold-working is much less. This is illustrated in Table 8.

TABLE 8 MAXIMUM AND MINIMUM CHIP HARDNESS

	Diamond-pyramid hardness (average)				
Steel condition	Uncut	Maximum	Increase	Minimum	Increase
Annealed 183 Bhn.....	194	407	213	337	143
Heat-treated 311 Bhn..	327	511	184	419	92
Heat-treated 352 Bhn..	362	556	194	445	83
Heat-treated 401 Bhn..	415	584	169	458	43

The maximum and minimum values of the chip hardness bear an interesting relationship to the hardness of the uncut stock.

From Fig. 10 and Table 8 it is evident that an increase in the hardness of the workpiece results in a higher hardness of the chip surface. The maximum work-hardening effect is of the order of 213 dph numbers, and it occurred with the softest (annealed) stock. The hardest stock revealed the least increase in hardness at low cutting speeds.

The various hardness minima are greater than the uncut hardness, the range being from 43 to 143 dph numbers with the greater difference again occurring in the softest workpiece.

If the chip hardness of the heat-treated steels is compared at a selected cutting temperature, 1200 F, it is noted that the relationship is a linear one, i.e., the diamond-pyramid hardness of the separating surface of the chip is a linear function of the Brinell hardness of the uncut stock at a cutting temperature of 1200 F. This is shown by the upper curve in Fig. 5.

Contemplated future tests will extend the heat-treated hardness range to a minimum of about 225 Bhn.

Conclusions

1 All carbide materials in the tool-work thermocouple, as herein applied, must be made from the same lot of carbide mixture and by the same method of manufacture.

2 The heat-treatment of the steel member of a carbide-steel thermocouple has a definite effect upon the temperature-emf relationship.

3 Lower cutting temperatures obtain with tungsten-carbide tools than with triple-carbide compositions.

4 Tungsten-carbide tools exhibit a greater tendency to adhesion of the chip and the tool, resulting in a rough chip surface.

5 The roughness of the chip surface affects the millivolt reading in the tool-work thermocouple.

6 Within the limits of this investigation the cutting speed for a selected cutting temperature decreases linearly as the hardness of the heat-treated workpiece is increased.

7 Within limits the chip thickness decreases with increase in cutting speed. An increase in workpiece hardness results in decreased chip thickness.

8 Within limits the chip hardness decreases with increase in cutting speed. An increase in workpiece hardness results in increased chip hardness.

9 The increase in chip hardness due to cold-working becomes less as the hardness of the workpiece is increased.

Acknowledgments

The author herewith expresses his appreciation to Vascoloy-Ramet Corporation and Carboloy Company, Inc., for the carbide materials used in these tests. Acknowledgment is made to Mr. H. W. Highriter, Vascoloy-Ramet Corporation, and to Mr. George F. Schrader, Mechanical Engineering Department, University of Illinois, for valuable help during the investigation.

BIBLIOGRAPHY

1 "Progress Report No. 1 on Tool-Chip Interface Temperatures," by K. J. Trigger, Trans. ASME, vol. 70, February, 1948, pp. 91–98.

2 "Physics of Metal Cutting," by H. Ernst, *Machining of Metals*, ASM, Cleveland, Ohio, 1938, pp. 14–17.

3 "Investigation of the Processes in the Wear of Cemented Carbide Tools," by Walter Dawihl, *Zeitschrift für Technische Physik*, vol. 21, 1940, pp. 337–345.

4 "Thermoelectric Thermometry," by W. F. Roeser, *Journal of Applied Physics*, vol. 11, 1940, p. 389.

5 "Basic Mechanics of the Metal-Cutting Process," by M. E. Merchant, *Journal of Applied Mechanics*, Trans. ASME, vol. 66, 1944, p. A-168.

6 "Mechanics of the Metal Cutting Process, I, Orthogonal Cutting and a Type 2 Chip," by M. E. Merchant, *Journal of Applied Physics*, vol. 16, 1945, pp. 267–275.

7 "Mechanics of the Metal Cutting Process, II, Plasticity Conditions in Orthogonal Cutting," by M. E. Merchant, *Journal of Applied Physics*, vol. 16, 1945, pp. 318–324.

Discussion

O. W. Boston.[4] The present paper is an appropriate follow-up of the author's previous report and shows the results of a great deal of painstaking work. He is to be commended on his efforts. In work carried out on the same subject, the writer found that the specific materials used as cutting tools had to be used in the calibration tests. The tools were of high-speed steel, which may account for this variation. The author's experiments show less variation between different pieces of sintered carbide of the same type, even from different manufacturers, than the writer experienced with the high-speed steel tools. It is of further interest that the sintered tungsten-carbide tools gave practically the identical results to those of the triple-carbide type. This of course would be expected, but it is always of interest and value to have these points proved.

---

[4] Professor of Metal Processing, and Chairman, Department of Metal Processing, College of Engineering, University of Michigan, Ann Arbor, Mich. Mem. ASME.

In the writer's early tests, it was found that as long as the tool itself was insulated from the toolholder, a second lead taken from any part of the lathe to the potentiometer was satisfactory.

It is interesting to see the relationship between the cutting speed and the interface temperature for the NE9445 steel at three quenched and tempered hardnesses of different values and one mill-annealed hardness. This definitely confirms the previous work on the relationship between cutting speed and tool life for alloy steels of corresponding hardnesses. It might be expected, however, that the slope of the cutting temperature-cutting speed line for the mill-annealed steel in Fig. 3 of the paper, might be of another slope, as was found in the case of tool-life data. This is brought out in the author's discussion of Fig. 3 in which equations for all four lines are given. The slope of the lines for the steels quenched and tempered averages 0.195, while that for the annealed steel is 0.212—somewhat higher. These equations are of nterest and should probably be correlated with the Brinell hardness. It would also be interesting to see if the same equations for steels of other analyses would follow these same laws. It is beieved that they would in a general way be similar but not equivaent.

The writer has also found that chips from a given steel are not always alike when cut at the same speed and other cutting conditions, as shown by the author in his Fig. 6. This is one of the easons why it has been difficult to accept the idea that machinability can be represented by chip ratio and other similar bases. It is for this reason that the writer has prepared a list of some 18 different methods which have been used to evaluate machinabilty, and it is proposed to secure some 30 or 40 steels and alloys of copper, aluminum, and magnesium so that all of these 18 tests can be run on each of the samples by a number of investigators in their own laboratories to learn the possibility of such correlations. So many times the work of one experimenter cannot be compared directly with that of another because of different conditions used in the test or because of different types of tests, and it is believed hat this lack of co-ordination has led to erroneous conclusions.

The writer is in general agreement with the author's conclusions. It is hoped that this work can be extended to other maerials with a view of proving that the conclusions arrived at on ne analyses apply also to materials of other analyses. Further, t would be most helpful to have a short test based upon cutting emperatures developed as a means of evaluating the machinaility of any given material. This work is definitely in that direcon.

M. E. Merchant.[5] The author's careful studies on tool-chip nterface temperatures are adding much to the fundamental nowledge of the metal-cutting process. Such studies as the resent one are greatly needed, and we wish to congratulate the author on the excellent work presented here. It is a pleasure also o know that the author plans to continue these studies.

The first point which the writer would like to discuss is the matter of the lower temperature and greater tendency to chip adhesion observed when cutting with tungsten-carbide tools as compared to triple-carbide tools. Greater tendency to chip adhesion, in general, indicates higher friction between chip and tool. It has been the writer's experience that lowered tool-chip interface temperature is a "cause" of higher chip friction. The two go hand in hand. The question then arises as to the reason for the lower temperature in the case of the tungsten-carbide tool. Although the writer does not have exact data at hand, it is his understanding that the heat conductivity of the tungsten-carbide composition is slightly greater than that of the triple-carbide composition. This greater heat conductivity should be the cause of the observed lower tool-chip interface temperature which in turn should cause the greater tendency to chip adhesion found with the tungsten-carbide tool.

The author's measurements of chip thickness are quite interesting, and the method used appears to give reasonably good results. However, the technique would be rather tedious if applied to a variety of different cutting conditions with different metals and tools, since the multiplier used to obtain average chip thickness from maximum chip thickness (0.91 in the present case) will vary with these changing conditions. The writer believes that a quicker and more accurate technique is the "chip weight" method.[6] In this method a short section of chip is weighed and its length accurately measured. The mean chip thickness can then be calculated from the weight per unit length.

The author's use of the chip-thickness values to calculate values of shear angle seems quite justifiable. The conditions of cutting which he used are a fair approximation to orthogonal cutting, and therefore the use of the equations for orthogonal cutting should result in values which represent a good approximation. As relative values they should be particularly reliable. However, even the absolute values of shear angle obtained by the author appear to agree well with values obtained by the writer[7] under true orthogonal conditions on a similar steel. The author reports that the shear angle increases with increasing cutting speed and also with increasing hardness of the work material. This agrees with the writer's experience. We would, however, offer a simpler explanation than that given by the author for these trends. The shear angle is to a first approximation a very simple function of three variables,[8] namely

$$\phi = \frac{C - \tau + \alpha}{2} \quad \ldots\ldots\ldots\ldots\ldots\ldots [1]$$

where

ϕ = shear angle
α = rake angle of tool
τ = friction angle, a direct measure of coefficient of friction between chip and tool
C = machining constant, directly related to plastic properties of workpiece

The principal reason for the increase in shear angle with increasing cutting speed is that the coefficient of friction between chip and tool decreases (i.e., the angle τ decreases) with increasing speed. Thus the shear angle should rise, in accordance with Equation [1]. The major reason for the increase in shear angle with increasing hardness of the workpiece is no doubt the higher value of machining constant C usually characteristic of the plastic properties of quenched and tempered steels, which should of course also make the shear angle rise in accordance with Equation [1].

---

[5] Senior Research Physicist, The Cincinnati Milling Machine ompany, Cincinnati, Ohio.

[6] "New Methods of Analysis of Metal Cutting Processes," by M. E. Merchant and N. Zlatin, Proceedings of the Society for Experimental Stress Analysis, vol. 3, no. 2, 1946, pp. 4–19.

[7] Refer to the author's Bibliography, item (6).

[8] Refer to the author's Bibliography, item (7).

The chip-hardness measurements made by the author present an interesting study. The writer has found that these hardness values can be explained quite rationally in terms of the data obtained from the chip-thickness measurements together with a knowledge of the tempering temperatures of the heat-treated steels. It has been shown by Zlatin and Merchant[9] that the amount of hardening of a chip by the deformation occurring in the process of chip formation is a direct function of the shearing strain undergone by the metal in that process of deformation. This shearing strain is a function of the shear angle ϕ and the rake angle of α and is given by the equation

$$\epsilon = \cot \phi + \tan (\phi - \alpha) \quad \ldots\ldots\ldots\ldots\ldots [2]$$

where

ϵ = plastic shearing strain undergone by chip metal.

It was found in this earlier study that the amount by which the chip is increased in hardness above the hardness of the parent workpiece is a linear function of the shearing strain. Shearing-strain values have been calculated from the chip-thickness data presented by the author and it has been found that, in the case of the annealed sample of NE9445 steel at least, a similar linear relationship exists. This is shown in Fig. 11 of this discussion. In this figure the hardness increases for the chips obtained at all the different cutting speeds and from all four different heat-treatments of the NE9445 steel are plotted as a function of shearing strain values calculated from Equation [2]. While the linear relationship holds throughout for the annealed sample, it is evident that there is a departure from the linear trend in the case of the quenched and tempered (unstable) samples. This, however, can be attributed to the annealing or tempering of the chips from these unstable steels by high chip temperatures.

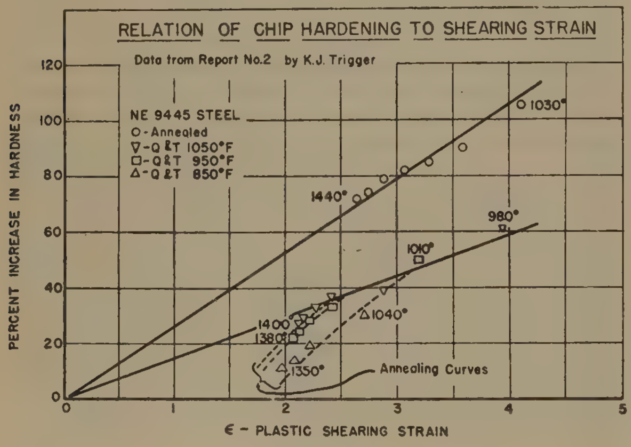

Fig. 11

Values of the tool-chip interface temperatures observed for the highest and the lowest cutting speeds used on each steel have been written opposite the corresponding plotted points in Fig. 11. It can be seen that, in general, where these temperatures are below or only slightly above the tempering temperature for the given sample, the plotted points lie on the lower full straight line passing through the axis. However, where these temperatures considerably exceed the tempering temperature, the plotted points fall below this curve. Thus it may be assumed that the chips removed from the quenched and tempered samples are all hardened by the initial deformation to a value corresponding to the full straight line, but that where the final chip temperature exceeds the tempering temperature, the chips quickly soften, dropping to final hardness values corresponding to the dotted annealing curves shown in the figure. The reason for the lower slope of the full straight line representing the hardening in the case of the quenched and tempered samples as compared to the line for the annealed sample in Fig. 11, is due to the lesser strain hardenability of the quenched and tempered samples.

It was found in the previous study that the slopes of these lines are greater the greater the strain-hardenability of the metal. Apparently all three quenched and tempered samples have approximately equal strain-hardenability of a fairly low value while the strain-hardenability of the annealed sample is appreciably greater. We would like to suggest that the author make Meyer strain-hardenability measurements on these steels to check these points.

Author's Closure

The author is grateful to Professor Boston and to Dr. Merchant for their kind remarks and for the pertinent contributions to the subject matter of this paper.

Professor Boston has brought up a number of interesting points for consideration.

The principal reasons for insulating both leads of the tool-work thermocouple were to avoid the possibility of parasitic emfs, and to facilitate the detection of short circuits caused by chip fragments which may have been lodged in the tool post. In one series of tests under constant cutting conditions, the second lead was attached alternately to the brush and to the tailstock of the lathe. Under specific cutting conditions, the millivolt readings averaged 13.12, when the lead was attached to the brush, as against 12.94 with the lead attached to the tailstock. While this difference is not great, it may be eliminated readily by the use of a brush made from a section of the workpiece. A further benefit in favor of the insulated brush is that the circuit was more sensitive. When the lead was attached to the brush the potentiometer could be balanced in about one third of the time required when the lead was attached to the lathe. Presumably parallel electrical paths cause the sluggishness. In some of the early tests a bronze bearing housing was suspected of causing a parasitic emf of nearly 0.5 mv magnitude. This lathe is not used now for the cutting-temperature tests.

The effect of steel hardness upon the slope of the cutting speed-cutting temperature relationship is, essentially, as has been pointed out by Professor Boston, that is, the exponent is greater for an annealed steel than for one in the quenched and tempered condition. Some tests performed subsequent to the presentation of the paper under discussion have indicated that NE9445 quenched and tempered to 283 Bhn had an exponent of 0.189, of the same order as that for the quenched and tempered steels reported upon, whereas two samples of annealed NE8640, 173 and 178 Bhn had exponents of approximately 0.22. All tests to date indicate that the curves are steeper for the annealed steels than they are for the quenched and tempered steels. The evidence points to a possible correlation of slope to Brinell hardness, although a greater variety of steels need to be tested before such a correlation is attempted.

A vast majority of the tests reported in this paper and its predecessor have been conducted on bars from the same heat of NE9445 steel. Such a procedure has been followed in order to eliminate the variable of chemical composition, until the cutting speed-cutting temperature relationship had been definitely established. A few tests with NE8640 and NE8640 sulphite-treated steels have confirmed the general cutting speed-cutting temperature relationship.

---

[9] "Distribution of Hardness in Chips and Machined Surfaces," by N. Zlatin and M. E. Merchant, Trans., ASME, vol. 69, 1947, annual bound volume only; also, *Iron Age*, vol. 159, May 22, 1947, pp. 69–75.

Recently, some tests have been conducted on cold-drawn low-carbon seamless tubing of 194 Bhn, having an approximate outside diameter of $7^{7}/_{8}$ in. and wall thickness of 0.1 in. In such tests only the side cutting edge was active and the cutting speed-cutting temperature relationship was the usual straight line on logarithmic co-ordinates. In a specific test at 0.01 in. per revolution feed, the equation was $T = 288\ V^{0.244}$. A number of tests have been conducted to evaluate the effect of feed over an approximate range from 0.0025 to 0.0147 in. per revolution. In each instance the equation of the line follows the general law $T = CV^{n}$ and from the tests the relationship of feed to cutting temperature has been developed into the general law $T = kf^{m}$.

This phase of the work is treated more completely elsewhere[10] and need not be repeated here. All tests with steel have resulted in the same general cutting speed-cutting temperature relationship, the constant and exponent of which depend upon the steel, its hardness, and the cutting conditions. Future tests are to be conducted on aluminum and other nonferrous alloys as well as some additional steels.

Professor Boston's plan for correlation of the various methods to evaluate machinability should go a long way toward a better understanding of machinability and metal cutting. One of the objectives of this study is to develop, if possible, a short test for evaluation of machinability by cutting-temperature relationships. It may be that the chip hardness must also be considered in conjunction with tool-chip interface temperature.

Dr. Merchant has raised some interesting aspects of the problem relating to the lower cutting temperatures and greater tendency to adhesion when the tungsten-carbide tool was used. The two grades of carbide used for the cutting tests shown in Fig. 4 of the paper were reported by the manufacturer as having the following approximate thermal conductivities: 0.100 and 0.190 cal/deg C/cm²/cm/sec for the triple carbide and tungsten carbide, respectively. This difference in conductivity is a probable cause of much of the observed difference in cutting temperature.

Undoubtedly, the temperature at the tool-chip interface has an important bearing upon the tendency of the chip to adhere to the tool. This may be observed at the beginning or end of a cutting test in which the conditions of the cut are such that a type 2 chip is obtained during the test. Due to backlash in the feed mechanism, both the initial and final portions of the chip are obtained under the equivalent of a fine feed. This fine feed results in lower cutting temperatures (see a foregoing part of this closure), and the separating surface of both the beginning and the end of the chip are roughened owing to the presence of a built-up edge on the tool. Since the cutting speed is essentially unchanged, the decrease of cutting temperature is the probable cause of the greater tendency to adhesion of the chip and the tool. This however, is not the only factor involved. If the separating surface of the chip from a tungsten-carbide tool is compared to that from a triple-carbide tool at the same tool-chip interface temperature, it is seen that the chip from the tungsten-carbide tool is still rough whereas the chip using the triple carbide is smooth on the separating surface.

As a case in point, compare the chip surface of the tungsten-carbide series, Fig. 7, at 211 sfpm with that of the triple-carbide group, Fig. 8, at 153 fpm. (The cutting temperature is essentially the same, 1130 F.) It is apparent that there is a considerable difference in the "welding-on" tendency of the chip and tool even though the cutting temperatures are equal. The tendency to adhesion must, then, be a characteristic of the composition of the carbide. The presence of a built-up edge on the tool has always accompanied a lower indicated tool-chip interface temperature. This is also a factor in the lower-cutting temperatures obtained with tungsten-carbide tools.

The manufacturers report a higher coefficient of friction for the triple-carbide grade, particularly at the lower cutting speeds. This is at variance with the general observation that a higher coefficient of friction is associated with greater tendency to adhesion of the chip and tool. Dawihl[11] reports the various welding-on temperatures of different grades of cemented carbide against steel. The tests were conducted by butting samples of steel and cemented carbide, at a contact pressure of some 4200 psi and heating them in a hydrogen atmosphere. In this way the temperature of incipient welding was obtained under conditions of thermal equilibrium. Dawihl's tests have significance, but it is well to remember that they were conducted under static conditions whereas in actual cutting large relative velocities often obtain.

Equation [1] of Dr. Merchant's discussion is convenient for the estimation of the shear angle ϕ although no attempt has been made to apply the equation in the analysis of these data. Dr. Merchant's excellent analysis has been of tremendous help in the understanding of the basic mechanics of the metal-cutting process and of the plasticity conditions during cutting. However, it appears that his Equation [1] is subject to certain limitations. It does not seem that the machining constant C is always a constant. Rather it is dependent upon the rate of shear and definitely upon temperature, especially in the range of recovery and recrystallization. Dr. Merchant recognizes these limitations in his papers,[12] and undoubtedly he has given a great deal of thought to possible methods of attack on the difficult problems involved.

Barrett[13] has discussed the effect of temperature upon strain-hardening and has shown the effect of various testing temperatures on the strain-hardening characteristics of aluminum and magnesium crystals. The curves reveal that strain-hardening is pronounced at about 65 F (18 C) and of minor magnitude at 575 F (300 C). Since recrystallization may occur well below this temperature (depending upon the magnitude of the shearing strain) the amount of strain-hardening becomes nil at elevated temperatures. The curves further reveal that shearing rate has a significant effect upon the magnitude of strain-hardening when at elevated temperatures, but that the effect is minor at lower testing temperatures. Steel chips may reach recrystallization temperatures during cutting and, as a consequence, a machining constant which was evaluated at room temperature should probably be modified. This presents a challenging problem.

With reference to Fig. 11 of Dr. Merchant's discussion, it appears reasonable to conclude that the divergence from the straight-line relationship of the plastic shearing strain to per cent increase in hardness is caused by further tempering of the quenched and tempered steels. Since the test logs were tempered for 5 hr, they should be structurally stable up to the respective tempering temperatures. Cutting temperatures significantly greater than the tempering temperature would provide further tempering action and thereby cause softening of the chip. From Fig. 11 it may be noted that the greater divergence is associated with the lower tempering temperatures, an observation in accord with the foregoing reasoning.

The strain hardenability as shown by the Meyer analysis[14] has been conducted using an $^1/_8$-in. steel ball under loads of 45, 60, 100, and 150 kg, respectively. While various observers obtained somewhat different results, the values of the Meyer exponent n were 2.25 for the annealed steels, and 2.14 to 2.18 for the quenched and tempered steels.

---

[10] Discussion of "Distribution of Heat Generated in Drilling," by A. O. Schmidt and J. R. Roubik, preprint No. 48—SA-10, presented at the Semi-Annual Meeting, Milwaukee, Wis., May 30–June 5, 1948, of The American Society of Mechanical Engineers.

[11] Bibliography of paper, reference (3).

[12] Bibliography of paper, reference (7).

[13] "Structure of Metals," by C. Barrett, McGraw-Hill Book Company, Inc., New York, N. Y., 1943, pp. 300–301.

[14] "The Hardness of Metals and Its Measurement," by Hugh O'Neill, Chapman and Hall, London, England, 1934.

The author is of the opinion that the strain hardenability as determined by a Meyer analysis at 70 F may not be directly applicable at temperatures where recovery or recrystallization may occur. Apparatus is being constructed which will permit the measurement of strain hardenability at elevated temperatures.

Automatic Control of Turbojet Engines

By C. S. CODY,[1] LESTER, PA.

This paper presents the requirements for automatic control of a turbojet engine in order to meet the needs of military aviation and to realize the full operational performance of the engine. The author describes how these requirements were established, and outlines the recommended approach to the design of an optimum engine power control.

INTRODUCTION

FROM the military pilot's standpoint, a single cockpit control lever should be all that is required to operate the turbojet engine over its full range of thrust, along a line of optimum practical economy, and within its safe limitations for turbine speed (rpm), temperature, and burner operation. Moreover, the control-lever sensitivity must be such that predetermined thrust settings may be selected without difficulty.

In order to retain the operational simplicity of single-lever power control of the engine in the face of increasing stringent operating requirements for the turbojet engine, it has become necessary for the turbojet-engine manufacturers to expend a major part of their development effort toward perfection of automatic engine-control elements. During the early development of the turbojet engine, it was reasonable to expect that greater emphasis would be placed on the design of the basic engine than upon the controls, because it was considered that simple manual controls would be adequate; however, since it has been generally realized that control performance has lagged basic engine development, a concentrated effort has been made to provide automatic engine controls which permit the full range of engine performance to be realized without detracting the military pilot's attention from his primary combat duties. As this automatic-control development has progressed, flight experience has dictated more and more stringent operating requirements as represented by closer speed regulation, faster acceleration, and increased service life. These requirements have been combined to make this development a difficult one, particularly as it has been desired that these improvements be incorporated promptly into engines already in operation in the field and in those coming off the production line.

The primary object of this paper is to acquaint the control designer with the general requirements for control of turbojet engines so that he can better anticipate the problems which will arise while developing controls for specific turbojet applications. Although the information presented is basic in nature, it is presupposed that the reader is generally familiar with the fundamental principles of jet propulsion and the functional arrangements of turbojet-engine components. For those less familiar with the major components of the turbojet engine, a recommended reference is a paper by A. H. Redding.[2]

FUEL CONTROLS

The thrust output of a fixed-area jet engine is a direct function of fuel flow. Therefore all devices for controlling thrust, by one means or another, must regulate engine fuel. As engine fuel requirements are affected by variations in pressure altitude, flight velocity, and ambient temperature, there must be some practical means for maintaining the selected percentage of available thrust for these changing conditions. Thus if the fuel to the engine is regulated only by the manual positioning of a variable fuel-metering orifice, or "throttle valve," it would be necessary to reposition the throttle lever after every change in the engine load in order to maintain the thrust setting.

An early solution to this problem was a scheduling means which consisted of providing an aneroid-operated fuel by-pass valve for use in conjunction with the manual throttle valve. Such a valve, usually known as the "Barostat," responds to changes in total air pressure at the inlet to the engine to by-pass all fuel pumped in excess of actual engine requirements for any given flight condition. This fuel valve, controlled by the aneroid element, is profiled to a definite fuel schedule which is applicable to only one basic engine-fuel-requirement curve for a fixed exhaust-nozzle jet area. Scheduled controls of this sort can establish only an approximate relationship between engine fuel-flow and flight conditions, and therefore do not hold the selected thrust settings over full range of throttle movement under changing flight conditions.

In order to overcome the limitations of scheduling, it is necessary to utilize some control parameter which is a function of the engine fuel requirements and which lends itself to simple and positive measuring means. The only parameter which fulfills this need is engine rpm. Engine control to maintain constant rpm provides the maximum thrust available for all flight conditions at the maximum allowable engine rpm, and at the same time holds a constant percentage of the thrust available for all partial throttle settings over the full range of flight conditions.

This direct measurement is then used to regulate the fuel flow to the engine to maintain the rpm at a constant selected value. Such a control means is the speed-responsive governor, well known for its innumerable applications on steam turbines, aircraft propellers, and reciprocating engines of all types.

Among the numerous speed-sensing governor elements, suitable for turbojet-engine application, are the following:

1 The centrifugal flyweight, measuring speed by radial displacement of rotating masses.

2 The positive-displacement pump, measuring speed as a linear function of pump volumetric output or a function of pump pressure.

3 The direct-current generator measuring speed in terms of output voltage.

4 The alternator, measuring speed in terms of alternating-current electrical frequency.

The speed measurements, or output signals, from any of these governing elements are usually applied either directly, or through suitable hydraulic or electrical amplification, to position a variable fuel-metering orifice or to vary the output of a variable-volume fuel-metering pump. In order to select a new governed engine speed, a signal in opposition to the speed measurement is introduced into the governing means by the pilot's control lever.

---

[1] Section Engineer, Engine Auxiliaries, Aviation Gas Turbine Engineering Department, Westinghouse Electric Corporation. Mem. ASME.

[2] "Current Problems in Developing Major Components for Aviation Gas Turbines," by A. H. Redding, *Aeronautical Engineering Review*, vol. 5, December, 1946, pp. 30–35 and 91.

Contributed by the Aviation Division and presented at the Aviation Conference, Dayton, Ohio, September 20–21, 1948, of THE AMERICAN SOCIETY OF MECHANICAL ENGINEERS.

NOTE: Statements and opinions advanced in papers are to be nderstood as individual expressions of their authors, and not those of he Society. Paper No. 48—AV-3.

For example, let us consider an engine governor of the simplest centrifugal flyweight type. Assuming that the flyweights, rotating at some function of engine speed, are directly linked to the main fuel-metering orifice, as the rpm increases, the weights are displaced outwardly, and the fuel-metering orifice is made smaller. Conversely, as the rpm decreases, the weights are displaced inwardly and the metering orifice becomes larger. The centrifugal action displacing the weights outward is opposed by a spring, known as the "speeder spring," and the force exerted by this spring is established by the position of the pilot's throttle through suitable linkages, cams, etc. When the spring force is just sufficient to balance the rotating weights, the governor is said to be "on speed," and the engine is operating at a constant rpm. Should the load on the engine start to decrease, such as during a climb to a higher altitude, the engine will be receiving fuel in excess of its requirements for the selected rpm, and therefore the engine rpm will begin to increase above the selected value. However, the governor will sense this increase in rpm and will move to close off the fuel-metering orifice until the rpm is reduced.

It is an unfortunate characteristic of all simple speed-responsive governors, consisting of only those basic elements so far discussed, that with a change of engine load calling for a reduced fuel supply, the governor is unable to maintain exactly the original rpm setting. This fact is made apparent when one remembers that there is a definite position of the metering orifice for each position of the flyweights; thus when a change in engine load takes place it is necessary for the weights to be displaced a certain amount in order to alter the fuel supply, and the weights can retain their new position only at a changed engine speed. For the simple uncompensated governor, which has just been considered, a reduction of engine load necessitates that the weights displace outwardly until they are just balanced by the new spring force created by the resultant compression of the speeder spring. The engine speed at which this new balance point is achieved will be somewhat higher than the desired speed originally selected by the pilot's throttle, and this increment of governed speed increase, resulting from the engine-load change, is commonly known as "governor droop." Referring to Fig. 1, the sloping vertical lines are the governing-control curves and indicate this droop characteristic.

At this point it should be emphasized that, although governor droop is very undesirable from a constant-speed standpoint, all governors require some stabilizing influence such as droop in one form or another, and that, in general, the greater the droop the greater is the tendency toward stability. It is obvious that if the control curves were absolutely vertical (representing zero droop), there would be no set fuel flow for the selected rpm and consequently the rpm could not be held by the governor. Hence stability is obtained by controlling transient changes along the dotted sloping control lines, as shown in Fig. 1. As the slope of these curves, in general, represents excessive speed change with load, it is necessary to reset these control lines, as soon as stable conditions are reached, into a resulting control curve having acceptable droop characteristics. As the sloping control lines are effective only during a transient condition, the governor is said to have "temporary droop." As soon as stable conditions are reached, the governor controls along the reset steeper curve with "permanent droop."

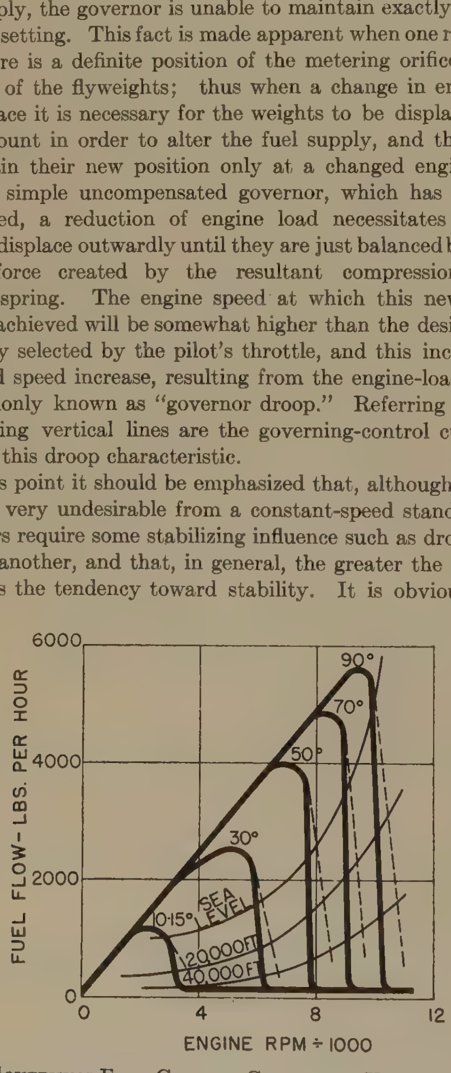

Fig. 1 Governing Fuel-Control Curves for Various Throttle Settings in Relation to Engine Fuel Requirements for Different Altitudes

The importance of the permanent-droop characteristic of the governor cannot be overemphasized from an operating standpoint, for it controls the variation in the set speed of the engine. This allowable variation in maximum (military) rpm is limited closely by the basic engine design. A drop off in military rpm is even more closely limited, as it represents a drop off in thrust which reduces the military performance of the aircraft.

The problem of compensating for governor droop, in order to provide acceptable speed governing, may be approached in various ways. In the illustration of the simple uncompensated fly-ball governor used in the foregoing, it will be recalled that the speed droop resulted from the inability of the weights to displace outward sufficiently to reduce completely the fuel flow to the new lower engine requirements. It will be further recalled that it was the increased compression of the speeder spring which prevented the weights from realizing the full displacement required to maintain constant rpm. This suggests the possibility of reducing permanent droop by reducing the initial speeder-spring compression in proportion to the reduction in engine load. This has been accomplished in some fuel-control governors by opposing the speed-sensing element by two separate speeder springs, the compression of the main speeder spring being accomplished by the pilot's throttle lever, while the compression of the auxiliary speeder spring or "reset spring" is varied by means of a piston positioned by a pressure which is a function of engine speed. Such a proportional pressure may be either engine fuel-nozzle manifold pressure, the pressure differential across a Venturi in the metered fuel line, or compressor-outlet total pressure. Another means of compensating for droop caused by changes in ambient-air conditions is to provide a barometric valve in the metered fuel line to by-pass a scheduled quantity of fuel just equal to the difference in fuel requirements between the fuel provided on the temporary droop curve and that desired to give the required stabilized speed.

So far in the discussion, all corrective measures outlined to compensate for excessive droop are scheduling devices which depend on their successful operation by determining in advance the fuel correction which will be required for various loads and engine rpm. As load changes occur with changes in ambient temperature, flight speed, flight attitude, and altitude, it is obviously nearly impossible to compensate accurately for all these variables using scheduling means and still operate the engine within acceptable limits. For these reasons, the ultimate objective of the control development is to attain true constant-speed or "isochronous" governing.

The isochronous governor senses the set speed directly and moves the throttle valve until this speed is reached, at which time the error signal becomes zero, and the speed-sensing means is restored to its original or synchronous-speed position. This type of governing employs the same principles as outlined, using the sloping temporary droop curve; however, in this case permanent droop is zero. The principle advantage of this type of governing is that no scheduling of load variables is necessary, and therefore the selected speed may be maintained regardless of load change vithin the accuracy of the apparatus to measure speed. A schematic arrangement of such a governor is shown in Fig. 2.

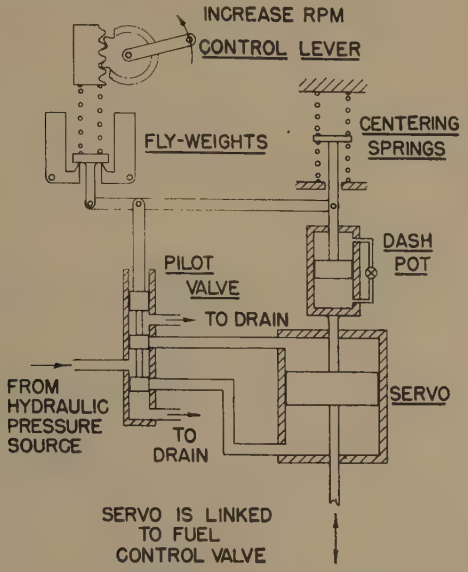

FIG. 2 SCHEMATIC ARRANGEMENT OF ISOCHRONOUS FUEL-CONTROL GOVERNOR FOR TURBOJET ENGINE

SPEED SENSING BY ELECTRICAL MEANS

As previously noted, speed sensing may also be accomplished electrically by a number of means, each having its advantages and disadvantages. The first of these types to be considered is the direct-current generator which is arranged to have a constant field strength. This device provides an excellent means for measuring the speed of engines which are not subjected to wide ranges of pressure altitudes.

One of the important advantages of this device lies in the linear relation between output voltage and speed. Another advantage is that a certain amount of power may be taken from this type of indicator without affecting seriously either the sensitivity or the speed of response.

The two major disadvantages of the direct-current generator are the difficulties in obtaining satisfactory brush operation over the entire range of altitudes, and the problem of providing a satisfactory voltage reference to use for a speed reference.

Another device which may be used for measuring speed is the so-called "drag-cup generator." This is essentially a two-phase nduction motor which is driven at a speed considerably lower han its synchronous speed. One of the two phases is excited rom a constant-voltage and constant-frequency supply. An lternating-current voltage is then induced in the second phase vhich is proportional to the speed of the motor. The frequency of this voltage is the same as that of the supply voltage.

The drag-cup generator eliminates the brush difficulties which are encountered with the direct-current generator. There remains, however, the difficulty of providing a satisfactory voltage eference to use as a speed reference.

The last type of speed-sensing device which will be considered n this paper is an alternator which is connected to a frequency neter. In so far as the stability of calibration under conditions f varying temperature and pressure is concerned, this appears o be the most satisfactory of all the methods for measuring peed. Its stability of calibration depends on the quality of the lectrical components in the frequency meter only. A further dvantage of this type of circuit is that the frequency meter may be arranged to give a zero signal at the set speed. As the result of this, the need for a reference voltage disappears.

In general, an alternator and frequency meter heretofore have not been satisfactory for aircraft application because of the large size and weight of the frequency meter. However, recent developments have made available a frequency-measuring circuit which is both small and light, and this system therefore offers great promise.

There are many different methods for utilizing the error signal produced by the speed-sensing circuit. However, the ultimate circuit will give identical control to that discussed under hydraulic mechanisms. This consists of the usual proportional temporary droop curve which is reset to give isochronous control.

To produce the proportional droop curve, the main control amplifier may be arranged so that its input signal is the difference between the error signal and a position-indicating signal from the final control element. Thus torque or force is applied to the final control element only when its position is different from that required by the error signal.

One accurate method for developing the reset signal requires the use of another amplifier and a small actuator. The purpose of this actuator is slowly to upset the relation between the final control-element position and the position-indicating signal. The amplifier is arranged to drive the motor at a rate porportional to the error signal and in the direction to reduce the error signal to zero.

Should an electrical system be selected, the power source must be self-contained within the control system as it is not advisable to depend upon the power source of the air frame for main-engine control operation. Also, in the development of an electrical system, due consideration must be given to the high-altitude characteristics of the control elements when the circuits are first being considered, in order to avoid the possibility of a complete redesign of a suitable sea-level control in order to meet high-altitude ambient conditions.

The electrical system has one distinct advantage over its mechanical-hydraulic competitor in that the development time should be somewhat shorter, particularly during the trying period when adjustments are being made while the control is first tried on the engine. In a hydraulic system these adjustments usually take the form of remachining new parts of a slightly different characteristic or size. On the other hand, on an electrical control, it usually means merely a manual resetting of resistance or capacitance.

In the early days of fuel controls, the fuel-control lever was generally scheduled so as to realize a linear relationship between its movement and engine rotative speed. As shown in Fig. 3, this arrangement provides an extremely thrust-sensitive control lever at higher values of thrust and, subsequently, low sensitivity at low values of thrust. Since, from a flight standpoint, control of airplane speed is a direct function of thrust and not rpm, a schedule of this nature makes it necessary to interconnect the pilot's control lever to the fuel-control lever by means of cams and shafting in place of a simple bell crank-and-pulley arrangement.

As a result of experience gained from turbojet-engine installations and flight testing, design changes were introduced to incorporate a nearly linear variation of thrust with the control-lever position substantially as shown in Fig. 4. This schedule does afford one disadvantage in that the control lever is sensitive to rpm changes at the low speed, and the establishment of the idle-speed setting becomes a problem if any backlash exists in the control linkage. The situation is remedied, however, by designing a flat-spot rpm schedule which permits the control arm to be moved a number of degrees at the idle setting without any response in rpm or thrust. Fig. 5 illustrates the optimum throttle-lever schedule for turbojet engines.

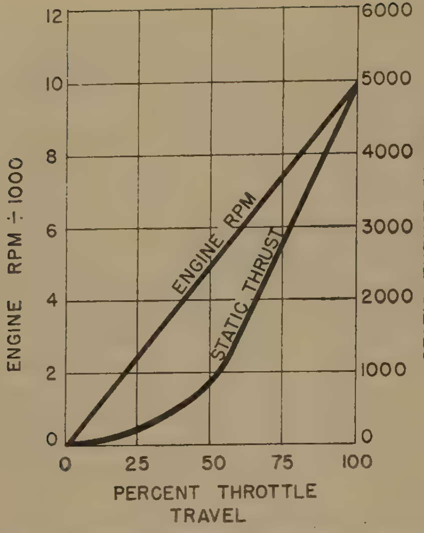

Fig. 3 Control-Lever Schedule of Early Turbojet-Engine Controls

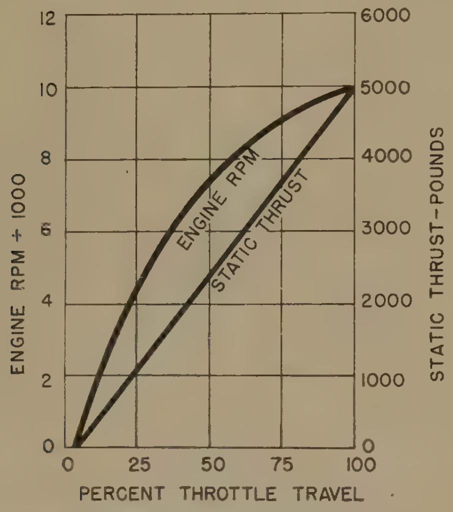

Fig. 4 Revised Control-Lever Schedule Giving Linear Relationship Between Thrust and Throttle Movement

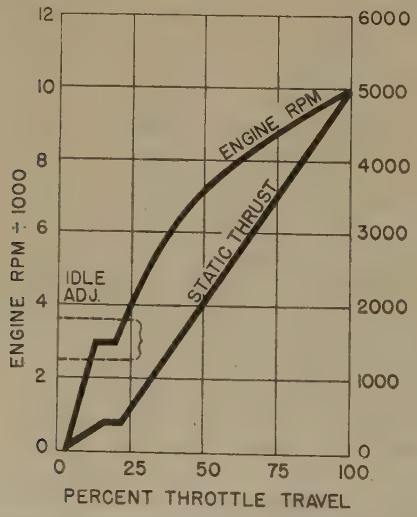

Fig. 5 Revised Control-Lever Schedule With Adjustable "Flat-Spot" Idle Setting

Acceleration Controls

An increase in engine rotative speed is obtained by delivering fuel to the combustion chamber at a rate over and above the steady-state requirement. The magnitude of this increased rate is limited primarily by three important factors. These are a possible stalling condition encountered in the compressor under certain adverse conditions, the limiting temperature that the turbine blades and nozzles will withstand, and a combustor "blow-out" condition, encountered under certain extremes of altitude. All of these elements are present in aviation gas turbines to a greater or lesser degree, and continuous effort is being made by industry to lessen their effect, in order to improve further the operation of the engine.

Stalling of an axial-flow compressor is caused by excessive pressure ratio either across the entire compressor or across any one stage of the compressor. This excessive pressure ratio causes the air flow along the blade path to deviate from the designed flow path and further decreases the pumping ability of the blade, which results in a momentary drop in discharge pressure. This in turn decreases the compression ratio until the air flow again follows the blade path and builds up the compression ratio sufficiently to repeat the cycle. This condition may occur at frequencies of approximately 20 to 30 cycles per sec (cps) and is often accompanied by excessive engine vibration.

Engines are so designed that stalling does not occur under steady-state operation. However, high acceleration, by increasing the back pressure on the compressor temporarily, will cause a borderline steady-state operation to stall under extreme acceleration rates. In actual engine operation compressor stall is avoided on conventionally designed compressors merely by limiting the rate of acceleration. Such a condition is shown by curve A in Fig. 6 which illustrates the maximum allowable turbine temperatures that can be experienced without stalling a hypothetical compressor. Since the temperatures are total values, a change in the ambient conditions will relocate this curve as shown by curves B and C.

Maximum thrust at "military rating" of the engine is obtained by operating at the maximum allowable turbine-inlet temperature. The engine design and metallurgical properties of the high-temperature materials are such that adequate life of the engine is obtained at this temperature. Referring to Fig. 7, the rapid drop-off in engine life which is encountered when military temperature is exceeded is clearly shown. As has been pointed out, engine

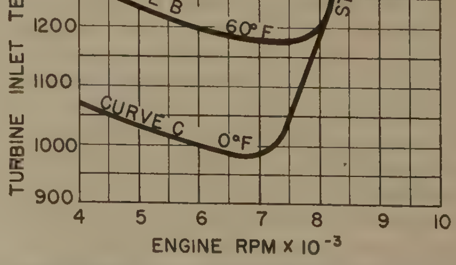

Fig. 6 Curves Showing How Stall Characteristics of a Hypothetical Turbojet-Engine Compressor Can Limit the Maximum Allowable Turbine Temperatures

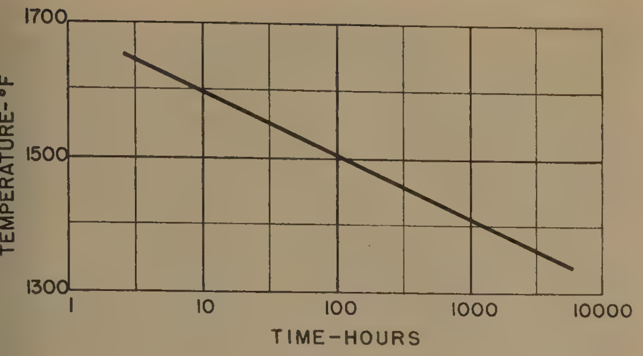

IG. 7 Effect of Maximum Turbine Temperature on Engine Life, Using a Conventional Turbine-Blade Material

cceleration can be accomplished only by increasing the tempera- ure required to maintain steady-state operation. In order not o affect engine life adversely, due consideration must be given to imiting the temperature rise over maximum steady-state condi- ions during accelerations. At the same time, the rate of accel- ration must be sufficiently fast to give satisfactory aircraft- arrier wave-off operation. This is accomplished by both limit- ng the top temperature to a reasonable maximum and making he acceleration period short enough so that the blades and ozzles do not have an opportunity to reach the actual gas tem- erature. In practice, this acceleration period, on typical fixed- rea-exhaust jet engines, is approximately 8 to 15 sec from idle to ilitary rpm.

The third factor, combustor blow-out, occurs under the ex- remes of altitude operation and is evidenced by an inability to aintain a fire in the combustion chamber. This phenomenon is ndicated at altitudes approaching the maximum when an accel- ration is attempted from a steady-state condition of operation. he additional fuel suddenly required for acceleration alters the ir-fuel ratio in the combustor in a direction to produce flame in- tability and blow-out at altitudes lower than the steady-state- ltitude limit. Acceleration rates under these conditions must e slower than normal to prevent this occurrence. This correc- ion must be incorporated into the control until combustion de- elopment raises the point at which this occurs to a limit mate- ially above the aircraft operational level.

From a study of these limitations it is evident that the fuel ow to the engine during an acceleration must be varied for each perating condition, in order to give the fastest acceleration and till not infringe upon these engine operational limitations.

One method of accomplishing this is, of course, the manual ethod in which the pilot varies the rate of fuel flow by moving he throttle at a rate so as not to exceed an established maximum urbine temperature. This leads to an acceleration rate slower han the optimum and also does not insure against the possibility f over-temperaturing by rapid movement of the pilot's control ever during an emergency.

The method that is now in general usage is the automatic ac- eleration control which is an integral part of the automatic fuel- ontrol system. Many arrangements embodying this feature re being used.

One method is the rate-of-pressure-rise system which is cor- ected for altitude, in which auxiliary relief valve and accumula- or valve act to control the rate of pressure rise in the fuel control uring an acceleration, and thereby control the rate of flow to the ombustion chamber.

Another method simply incorporates a barometrically con- olled auxiliary relief valve which acts to by-pass a certain mount of fuel pumped by a positive-displacement pump on a predetermined schedule and therefore limits the fuel available for acceleration.

Still another hydraulic method makes use of a dashpot system which is linked to the fuel-control lever, and, regardless of the rapidity with which the control lever is moved, the dashpot will act to control the elements of the fuel-control system so as to deliver fuel to the engine at a scheduled rate.

All of these methods possess one major flaw, viz., the fact that it is almost impossible to design a hydraulic system that will follow the optimum curve such as described previously, in order to secure a maximum acceleration rate.

It has been evident for some time that the major objections, as listed, to scheduling controls may be overcome by accelerating against a direct temperature measurement. Active development work has been in effect using this principle for the past several years. Numerous arrangements for measuring top turbine temperature have been considered, such as fuel-air-ratio measurement, optical pyrometry, differential-expansion capillary-tube gas-density method in which the pressure drop through an orifice is a function of absolute temperature, and direct-temperature measurement.

An extremely important consideration in the use of any of these methods, however, is the radial and circumferential temperature distribution generally present in all aviation gas-turbine engines. Generally speaking, from a stress standpoint, the radial temperature distribution of the gas entering and leaving the turbine is arranged to give a curve such as indicated in Fig. 8, in order to keep blade creep and fatigue strength proportioned to the stresses imposed along the blade. The temperature at the base of the blade is therefore lowest, and the temperature rises toward the tip as shown. Physical limitations between engines, however, necessitate a variation of this curve as shown which complicates any temperature measurement taken from any one radial position. Fig. 9 shows the increase in accuracy to be obtained with the use of an increased number of thermocouples in parallel.

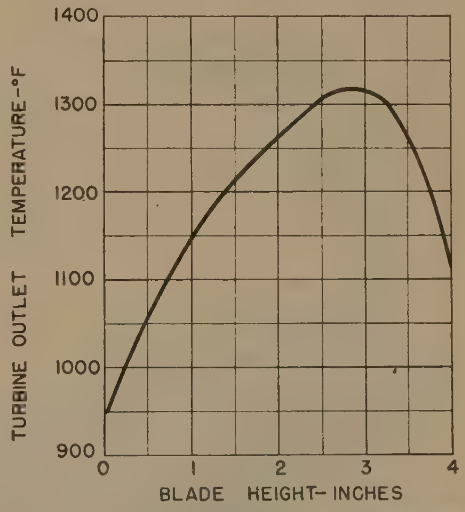

Fig. 8 Typical Radial Distribution of Temperature Along Turbine Blades

At this point it perhaps would be well to discuss briefly the effect of response rate of thermocouples on the indicated reading during a transient condition. The first requirement of a top-temperature control, similar to that being discussed, is to give adequate protection to the turbine blades. With this in mind, experiments were conducted to determine the response rate of the actual blades themselves. It is evident that the temperature pickup must have a faster response rate than the blade during

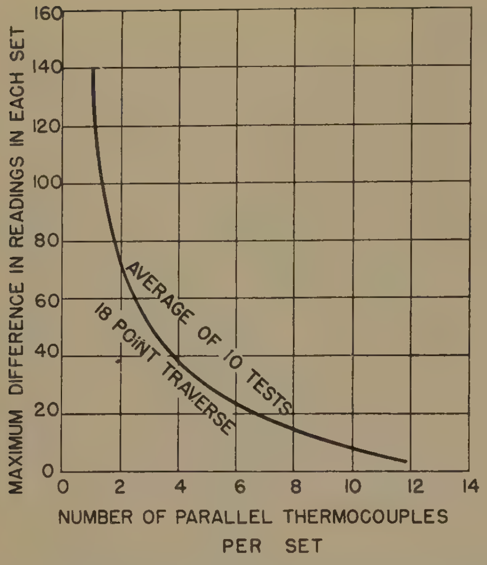

Fig. 9 Increased Accuracy of Indicating Average Turbine-Outlet Temperatures by Paralleling Thermocouples

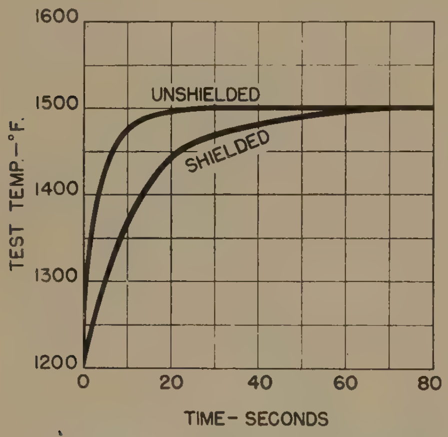

Fig. 10 Comparison of Thermocouple Response Rates

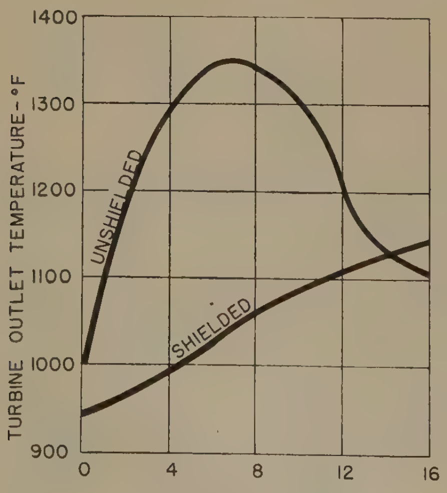

Fig. 11 Effect of Thermocouple Response Rate on Indicating Turbine-Outlet Temperature During an Engine Acceleration

a transient in order to prevent overheating of the blades. These tests showed that the blade-response rate at the trailing edge was 2 to 3 sec and 12 to 14 sec on the leading edge. Response rates of the shielded stagnation type of thermocouple ran as high as 12 sec, and it was of course evident that a couple such as this would not provide suitable protection. Further development along this line resulted in the unshielded type of thermocouple having suitable response rates. Comparative performance is shown by the curves in Fig. 10.

Further comparison indicating the effect of response rate of these two types of thermocouples during an actual engine acceleration is shown in Fig. 11. In both cases the actual turbine-outlet temperature was comparable. It will be noted that during the acceleration the stagnation type of couple actually indicated several hundred degrees lower temperature than the couple having a much higher response rate.

Mechanical Design Requirements

The primary requirement for the engine power control is reliability, as safety of flight will always be the most vital consideration in designing any aircraft component. Lacking this high degree of reliability in turbojet-engine controls developed thus far, the Air Services have found it necessary to require that the engine manufacturer furnish stand-by, or emergency controls which will assure manual operation of the engine in the event of flight failure of the primary automatic controls.

In nearly all cases, the designers of military airplanes crowd the engine installation into the smallest possible space in order to achieve optimum aerodynamics proportions for the airframe; therefore compactness is an essential requirement for the engine-power control. With the advent of the small frontal-area axial-flow turbojet engine, accessory compactness has become a consideration of even more vital importance, because, in general, it is desired that the primary controls and accessories of the engine be mounted directly on the engine to provide a packaged power-plant installation. In order to meet this latter requirement without compromising the big advantage of small diameter in the axial-flow turbojet design, it has been necessary to give considerable attention to assembling the control elements into packaged units utilizing internal passages instead of external fluid lines wherever possible. A good example of the ingenuity employed is illustrated in Fig. 12, showing a turbojet-engine fuel-control governor complete with fuel pump, acceleration control, and all auxiliary valves in a single packaged unit. An over-all view of a typical axial-flow turbojet engine, showing the relative location of this fuel-control governor and other engine accessories is shown in Fig. 13.

A further mechanical design requirement for the engine power control is light weight. In an aircraft, the saving of even a few pounds can improve significantly the over-all flight performance of the airframe and engine combination.

In the design of the fuel control, due consideration must be given to the pressure drop through the controlling elements, as this drop adds directly to the already severe fuel-pumping requirements for turbojet engines. As these requirements are of major importance, a brief review of the difficulties involved will be given.

In general, the top fuel pressure of the system is determined by the range in fuel flow required by the engine. This is represented by the ratio of the fuel required for high-speed cold-day sea-level flight versus high-altitude idling. This ratio may be as high as 35 to 1. Assuming 3-psi drop in the fuel nozzle is the minimum required for barely acceptable atomization, this will require a maximum nozzle drop of 3600 psi to obtain the required flow through fixed-area nozzles. As this pressure verges on the impractical, sacrifices have been made in the permissible fuel range of the engine. In addition, intensive development effort is being made to obtain acceptable low-pressure fuel nozzles. In view of the limitations covered by this situation, every consideration must be given in the fuel-system design to hold the required pressure drops through the other fuel-system elements to a minimum.

One of the most serious problems encountered with the modern type of fuel control is the malfunctioning of the control elements due to contaminated fuel. This condition is experienced with controls whose elements are subjected to the same fuel that is eventually delivered to the combustion chamber. Since the fuel that is used in the present-day engines has a very low viscosity, small clearances are required between sliding valves and their sleeves for pressure sealing.

Early models of fuel controls made use of the synthetic-rubber "O" ring seal as a piston ring and thereby permitted large clearances. However, this did not prove satisfactory, as it was not possible to obtain a suitable synthetic material that was fully resistant to the entire range of fuels. The materials used would increase in size when exposed to fuel for any length of time and cause additional resistances or would shrink after being subjected to a different type of fuel which would cause pressure leakage.

There are several partial solutions to this problem. One method is to use a micronic filter in the fuel supply to remove the contamination. This necessarily requires a micronic filter of large size and introduces additional pressure drop in the fuel system, and at the same time increases the weight materially. In addition, this type of filter causes serious pressure drops in cold-weather operation due to the formation of ice crystals from water which is normally carried in solution in the fuel at normal temperatures. A more desirable alternate method is to design the fuel system such that there is a definite pressure drop across the sliding portion of the control valves and to filter only the leakage fuel to the valve. This method uses several small filters of greatly reduced size and has the advantage of not increasing the weight as much as one large filter, as only a small part of the fuel must be filtered.

Since the use of micronic filters is generally undesirable, every

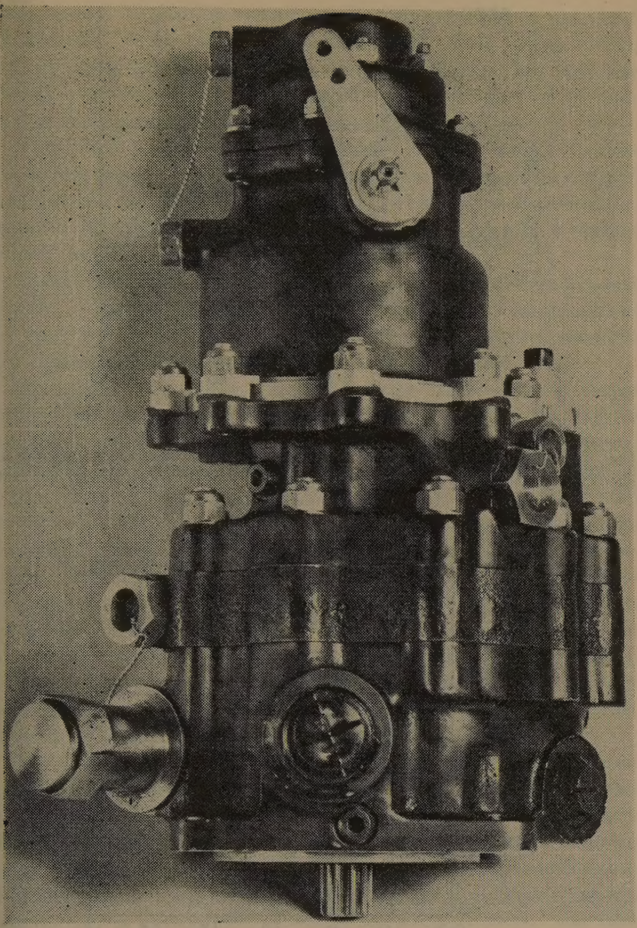

Fig. 12 Fuel-Control Governor for Turbojet Engine (Courtesy Woodward Governor Company.)

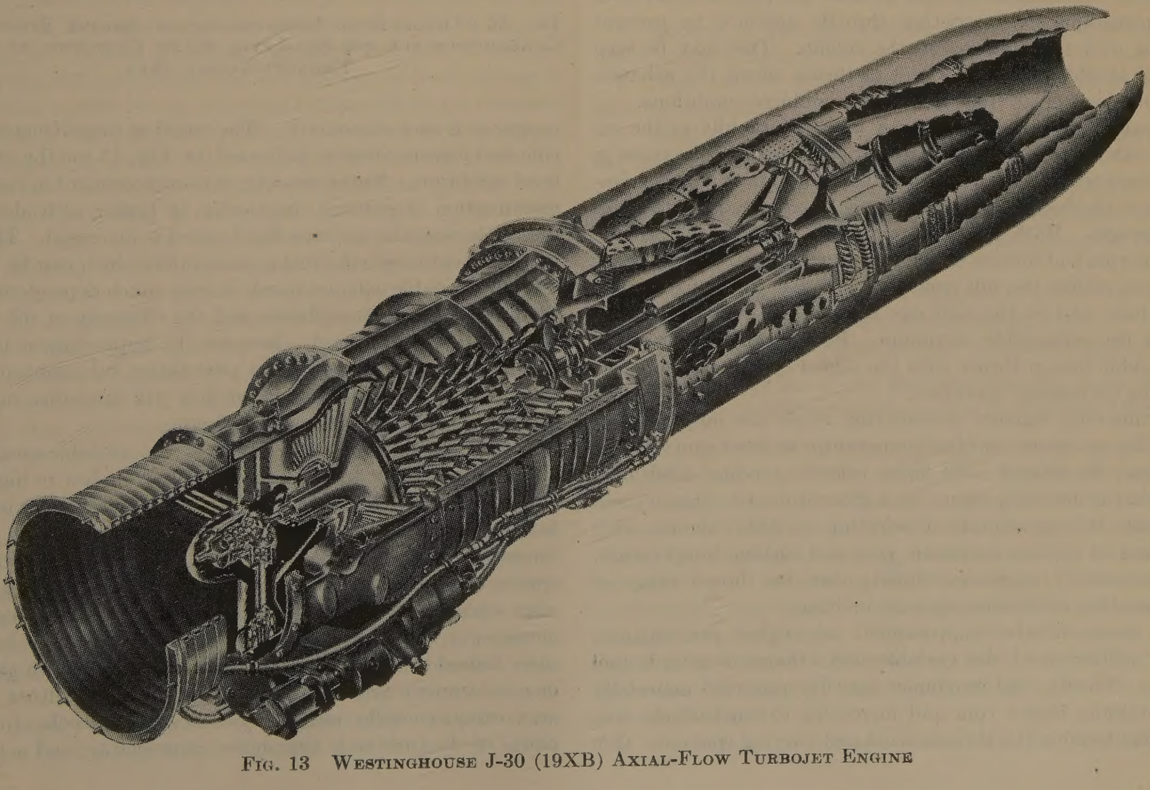

Fig. 13 Westinghouse J-30 (19XB) Axial-Flow Turbojet Engine

consideration should be given to a design in which the valves will operate satisfactorily with contaminated fuel. This can be done by designing the valves such that there is no pressure drop across the sliding portions, thereby preventing foreign material from being washed into the clearance between the valve and the bushing. The use of poppet-type valves seating on some type of resilient seat has given the most promise of operating on contaminated fuel. This is possible since there are no sliding parts to stick, and if some foreign material does get under the valve it will be pressed into the resilient seat and good sealing properties of the valve are retained.

Because it is not always possible to design all valves for satisfactory operation on contaminated fuel, the only other alternative is to operate the valves in a medium separate from the fuel. This can be done by having all the control valves, with the exception of the main fuel-control valve, operate in a liquid-sealed system which can be kept free of contamination by the use of a small filter. Although this will overcome the contamination problem, due consideration must be given to the viscosity curve of this liquid, as it is mandatory that satisfactory operation be secured down to —67 F.

Variable-Area Exhaust Nozzle

So far, the discussion has considered only the operation of the turbojet engine with a fixed exhaust-nozzle area which gives optimum operating conditions of the engine under only one combination of temperature, flight speed, and altitude. In addition to this, it places certain limitations on the acceleration characteristics of the engine which result in slower acceleration and certain sacrifices in engine economy.

If the design of the engine incorporates a variable-area exhaust nozzle, improved performance is obtained in three ways as follows:

1 Maximum military thrust is available for all flight conditions, as the engine can always be operated at maximum rpm with the maximum allowable turbine-inlet temperature. This is of advantage not only because increased thrust is available under some comditions, but also because the pilot is relieved of the responsibility of restricting throttle advance to prevent damaging over-temperatures in the engine. This may be seen from Fig. 14 which provides a plot of thrust versus the exhaust-nozzle area for a given rpm and different ambient conditions.

As would be expected, the thrust increases rapidly as the exhaust-nozzle area is reduced, with an accompanying increase in turbine temperature. It may be noted that limiting turbine temperature is reached at different exhaust-nozzle areas as the ambient changes. With a fixed nozzle area, selected to provide maximum rpm and turbine temperature on a standard day, it is not possible to realize the full rpm on a hot day without excessive temperature, and on the cold day the turbine temperature will be below the permissible maximum. Both conditions represent a measurable loss in thrust with the added danger of over-temperaturing on hot-day operation.

Unfortunately, ambient temperature is not the only offender in affecting maximum turbine temperature at fixed rpm and exhaust area, for altitude and flight velocity produce additional changes in turbine temperature at a given rpm and exhaust area. Here again, the opportunity of selecting variable exhaust areas as required to achieve maximum rpm and turbine temperature, and consequently maximum thrust, over the broad range of flight operating conditions, appears inviting.

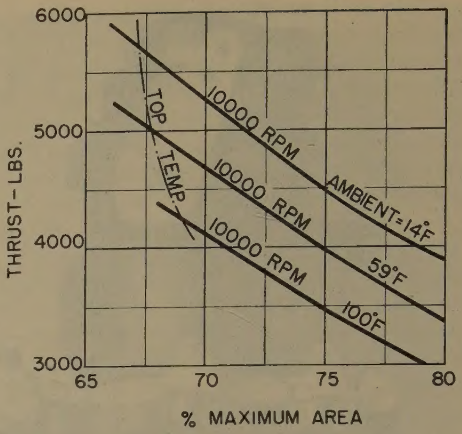

Fig. 14 Effect of Varying Exhaust-Nozzle Area at Constant Engine RPM to Maintain Military Thrust With Varying Ambient Temperatures

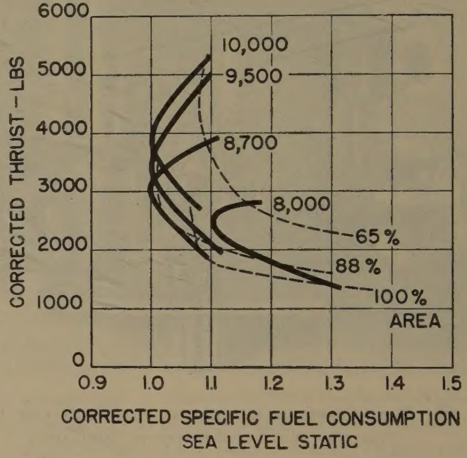

Fig. 15 Theoretical Improvement of Engine Specific-Fuel Consumption for the Sea-Level Static Condition by Varying Exhaust-Nozzle Area

2 A factor in the improvement of engine performance, through utilization of the variable-area exhaust nozzle, is fuel economy. Ideally, fuel economies may be improved materially by maintaining higher rpm and increasing exhaust-nozzle area rather than holding the jet area fixed and varying rpm over wide ranges as is now customary. The trend of improvement in specific fuel consumption is indicated by Fig. 15 for the static sea-level condition. Unfortunately, this improvement in specific fuel consumption is reduced drastically at higher altitudes, and is further lessened as airplane flight speed is increased. The actual improvement in specific fuel consumption which can be achieved with the variable exhaust nozzle is very much dependent on both the aircraft-engine installation and the efficiency of the variable-area exhaust nozzle used. Because the improvement in specific fuel consumption is attained at part thrust by maintaining high rpm, the resulting increase in air flow will introduce duct losses which may invalidate the expected gain.

3 Yet another factor in favor of the variable-area exhaust nozzle is the ability to accelerate rapidly from low to high thrust. It has been an unfortunate characteristic of jet engines now in the field that acceleration time from idle to military thrust has been excessively long, usually in excess of 8–15 sec. This long acceleration time is a function of two major factors. The first is the large rotor inertia, coupled with comparatively low accelerating horsepower available in the turbine under the high back pressures caused by the restricting exhaust nozzle. With the greatly increased nozzle areas employed at low thrusts with a variable-area exhaust-nozzle engine, the available accelerating horsepower of the turbine is augmented appreciably, and accelerating

imes from idle to military rpm can be reduced to ${}^{1}/_{3}$ or less of the omparable value for fixed exhaust-nozzle area. In addition, tilization of the variable-area exhaust nozzle does not limit the lesign of the basic engine components in order to avoid encounering compressor stall during acceleration.

The foregoing advantages obtainable by incorporating a variale-area exhaust nozzle in the engine, of course, must be weighed gainst the added complications, somewhat reduced reliability, reater duct losses in the aircraft, and increased engine weight vhich may be of considerable magnitude.

In analyzing the control means for the variable-area exhaust ozzle, it is first necessary to examine the various combinations f rpm and exhaust-nozzle area to obtain the control schedule or optimum economy.

Again referring to Fig. 15, which shows the relation of thrust ersus SFC at various rpm's and tail areas for our hypothetical ngine, it will be noted immediately that the conditions of maxinum-economy cruise operation are defined by the envelope of urves in the direction of low SFC values. As has been indicated reviously, it is definitely of advantage in the upper thrust range o hold maximum speed and increase exhaust-nozzle area to reluce thrust from maximum. For the particular characteristics f our hypothetical engine, a condition is reached in the process f reducing thrust at which it is advantageous to reduce rpm imultaneously with further increase of exhaust-nozzle area. inally, full-open exhaust-nozzle position is reached and further eduction in thrust is accomplished by reductions in rpm to idle. his is the schedule for best economy.

For best acceleration, maximum exhaust-nozzle area should e maintained until full rpm is reached, after which the exhaust rea can be reduced to achieve maximum thrust. To follow such schedule for steady-state operation would represent a compronise with best cruise economy, but with proper attention to conrol characteristics it will be found that no appreciable control omplexity is introduced in following approximately the best cceleration schedule during transients and best economy schedle for steady-state operation.

The regime of control variables, as a function of power-control ever position, for these respective schedules is shown in Fig. 16. ssuming an all-speed governor regulating fuel flow to control pm over the indicated range and as a function of lever setting, it emains only to provide an actuating system regulating exhaustozzle area in the scheduled relation to control-lever position. uch an actuating system can be the simplest form of hydraulic r electric servo to provide a predetermined exhaust area for each crement lever position in the partial-load range. As has been oted previously, turbine temperatures vary widely over the ange of ambient conditions, and the simple scheduled relation f exhaust area to control-lever position cannot hold for maxium-thrust conditions. This problem may be made by providg an overriding signal into the exhaust-nozzle servo, directly ensing turbine temperature or a temperature directly related to rbine temperature, and limiting the minimum exhaust-nozzle rea such that maximum turbine temperature is not exceeded, gardless of control-lever position or influence of ambient conitions.

When a variable-area exhaust nozzle is utilized, the design of e fuel-control system must provide means for a more rapid reonse to load changes on the engine, both from a stability standoint and from a safety standpoint, than is required with the xed-area exhaust nozzle. Sluggish or slow response can duce instability and result in hunting. Slow response in ecognizing sudden load changes can also cause destructive overeeds. As an example, assume that the exhaust area is made ddenly larger; then the control must immediately prevent exssive fuel from going to the engine in order to prevent overspeeding. On the other hand, if the pilot demands full engine power for a carrier wave-off and the exhaust area is reduced abruptly, the control must supply the added fuel needed to maintain engine rpm within acceptable limits. In general, full movement of the throttle valve must be possible in something less than ${}^{1}/_{4}$ sec.

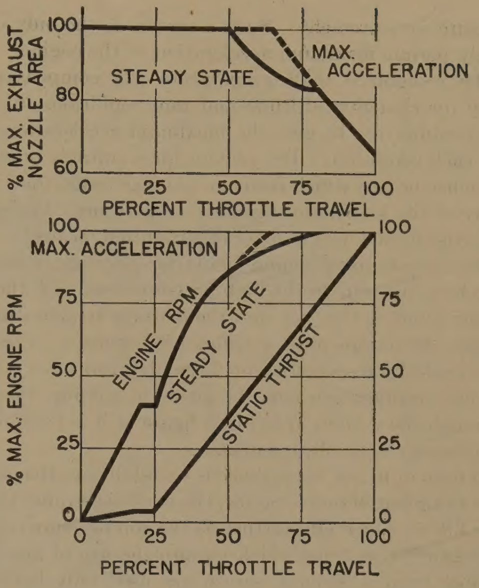

Fig. 16 Control-Lever Schedule Giving Optimum Co-Ordinated Control of Engine With Variable Exhaust Nozzle

Conclusions and Recommendations

Based on engine operational experience and engineering design studies of control problems, the following requirements are considered the primary requisites for a turbojet-engine power control, in order to meet the needs of military aviation and to realize the full operational performance of the engine:

1 Control to hold the selected thrust stable within specified limits for each flight speed and altitude.

2 Basic control design based on direct measurements rather than on scheduling.

3 Single-lever control of the engine to give a linear relationship between thrust and throttle movement.

4 Control to permit engine acceleration to be as rapid as the temperature and aerodynamic limitations of the engine permit.

5 Fast response rate to provide for rapid changes in the operating loads on the engine.

6 Controlling elements to be designed to give a low fuel pressure drop, in order to minimize fuel-pumping loads.

7 Control to operate satisfactorily on contaminated fuel.

Intensive study has shown that the following trend offers the best promise of fulfilling requirements of the military Air Services:

1 The speed-sensing means should be an all-speed isochronous governor, as no other means offers promise of maintaining the set engine speed for all load changes within the accepted requirement of plus or minus 1 per cent. Reset should be accomplished by direct speed-sensing, as experience has shown the impracticability of scheduling the exact degree. Of course the speed-sensing may be either the mechanical flyweight type or by suitable electrical means. Either system will operate through hydraulic or electrical servo systems; the choice will be indicated by an over-all study of the system based upon reliability, weight, and simplicity.

2 Acceleration of the engine should be accomplished by direct

temperature measurement. Such a system is the only one that will safely permit maximum acceleration of the engine. Also, it should be recognized that temperature will compensate automatically for changing altitude and ram conditions by varying the acceleration rate to give the maximum acceleration permissible for each condition. The pickup for a suitable temperature reading must be one which reads an average value that is represen tative of the maximum allowable temperature. Probably this can be accomplished by a number of recognized means.

3 The fuel-pumping requirements for jet engines have been found to be severe due to the high pressures required, the lack of lubrication value in the fuel, and the extreme temperature range over which the pumps must satisfactorily operate. The control has been partially responsible for these high pressures. For this reason due consideration must be given to holding the pressure drop through the system to as low a figure as it is possible to obtain satisfactory control pressures.

4 An item of major importance is the ability of the control to handle contaminated fuel. So far, the controls require the use of micronic filters, which add further to the top pressure of the system. In general, systems which require the use of any filtering means finer than a 60-mesh screen are used only because fuel systems capable of operating successfully on contaminated fuel are not as yet available for production engines.

5 It is expected that many new turbojet engines will have a variable-area exhaust nozzle, in order to realize the benefits in thrust, economy, and increased acceleration rate of the engine. The proper operation of this nozzle is of course a control function. As this adds a second controlled variable, it adds immeasurably to the problem to be considered in the design of the control. In addition, it means that the entire control must be designed as an integrated whole, as studies have shown that the speed and temperature components must be interrelated properly in order to obtain a stable system. At this time it should be emphasized that in the development of a control of this type, it is practically mandatory that proper mathematical considerations be taken into account to assure that the over-all system will be basically stable. These studies then should be supplemented further on a suitable transient analyzer in order to confirm the results of the original equations over the entire operating range.

As the development of the control progresses, consideration should be given to ease of service in the field. By now it will be recognized that a full understanding of the operation of the complete control system will be understood by only a comparatively few technicians in the field. On the other hand, all line maintenance and trouble-shooting will be done by semiskilled personnel, and it becomes nearly impossible for them to locate and correct troublesome items expeditiously. Therefore it is strongly suggested that provisions be made in the design for the use of a field-service check kit. With such an apparatus it will be possible for the average personnel to check each component on a "go–no-go" basis. The faulty component would then be replaced and returned to the overhaul base or manufacturer for repair. It is now recognized by the Air Services that such a procedure is almost mandatory.

The development of a completely suitable automatic power control for a turbojet engine is a tremendous engineering project. It is belived that such a control can be realized only by giving detailed attention during the development stages to the requirements outlined in this paper. Such a control should result in an easily serviceable unit, of excellent reliability and performance, and one which will permit the full utilization of engine possibilities as to thrust, economy, and acceleration from a single power-control lever in the pilot's cockpit.

ACKNOWLEDGMENT

The author wishes to express his appreciation to the engineers of the Engine Auxiliaries Section, Westinghouse Aviation Gas Turbine Division Engineering Department, for their invaluable aid in the preparation of this paper.